Three-dimensional study of the Iberian red deer antler (Cervus elaphus hispanicus): application of geometric morphometrics techniques and other methodologies

Débora Martínez Salmerón

Three-dimensional study of the Iberian red deer antler (*Cervus elaphus hispanicus*): application of geometric morphometrics techniques and other methodologies

Débora Martínez Salmerón

PhD Thesis

Barcelona, 2014

Facultad de Biología
Departamento de Biología Animal
Programa de Doctorado de Biodiversidad

Three-dimensional study of the Iberian red deer antler (*Cervus elaphus hispanicus*): application of geometric morphometrics techniques and other methodologies

Memoria presentada por
Débora Martínez Salmerón
para optar al título de
Doctora por la Universidad de Barcelona

Barcelona, 2014

VºBº de los directores:

Director/Tutor
Adrià Casinos Pardos
Depto. Biología Animal
Universidad de Barcelona

Directora
Concepción Azorit Casas
Depto. Biología Animal,
Biología Vegetal y Ecología
Universidad de Jaén

Abstract

Over time, many studies based in classical morphometry about deer antlers have been done. The present study propose a new perspective on antler study, taking as model the Iberian red deer subspecies (*Cervus elaphus hispanicus*) from Sierra Morena (Spain), introducing new techniques able to provide more detailed information about them. The objectives addressed in this work have been principally focused on the use of geometric morphometrics methods and photogrammetric systems based on CAD-3D technology. Three-dimensional coordinates of 217 antlers, concerning both the full and half antler structure, were adapted for each objective of the study, and subjected to several multivariate statistics analyses. Consequently, the exhaustive characterization of the shape changes of different antler parts, from different ages, was carried out, as well as the exploration of the existence of a possible optimal age for the obtention of the best hunting trophies. The antlers of youngest individuals (2 to 3 years old) showed smaller but more elongated near the skull, with straighter and vertically oriented tines; while the antlers of fully-grown individuals (6 to 9 years old) were shorter near the skull and more arched distally, presenting longer and curved tines. The allocation of an own antler categorization, based on some key measures used in hunting protocols, made possible the observation of a noticeable improvement in the quality of antlers of individuals aged between 4 and 9 years, as well as some deterioration from 10 to 13 years. This implies important aspects to consider for deer management in the area studied, which also might be applicable to other species. In turn, the high variability of antlers in terms of asymmetry was studied through the evaluation of the presence of Fluctuating asymmetry (FA) and Directional asymmetry (DA). Generally,

previous studies on antlers only shown FA. However, the presence of FA and DA was significant in the sampled antlers, being the amount of DA higher than FA. The predominance of DA, rejected the possibility of considering FA as individual quality indicator. In addition, the DA presence involved new insights about the antler asymmetry and its development, pointing to a stronger action of the genetic component of antlers, and to a more intense use of the right antler side. On the other hand, the annual capacity of antlers to regenerate, where multiple pathways and mechanisms interact, led us to the idea that antlers may act as modular structures. Accordingly, five modularity hypotheses of different biological interest were proposed, taking into account both the variation among individuals and the variation suffered at direct developmental pathways. Modularity and integration were found, highlighting the tight relationship between both phenomena in antlers. This last fact, reflected the interaction of multiple pathways along the antler growth, as well as the existence of developmental interactions transmitting the effect of random perturbations throughout the whole structure. Thus, the antlers generally act as single integrated modules, performing a common function as head and eyes protection during fights. However, the modularity observed also suggested the relative independent behaviour of some antler parts, as the trez tines, during antler development. Finally, a Photogrammetric Interactive Measure Method (PhIMM), based on the combination of digital methods and the use of a parametric CAD system, was proposed to complete the study. This methodology, represents advantages from the data-taking point of view, since the use of digital photographs allows to sample in the field in an economic and fast way. Furthermore, the lack of taking measures in the

field is not a problem, since the CAD-3D technology allows to create three-dimensional models of the structures on which we can perform all the measurements desired, including volumes and perimeters. In addition, the information extracted from this models can be directly shown in excel sheets, facilitating the data processing and even the introduction in other programs.

Resumen

A lo largo de los años, muchos han sido los estudios de morfometría clásica realizados sobre astas de ciervo. El presente estudio propone una nueva perspectiva acerca del estudio de las mismas, tomando como modelo la subespecie de ciervo Ibérico (*Cervus elaphus hispanicus*) de Sierra Morena (España), e introduciendo el uso de nuevas técnicas capaces de proporcionar información más detallada sobre dicha estructura que las aplicadas hasta el momento. Los objetivos planteados en este trabajo se centran en la utilización de morfometría geométrica y métodos fotogramétricos basados en tecnología CAD-3D. Para ello, fueron adaptadas a cada objetivo, y sujetas a diferentes análisis estadísticos, coordenadas tridimensionales tanto de la mitad como de la totalidad de 217 cornamentas. De esta manera, se llevó a cabo tanto la caracterización exhaustiva de los cambios de forma de diferentes partes de la cornamenta en función de la edad de los ciervos, como la exploración de la existencia de una posible edad óptima para la obtención de los mejores trofeos de caza. Las cornamentas de los individuos más jóvenes (2-3 años de edad) resultaron ser más pequeñas y alargadas en la parte más próxima al cráneo, con puntas generalmente rectas y orientadas verticalmente; en cambio, las cornamentas de individuos más desarrollados (6-9 años de edad), resultaron ser más cortas en su parte más próxima al cráneo, arqueadas distalmente y con puntas más largas y curvadas. La asignación de una categorización propia basada en medidas utilizadas en protocolos de caza, hizo posible la observación de una mejora en la calidad de las cornamentas de individuos entre 4 y 9 años de edad, así como un deterioro en las de individuos entre 10 y 13 años de edad. Dichos resultados son importantes para el manejo del ciervo Ibérico en el área de estudio, lo que

también podría ser aplicable a otras especies. A su vez, mediante la evaluación de la presencia de asimetría fluctuante (FA) y asimetría direccional (DA) se estudió la elevada variabilidad observada en cornamentas, en cuestión de asimetría. En general, los antecedentes bibliográficos únicamente muestran la presencia de FA. No obstante, la presencia tanto de FA como DA fue significativa, siendo DA más abundante que FA. El predominio de DA, supuso la imposibilidad de considerar FA como indicador de calidad individual. Asimismo, la presencia de DA planteó nuevas perspectivas acerca de la asimetría y desarrollo de las cornamentas, apuntando hacia una mayor influencia por parte del componente genético de las mismas y, en este caso concreto, hacia un uso más intenso de la rama derecha. Por otro lado, la capacidad de regeneración anual, donde múltiples vías y mecanismos de desarrollo interactúan, sugirió la idea de que las cornamentas pudieran comportarse como estructuras modulares. Debido a ello, se propusieron cinco hipótesis de modularidad de distinto interés biológico, con el fin de obtener una visión más global del comportamiento de las cornamentas teniendo en cuenta tanto la variación entre individuos, como la debida a vías directas del desarrollo. La presencia de modularidad e integración, resaltó la estrecha relación entre ambos fenómenos. Ello, a su vez, reflejó la interacción de las múltiples vías que actúan a lo largo del proceso de crecimiento de las cuernas, así como la existencia de interacciones del desarrollo capaces de transmitir el efecto de perturbaciones aleatorias a lo largo de toda la estructura. Así, se podría decir que las cornamentas actúan generalmente como un único módulo integrado, cuya finalidad es realizar una función común, tal como proteger la cabeza y ojos durante las

luchas. Sin embargo, la modularidad observada también sugirió cierta independencia de algunas partes de la cuerna, como los candiles, a lo largo del proceso de desarrollo de las mismas. Finalmente, se propuso la implementación de un método fotogramétrico interactivo de medida (PhIMM), basado en la combinación de métodos digitales y el uso de un sistema CAD paramétrico, para el estudio de estructuras biológicas del tipo cornamentas. Dicha metodología supone ventajas desde el punto de vista de recolección de datos, puesto que la realización de fotografías digitales permite trabajar en el campo de manera rápida y económica. De esta manera, la falta del registro de algunas medidas en el campo no sería un problema, ya que la tecnología CAD permite crear modelos tridimensionales de estructuras, a partir de las cuales se pueden tomar todas las medidas deseadas, incluido el cálculo de volúmenes y perímetros. Además, la información extraída de dichos modelos puede ser directamente registrada en hojas Excel, facilitando así el procesado de los datos e incluso su introducción en otro tipo de programas informáticos.

1. Introduction

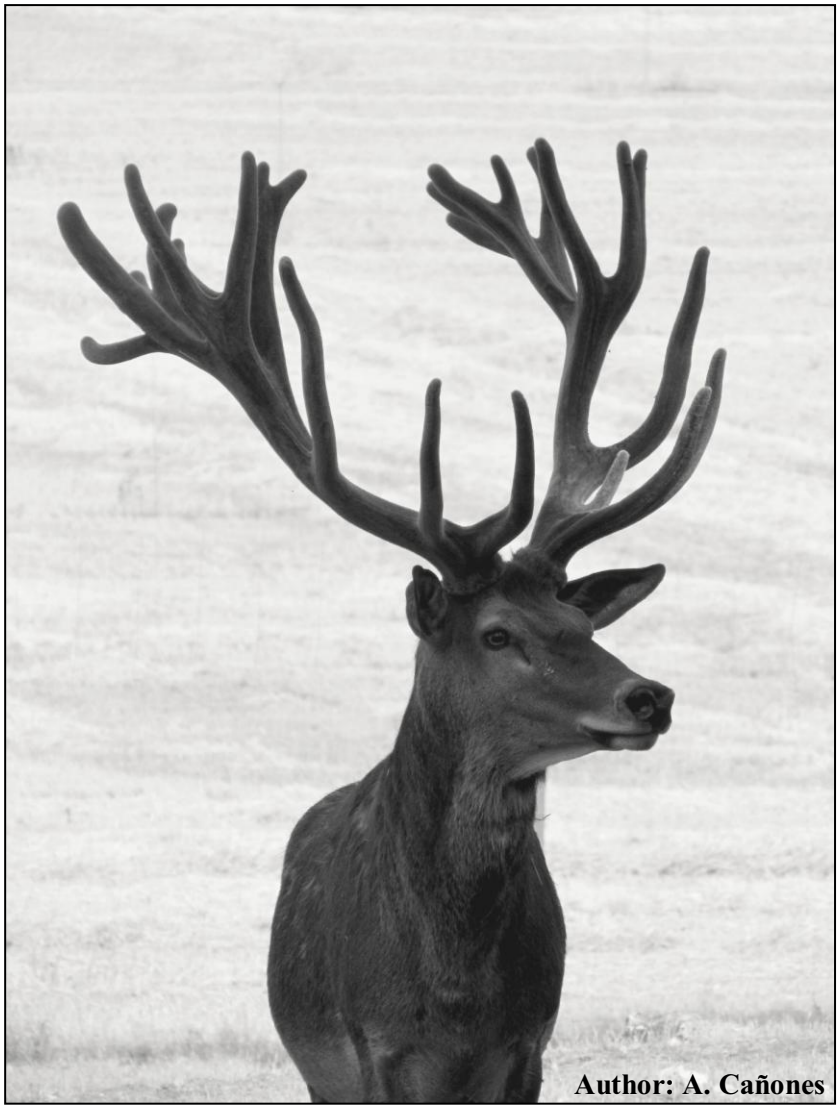

1. Introduction

1.1 Geometric morphometrics brief history

The origin of morphometrics, defined as the study of the shape variation and its covariation with other variables (Bookstein 1991; Dryden and Mardia 1998), dates back several centuries. The painter Albrecht Dürer (1528) was the first to use shape transformations of the human head for the study of human proportions. However, were the advances introduced by mathematicians of the 19th century who contributed to the current approaches that morphometry allows (Van der Molen et al. 2007). Among them, D'Arcy Thompson (1917) synthesized for the first time geometry, statistics and biology, suggesting that shape changes suffered by a biological structure could be modelled and described by transformation grids. Francis Galton was the first to introduce the use of statistics methods for the analysis of biological variation by using several variables simultaneously (Sokal and Rohlf 1997). Karl Pearson contributed with the introduction of descriptive statistics and correlation methods (Pearson 1895). Later, Ronald A. Fisher, who was interested in genetics and evolution of morphological traits, participated in the development of several concepts widely used even today, as for example the analysis of variance (Fisher 1935). By the same time, Julian Huxley and Georges Teissier, developed the theory of allometry and designed analytical methods for the interpretation of biological quantitative data (Huxley 1932). All these contributions together with many others (Bookstein 1998), form the basis of traditional morphometrics but also that of geometric morphometrics (Adams et al. 2004; Van der Molen et al. 2007). Thus, traditional morphometrics (Marcus 1990; Reyment 1991), bivariate or multivariate morphometrics (Blackith and Reyment 1971), consisted in

the application of statistics to groups of morphological variables generally based on linear measurements, but also on ratios and angles (Adams et al. 2004). On the other hand, geometric morphometrics methods are characterized for combining geometrical and biological information (Bookstein 1982 and 1984), to study in a two or three-dimensional spaces the quantitative shape change of the structures (Bookstein 1982; Zelditch et al. 2004). In addition, geometric morphometrics methods (GMM) are attractive due to its many advantages, and even the possibility to explore a large number of different phenomena involved in the shape change of biological structures, as for example asymmetry, integration or modularity. For that reason, it has been the technique chosen for carrying out the present research, since it is apparently the most suitable method to work with complex biological structures, as Iberian red deer antlers (*Cervus elaphus hispanicus*), the present case study.

1.1.1 *Traditional morphometrics vs. Geometric morphometrics*

Although it has been shown that traditional morphometrics and geometric morphometrics methods have common basis, there are many differences between them.

Briefly, traditional morphometrics principally consists in the use of lineal measurements, as lengths, depths or widths. This kind of measurements generally present little information about shape, since they sometimes overlap or run in similar directions ignoring the spatial relationships among them (Zelditch et al. 2004). Furthermore, they usually are highly correlated with the size of the object, biasing the patterns of shape variation (Bookstein et al. 1985). Moreover, some of these measurements are not exactly independent, which could result in correlated measurement error (Zelditch et al. 2004). Additionally, some lineal measurements, such

as the maximum width or height of an object, cannot be defined by homologous points (Van der Molen et al. 2007; Zelditch et al. 2004), which may result in identical values from two different forms, as it occurs with the classical example of the drop and the ellipse (Fig. 1.1).

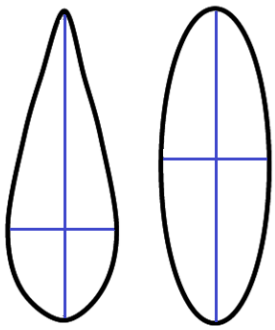

Figure 1.1. Classical example of disadvantage in traditional morphometrics are the drop and the ellipse, where the same set of measures, width and length, can be obtained from two different shapes. Scheme extracted from Van der Molen et al. 2007.

All these observations, coupled with the inability to visualize the shape change using traditional methods, would underestimate the shape information collected (Zelditch et al. 2004).

The different drawbacks mentioned led to the geometric morphometrics development (Van der Molen et al. 2007). Geometric morphometrics is characterized for being a landmark-based method (non-linear measurements) (Baab et al. 2012), which allows to deduce the organism shape understood as the remainder geometric information when the location, rotation and scale effects are removed (Kendall 1977) (Fig. 1.2). Furthermore, this procedure always maintains the physical integrity of the organisms studied (Bookstein 1991; Van der Molen et al. 2007; Zelditch et al. 2004). Thanks to the rigorous statistical theory created by some statisticians, as David Kendall (1984), geometric morphometrics allows to combine the use of multivariate statistics and methods for the direct

visualization of the results (Adams et al. 2004). Therefore, we can observe solely and exclusively the changes due to shape variation (Zelditch et al. 2004). In addition to the above information, it should be noted the progress occurred in the design of specialized software to perform geometric morphometrics analyses, which is mostly free available. This is the case of MorphoJ, the main software used in this study, which in turn is interesting for its remarkable statistical power (Klingenberg 2011).

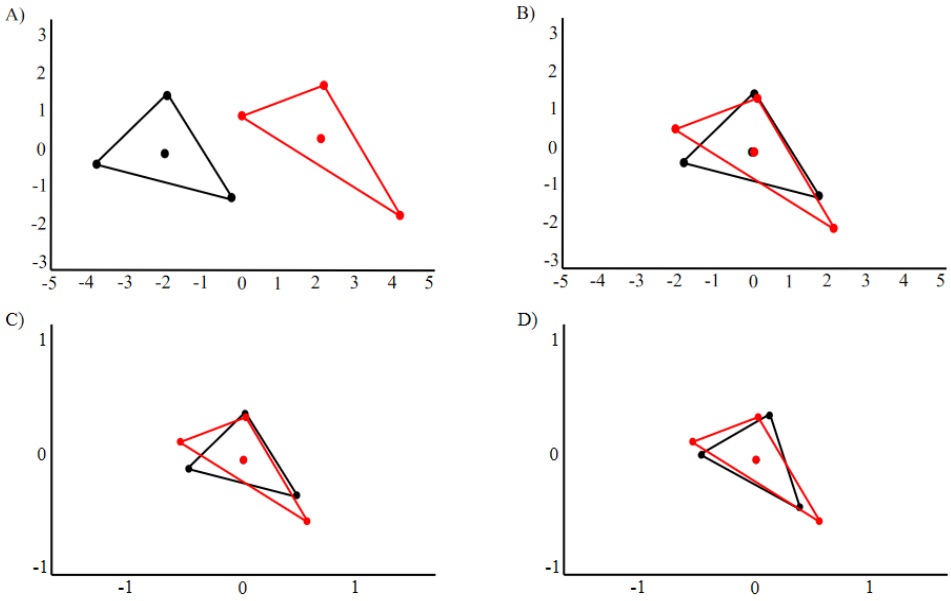

Figure 1.2. Scaling, translation and rotation effects over two different configurations of landmarks represented by triangles. A) Original landmark configurations; B) Translation to the origin; C) Scaling to unit the Centroid size and; D) Rotation to minimize the squared distances between the corresponding pairs of landmarks. Example modified from Baab et al. 2012.

1.1.2 *Shape space and dimensionality*

The significant contribution of the statistician David Kendall, allowed the visualization of the different shape changes of structures and organisms. This visualization occurs in a shape space or Kendall space (Kendall 1981 and 1984), which is defined as a non-Euclidean space represented by a spherical surface (Zelditch et al. 2004). Due to the complex interpretation of this multidimensional space for configurations of more than three landmarks, the corresponding morphological points can be projected onto a tangent linear space. This tangent space stands for an Euclidian approximation of the Kendall shape space of the same dimension (Van der Molen et al. 2007), where multivariate statistics methods can be easily used (Zelditch et al. 2004) (Fig. 1.3).

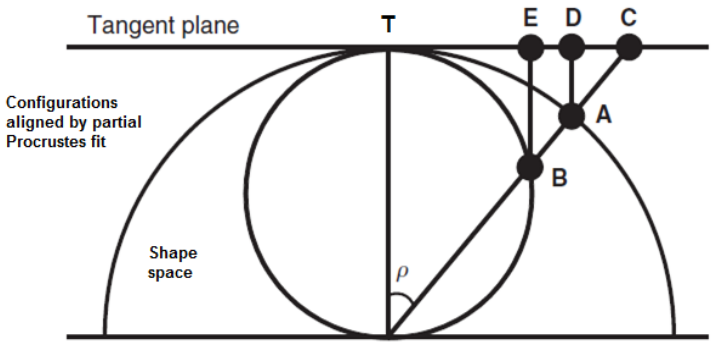

Figure 1.3. Relationship between Kendall's shape space and the tangent space, for configurations of triangles. The outer hemisphere is a shape space section, which represents the alignment of the triangle configurations to unit the Centroid size by partial Procrustes fit. The inner circle, is a Kendall's shape space section where shapes are scaled, centered and aligned to cos (ρ). B represents a triangle in the Kendall shape space, while A is the same shape scaled to unit the CS. C, D and E, represent alternative projections of a single shape onto the tangent plane. T represents the tangent point, which in turn, corresponds to the Procrustes average shape. Figure modified from Zelditch et al. 2004.

Regarding the dimensionality of this space, it depends of the number of landmarks and data dimension used. Thus, for 2D data the shape dimension would be $2k$ - 4, where k is the number of landmarks, and four the number of dimensions reduced due to the removal of the location (2 dimensions), rotation (1 dimension) and scale (1 dimension) effects from each landmark configuration (Klingenberg et al. 2002). However, for 3D data such as the study case, the shape dimension is $3k$ - 7, since one dimension is reduced for the scale effect, but three for the location effect and other three for the rotation effect (Klingenberg et al. 2002).

1.1.3 *Shape components*

Generally, the total shape change of the structures can be decomposed in two components: the uniform and non-uniform (Bookstein 1991). The uniform shape component takes into account the shape changes due to geometry, which are characterized for equal affect on all the sampled points, once the scale, location and rotation effects have been removed, so that parallel lines remain parallel (Zelditch et al. 2004) (Fig. 1.4). By contrast, the non-uniform shape component refers to all the other potential shape changes concerning to non-linear movements, but local variations of certain landmarks (Van der Molen et al. 2007). However, despite we are able to separate both components, it is the study of the total shape variation what more interest arouses in biological studies, and what has been taken into account when studying antlers.

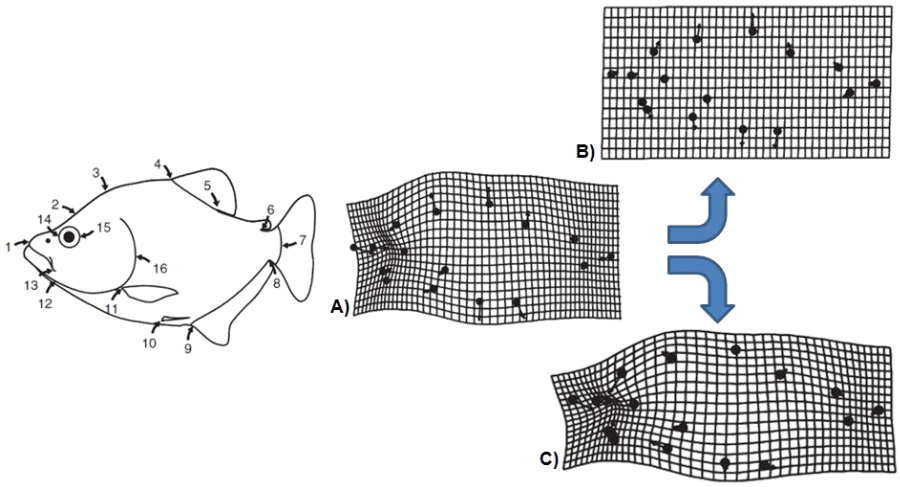

Figure 1.4. Example of shape decomposition in *Serrasalmus* gouldingi (subfamily of piranhas). A) Total shape deformation including its two components; B) uniform component and; C) non-uniform component. Figure modified from Zelditch et al. 2004.

1.2 Photogrammetric Interactive Measure Method (PhIMM)

The application of geometric morphometrics methods (GMM) on biological structures, has been a revolutionary tool for the specific study of the shape changes associated to them, especially due to the accuracy of the results. However, a constant and continuous technological updating, innovation and progress is always necessary. Therefore, new tools and methodologies to facilitate and accelerate the collection and processing of geometric data are necessary. This is where the Photogrammetric Interactive Measure Method (PhIMM) will play an essential role.

As the name of the method suggests, it is characterized for combining photogrammetric techniques, such as the taking of digital photographs directly in the study field, and the application of a parametric software based on three-dimensional Computer Aided-design technology (CAD-

3D). Thus, from a few digital photographs taken from each measured structure and CAD-3D technology, it would be possible to extract the geometric information of the structures under study and generate three-dimensional models of the same.

From the point of view of deer hunting, there is a growing interest in trophy evaluation to homologation. For that reason, the validity of this new method was tested through its application for the evaluation of the quality of different antler trophies from Sierra Morena, in the same way that it has been traditionally done by using different measures defined in hunting protocols.

1.3 Antlered deer ancestors

Since this work is principally focused on the study and application of GMM and the PhIMM on Iberian red deer antler, it is interesting to know how this structure appeared along the phylogenetic history.

Cervid anagenesis has changed slowly over time (Gingerich 1984). Cervids have a tropical origin, although they have always been primarily confined to temperate climate lands (Clutton-Brock et al. 1982). However, along the Tertiary cervids evolved, in such a way that they colonize cold climates, originating two subfamilies, one in the Old World and another one in the New World, differentiated among other things by their autopod (Geist 1998). Concretely, Old World cervids were considered *plesiometacarpalian*, since the second and fifth metapodials were lost except for their proximal ends, while the New World cervids were considered *telemetacarpalian*, since they only retained the distal ends of the same toes (Geist 1998) (Fig. 1.5).

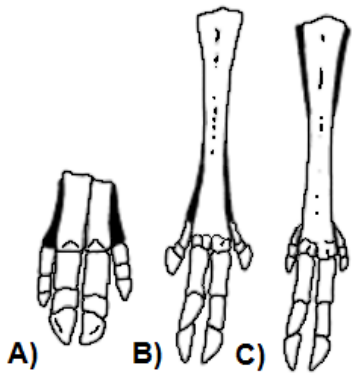

Figure 1.5. Deer metapodials condition. A) Holometacarpalian condition: the one found in pigs, is characterized in that the second and fifth metapodia (in black) are intact; B) Telemetacarpalian condition: typical of New World deer and various extinct ruminants families, is characterized by the reduction to distal splinters of the second and fifth metapodia; C) Plesiometacarpalian condition: typical of Old World deer, is characterized by the reduction to proximal splinters of the second and fifth metapodia. Figure modified from Geist 1998.

Among the characteristics of early cervids were small size, great development of the upper canines and antler absence, especially in those living in tropical climates, including the Asian water deer (*Hydropotes inermis*) from a temperate climate (Geist 1998). According to the fossil record, cervids appear in the Oligocene (mid-Tertiary period), approximately 40 million years ago (García et al. 2010). The first antlers appeared during the early Miocene, approximately 20 million years ago (Clutton-Brock et al. 1982). Specifically, antlers appeared in the genera *Syndioceras* (from North America) (Fig. 1.6) and *Climacoceras* (from Eurasia) (García et al. 2010). In both genera, originated in the Oligocene (Clutton-Brock et al. 1982), the antlers were characterized for being coated with a skin similar to that of giraffes (Geist 1998). Parallel in time, true antlers appeared in the North American ascendants of the family *Antilocapridae* (García et al. 2010), and were characterized for not being renewable (Geist 1998).

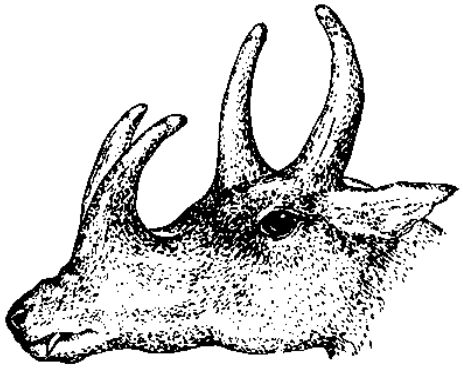

Figure 1.6. *Syndioceras* genus. Image extracted from Goss 1983.

The first cervids to have renewable antlers were those of the genera *Dicrocerus* and *Stephanocemas*, from Asia and Europe respectively, during the mid-Miocene (Clutton-Brock et al. 1982; Geist 1998; García et al. 2010). These antlers, despite being deciduous and forked did not show the same pattern of mineralization than current antlers (Geist 1998). Conversely, which considered as the first antlered cervid was an Old World form, a muntjaclike cervid from Europe (*Euprox minimus*), which displayed also short tusks (Geist 1998). This species radiated originating true deer during the late Pliocene, approximately 5.3 million years ago (Clutton-Brock et al. 1982), as the genus *Odocoileus* (Kurtén and Anderson 1980). Larger animals originated endowed with more complex antlers and reduced canines, as reviewed by Goss (1983) (Fig. 1.7). From this radiation originated *Cervus* sp. characterized by the progressive complexity of their antler shape, especially at its top (Clutton-Brock et al. 1982), until reaching the current antlered deer morphologies. However, it is interesting to note that in the late Pleistocene, *Cervus elaphus* specimens were much larger than members of the same species of post Pleistocene or present times (Walvius 1961; Clutton-Brock et al. 1982). A hypothetical explanation to the body and antler size decline, is a delay in

the animals growth due to a mineral-poor environment, beyond genetic changes, as it apparently occurred with the Rhum deer, from the highlands of Scotland (Clutton-Brock et al. 1982).

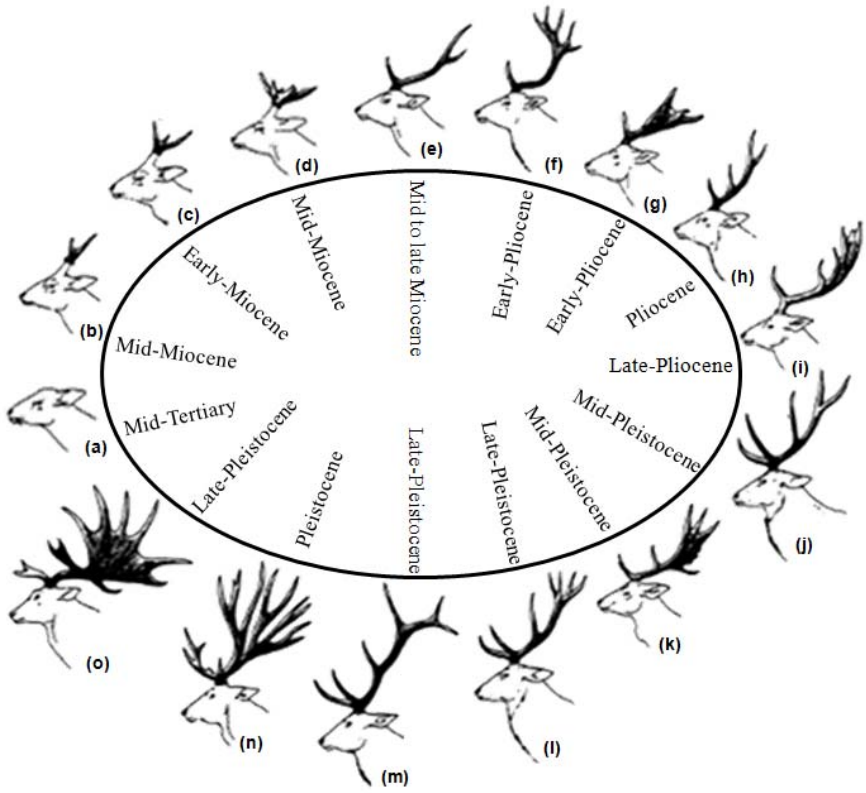

Figure 1.7. Antler evolution. (a) Hypothetical mid-Tertiary tropical, tusked deer; (b) Two-pronged mid-Miocene Muntjac-like deer (*Eustylocerus*); (c) *Dicerus*, early-Miocene; (d) *Stephanocemas*, mid-Miocene; (e) Three-pronged deer from mid to late Miocene; (f) *Rucervus*, from approximately late-Miocene; (g) *Cervavitas*, early-Pliocene; (h) Four-pronged deer, genus *Cervus*, Pliocene; (i) *Anaglochis*, late-Pliocene; (j) Five-pronged Ice Age deer, *Cervus elaphus acoronatus*, mid-Pleistocene; (k) *Dama dama*, mid-Pleistocene; (l) *C.e.hipelaphus*, late-Pleistocene; (m) Six-pronged Ice Age deer, wapiti, *C.e.canadiensis,* late-Pleistocene; (n) *Eucladoceros*, Pleistocene; (o) *Megaloceros gigantheus*, late-Pleistocene. Image modified from Geist 1998.

1.4 *Cervus elaphus hispanicus*: systematic aspects and distribution

In the same way that historical references about the appearance of antlers are important, it is also interesting to know some general aspects about the subspecies under study.

The red deer (*Cervus elaphus*) is a hoofed ruminant mammal, which belongs to the order Artiodactyla and family Cervidae (Price et al. 2005; Garde et al. 2010). This family includes 16 or 17 genera, depending on the author (Ellerman and Morrison-Scott 1951; Price et al. 2005; Garde et al. 2010), including about 41 species (Garde et al. 2010). *Cervus* sp. (Linnaeus 1758) includes 10 species distributed in Asia, Europe (including Corsica and Sardinia Islands) and Africa (Maghreb) (Corbet 1978; Whitehead 1993; Carranza 2004; Garde et al. 2010). *Cervus elaphus* comprises several subspecies (Clutton-Brock et al. 1982; Whitehead 1993), and the present research focus on the Iberian red deer (*Cervus elaphus hispanicus*; Hilzheimer 1909). The Iberian red deer is characterised for being one of the smallest subspecies of the genus (Huxley 1931; Whitehead 1993; Fierro et al. 2002), with the subspecies *C. e. barbarus* native from North Africa (Bennett 1833). *C. e. hispanicus* is endemic from the Iberian Peninsula (Garde et al. 2010), with exception of the North Western and Northern regions (Carranza 2004) (Fig. 1.8). The Iberian red deer is also characterised by having a coat of a more brownish colour than other subspecies (Azorit et al. 2002a), which presenting white spots during the first three months of the specimen life (Geist 1998; Carranza 2004). The Iberian red deer are crepuscular and usually gregarious, despite both sexes remain separated during almost the whole year, except in the breeding season, when their polygynous social structure involves the formation of harems (Carranza 2004; Garde et al

2010).

Figure 1.8. Pair of *Cervus elaphus hispanicus* males.

Despite the systematics mentioned above, it is interesting to note that some studies (Ludt et al. 2004; Sommer et al. 2008; Skog et al. 2009) have shown that mitochondrial DNA differences within populations of *Cervus elaphus* from Western Europe, are not enough robust to recognize subspecies. If we take into account this fact, the material studied in this research should be considered within the lineage *Cervus elaphus elaphus* (Sommer et al. 2008; Skog et al. 2009).

1.5 Economic interest of the Iberian red deer in Sierra Morena

The socio-economic value of the Iberian red deer in Sierra Morena is especially important, because it represents the most important exploitation of game species in the South of Spain (Carranza 1999; Azorit et al. 2002b; Garde et al. 2010; García et al. 2010). The principal deer hunting method

used is the commercial practice called *montería*, which requires the use of dogs for leading deers to open areas where are shot by hunters hidden at fixed points (Torres-Porras et al. 2009b). All resources obtained from hunting animals have commercial use (meat, skin, antlers, etc.); however, the principal objective of their exploitation is obtaining the best hunting trophies, which normally implies to obtain good specimens with larger and most symmetrical antlers (Carranza 2004; García et al. 2010) (Fig.1. 9).

Figure 1.9. Iberian red deer specimens bearing antlers of high economic value.

Therefore, the interest in the obtention of specimens with an optimal antler pattern is more and more ingrained (Fierro et al. 2002). Consequently, sometimes state landlords restock populations with specimens from France, Belgium or Germany (Fierro et al. 2002; García et al. 2010). Of course, this restocking could imply the improvement of antler trophies but at the same time increases heterosis (García et al. 2010), which has been correlated positively with antler size (Pérez-González et al. 2010). In turn, this heterosis represents a threat from the genetic point of view, since they could produce changes able to cause the disappearance of the autochthonous red deer (Carranza 2004). Therefore,

there is controversial whether restocking is a correct population management. Additional problems could also be the artificial selection exerted by breeders or the habitat fragmentation due to the presence of hunting fences (Carranza 2004). Thus, it is obvious the requirement to have a good knowledge of the antler development and structure for a correct management of the Iberian red deer populations, as a way to reconcile economic efficiency with conservation of areas of high natural value (Carranza 1999; Carranza 2004).

1.6 Antler traits and structure

Antler and bigger size are sexual dimorphic characters of Iberian red deer males (Clutton-Brock 1982; Carranza 2004; Garde et al. 2010). Antlers have different functions (Clutton-Brock 1982), being specially important that of acting like weapons of attack and defence in intraspecific fights during the breeding season (Clutton-Brock 1982; Lincoln 1992; Carranza 2004; García et al. 2010). However, antlers also serve to defend against predators, for temperature regulation, female claiming, force demonstration performances (García et al. 2010), or individual quality indicators (Schmidt et al. 2001). In this way, it is important to remark that antler development is highly sensitive to high population densities (Azorit et al. 2002a; Carranza 2004; Torres-Porras et al. 2009a) and bad environmental conditions, being specially important the food and mineral availability (Carranza 1999; Putman and Staines 2004). Some farmers try to mitigate the effect of the lack of food providing extra provisions at certain times of year (Carranza, 1999; García et al. 2010). Despite the existence of such possibility, it is discussed the positive effect of this practice (Carranza 1999; Carranza 2004; García et al. 2010), since negative consequences are also known about it. For example, there is a

possibility of increase the population density in certain areas (Carranza 1999), which in turn may lead to a habitat deterioration (Putman and Staines 2004). Consequently, from a scientific point of view, antlers can provide an insight into the genetic rank of the specimens (Ditckoff et al. 2001). Briefly, optimum antlers are provide by the conjunction of genetics and environmental situation (Carranza 1999).

The Iberian red deer antler develops from a cranial outgrowth of the frontal bone called pedicle (Price and Allen 2004; Hall 2005; Price et al. 2005; Kierdorf et al. 2007; García et al. 2010). From the pedicle a principal axis called beam emerges surrounded in the base by a rough area called burr (García et al. 2010) (Fig. 1.10).

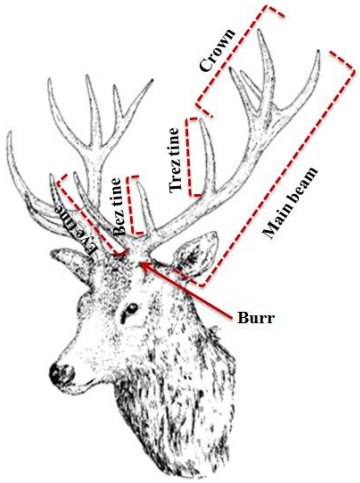

Figure 1.10. Antler parts represented on a specimen of *Cervus elaphus*. Image modified and extracted from Goss 1983.

In the youngest individuals (known as "*varetos*") of approximately one year old, the beam is not branched (Carranza 1999; García et al. 2010). From the first antler development onwards, antlers tend to be larger and morphologically more complex in number of branches (tines) appearing different ramifications: eye tines, bez tines, not always present in adults,

trez tines, and crowns. This later structure consists of a variable number of tines (Carranza 1999; Azorit et al. 2002a; Carranza 2004; Kierdorf et al. 2007; García et al. 2010) (Fig. 1.10).

Besides present a highly variable morphology, the antler is one of the most interesting bone structures due to its capacity to fall and regrow every year (Suttie et al. 1991; Stéger et al. 2010; Gaspar-López et al. 2010), since it has been shown the general inability of mammals to regenerate complex appendages (Kierdorf et al. 2007). In this way, antlers can change its morphology every year, for which different theories have been collected in the work of García et al. (2010), for example: to look like females to avoid predation, for antler size adaptation to body size, or for the repair of damaged antlers due to fights or frosts. The capacity for the annual antler regrowth is similar in some aspects to urodele limb regeneration (Kierdorf et al. 2007). This capacity probably makes antlers one of the tissues with a fastest growth in the animal kingdom (Price and Allen 2004; Price et al. 2005), since it only needs 4-5 months to complete all the developmental stages, ossification and mineralization included (García et al. 2010). However, the growth process needs a minimum time to result in a normal antler development (García et al. 2010), taking approximately 158 days in adult Iberian red deer (Gaspar-López et al. 2010). On the other hand, antler regeneration can involve strong variations in antler shape between years (Pélabon and Joly 2000).These variations could be due to environmental differences throughout the regeneration process, which in turn could result in diverse asymmetry levels at different antler parts (Swaddle 2003; Mateos et al. 2008).

Maximum antler development is coincident with reaching full sexual maturity, which is attained between 7-12 years old, according to different authors (Nahlik 1992; Carranza 1999; Montoya 1999; García et al. 2010).

The sexual maturity is followed by the antler regression phenomenon and consequently for deer aging (García et al. 2010).

1.7 Antlers vs. Horns

Antlers are bone (García et al. 2010) unlike bovine horns, which have a dermal origin (Santiago-Moreno et al. 2010). According to Ullrey (1982), Cuvier (s. XIX) was the first author to affirm that mature antler was a bony structure. Until then some people thought that it was made of wood (Goss 1983).

As Aristotle report many years ago in his treatise *Historia Animalium*, the antler is the only appendix totally hard and filled from end to end, whereas the horns are partially empty (Fig. 1.11).

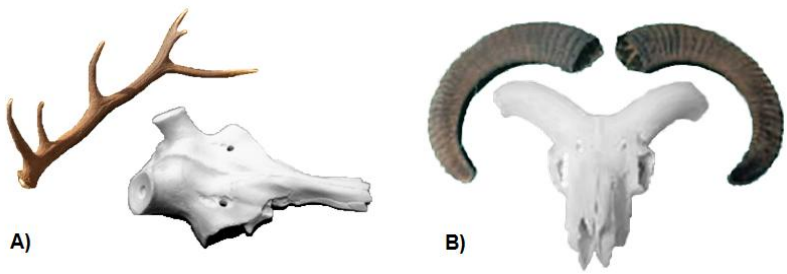

Figure 1.11. Comparison between antler and horn. A) Antler cast totally filled from end to end, and deer skull with its permanent pedicles; B) Horn partially empty, which acts as a corneal sheath overlying the skull bone of different bovid species, such as the bighorn sheep. Image B extracted and modified from Santiago-Moreno et al. 2010.

Moreover, horns present a rigid cover impossible to modify once formed (Goss 1983), which make them permanent structures along life (Santiago-Moreno et al. 2010). Another difference between antlers and horns lies in how they grow, since the antler, mesenchymatic (Price and Allen 2004),

grows by its tip area (Price et al. 2005) and bovine horn, ectodermic, grows by its base (Goss 1983).

Despite their differences, antlers and horns also have similarities, as for example that both are considered secondary sexual characters (García et al. 2010; Santiago-Moreno et al. 2010), or the fact that its shape is highly influenced by environmental variables as the temperature, food availability or photoperiod (García et al. 2010; Santiago-Moreno et al. 2010).

1.8 Objectives and justification

The main objective of this thesis has been to analyze the Iberian red deer antler (*Cervus elaphus hispanicus*) from the Eastern area of Sierra Morena (Jaen, Spain), through the use of three-dimensional geometric morphometrics methods and other methodologies. To do it, we have tried to delve into different antler aspects, which correspond to the different objectives of the research.

The high economic interest of the Iberian red deer antler (Azorit et al. 2002b; García et al. 2010), focus in obtaining the best hunting trophies. It implies to bring down the specimens of larger and apparently more symmetrical antlers, since it has always been suggested that only high-quality males are capable to produce this type of ornaments (Moller 1992; Pélabon and Joly 2000; Carranza 2004; Dicthkoff and Defreese 2010). Therefore, the need to have the best possible knowledge about the management of the species is necessary to obtain specimens with antlers of great economic value (Fierro et al. 2002). Geometric morphometrics methods, as well as the use of PhIMM, could serve as very useful tools for the management and conservation of hunting trophies, species and its

environment. Additionally, is the first time that both methodologies are applied to deer antlers, what makes the study not only extremely novel, in the opinion of more than one specialist in the field, but also accurate due to the methods used. Furthermore, these technologies could be a positive support for the established official protocols evaluating the quality of hunting trophies. In turn, it would be possible to learn more about the antler behaviour and its development, leading us to a better understanding of the diverse levels of interaction existing between the different antler parts. In line, the knowledge of the antler condition, as well as some weather information of each hunting season, could help to recognize the environmental situation of the studied area. Consecutively, this study could provide information about nutritional demands in the study area, or indicate the presence of a possible good quality genetic strain among the sample. Therefore, the specific objectives of the study are:

1) Describe and quantify the shape variability among Iberian red deer antlers from different age classes by using geometric morphometrics methods, as well as evaluate the presence of an optimum trophy age in the study area. Thus, a detailed description of the overall shape variation observed in antlers would be obtained, being of special interest the changes experienced by the main axes of the structure, as well as by those tines common to all age classes, such as the eye and trez tines. On the other hand, to evaluate the existence of a possible optimal age class for antlers in terms of trophy quality, different antler categories are established from the knowledge of several measures used in the corresponding trophies approval protocols.

2) To quantify the asymmetries present between the left and right antler sides of the Iberian red deer, focusing on the presence of fluctuating

asymmetry (FA), and determine whether it is possible to use FA as a reliable *fitness* or individual quality indicator. The annual antler regrow provides a valuable source of information about the status of the individuals every year, but in turn could lead to deviations from perfect bilateral symmetry of the structure, largely due to environmental stresses. For that reason, some studies suggest the idea of using antler asymmetries as environmental indicators. In this sense, we would be able to see if the shape changes due to the asymmetric component of antlers are affected by factors such as the age or environmental variables.

3) To determine whether the Iberian red deer antler can be defined as a single integrated structure or as a modular entity. Therefore, in order to test the presence of modularity and integration between the different antler parts, several hypotheses of diverse biological interest have been proposed. Each hypothesis suggested tested by focusing on both, the general variation of traits among individuals, where the different mechanisms involved on antler development are included, and on variation due to FA, which exclusively represents the interactions between developmental processes.

4) To develop and apply a Photogrammetric Interactive Measure Method (PhIMM) based on parametric CAD-3D technology to assess the quality of different deer hunting trophies. This part of the study is based in tuning the use of the PhIMM and assess its reliability and accuracy in geometric data collection. The reduced number of photographs required by antler, would allow the study of a big number of individuals in a fast way. Thus, this method would facilitate the field work and the obtention of large amounts of information. In addition, the CAD-3D technology would help us to perform a three-dimensional modelling of the structures under study.

2. Material and methods

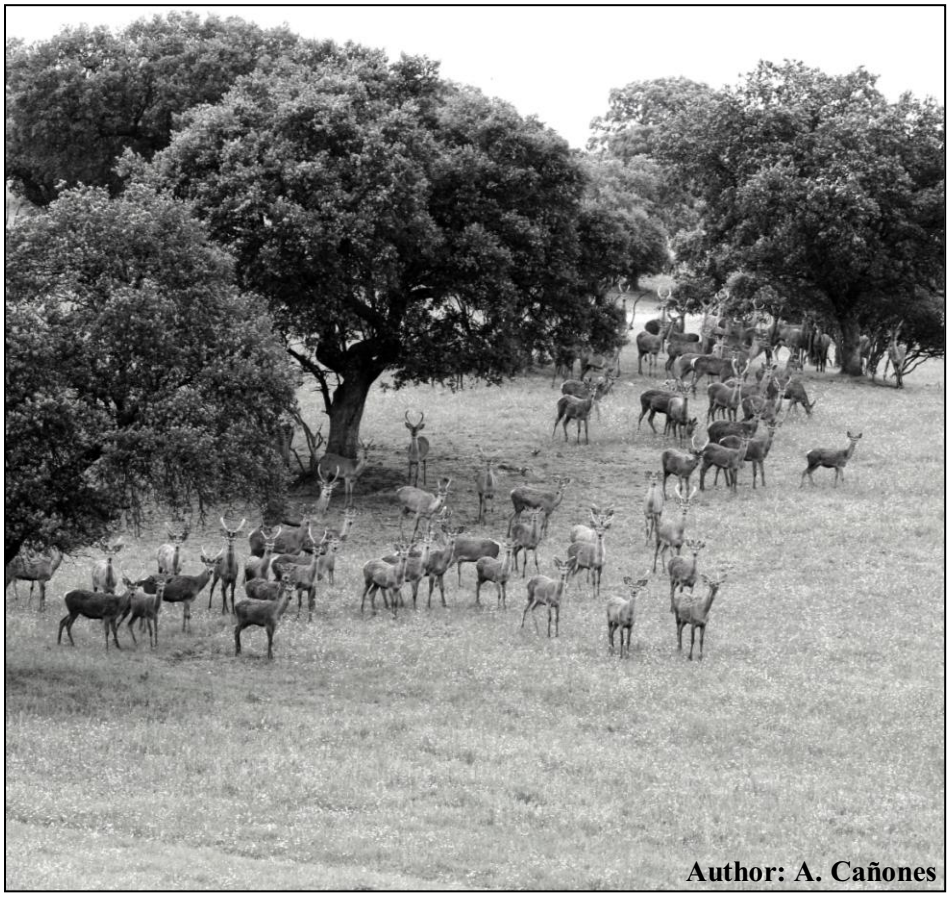

2. Material and methods

2.1 Study area and material collection

The Iberian red deer inhabits almost all types of habitats in the Iberian Peninsula, from sea level to high mountain areas (Carranza 2004). However, the species has preference for transition areas, characterized by suffer daily and seasonal variations, such as forest clearings or grasslands, with production of herbaceous plants mainly consumed in winter and spring, and shrub species mainly consumed during summer and autumn (Carranza 2004). These are the characteristics of the studied area, which is focused in the Eastern part of Sierra Morena, located in the region of Andalusia (South of Spain), province of Jaen (Fig. 2.1). This area includes approximately 150 big game states and two Natural Parks (Despeñaperros and Sierra of Andújar). Sierra Morena is especially interesting from the conservation point of view since it is included in the Natura 2000 Network. The typical Mediterranean climate of the area, is characterised by an irregular distribution of rainfall throughout the year (Azorit et al. 2002c; Azorit et al. 2003).

The 217 antlers used to conduct this study, were collected from several big game states of Sierra Morena. Concretely, the material was harvested along three different hunting seasons (2007/08, 2009/10 and 2011/12), which last approximately four months, from October of one year to February of the next year. Accordingly, in some cases both the license and collaboration with the corresponding guards and farm keepers was necessary. Likewise, when the visit to the different big game states was not possible, the material measurement process was carried out by accessing taxidermy rooms. Therefore, all the antlers measured were

hunting trophies. In parallel, weather variables of interest for the research, as for example the winter rainfall and winter temperature of the study area or each hunting season, were extracted from different climatic stations surrounding the area studied (available at www.juntadeandalucia.es).

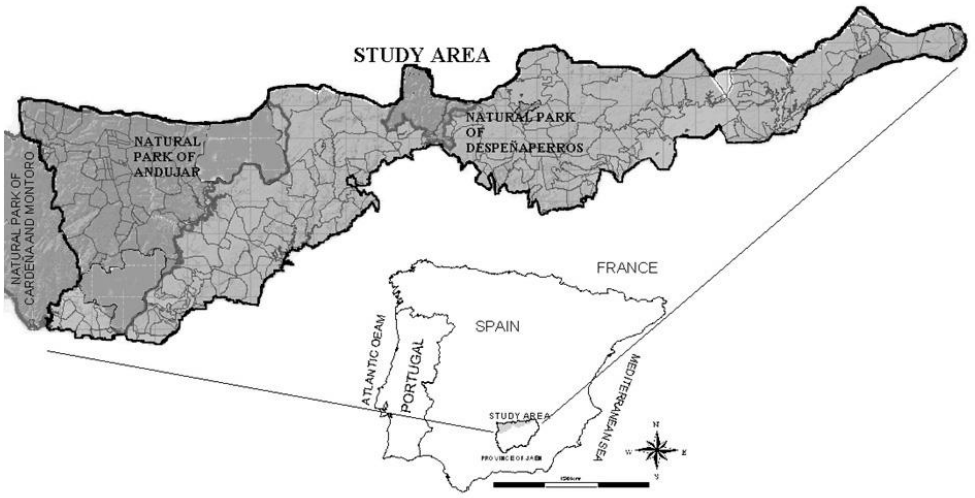

Figure 2.1. Study area. Map of Spain showing the location of Andalusia and Sierra Morena.

2.2 Age determination

The age has a significant influence over the antler development. For that reason, its determination for each one of the specimens of the sample was of great importance. Due to the fact that age identification methods based on animal dentition always have been the most reliable (Azorit 2011), the lower jaw of each individual measured was collected. The different mandibles were cleaned and cut between the two cusps of the first molar (M1), in order to count the cement layers deposited in, and were observed under a magnifying glass. The cement layers corresponded to growth and

rest marks of the cellular interadicular cementum of M1, which normally give place to wide bands of rapid growth (in spring-summer) and narrow bands, corresponding to periods of slow deposition of calcified material (in autumn-winter) (Azorit et al. 2002d; Azorit 2011) (Fig. 2.2). However, the cause of the different bands formation is not exactly known. The count of narrow bands, or rest lines, for age determination in Iberian red deer is accepted, but we must to take into account that the first one appears at 6 months old (Azorit et al. 2004; Azorit 2011). From here, a new rest line appears each consecutive year. The reliability of the process is very high, representing a 75% of success if we consider an age determination error of half year (Azorit 2011).

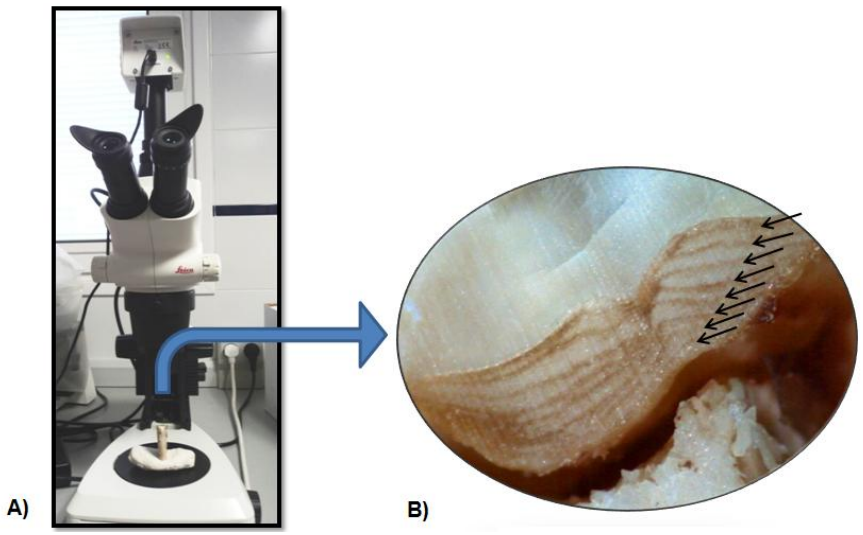

Figure 2.2. Age determination. A) Deer jawbone cut under a magnifying glass to count the cement layer deposition; B) Interadicular narrow strips or rest lines, observed at first molar level.

Depending on the age established to each specimen, they were grouped into different age classes (from 1 to 6). The age class 1 included individuals from 2 (since it is the minimum legal age to hunt a deer) to 3 years old; age class 2 included individuals from 4 to 5 years old; and so, up to the age class 6, with individuals from 12 to 13 years old. The grouping of the specimens into age classes, facilitated the study of the changes suffered by the sampled antlers along different developmental stages.

2.3 Data obtaining and treatment

2.3.1 *Landmarks and semilandmarks*

To study the antler shape change through geometric morphometrics methods, it was necessary the use of configurations of landmarks, defined as homologous points found in geometric locations corresponding to the position of the same particular traits in all the structures of the sample (Bookstein 1991; Van der Molen et al. 2007; Baab et al. 2012). In this case, the landmarks were specified by three Cartesian coordinates (*x*-, *y*- and *z*-) (Baab et al. 2012), since the present study has been defined in a three-dimensional space. However, it is also possible to work in a two-dimensional space (Bookstein 1991). Besides the use of landmarks, sometimes it was also necessary the use of semilandmarks, defined as anatomical points positioned along the curves or surfaces of the structures (Baab et al. 2012), which are located between two true landmarks (Van der Molen et al. 2007). The semilandmarks were not considered true landmarks due to its arbitrary placement. For that reason, it was necessary the application of algorithms to correct their position across the sample before to start to work with them (Baab et al. 2012). Thus, the landmark

and semilandmark data help to preserve the spatial relationships among the dimensions used, providing us individual landmark configurations for each one of the sampled specimens (Baab et al. 2012).

2.3.2 *Antler landmark definition*

The landmark definition on the Iberian red deer antlers was specially complicated since there was no previous reference about geometric morphometrics studies on them. Therefore, no previous pattern of landmarks defined on antlers existed. For that reason, the observation of as many possible different antlers was necessary in order to try to determine the position of those most suitable landmarks and semilandmarks. The highest problem was the fact that we wanted to compare antler shapes corresponding to specimens of different ages, which meant different developmental stages of the same structure and above all, a different number of tines. It represented one of the main challenges of the study.

Thus, the landmark and semilandmark digitalization was performed following the theory proposed by Oxnard and O'Higgins (2009), so that the occurrence or not-occurrence of the different antler tines was considered as potentially developable structures along the different antler casts. Hence, these potential structures were digitized in those individuals where they were present, as they were duplicated in those that did not had these tines without incurring a bias when analyzing the data (Oxnard and O'Higgins 2009). Taking into account this, a total of 115 landmarks were digitized on each one of the sampled antlers (Fig. 2.3).

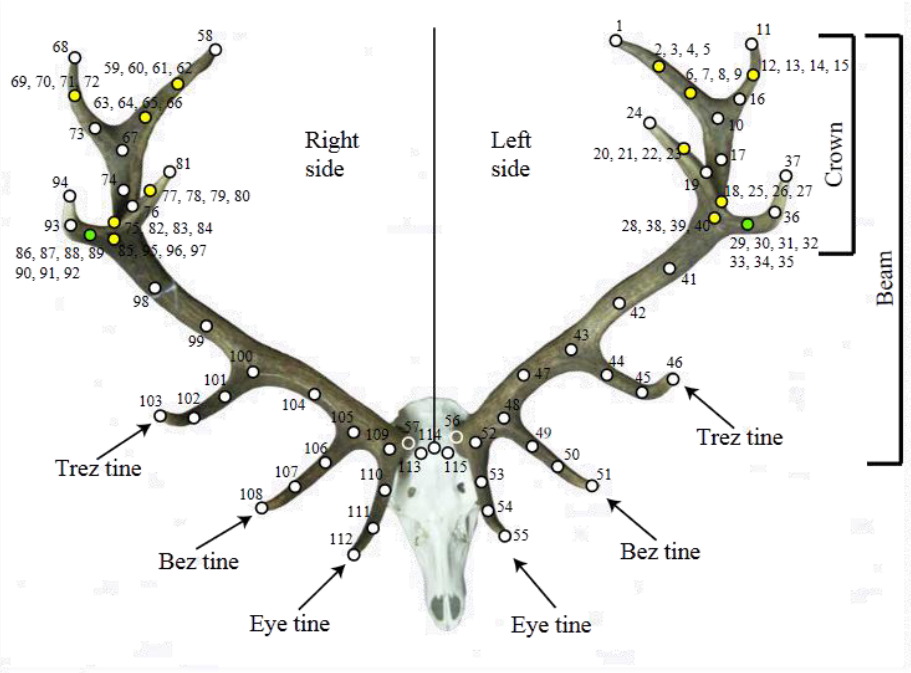

Figure 2.3. Total of landmarks registered on each one of the antlers sampled. Top view. Landmarks 56 and 57, represented by transparent landmarks in the figure, are not in the antler surface but located under the burr base. Yellow landmarks are duplicated four times and green landmarks seven times due to the potential occurrence of tines in those antler positions during development.

2.3.3 *Centroid size and allometry*

In GM we use the term shape and not form, since the last one usually includes both, shape and size of the object study (Van der Molen et al. 2007). The necessity to erase the scale before any shape analysis implies the separation of shape and size (Zelditch et al. 2004), which allowed us to study the shape change of Iberian red deer antlers with different sizes and belonging to different ages (from 2 to 13 years old). However, size and shape are not statistically independent. They are associated through

the allometry, which is principally defined as the influence of size on shape (Mosimann 1970; Klingenberg 2009). The allometry, normally exert influence over all the parts of the organisms (Klingenberg 2013). For that reason, the allometric effect was tested in each one of the studies developed in this thesis, by performing the corresponding multivariate regression of shape on size (Monteiro 1999; Drake and Klingenberg 2008a; Klingenberg 2009; Klingenberg 2013). The estimator of size in GM is the Centroid size (CS) (Van der Molen et al. 2007; Baab et al. 2012), which is calculated as the square root of the sum of the squared distances of each landmark respect to the centre (Centroid) of the form (Bookstein 1991; Bookstein 1996; Zelditch et al. 2004), and is the one mathematically independent of shape (Zelditch et al. 2004) (Fig. 2.4). Despite that, it is also possible to calculate the log-transformed Centroid size (log CS), especially useful when there are high size differences in the sample, and most of the shape variation occurs among the smaller specimens (Klingenberg 2013).

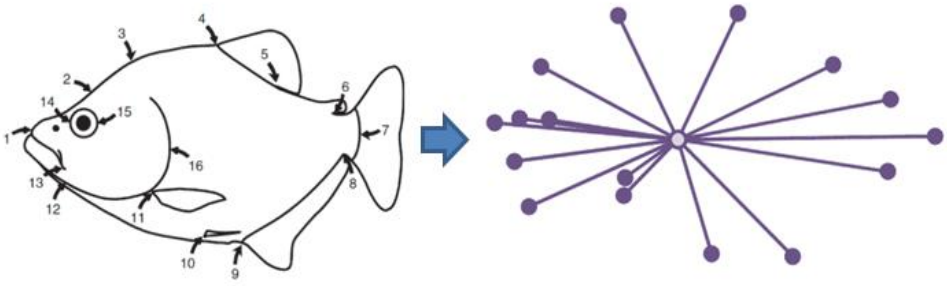

Figure 2.4. Centroid size visualization in a piranha's example. The central circle corresponds to the Centroid size of the piranha, while the lines connecting the Centroid to each one of the 16 landmarks represented are the distances used to calculate it. Images extracted from Zelditch et al. 2004.

2.3.4 *Procrustes Superimposition (GPA) or Procrustes fit*

In order to start to work with the collected and transformed coordinates of each antler, first of all we transformed the data, scaling, rotating and translating the different landmark configurations with respect the original configuration (Van der Molen et al. 2007). To do it, a Procrustes superimposition was performed (Dryden and Mardia 1998). The scaling process transformed the CS to the unit (1.0) by dividing each landmark coordinate by the CS. The translation process, shifted the CS to the coordinate (0,0,0) (or (0,0) in 2D) by averaging the *x*-, *y*- and *z*-coordinates of all the landmarks and subtracting them. Finally, the best fit between the landmark configurations, which corresponds to the minimum sum of squares between corresponding landmarks, was achieved through the rotation process (Rohlf and Slice 1990; Dryden and Mardia 1998). Then, it was possible to obtain a consensus configuration, id est., an average configuration of landmarks obtained from all the landmark) configurations of the sample (Corti and Crosetti 1996; Zelditch et al. 2004) (Fig. 2.5), as well as the principal warps (PrW) which allowed to describe the relative movements of the consensus landmark configurations in the *x*-, *y*- and *z*- planes (Van der Molen et al. 2007). In addition, every PrW had associated a partial warp (PW), defined as combinations of the PrW on the different coordinate axis, which facilitated the interpretation of the principal warps and were used for further analysis (Van der Molen et al. 2007).

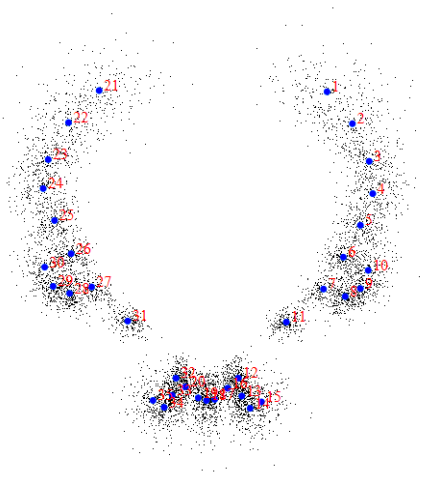

Figure2.5. Procrustes superimposition visualization over the antler sample used in the first study of this thesis. The small black points, which correspond to each one of the landmarks digitized for each antler, show the best fit between all the landmark configurations of the sample. The blue points represent the average landmark configuration from all the original configurations of landmarks aligned.

2.3.5 *Multivariate statistics*

After the GPA and the obtaining of the partial warps, we extracted a covariance matrix of the variables under study, and applied multivariate statistics such as Principal component analysis (PCA). The PCA produced a new set of shape variables, called Principal components (PCs) or relative warps (RW) (Van der Molen et al. 2007). The PCs were useful to observe easily patterns of shape variation in the whole dataset (Klingenberg and Zaklan 2000), providing the maximal amount of uncorrelated information from complex multidimensional data (Zelditch et al. 2004) by reducing its dimensionality (Klingenberg et al. 2001). The first PCs generally accounted for most of the shape variability among specimens (Klingenberg et al. 2003). However, we could also capture differences among groups, if present, through the use of Canonical variates analysis (CVA), or discriminate only between pairs of groups by using a Discriminant function analysis (DFA) (Zelditch et al. 2004). Otherwise, we could use one-way analyses of variance (ANOVA) in order to test

possible mean differences between groups of specimens, very useful when we had one trait and more than two groups (Zelditch et al. 2004). Subsequently, in this case we tested whether the antlers from several age classes could be considered morphologically different between them; so that they could be classified correctly within each age group. However, if we wanted to compare a complex trait as shape with different categorical variables, a multivariate analysis of variance (MANOVA) was recommended. It was useful to test for shape differences between the specimens collected in different capture years (Zelditch et al. 2004).

2.3.6 *Symmetry and asymmetry*

In geometric morphometrics, the different parts of an organism can show one of the two possible types of symmetry, Object symmetry or Matching symmetry (Klingenberg et al. 2002). In our case the red deer antler, generally considered as a symmetrical bilateral trait (Mateos et al. 2008) shows Matching symmetry, id est., there are two separate copies on each body side or plane of symmetry, which can be considered as mirror images of one another in the same way that fly wings (Klingenberg et al. 2002) (Fig. 2.6).

In contrast, structures with Object symmetry have internal symmetry, which imply the presence of a symmetry axis located in the mid body plane, as for example the head of vertebrates (Klingenberg et al. 2002) (Fig. 2.6). Deviations from perfect symmetry occur especially due to genetic or environmental factors (Parsons 1992; Ditchkoff and DeFreese 2010), generating certain asymmetry between the left and right sides of the structures (Fig. 2.7).

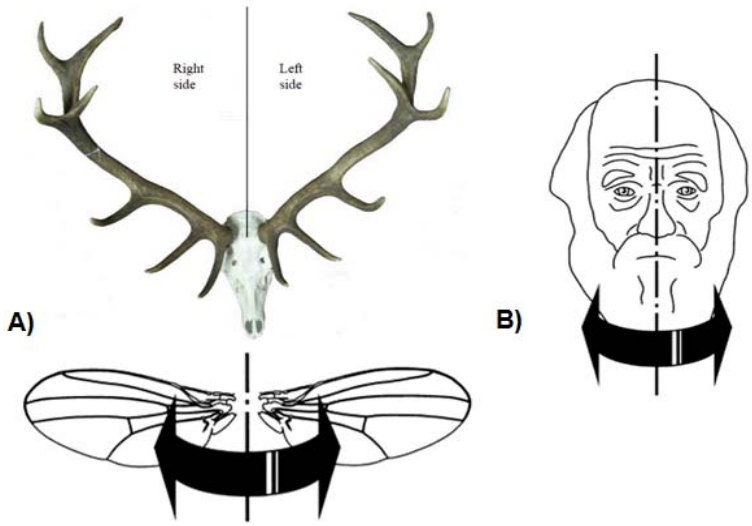

Figure 2.6. Matching symmetry and object symmetry. A) the Iberian red deer antler as well as the fly wings show matching symmetry, since both structures are present in two separate copies on the left and right body sides as if they were mirror images; B) the vertebrate head shows object symmetry, since all the structure is crossed by the mid body plane becoming symmetrical by itself. Fly wings and vertebrate head images extracted from Klingenberg et al. 2002.

In this sense, we can talk about the two principal types of asymmetry considered, Fluctuating asymmetry (FA) and Directional asymmetry (DA) (Van Valen 1962; Leamy 1984; Palmer 1994). Thus, the FA would be related to random changes on the left and right antler sides, principally associated to environmental changes (Palmer 1994; Mateos et al. 2008). Furthermore, FA is characterized for being used as a measure of developmental instability (Klingenberg and McIntyre 1998). However, DA represents internal and external conspicuous asymmetries of the structures (Palmer 2004), which are characterized for being consistent across the sampled specimens causing further development of one side

than the other side (Palmer 1994). In order to quantify the FA or DA levels in Iberian red deer antlers subjected to geometric morphometrics analyses, the differences between the original settings of landmarks and their corresponding mirror images were computed. It normally occurred through a two-way ANOVA, for linear measurements (Palmer and Strobeck 1986; Palmer 1994), but in our case a Procrustes ANOVA was used, since it was adequated for shape data (Klingenberg and McIntyre 1998; Klingenberg et al. 2002). The Procrustes ANOVA was characterized for providing a range of different effects such as the FA, which would be represented by the variability in the differences between the left and right antler sides among specimens; the DA represented by the average difference between antler sides; the individual effect, represented by differences among specimens; and the measurement error, which allowed us to discern whether the asymmetries observed were real or due to inherent errors during the measurement process (Klingenberg et al. 2002) (Fig. 2.7).

Figure 2.7. Some examples of the asymmetries observed between the left and right sides of Iberian red deer antlers.

2.3.7 *Integration and modularity*

As Klingenberg (2008a) said "integration and modularity are two closely related concepts". Generally, the organisms are composed of different parts resulting from the interaction of developmental, genetic, functional and evolutionary processes (Klingenberg 2008a). This fact could imply the existence of relatively independent modules along the structures, as for example the Iberian red deer antler and its tines, which were characterized by a minimal correlation between them (Klingenberg 2008a) (Fig. 2.8). Despite that, the possible modules always have certain degree of integration between them (Klingenberg 2008a and 2009). Thus, in order to identify the presence of hypothetic modules (sets of landmarks) along the antlers, and quantify the integration and modularity levels among them, there were some analytical methods based in geometric morphometrics.

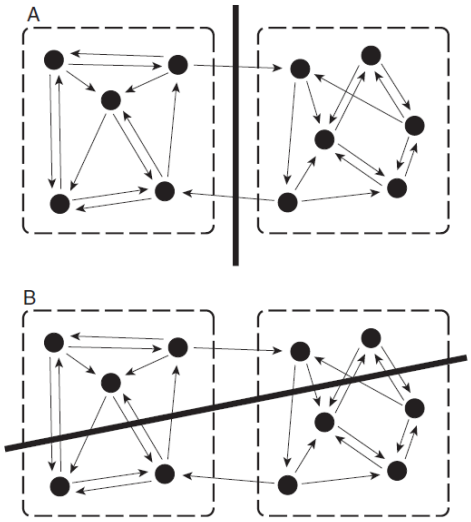

Figure 2.8. Detecting modularity presence. The dashed lines represent two hypothetic modules, internally integrated (arrows). The black lines show two different partitions. A) the line coincides with the limit between modules suggesting the relatively independence from each other; B) the partition goes across many intersections of the modules, so that strong covariation would be expected between subsets. Scheme extracted from Klingenberg 2009.

However, before that, to test for the presence of allometry (Monteiro 1999; Klingenberg 2009) was necessary, since it is well known its effect over the integration and modularity levels (Klingenberg 2009). Accordingly, the residuals generated through the allometry correction regression were used for further analyses (Klingenberg 2009). The different modularity hypotheses proposed were tested by comparing alternative antler partitions and obtaining the RV coefficient, which indicates the degree of association between modules (Escoufier 1973). Then, in order to observe and study the covariation between the subsets defined, a Partial-Least-Squares (PLS) was performed (Klingenberg and Zaklan 2000; Rohlf and Corti 2000; Bookstein et al. 2003). Since the PLS analyses could use two different criteria in terms of Procrustes superimposition (Klingenberg 2009), the first step was to decide which approach was going to be used. If the principal idea was to consider that the structure under study behaved like a whole, we would expect a simultaneous variation of all the parts. Therefore, all the landmarks were subjected to a single Procrustes fit by a PLS within configuration, independently of the modules proposed (Klingenberg 2009). In contrast, if the sets of landmarks proposed would have been considered as different units, a separate Procrustes fit for each module would have been more appropriate (Klingenberg 2009) and therefore, a Two-Block Partial Least Squares (2-B PLS) would have been used. We focused on the first approach and the use of a PLS based on a single Procrustes fit.

2.3.8 *Digitalization methods*

In traditional morphometry, the most commonly measuring systems used were callipers and tapes (Elewa 2010), since they were cheap and easy to handle and transport. However, the process of data collection for geometric morphometrics studies can be accomplished through various methods as for example, CT scans, digitizers or digital photographs (Van der Molen et al. 2007). The use of digital images (photographs), is a fast and low-cost method but it is necessary that all the images are oriented in the same way (Van der Molen et al. 2007). The digital images does not allow to work directly in a three-dimensional space, but the 2D information extracted from them can be transformed in 3D coordinates through the use of mathematical transformations (Elewa 2010). Another inexpensive option to work in two dimensions, would be the use of flatbed scanners whose disadvantage is that they are only effective with fairly flat objects as for example, dragon-fly wings (Sadeghi et al. 2009). In parallel, there are different devices adapted to work in 3D as for example, digitizing arms (e.g. the MicroScribe G2X used in this study, characterized for having 50" of sphere and 0.009" (0.23 mm) of accuracy (Fig. 2.9)) (Van der Molen et al. 2007).

Figure 2.9. MicroScribe digitizer G2X

Digitizers, are characterized for being portable and for having a stylus at one end (Baab et al. 2012), allowing a rapid data collection directly transferred to a computer to be analyzed. The drawback is that during the measurement process the study object must be immobilized (Van der Molen et al. 2007). A powerful alternative is the use of computed tomography (CT scans) (Van der Molen et al. 2007; Elewa 2010). This technology consists in scanning thin object slices by using X-ray or magnetic resonance (Elewa 2010), in order to register both the surface and volume of the objects (Spoor et al. 2000). Thus, this method would provide a large amount of information, but it is also the most expensive (Van der Molen et al. 2007).

2.4 Tools for the application of the PhIMM

The Photogrammetric Interactive Measure Method (PhIMM) comprises the use of two types of tools. On one hand, the photogrammetric part of the process requires to take two digital photographs from different perspective by antler studied. Each photograph must include a metric reference, in this case represented by a flat, rectangular piece of 50x50 cm to obtain common benchmarks in the different antlers used. Some basis are the same for both methods, GMM and PhIMM, since a series of homologous points have to be defined over the studied structure. In this case, the photographs were obtained through two handheld PowerShot SX210 IS digital cameras, with a resolution of 4320x3240 pixels. On the other hand, for the photo processing a software based on Computer Aided-design technology (CAD-3D) called SolidWorks (from Dassault systems) was used. This software allows us to make a virtual recreation of the space in which objects are photographed modelling them three-dimensionally.

Furthermore, it would be possible to extract valuable information about the objects studied, not necessarily collected in the field, such as lengths or perimeters. In parallel, all the obtained data can be easily transferred to an Excel template file, being available for an easy use with other software.

3. Geometric morphometric analysis of antler development in Iberian red deer (*Cervus elaphus hispanicus*)

3.1 Abstract

This study describes and quantifies antler shape variation in Iberian red deer (*Cervus elaphus hispanicus*) from Sierra Morena (Spain) to both characterize age related changes and identify optimum trophy age. 35 landmarks were recorded using a MicroScribe 3D digitizer on 209 red deer antlers. Through geometric morphometrics analyses overall antler shape variation was explored and morphological variations of the common parts of antler trophies (beams, trez tines and eye tines) were localised. The degree of covariance with antler shape of several environmental and developmental factors (age, capture year, presence of bez tines, total tines, and crown tines) and antler size was also assessed.

The shape analyses indicated that, in young individuals (2 to 3 years), antlers are relatively more elongated near the skull and their beams are closer distally, while the antlers of fully-grown individuals (6 to 9 years) are relatively shorter near the skull and more arched distally. Shape variations linked to age were also identified in specific tines: trez and eye tines were straighter and more vertically oriented in the youngest individuals, becoming longer and more curved in older individuals. A PCA allowed us to observe that the shape changes associated to the first three PCs described how the antler progressively transforms to accommodate an increasing number of tines during a deer's life history, both elongating and separating the beams, but also reorienting its trez tines, eye tines and crown. The main factors associated with red deer antler size and shape differences were presence of bez tines, age, total number of tines and number of crown tines, although environmental effects (capture year) were also significant. Each antler was assigned a

trophy quality score (TQS) based on different measurements commonly used in hunting protocols. Then, a multivariate regression of shape on TQS was carried out to visualize the associated shape variation. Trophy quality (TQS) improved between age classes 2 and 4 (4 to 9 years), with some deterioration in quality in age classes 5 and 6 (10 to 13 years). These findings have implications for the management and conservation of Iberian red deer in Sierra Morena.

3.2 Introduction and objectives

Hunting is a popular practice in the south of Spain, and as such, a high economic interest has aroused in the exploitation of hunting in that area (García et al. 2010). In eastern Sierra Morena (Jaén, Spain), where the study area of this work is centered, the main big game species is the Iberian red deer (*Cervus elaphus hispanicus*), whose biology has been thoroughly studied, often in relation with its hunting importance (Carranza 1999; Azorit et al. 2002a; Azorit et al. 2002b; Fierro et al. 2002; Azorit et al. 2003; Gaspar-López et al. 2007; López-Parra et al. 2009; García et al. 2010; Garde et al. 2010). For that reason, there is a growing interest in optimizing the quality of red deer antlers. Both antler size and symmetry between branches are especially important criteria to assess antler quality (Azorit et al. 2002a; Azorit et al. 2002b; Gaspar-López et al. 2007).

The red deer antler is a complex bony structure (García et al. 2010; Santiago-Moreno et al. 2010), which has a general pattern of development consisting in the growth of several tines along a principal axis called beam, usually in the same order: eye tines, bez tines (not always present), trez tines, and crowns (Montoya 1999; Azorit et al. 2002a; Fierro et al.

2002; García et al. 2010). In order to facilitate the description of the different parts of the antler, in this work we will use the term beam to describe only the part of the main axis ranging from the base of the antler to the crown base (Fig. 3.1), and not to the end of the principal tip in the crown, as classically defined (Mateos et al. 2008).

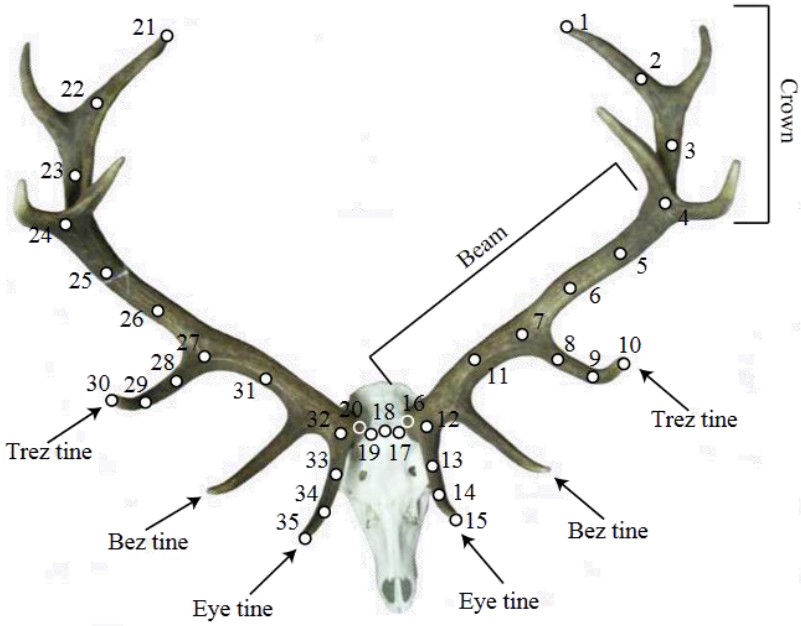

Figure 3.1. Landmarks measured on each antler. Top view. Landmarks 16 and 20, represented by empty circles, are located under the burr base and thus cannot be directly shown on the figure.

Generally, as deers grow in size, there is an increase in the number of antler tines, especially at the crown (Carranza 1999; Azorit et al. 2002a). This pattern of antler development carries on beyond two thirds of their life span, until 8-11 years of age according to most authors (Montoya 1999; Azorit et al. 2002a; Carranza 2004; but see Nahlik 1992; around 11-12 years old). From that age decay starts and antler size and tine number

begin to regress (Marcos 1989; De los Reyes 1990; Carranza 1999; Azorit et al. 2002a; Carranza 2004; García et al. 2010), to the point that it is possible to find old individuals whose antlers consist only of the beams, like the youngest deers (Marcos 1989; De los Reyes 1990; García et al. 2010). Thus, the number of tines is not a reliable indicator of an individuals' age (García et al. 2010), being teeth the best age indicator (Klein et al. 1981; Azorit et al. 2002c; Azorit et al. 2002d; Azorit et al. 2002e; Azorit et al. 2002f).

Previous studies have shown that antler shape variation is related with several factors, such as age (Azorit 2002a) and environmental parameters (e.g. the rainfall throughout the year, higher population densities and especially food availability; Carranza 1999; Azorit et al. 2002a; García et al. 2010). Sierra Morena (Fig. 3.2), the study area of the present work, shows a typical Mediterranean climate, with dry and hot summers and cold and rainy winters (Azorit et al., 2003; Torres-Porras et al. 2009a).

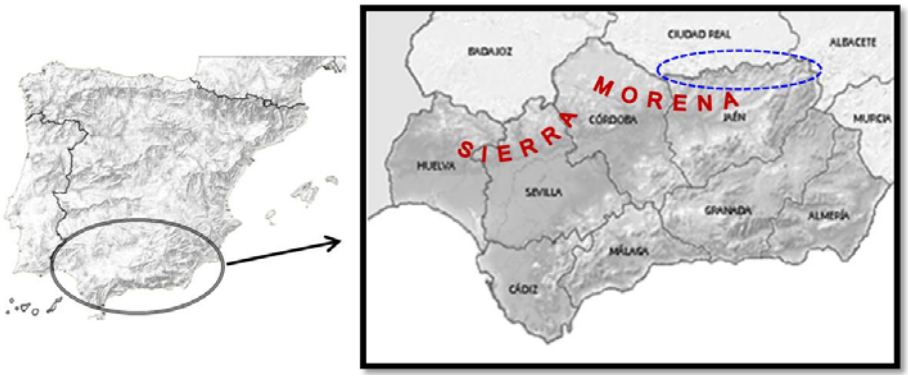

Figure 3.2. Study area. Map of Spain showing the location of Andalusia and Sierra Morena. The blue ellipse represents the study area: Eastern Sierra Morena, in the province of Jaén.

However, climate irregularities are common, especially regarding rainfall, since some years there is high precipitation and others are marked by long periods of drought. It has been shown that harsh winters can result in low quality trophies, probably related to changes in antler mineralization (Landete-Castillejos et al. 2010). Furthermore, soil moisture, which is related to winter rainfall, is one of the main factors determining food quality and availability during the spring (Carranza, 1999), season in which antlers develop. Thus it has been considered one of the principal traits to determine trophy quality (Chapman 1975; Carranza, 1999; García et al. 2010). With this in mind, capture year was used as a proxy for the environmental conditions leading up to the sampled antlers growth (Azorit et al. 2002a). For each year, rainfall and temperature data corresponding to the winter previous to the spring, when the sampled antlers grew up, were collected and averaged.

The morphological variability of red deer antler is enormous, both in size and shape. For that reason, the aims of this study are, on the one hand, to describe and quantify the main morphological variations of the common parts of antler trophies (beams, trez tines, and eye tines), and on the other hand, to try to determine an optimum trophy age. If a specific age class providing the best antler trophies could be found in our sample, it would be of special interest from the point of view of the Iberian red deer management in Sierra Morena. Moreover, determining trophy quality through antler shape could help in the indirect knowledge of the quality of individuals or their environmental situation, which also provides insightful information for the management of big game estates. Finally, it is worth noting that this methodology is non-invasive and, as such, it does not cause any damage to the antlers as prized hunted trophies.

3.3 Material and methods

To describe and quantify antler shape variation, we used 3D geometric morphometric methods. This methodology constitutes a powerful and precise tool for the quantification of the shape variation and morphological transformations observed on a structure, allowing us to combine it with statistical analyses (Adams et al. 2002). The degree of covariance with antler size and shape of several environmental and developmental factors (age, winter rainfall, presence of bez tines, capture year, crown tines and total number of tines) was also assessed, since all of them can influence the final quality of trophies (Carranza 1999; Azorit et al. 2002a; García et al. 2010).

The sample studied consisted of 209 red deer antlers, still attached to the animal's skull, from several big game estates in eastern Sierra Morena (Jaén, Spain) (Fig. 3.2) during the 2007/08, 2009/10 and 2011/12 hunting seasons. The antlers were harvested between October and February, the hunting season's duration (Azorit et al. 2002a), and came from a hunting practice called *Montería*, the most common and widely hunting technique used in Spain (for more details see Torres-Porras et al. 2009b). Furthermore, this hunting technique has been considered the less biased method when working with data about hunted animals (Martínez et al. 2005; Torres-Porras et al. 2009b).

Geometric morphometrics are landmark-based methods, which allow analyzing the shape of the object study exclusively, that is, the geometric information left after removing translation, rotation and scale effects (Rohlf and Slice, 1990; Bookstein 1991; Dryden and Mardia 1998; Kerschbaumer and Sturmbauer 2011). Thus, for each specimen, we

digitized the 3D coordinates of 35 landmarks and semilandmarks (hereafter landmark configuration) using an Immersion MicroScribe G2X digitizer (Solution Technologies, Inc., Oella, MD, USA) (Fig. 3.1 and Table 3.1).

Table 1. Landmark definitions.

Landmark	Definition
1	Tip of the left beam
2 – 6	Semilandmarks along the upper part of the left beam
7	Left trez tine base
8, 9	Semilandmarks along the edge of the left trez tine
10	Tip of the left trez tine
11	Semilandmark between the left trez tine base and the left eye tine base
12	Left eye tine base
13, 14	Semilandmarks along the edge of the left eye tine
15	Tip of the left eye tine
16	Left burr base
17	Left midpoint of the coronal suture
18	Intersection between the coronal and sagittal sutures
21	Tip of the right beam
22 – 26	Semilandmarks along the upper part of the right beam
27	Right trez tine base
28, 29	Semilandmarks along the edge of the right trez tine
30	Tip of the right trez tine
31	Semilandmark between the right trez tine base and the right eye tine base
32	Right eye tine base
33, 34	Semilandmarks along the edge of the right eye tine
35	Tip of the right eye tine
20	Right burr base
19	Right midpoint of the coronal suture

Landmarks (LM) are anatomically corresponding points to each antler, while semilandmarks are points constructed between two traditional landmarks which allow the accurate description of lines and curves on the structure (Van der Molen et al. 2007; Gómez-Robles et al. 2007). However, it was necessary to transform these semilandmarks into proper landmarks before carrying out any analysis. This transformation implied true homology (Kerschbaumer and Sturmbauer 2011), and in the present study it was performed through the program Resample (Raaum 2006), which recalculated distances between target semilandmarks localized between two true landmarks. Once semilandmarks had been transformed, a Procrustes superimposition (GPA) on the original configurations of landmarks (Dryden and Mardia 1998) was carried out to minimize the sum of the squared distances between homologous points. It resulted in a consensus configuration or mean shape, and a set of shape variables (principal warps) that showed the specific variation for each landmark from the original configuration to the consensus configuration (Van der Molen et al. 2007), and which were subdivided into partial warps (PW), projections of the principal warps on the x, y and z axes, to describe the shape change more accurately (Bookstein 1989). Then, a principal component analysis (PCA) was performed to reduce the dimensionality of the data, obtaining a lower number of variables, which provided as much information as possible with no repetition (Terrádez-Gurrea 2002; Van der Molen et al. 2007). These new variables were called relative warps (RW) or principal components (PC) (Frieß 2003; Gómez-Robles et al. 2007) and always appear ordered according to decreasing percentage of information explained.

We also tested whether size had a significant effect on antler shape variation. In order to do that, we carried out a multivariate regression of the shape variables (PCs) on antler size, represented by the centroid size (CS), defined as the square root of the sum of the squared distances of all landmarks from the centroid of the structure (Bookstein 1996), and the log-transformed centroid size (log CS), of each landmark configuration. To quantify the relationship between antler shape and factors like age class, environmental factors (capture year), presence of bez tines, number of crown tines, and total number of tines, we also performed multivariate regressions of shape on each factor.

The factors related to tine development (presence of bez tines, number of crown tines and total number of tines) were derived from each specimen in the sample. Depending of the hunters, antlers with no bez tines were considered poor quality trophies (Fierro et al. 2002). For that reason, the presence or absence of bez tines sometimes has been considered somewhat subjective. The capture year of each Iberian red deer was registered, as well as climatic parameters relative to that year, namely: the winter rainfall (from December of the previous year to March of the capture year; following the statements of Carranza 1999 and the work of Landete-Castillejos et al. 2010), and the mean winter temperature. The climatic parameters were obtained through different weather stations located close to the study area (Junta de Andalucía 2012).

As age is a known determinant of Iberian red deer antler shape (Huxley 1931; Lincoln 1992; Azorit et al. 2002a; Fierro et al. 2002), we needed to accurately determine the age of each specimen. Since the teeth are the best part of the animal anatomy to do that (Klein et al. 1981), the lower jaw of each specimen was collected and cleaned. Afterwards, age was

determined studying the cementum layer deposition of the lower first molar (M1), the first permanent tooth to grow, since it has been shown to produce the most accurate age estimations (Azorit et al. 2002c; Chritz et al. 2009). To count the cementum layers, it was necessary to cut M1 transversely between its two cusps. For what a circular saw DIMAS TS 2301 with a RUBI disc 30966 of 200 mm diameter and a thickness of 1.5 mm was used. Then, the cementum layers were observed under a magnifying glass (8 increases). Despite it is the most reliable method established for age determination it is possible to underestimate the age in some oldest deer because of compaction of the firsts cement layers formed (Azorit, 2004, 2011).

Counting cementum layers we classified each individual into one of six age classes (1 to 6), being the age class 1 formed by individuals from 2 to 3 years old, the age class 2 from 4 to 5 years old, and successively until age class 6, which is formed by individuals from 12 to 13 years old. However, it is important to note that with this method it is assumed that probably some of the oldest deer can be older than estimated.

In order to determine an optimum trophy age, it was necessary to establish our own categorization of the measured trophies, since the official scoring protocols use a set of distances, diameters, tine counts and arbitrary descriptors not suited to landmark data. Thus, we created an index to categorize trophy quality using different size-related measures based in some variables used by the Junta Nacional de Homologacion de Trofeos de Caza (2010). All distances used in this index were obtained from the landmarks previously digitized for each specimen. We called the index Total Quality Score (TQS), which was calculated as follows:

$$TQS = \frac{L_{beam}}{2} + \frac{L_{eye} + L_{trez}}{4} + W,$$

were L_{beam} was the average length of the beams (in cm), L_{eye} was the average length of the eye tines (in cm), L_{trez} was the average length of the trez tines (in cm), and W was the maximum separation between the left and right antler branches (S) relative to average beam length (L_{beam}). After calculating its corresponding S/L_{beam} ratio, each specimen was assigned a W score from 0 to 3 as follows: 0 if $S/L_{beam} < 0.60$; 1 if $0.60 \leq S/L_{beam} < 0.70$; 2 if $0.70 \leq S/L_{beam} < 0.80$; and 3 if $S/L_{beam} \geq 0.80$. Then, to simplify TQS interpretation, TQS scores between 71 and 80 were considered to be a very good trophy (VG), 61 to 70 a good trophy (G), 51 to 60 a medium trophy (M), 41 to 50 a poor trophy (P), 31 to 40 a bad trophy (B), and 30 or less to be a very bad trophy (VB).

All geometric morphometric analyses were performed using the MorphoJ software package (Klingenberg 2008b; Klingenberg 2011).

3.4 Results

The first six principal components (PCs) of the PCA accounted for 68.53% of the total shape variation observed in Iberian red deer antlers (Table 3.2; Fig. 3.3). The first principal component (PC1) explained 28.10% of the observed shape variation (Table 3.2, Fig. 3.4-PC1), and its extreme positive values were characterized by antlers relatively more elongated near the skull and presenting beams (LM 4, 5, 6, 7, 11, 12/ LM 24, 25, 26, 27, 31, 32) drawn closer with respect to the consensus configuration.

Table 3.2. Percentage of shape variation associated to the first six principal components (PCs) of the PCA.

PC	Eigenvalues	%Variance	%Accumulated	PC	Eigenvalues	%Variance	%Accumulated
1	0.006651557	28.097	28.097	4	0.0016606	7.015	59.003
2	0.00373937	15.796	43.893	5	0.00124307	5.251	64.254
3	0.00191645	8.095	51.988	6	0.00101107	4.271	68.525

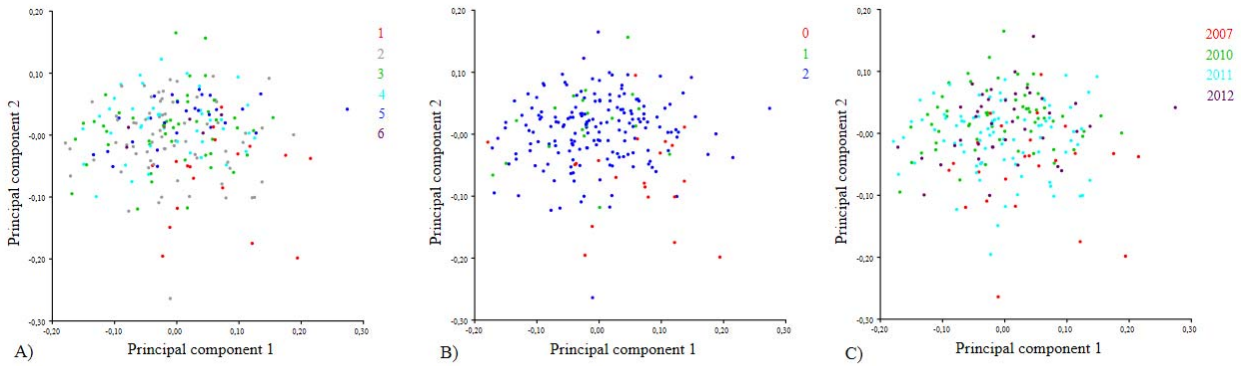

Figure 3.3. PC1 vs PC2 coloured by different study variables. A) coloured by age class; B) coloured by number of bez tines; C) coloured by capture year.

The crowns (LM 1-4 / LM 21-24) drew a more obtuse angle with the beams, almost closing the antler contour, and were cranially oriented, while the trez tines (LM 7-10 / LM 27-30) and eye tines (LM 12-15 / LM 32-35) were straighter and more upwardly oriented (Fig. 3.4-PC1b, c). On the other hand, the extreme negative values of PC1 were characterized by antlers relatively shorter near the skull and with more distant beams (Fig. 3.4-PC1). The trez tines were slightly more curved and the eye tines were directed downwards with respect to the mean configuration (Fig. 3.4-PC1b). Finally, the crown was bent caudally, drawing a smooth curve (Fig.3. 4-PC1c).PC2 explained 15.79% of shape variation (Table 3.2, Fig. 3.4-PC2). Here, the extreme positive values were characterized by antlers having a relatively shorter and inwardly curved proximal part of the beam (from eye tine to trez tine; LM 7, 11, 12 / LM 27, 31, 32) and a longer and more arched distal part of the beam (from trez tine to the crown; LM 4-7 / LM 24-27). Furthermore, the crowns were much longer and curved than in the mean configuration, giving a broader and more globular appearance to the distal antler. The trez tines were long and curved, while the eye tines were also longer and more frontally oriented. At extreme negative values of PC2 (Fig. 3.4-PC2) the antlers became a smoothed V-shape, with markedly shorter and straighter crowns, which drew an obtuse angle with the beam. The trez tines were shorter and directed upwards, forming a more acute angle with the beam. The eye tines were also shorter and more laterally oriented than in the consensus shape. PC3 explained 8.10% of shape variation (Table 3.2, Fig. 3.4-PC3). Antlers with extreme positive values of this PC were characterized by slightly narrower shapes with longer trez and eye tines. At extreme negative values, the antler shapes were slightly wider and with shorter and straighter trez and eye tines,

which in turn were more upwardly oriented than in the mean configuration. Furthermore, the crown pointed caudally at the positive end of PC3, and cranially at the negative end. PC4, which explained 7.02% of shape variation (Table 3.2, Fig. 3.4-PC4), showed curved beams and a marked angulation between the beam and the crown at its extreme positive values. The trez tines were shorter and homogeneously curved than in the consensus. At extreme negative values of PC4, the antlers became extremely V-shaped, showing almost straight beams and crowns, and presented long trez tines, which were curved at the base and straighter near the tip. The shape of the eye tines did not vary significantly in PC4. Explaining 5.25% of shape variation, PC5 showed antlers whose trez and eye tines were long and only slightly curved (Table 3.2, Fig. 3.4-PC5). From the negative end of the PC to the positive end, the trez tines oriented themselves progressively more frontally, while the eye tines went from a downwards position at the negative end to an almost horizontal position at the positive end. Finally, PC6 explained 4.27% of shape variation (Table 3.2, Fig. 3.4-PC6). The extreme positive values of this PC showed a cranially projected upper part of the antler and longer tines, especially the eye tines. At extreme negative values of PC6 antler shapes presented a caudally projected upper part and shorter tines. The most striking feature of this PC, however, were the asymmetric shape changes detected in crown tip orientation (Fig. 3.4-PC6a) and tine length and orientation (Fig. 3.4-PC6c). On a side note, in agreement with hunting protocols but contrary to Azorit et al. (2002b), the shape changes described in our study place the greater separation between the right and left beams at crown base level, which in turn coincides with the point of highest beam curvature.

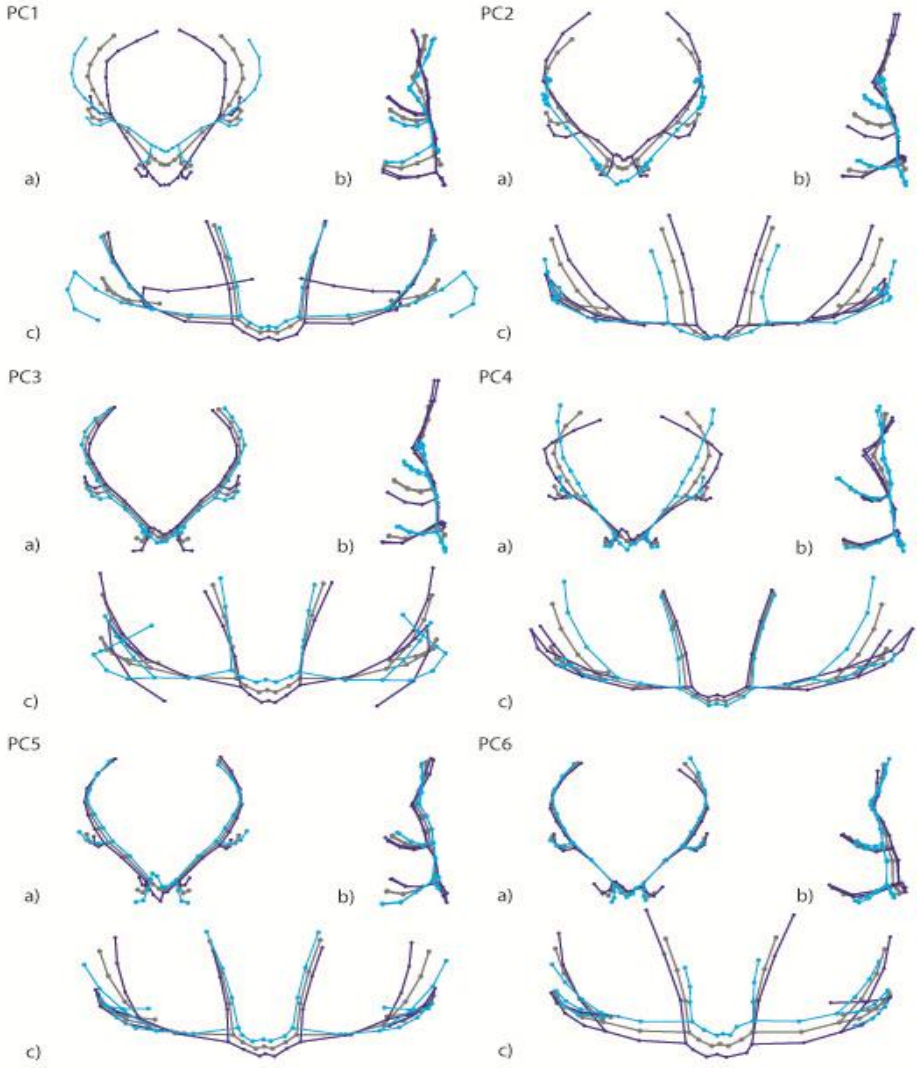

Figure 3.4. Shape changes associated to the first six principal components (PCs). a) Frontal view, b) lateral view, and c) ventral view. Dark blue configurations represent shape changes associated to extreme positive values; light blue configurations represent shape changes associated to extreme negative values; and grey configurations represent the consensus configuration.

Results of the multivariate regressions relating each factor to antler shape variation are shown in Table 3.3. The regressions of size on shape showed that the allometric effect on antler shape was highly significant. The allometric effect represents 8.85% of antler shape variation (P-value < 0.0001) when using CS, and 9.29% (P-value < 0.0001) if we use log CS (Fig. 3.5A and B). If we relate these results with the individuals' age class, we see that the youngest individuals generally have the smallest antlers and show the most different shapes, which could explain the different results of CS and log CS, since the latter magnifies changes at small sizes (Fig. 3.5A and B).

Table 3.3. Effect of the studied factors on antler shape variation. Abbreviations: %Pred., amount of antler shape variation explained by that particular factor; CS, Centroid size; log CS, log Centroid size; p-value, significance of the permutation test assessing factor effect on antler shape variation.

Factor	%Pred.	P-value
Size (CS)	8.85	<0.0001
Size (log CS)	9.29	<0.0001
Capture year	1.66	0.0019
Age class	2.65	0.0001
Presence of bez tines	3.09	<0.0001
Total number of tines	10.29	<0.0001
Number of crown tines	9.99	<0.0001
TQS	9.41	<0.0001

As it can be observed in Fig. 3.5D, the youngest individuals (age classes 1 and 2; 2 to 5 years old) seemed to present higher PC1 values, which corresponded to antler shapes with beams more elongated near the skull and running closer together, and whose crowns almost touch distally. Furthermore, the trez and eye tines of young individuals were straighter

and more vertically oriented. On the other hand, the antlers of fully-grown individuals (age classes 2 to 4; 4 to 9 years old) apparently tended to present high PC2 values, which relates to beams shorter near the skull and considerably arched in the upper part, acquiring the characteristic cup-like contour of Iberian red deers (personal comment Azorit C.). The trez and eye tines of old individuals were longer and more curved than in younger individuals.

Regarding factors other than size, all of them had also a significant effect, although the amount of antler shape variability it explained ranged from 1.66% in capture year to 10.29% in total number of tines (Table 3.3). Overall, the factors related to antler development (total number of tines, number of crown tines, presence of bez tines, and age class) had a greater effect on antler shape variation (Table 3.3). On the other hand, the environmental proxy (capture year) had the smallest effect, contrary to what would be expected from the results of previous studies on the effect of food availability on antler growth (García et al. 2010).

Additionally, the effect of each studied factor on each individual PC was assessed separately using the same methodology (Table 3.4). The shape changes described for PC1 (see above; Fig. 3.4 PC1) were related to antler development, since a significant effect on this PC was detected for the number of crown tines, the total number of tines, the antler size, and marginally the presence of bez tines. In the case of PC2, all the factors tested were significant, especially the number of crown tines, the total number of tines, and antler size, as observed for PC1, but with an even higher magnitude (from about 30% to about 20% of shape variation). Age class and the presence of bez tines also were significant, but most surprisingly, this was the only PC for which a significant effect of the

environmental proxy (capture year) was detected. Again similarly to PC1, in PC3 a significant effect of the number of crown tines, the total number of tines, and in a lower magnitude the presence of bez tines and antler size, was detected. The shape changes described for PC4 (see above; Fig. 3.4 PC4) were related to size and age class. Similarly, the shape changes described for PC5 (see above; Fig. 3.4 PC5) were related mostly to size, but also to age class, the presence of bez tines, and the total number of tines. Finally, PC6 was only marginally related to the presence of bez tines (1.9% shape variation; $p= 0.0430$).

Finally, regarding the Trophy Quality Score (TQS), first, since it is constructed as a sum of linear measurements, it could also be considered a size variable, which would explain the similar results of the regressions on log CS and on TQS (Table 3.3; Fig. 3.5). Second, observing the mean antler shape associated to each TQS category (Fig. 3.5C), we can see that higher scores are related to more arched antlers and longer and more curved tines. Third, we could observe that, with increasing TQS scores, antler shape variation also increased, since the scatter around the regression of shape on TQS got progressively wider (Fig. 3.5C). Finally, we were not able to define an optimum trophy age based on the regression of antler shape variation on TQS, since the best trophies appeared between age classes 2 and 5 (i.e., between 4 and 9 years old; similarly to the observations of Carranza, 1999). That is, our sample includes such great variability of shape in each age class as to prevent the definition of an age with optimal trophy quality.

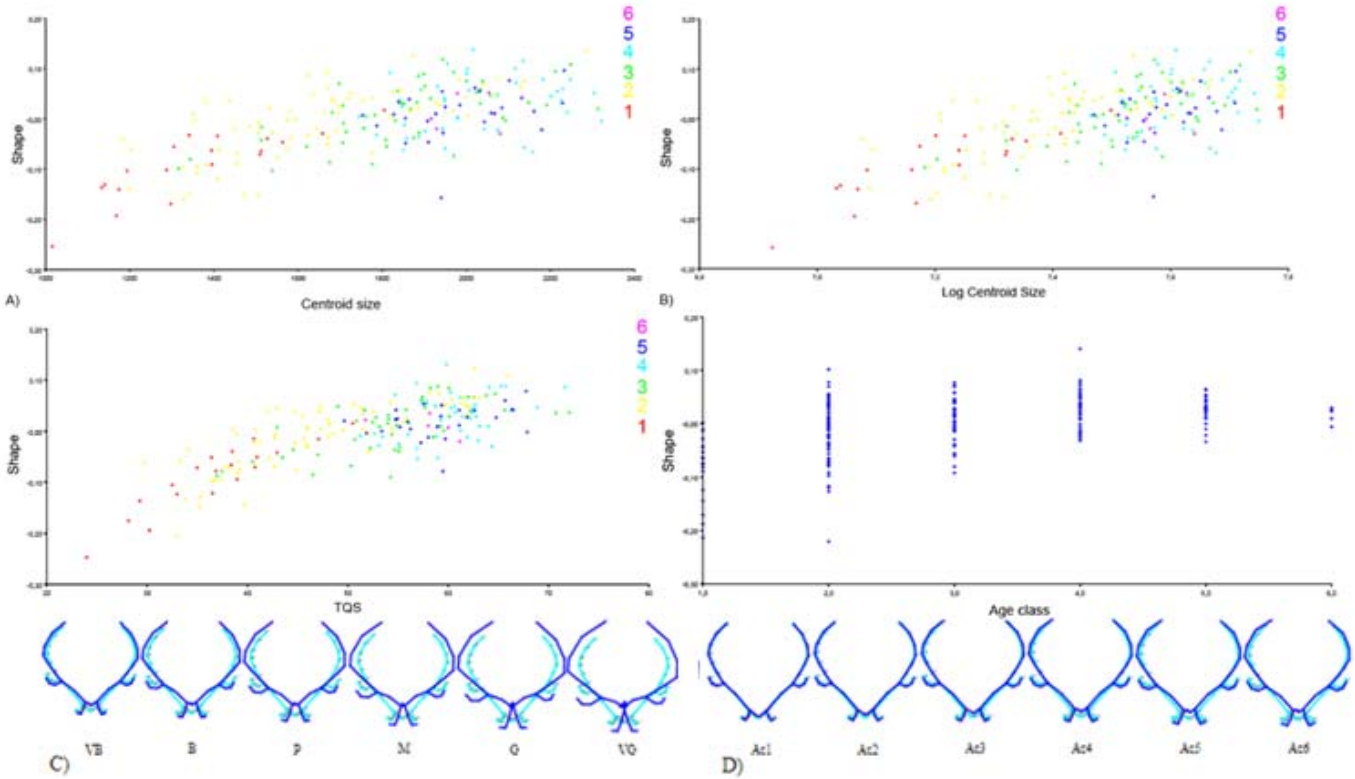

Figure 3.5. Regression of total shape on different studied variables. A) Shape on Centroid size (CS), coloured by age class; B) shape on log CS, coloured by age class; C) regression of shape on TQS coloured by age class and D) regression of shape on age class. Below regression (C) is represented the shape change (dark blue) associated to each category (from 20 to 70 scoring; from very bad (VB), to bad (B), poor (P), medium (M), good (G) and very good (VG) categories) respect to the mean configuration (light blue); below regression (D) is represented the shape change (dark blue) associated to each age class (Ac; from 1 to 6) respect to the mean configuration (light blue).

3.5 Discussion and conclusions

3.5.1 *How do the studied factors affect antler morphology?*

Despite the fact that there seems to be an age-related pattern of shape change in our sample (Fig. 3.3), as it has been also observed in other studies (Huxley 1931; Lincoln 1992; Azorit et al. 2002a; Fierro et al. 2002), it also seems that other factors have a greater effect on antler shape variation (e.g. the total number of tines, the number of crown tines) (Table 3.3).

As described above (see Results section), one of the shape changes associated to decreasing PC1 values (i.e. from positive to negative values) is a progressive separation of the beams, especially at the upper part of the structure. This separation of the beams has been related to an increase in the number of tines (Azorit et al. 2002b), which agrees with the significant effect of all tine-related factors on PC1 (i.e. number of crown tines, total number of tines, presence of bez tines; Table 3.4), and also of size, since a significant correlation between the number of tines and antler size has been previously documented (Azorit et al. 2002b). Furthermore, the youngest specimens (age class 1 and 2), whose right and left branches have the minimum separation between them, and which also posses the lowest number of tines, present the most positive values of PC1.

In the case of shape changes explained by PC2, the most striking feature is the elongation and increase in curvature of the crown from negative to positive values. A longer crown is usually related to a higher number of crown tines (Carranza 1999; Azorit et al. 2002b), hence the high correlation of this PC with the total number of tines and the number of crown tines and, as in PC1, with size (Azorit et al. 2002b). Furthermore,

high PC2 values are generally attributed to fully-grown individuals from 6 to 9 years old (age classes 3 and 4), which correspond to the age at which the Iberian red deer reaches their maximum antler development (Montoya 1999; Azorit et al. 2002a; Carranza 2004; Garcia et al. 2010) (Fig. 3.6). This association would explain the significance of age on PC2.

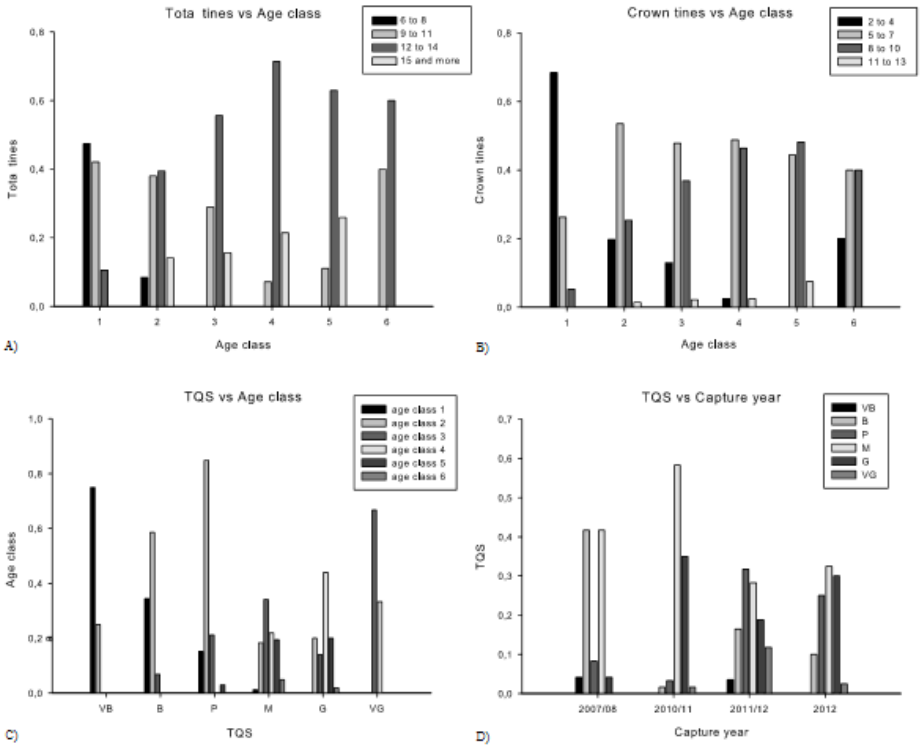

Figure 3.6. Histograms showing the relative frequencies of the total number of tines vs age class (A), the number of crown tines vs age class (B) the TQS vs age class (C), and the TQS vs capture year (D).

The exact same factors affecting the shape changes associated to PC1 were also found to be significantly related to the shape changes associated to PC3 (and also in a similar magnitude; Table 3.4). However, the relationship between these factors and PC3 is inverse to that with PC1, since the caudal displacement of the tip of the crown as more tines are subsequently added occurs with decreasing PC1 values and with increasing PC3 values (Fig. 3.4-PC1, PC3).

Thus, we propose that the shape changes associated to the first three PCs (i.e. PC1 to PC3) describe how the antler progressively transforms to accommodate an increasing number of tines during a deer's life history, both elongating and separating the beams, but also reorienting its trez tines, eye tines and crown.

The shape changes associated to PC4 principally described how the V-shaped antlers typical of young individuals transform into the curved shape of the adult, where the beam and the crown are no longer aligned, as described in previous studies (Marcos 1989; De los Reyes 1990; Carranza 1999; Montoya 1999; García et al. 2010). This would explain why the only significant factors affecting PC4 were age and size.

In the case of PC5 and PC6, the shape changes occur at a smaller scale, showing antlers with a similar shape to the mean configuration and only slight changes especially at eye tines level. PC5 was mostly affected by size, so maybe represents allometric changes in antler development (since age, presence of bez tines and total number of tines, were also marginally significant). In the case of PC6 there was no significant relationship with any factor studied except the presence of bez tines. It is interesting to note, however, that PC6 described different shape changes for the left and right branches. Since presence of bez tines accounts for this kind of asymmetry

(since it was code 0-1-2), it could explain its significant relationship with PC6.

Table 3.4. Effect of the studied factors on each individual PC. Abbreviations as in Table 3.3.

PC	Factor	%Pred.	p-value	PC	Factor	%Pred.	p-value
	Size (CS)	14.02	<0.0001		Size (CS)	5.55	0.0005
	Age class	0.50	0.3058		Age class	2.47	0.0218
	Presence of bez tines	2.87	0.0140		Presence of bez tines	0.92	0.1726
PC1	Capture year	1.67	0.0662	**PC4**	Capture year	0.14	0.5958
	Number of crown tines	15.38	<0.0001		Number of crown tines	0.48	0.3184
	Total number of tines	14.47	<0.0001		Total number of tines	0.83	0.1894
	Size (CS)	20.73	<0.0001		Size (CS)	10.17	<.0001
	Age class	9.96	<0.0001		Age class	5.27	0.0007
	Presence of bez tines	8.74	0.0001		Presence of bez tines	4.49	0.0022
PC2	Capture year	6.39	0.0007	**PC5**	Capture year	0.14	0.5832
	Number of crown tines	27.19	<0.0001		Number of crown tines	1.56	0.0747
	Total number of tines	29.58	<0.0001		Total number of tines	3.92	0.0043
	Size (CS)	2.48	0.0217		Size (CS)	0.30	0.4300
	Age class	0.71	0.2297		Age class	0.62	0.2624
	Presence of bez tines	2.98	0.0118		Presence of bez tines	1.94	0.0430
PC3	Capture year	0.25	0.4656	**PC6**	Capture year	0.00	0.9812
	Number of crown tines	11.37	<0.0001		Number of crown tines	0.22	0.4955
	Total number of tines	10.86	<0.0001		Total number of tines	0.55	0.2835

As a final remark, we would like to point out that the present study shows that the use of geometric morphometrics methods on antler morphology not only produces similar conclusions than traditional methods, as the appreciation of the antler branches separation with the increasing number

of tines (Azorit et al. 2002b) or the correspondence between deer ages and their maximum antler development (Montoya 1999; Azorit et al. 2002a; Carranza 2004; Garcia et al. 2010), but also allows a more precise study of the shape changes associated to each factor affecting antler morphology.

3.5.2 *Thoughts on antler quality optimization*

Although the shape variation at each age class was high enough to prevent the definition of an optimum trophy age, a deeper understanding of the causes behind this large shape variation would help us establishing an approximated age interval where trophy quality is higher.

In the case of our antler quality index, TQS, antler size is the main determinant of trophy quality, since TQS is calculated using linear measurements. As it has been already demonstrated, antler size increases with age and depends on food availability during the growth period (spring) (Carranza 1999), which is related to winter weather conditions, as also suggested by Landete-Castillejos et al. (2010). Thus, TQS should be related to age class and to environmental factors.

As expected, age class had a significant effect on TQS, explaining 41.31% of its variability ($p = <0.0001$). While the youngest individuals (age class 1) did present the lowest scores (VB quality), mostly due to their smaller size, the highest scores (VG quality) corresponded to age classes 3 and 4 (6 to 9 years old), not to the oldest individuals (Fig. 3.6C). However, good quality trophies (G) appeared in age class 2 through 5, which is an interesting fact, since good quality trophies in individuals of age class 2 are a rare event (Carranza, 1999). In fact, Azorit et al. (2002a) determined that Iberian red deer must be at least 7 years old (age class 3) to produce

good trophies. We propose then that these results could indicate the presence of individuals of exceptional genetic quality, able to produce good antler trophies at an early age, in our sample. The good qualities found in individuals of 2012 (cold and dry winter) and in age class 2 individuals of 2011 (coldest winter) further support this argument (see below). Finally, the scarcity of good trophies in age classes 5 and, especially, 6 could be explained by the antler decay phenomenon (Marcos 1989; De los Reyes 1990; Carranza 1999; Azorit et al. 2002a; Carranza 2004; García et al. 2010). According to Carranza (2004), antler decay normally starts from 9 years old (age class 4), which agrees with our finding of low qualities in age classes 5 and 6, but also coincides with our theoretical age of maximum number of tines (see below; Fig. 3.6).

We have also found that higher TQS scores are related to increasing shape variability (Fig. 3.5C). Since the total tine number is one of the main factors affecting antler shape variation, we studied the relationship between tine number and TQS (Fig. 3.7). As expected, this relationship proved significant (r^2= 0.580), which again relates to the theoretical maximum tine number at age class 4 (see below; Figure 3.6A).

Summarizing, although we could not find an optimum trophy age based on antler shape alone, the study of the factors affecting antler shape suggests that age class 4 (8 to 9 years old) produces the best quality trophies. Regarding environmental factors, since food quality and availability have a significant effect on antler development and those factors are determined by the winter rainfall (Chapman 1975; Carranza 1999; García et al. 2010), we would expect a significant positive correlation between our environmental proxy (capture year) and trophy quality (TQS).

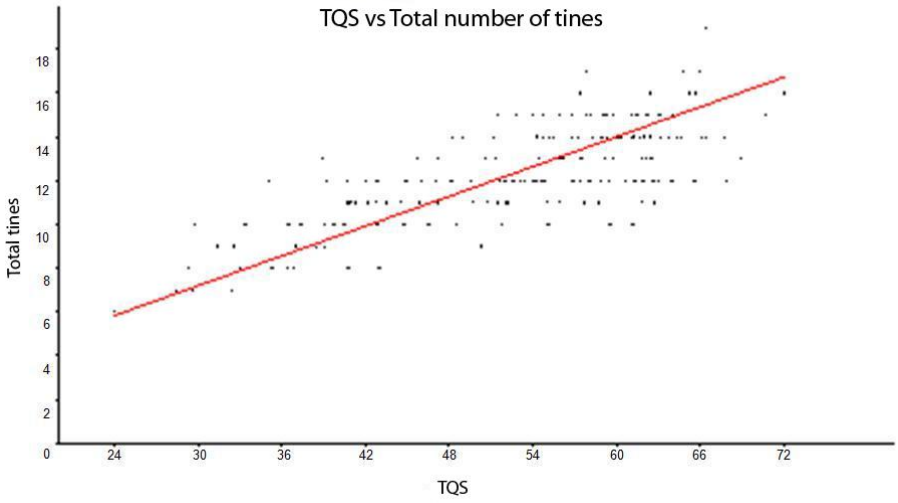

Figure 3.7. Regression of TQS on total number of tines (r^2= 0.57986; Y= 0.22638 + 0.42204x).

Indeed, capture year was significantly related to TQS (2.42 % of TQS explained by environmental factors, p = 0.0209). According to this, the year 2010, which had the rainiest and warmest winter (winter rainfall = 5.57 mm; mean winter temperature = 2.75 ºC), should have produced the best trophies. Most individual captured that year, however, were of medium quality (M), although there was also a fair share of good (G) trophies (Fig..3.6D). The antlers from 2012 correspond to the driest winter (winter rainfall = 0.34 mm; mean winter temperature = 1.39 ºC), which we would lead us to expect low-quality antlers, ranging from very bad quality (VB) to poor quality (P) (Landete-Castillejos et al. 2010). However, we found a balanced distribution of poor to good quality antlers. The year 2011 also presented a balanced quality distribution (although slightly skewed towards poor quality; Fig. 3.6D), even though it had the coldest winter (mean winter temperature = 1.26 ºC). Possibly the

abundant winter rainfall that winter (winter rainfall = 3.41 mm) counteracted part of the negative effect of the low temperatures. The year with worst antler trophies was 2007, with higher rainfall than 2012 but mean temperatures during winter closer to those of 2011 (winter rainfall = 1.19 mm; mean winter temperature = 1.28 ºC). Thus, contrary to previous studies (Ditchkoff et al. 2001; Azorit et al. 2002a; García et al 2010; Landete-Castillejos et al. 2010), although the environmental effects had a significant influence on trophy quality, winter rainfall and mean winter temperature were not good predictors of antler quality (at least using our quality index, TQS). A possible explanation to this could be that the animals would have been supplemented with fodder in the harshest winters. However, this is not a common practice in Sierra Morena. Instead, when a harsh winter is predicted, the largest estates would dedicate part of their extension to cultivate crops, which increases winter survival of the animals, but probably have no effect on antler growth during the spring. Small estates cannot afford this practice. Thus, supplementary feeding is probably not causing this low association between environmental factors and trophy quality.

3.5.3 *Modularity in antler development?*

One interesting observation is that, regardless the shape changes explained by each PC, those shape changes generally occurred in a coordinated way between the upper part and the lower part of the antler, establishing the trez tines as the midpoint of the structure. For instance, when the upper part of the antler narrowed, the lower part was normally elongated near the skull. On the contrary, when the upper part of the antler became more arched and consequently wider, the lower part generally became shorter,

especially near the skull. Furthermore, a more developed upper part (and thus a contracted lower part) seemed to be associated with longer and more curved tines, which normally correspond to the adult specimens (i.e. to more developed antlers). The increased length and curvature of the tines was, at the same time, usually associated with a change in tine orientation: longer and more curved eye tines were usually frontally oriented, while trez tines tended to be laterally directed from the beam. All of these findings seem to suggest the existence of modularity in antler development, which we believe should be further studied in the future, especially if the genes governing antler growth were mapped.

3.5.4 *Interactions between factors*

Even though we observed how several factors relate to antlers shape, we could not find a characteristic shape to any specific age class, likely because the interactions among the studied factors create a huge pool of variability at each age class.

The relationship between the tine-related factors is clear, since one is a linear combination of the others (total number of tines = 4 + presence of bez tines + number of crown tines). However, as reflected in the analyses of factor effects on individual PCs (Table 3.4), each of these three factors is related to different shape changes, especially in the small scale PCs (in our case, PC5 and beyond). A more complex relationship would be that of each tine-related factor with age.

For instance, in our sample, most of the individuals from age class and a few individuals from age class 2, did not present bez tines, which conforms to the developmental pattern described for the Iberian red deer in Sierra Morena, where the youngest individuals typically do not present

bez tines (Azorit et al. 2002a). This way, presence of bez tines is a factor more likely to affect older individuals. Nevertheless, the number of bez tines was not constant in any age class.

Regarding the total number of tines, our sample included antlers with 6 to 19 tines. As with presence of bez tines, it was not possible to assign a particular number of tines to each age class (Fig. 3.8A). In agreement with previous studies relating age with tine number (Huxley 1931; Nahlik 1992; Lincoln 1992; Carranza 1999; Montoya 1999; Azorit et al. 2002a; Fierro et al. 2002; García et al. 2010), the youngest individuals (age class 1) had the lowest total number of tines, ranging mostly from 6 to 11 tines. Age class 2 presented the highest variability in total number of tines, having the categories 9 to 11 tines and 12 to 14 tines a similar frequency. From there, most individuals in each subsequent age class presented between 12 and 14 tines. Thus, most of the studied specimens had 12 to 14 tines (Fig. 3.6A), in contrast to the frequent 10 tines observed by Azorit et al. (2002a) in the Iberian red deer populations of Sierra Morena ten years ago. This apparent increase in the overall quality of the antlers of Iberian red deer of eastern Sierra Morena, had already been suggested by Fierro et al. (2002), who proposed the recent introduction of deers from France and Central Europe in Sierra Morena as the source for this quality increase. Finally, in age class 6 (12 to 13 years old) a decrease in tine number is observed (Fig. 3.6), which agrees with Nahlik (1992), who states that antler decay (the decrease in antler size and number of tines) starts at about 12 years old depending on the food availability, but not with Montoya (1999), who supports 8 years as the age of antler decay starting (which would be our age class 4). The quadratic model in Figure 3.8 also allowed us to determine the age at which Iberian red deers tend to

have the maximum number of tines, which could be useful if trying to find an optimum trophy age using the standard hunting protocols. According to our results, the individuals of age class 4 (8 to 9 years old) should present the maximum number of tines, producing thus better trophies than both younger and older individuals.

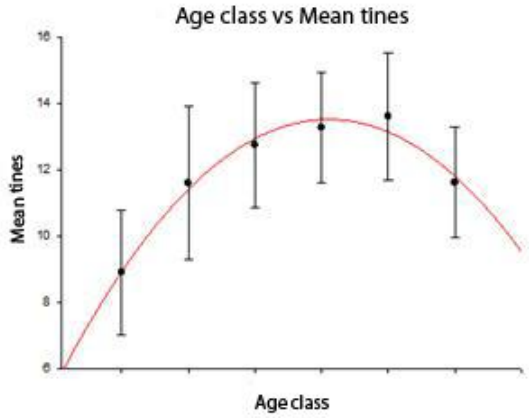

Figure 3.8. Changes by age class in the mean number of tines. The red line represents the best fit model derived by polynomial analysis (quadratic model: $Y= -0.47x^2 + 2.955X+ 8.920$; $r^2 = 0.97$).

Regarding the number of crown tines, most of our specimens had between 6 and 8 crown tines, since there is a maximum of six tines on the beams (one eye, one bez and one trez tine per beam) and most of our specimens presented 12 to 14 total tines. Most of the measured specimens of age class 1 (2 to 3 years old) present between 2 and 8 crown tines (one to four tines per crown) (Fig. 3.6B). Previous studies had already described 2 crown tines as characteristic for young individuals (Saénz de Buruaga et al. 1991; Azorit et al 2002a). However, according to Spanish hunting protocols (García et al. 2010), 3-years-old individuals are considered good

trophies when they have 10 tines or more (i.e. 4 or more crown tines). Thus, the studies proposing 2 crown tines as typical for young individuals were probably conducted on individuals from a poor year in terms of food availability or on individuals of mediocre quality. Most of the individuals from age class 2 (4 to 5 years old) presented between 5 and 7 crown tines, in agreement with García et al. (2010), who argue that individuals from this age onwards would be required to present at least 10 or 12 tines to be considered good trophies in Spain. From age class 3 onwards crown tine number ranged similarly to age class 2, but the frequencies progressively shifted to the higher categories (Fig. 3.6A, B). Finally, as observed for total tine number, there was a decrease in the number of crown tines in individuals of age class 6.

4. Asymmetry study of Iberian red deer antler (*Cervus elaphus hispanicus*) by using geometric morphometrics

4.1 Abstract

Due to the Iberian red deer antler complexity, the use of three-dimensional geometric morphometrics methods was proposed in order to test the presence of asymmetries in the structure. In the same way that most of the existing bibliographic background on antlers, this study tested the presence of fluctuating asymmetry (FA) and assessed its reliability as individual quality indicator. To do it, 434 half antlers were used in two different datasets. From each antler side, 56 landmarks and semilandmarks were digitized through and Immersion MicroScribe G2X. A Procrustes ANOVA performed over a first dataset, where some replicated antler measures were included, determined that the measurement error was small enough to consider it negligible. So, it could be assumed that the asymmetries observed were real. At first glance, the antlers FA level was significant; however, the directional asymmetry (DA) level was also significant, representing almost the double. A Discriminant function analysis (DFA) showed statistically significant differences between the right and left antler sides. In addition, the significant DA effect found in this case corresponded to a slightly more developed right antler side. All these results suggested that the FA found in Iberian red deer antlers, was not useful as individual quality indicator. In parallel, the effect over the asymmetric component of antlers of different variables considered of importance in final antler development, such as the age, total number of tines or capture year, was tested by performing MANOVA tests. Any of the variables studied had effect over the asymmetric component, which pointed to the fact that probably is the genetic component of individuals the principal cause of the significant

presence of asymmetries in the sample, and not the environment. Thus, the presence of DA provided new insights about the antler asymmetry and its development, leading us to think about different questions, as for example if there is a possible influence of DA on the mechanical constraints acting over the antlers so useful during fights.

4.2 Introduction

The antler, generally defined as prominent secondary sexual characters expensive to maintain (Estévez et al. 2008; Dicthkoff and Defreese 2010), is only present in red deer males. The antlers are bilateral structures supposedly encoded by the same genes, which implies that its right and left sides, are genetically programmed to develop symmetrically (Solberg and Saether 1993; Lagesen and Folstad 1998; Pélabon and Jolly 2000) and therefore, they would be controlled by the same genetic and developmental programs (Bartos et al. 2007). Nevertheless, it is important to take into account that the final development of any morphological trait, is under the influence of both individual genetic and environmental factors (Putman et al. 2000).

Clutton-Brock (1982) defined several antler functions, for example indicator of dominance rank or individual quality. However, the antler is also indicator of reproductive effort (Clutton-Brock et al. 1982; Berglund et al. 1996; Dicthkoff and Defreese 2010), and especially highlighted has been the antler role as weapons in intra-specific combats in order to defend harems during the rutting season (Clements et al. 2010; Stéger et al. 2010), or territories with high food productivity where females use to feed (Carranza 1999; Carranza 2004). This is what occurs with the antler

of the Iberian red deer (*Cervus elaphus hispanicus*), the subspecies under study.

Some antler asymmetry studies, emphasize the use of antlers primarily as weapons in male-male encounters, being its main objective the head and eyes protection (Mateos et al. 2008). This protective function could provide to some antler parts, as the eye and trez tines, a less functional importance probably helping to increase the presence of asymmetry on them (Mateos et al. 2008).

The antler has been considered a good structure for asymmetry studies, because it is thought that its annual renewal is a reflection of the hardships to which the specimens have been subjected during the year (Carranza 2004; García et al. 2010), as well as an easy way to predict the environmental situation (Dicthkoff and Defreese 2010). These hypotheses suggest that only high-quality males are capable to produce large and more symmetrical ornaments (Moller 1992; Pélabon and Joly 2000; Carranza 2004; Dicthkoff and Defreese 2010) and hence, that these males are expected to have higher fitness, since they could be preferred by females (Geist 1998; Moyes et al. 2009). Some authors disagree about this last assumption, and think that more symmetrical ornaments are exclusively a matter of sexual selection, while other authors simply believe that evidence lacks (Clutton-Brock 1982; Clutton-Brock et al. 1982; Malo et al. 2005).

Taking into account all the above information about antlers, and the increasing interest in their symmetry, it is important to introduce the two most important types of asymmetry studied in this research, fluctuating Asymmetry (FA) and directional asymmetry (DA) (Leamy 1984).

On one hand, fluctuating asymmetry (FA) is considered an epigenetic measure of stress (Parsons 1990; Moller 1992). It takes place when small random quantifiable differences appear between the right and left sides of bilateral characters (Van Valen 1962; Palmer and Strobeck 1986; Pélabon and Van Breukelen 1998), and they occur with no directionality (Moller 1994). It has been also suggested that these small departures from bilateral symmetry provide a measure of the sensitivity of development (Parsons 1990), and these departures vary predictably according to the different environmental stresses (Palmer 2013). For that reason, it is thought that FA could reflect developmental stability, which in turn could predict the individual fitness (Palmer and Strobeck 1986; Kruuk et al. 2003; Swaddle 2003; Mateos et al. 2008). The fighting ability of males, as well as, their ability to gain food or to deal with disease and parasitism, is also apparently reflected by FA level, especially in sexually selected traits as antlers (Moller 1992; Bateman 2000; Mateos et al. 2008). On the other hand, Directional asymmetry (DA) reflect systematic differences between the right and left and right body sides (Klingenberg et al. 2010) showing the propensity of a bilateral character to develop more in one side than in the other in a predictable manner and repeatedly in time (Palmer 1994). It is a phenomenon characterised by its genetic basis and sometimes related to a differential adaptive activity of the genome on each side (Palmer and Strobeck 1986; Palmer 1996). Examples are mammalian heart (Van Valen 1962) or human brain (Toga and Thompson 2003). But DA could be also related to a selective advantage, as it occurs in many vertebrate testes size, since generally large secondary sexual characters are associated with mating success and other sexual selection advantages. This last fact, made that some authors think about the use of DA as a fitness indicator and

even as a developmental stability measurement, in the same way as FA (Moller 1994). However, other authors argued (Graham et al. 1994; Palmer 1996) that DA could not reflect developmental stability and individual quality due to its genetic basis.

The antler asymmetry studies generally consider the presence of FA and not DA (Moller 1992; Solberg and Saether 1993; Bartos and Bahbouh 2006; Bartos et al. 2007; Mateos et al. 2008), since apparently most morphological characters show FA while very few of them show DA (Ludwig 1932). However, other studies suggest the possibility of a change from FA to DA in few generations (Graham et al. 1993; Moller 1994).

Traditionally, the classical way to measure asymmetries in any structure was the use of linear measurements (Moller 1992; Solberg and Saether 1993; Bartos and Bahbouh 2006; Bartos et al. 2007; Mateos et al. 2008). But due to the antler complexity, in this research–three-dimensional methods were used, as previously made by Dicthkoff and Defreese (2010) in white-tailed deer (*Odocoileus virginianus*).

The main goal of this study was to test the presence of asymmetries in Iberian red deer antlers, especially fluctuating asymmetry (FA), by using geometric morphometrics methods, and to assess its reliability as a quality or *fitness* indicator (Solberg and Saether 1993; Palmer 1994; Palmer 1996; Pélabon and Van Breukelen 1998; Putman et al. 2000; Ditchkoff et al. 2001; Mateos et al. 2008). Furthermore, as has been previously hypothesized by other authors (Moller 1992; Dicthkoff and Defreese 2010), we expected that FA decrease with antler size as well as with age, since it has been quoted above, it is assumed that only the best quality individuals are capable to produce large ornaments throughout its life. Furthermore, since some studies suggest the possibility of using antler

asymmetries as environmental indicators (Pélabon and Van Breukelen 1998; Dicthkoff and Defreese 2010), the effect of potential stresses during the traits development of individuals was assumed (Palmer and Strobeck 1986; Parsons 1990; Solberg and Saether 1993). As a null hypothesis, we would expect an increase of the FA levels in the years when the climatic conditions were worse. It would be especially evident if-rain lacked during the previous winter to the period of a new antler regrowth, since it would affect food availability (Carranza 2004). However, despite all this knowledge, it is also important to note the existence of studies where the FA is not considered as an individual quality indicator (Kruuk et al. 2003; Ditchkoff and Defreese 2010).

4.3 Material and methods

Antler measurements, were obtained from hunting trophies collected in several big game states from the Eastern part of Sierra Morena (Jaen, South of Spain), during the 2007/08, 2009/10 and 2011/12 hunting seasons. The data were divided in two different datasets, which were analyzed by using three-dimensional geometric morphometrics methods. Accordingly, 33 complete antlers, resulting in a total of 132 half antlers (66 left branches and 66 right branches), were measured twice to calculate the error measurement (Palmer 1994; Klingenberg and McIntyre 1998; Jojic et al. 2011). From each antler side, 56 landmarks and semilandmarks, corresponding to the different antler parts (eye tines, bez tines, trez tines, beams and crowns) (Fig. 4.1 and Table 4.1) were digitized through an Immersion MicroScribe G2X.

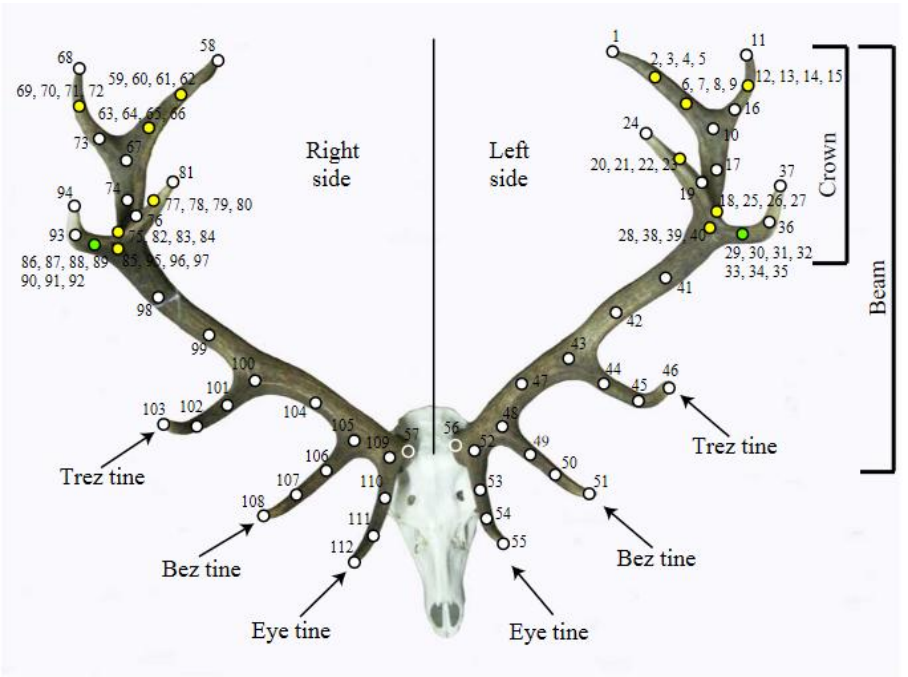

Figure 4.1. Antler parts and landmarks representation. Top view. Landmarks 56 and 57, represented by transparent landmarks in the figure, are not on the antler surface but underneath the burr base. Yellow landmarks are duplicated four times and green landmarks seven times, respectively, due to the potential occurrence of tines in those antler positions during development.

The same number of landmarks (anatomically homologous points) (Van der Molen et al. 2004; Zelditch et al. 2004) and semilandmarks (constructed landmarks) (Van der Molen et al. 2004) were registered on all the antlers, independently of their developmental stage, since individuals from different age classes were included.

Accordingly, the sample contained antlers with different numbers of tines, which were not always developed at the same places, or they could be present or missing.

Table 4.1. Landmarks (LMs) name. In order to facilitate the landmark definition, the crown tines were considered from crown base until the central tip of the beam as first, second, third and fourth tine. The corresponding potential tines were considered as daughter tines of each one of the four principal crown tines.

Left side LMs	Definition	Right side LMs
1	Tip of the fourth crown tine	**58**
2 and 6	Semilandmarks along the fourth crown tine	**59 and 63**
3 to 5	Semilandmarks along the first potential daughter tine of the fourth crown tine	**60 to 62**
7 to 9	Semilandmarks along the second potential daughter tine of the fourth crown tine	**64 to 66**
10	Shared base of the fourth and third crown tines of the left crown	**67**
11	Tip of the third crown tine	**68**
12 and 16	Semilandmarks along the third crown tine	**69 and 73**
13 to 15	Semilandmarks along the first potential daughter tine of the third crown tine	**70 to 72**
17	Crown midpoint semilandmark	**74**
18	Base of the second crown tine	**75**
19 and 23	Semilandmarks along the second crown tine	**76 and 77**
20 to 22	Semilandmarks along the first potential daughter tine of the second crown tine	**78 to 80**
24	Tip of the second crown tine	**81**
25 to 27	Semilandmarks along the second potential daughter tine of the second crown tine	**82 to 84**
28	Base of the first crown tine	**85**
29 and 36	Semilandmarks along the first crown tine	**86 and 93**
30 to 32	Semilandmarks along of the first potential daughter tine of the first crown tine	**87 to 89**
33 to 35	Semilandmarks along of the second potential daughter tine of the first crown tine	**90 to 92**
37	Tip of the first crown tine	**94**
38 to 40	Semilandmarks along of the third potential daughter tine of the first crown tine	**95 to 97**
41 and 42	Beam semilandmarks between the crown base and left trez tine base	**98 and 99**
43	Trez tine base	**100**
44 and 45	Semilandmarks along the trez tine	**101 and 102**
46	Tip of the trez tine	**103**
47	Beam semilandmark between trez tine base and bez tine base	**104**
48	Bez tine base	**105**
49 and 50	Semilandmarks along the bez tine	**106 and 107**
51	Tip of the bez tine	**108**
52	Eye tine base	**109**
53 and 54	Semilandmarks along the eye tine	**110 and 111**
55	Tip of the eye tine	**112**
56	Burr base	**57**

For that reason, following the same criteria than in Oxnard and O'Higgins (2009), we searched for the antler with apparently the highest number of tines, and from there we defined a configuration of landmarks and semilandmarks including all the observed tines. In this way, wherever a tine was not present, the corresponding number of landmarks and semilandmarks overlapped like if they were present, since they are structures that can be potentially developed (Oxnard and O'Higgins 2009). This landmark superposition does not imply a higher weight of the potential tines over the rest of the antler in the subsequent analyses, since they act as a single point (Oxnard and O'Higgins 2009).

The use of semilandmarks involves a necessary transformation prior to its use in subsequent analyses, in order to obtain true homology (Kerschbaumer and Sturmbauer 2011). In order to perform the last transformation, the software Resample (Raaum 2006) was used. These were the previous steps to perform a Procrustes Superimposition (GPA) and to align all the landmark configurations of the left and right antler sides, which are mirror images for each other. The objective was to obtain a symmetrical mean configuration among both sides (Klingenberg et al. 2002). In turn, the rotation, translation and scale effects were erased (Zelditch et al. 2004). In this way, the shape variation among individuals was studied by using the average configurations of the left and right antler sides, as well as the asymmetry resulting from the differences between the left and right antler side configurations of each individual (Klingenberg et al. 2002). This is the procedure for structures with matching symmetry, that is when there is an existing pair of separate copies of the structure on each side of the mid body plane (Klingenberg et al. 2002).

The error performed during antler measuring was tested to see whether it was small enough to consider the asymmetries found as such. The most usual way to test it and to quantify the magnitude of the effect of the possible asymmetries over shape data, by using geometric morphometrics methods, is a Procrustes ANOVA (Klingenberg and McIntyre 1998; Klingenberg et al. 2002). To apply it, the use of the dataset where some specimens were digitized repeatedly (Klingenberg 2011), was necessary. The Procrustes ANOVA divided the deviations of each one of the half antler configurations from the mean configuration, into the following effects (Klingenberg et al. 2002):

- **Individual effect**: Variation among individuals corrected for the effects of any type of asymmetry, which is equivalent to the degree of variation between the means of the left and right branches of each individual.

- **Side effect**: The side effect or repetition effect, it is equivalent to the degree of Directional Asymmetry (DA) present in the sample, which represents the average difference between the left and right sides.

- **Individual x side effect**: They are bilateral symmetry deviations or degree of Fluctuating Asymmetry (FA) present in the sample, which refers to the variability of left-right differences among individuals.

- **Measurement error**: Amount of error introduced into the sample through the measurements made, representing the difference between the original and repeated measures.

To compare the magnitude of the different effects showed in the sample by the Procrustes ANOVA, the mean square (MS) values were observed

(Jojic et al. 2011).

Afterwards, a new Procrustes ANOVA was performed by using a second dataset without repetitions, to analyze the symmetric and asymmetric antler components. In this case, 56 landmarks and semilandmarks from 217 complete antlers were digitized, comprising a total of 434 left and right branches. The same process of semilandmark transformation than in the first dataset was applied. In parallel, to assess whether the asymmetry levels found could be affected by the possible presence of antisymmetry, a Kolmogorov-Smirnov test was performed to observe possible departures from normality; the corresponding kurtosis value was calculated. Both results showed no presence of antisymmetry in the sample.

A Discriminant Function Analysis (DFA) was performed in order to test the presence of differences between the right (R) and left (L) antler sides. The reliability of the classification made by the DFA was tested by cross-validations, which leave out one individual each time by using a permutation test of 10000 iterations (Klingenberg et al. 2010). The cross-validations ensured a greater sensitivity and specificity in relation to the number of individuals classified correctly on each group R and L. Then, the shape changes and size differences associated to each antler side were observed by extracting their mean shapes.

The allometric effect was tested with the corresponding multivariate regressions of the symmetric and asymmetric components of the half antlers shape on log Centroid Size (log CS). As made by Jojic et al. (2011), these tests were based on regressions with a permutation test of 10000 iterations, under the null hypothesis of independence between size and shape from random exchanges of the log CS value. To quantify the

shape changes associated to the asymmetric component of the second dataset, a Principal Component Analysis (PCA) was performed. In the same way, a PCA over the symmetric component of the same dataset was also carried out. Additionally, since several variables as age or environment, being especially important the food availability (Carranza 1999; Azorit et al. 2002a; García et al. 2010), have effect over the antler development, we statistically tested the possible relationships between them and the antler asymmetries observed, by performing multivariate analyses of the variance (MANOVA) through the software SPSS version 15.0 (SPSS Inc., Chicago, IL, USA). In this case the available data were: age class, total number of antler tines, and capture year, which was used as a proxy variable of environmental conditions, including winter rainfall and winter temperature.

The individuals' age class was determined by collecting, cleaning and cutting the lower jaw of each specimen at first molar (M1) level, and counting the deposition of cement layers (Klein et al. 1981; Azorit et al. 2004; Chritz et al. 2009). By this process we classified the specimens of the sample in different age classes, from 1 to 6, comprising altogether specimens from 2 to 13 years old. All the morphometric analyses were conducted using the software MorphoJ (Klingenberg 2008b and 2011) and the software Morphologika2 version 2.5 (O'Higgins and Jones 2006).

4.4 Results

4.4.1 *Measurement error and FA-DA significance*

The Procrustes ANOVA results showed a measurement error quite small in comparison with the magnitude of the effect of the different

asymmetries observed, suggesting that the measurement error would not affect the analysis (Table 4.2). It would justify the use of a single copy for each antler in the subsequent asymmetry analyses (Jojic et al. 2011).

In parallel, a significant magnitude of the side ($p < .0001$; which represents DA) and individual x side ($p < 0.0001$; which represents FA) effects was observed. Then, as originally expected, FA was found in the sample studied, which suggests the possibility to use it as an individual quality indicator. Surprisingly, DA was also significant in the sample, and comparing the MS values of both, DA and FA, a difference of almost the double between them was observed (MS value of DA was 0.0002809688, while the MS value of FA was 0.0001440964; Table 4.2).

Table 4.2. Procrustes ANOVA results, including repeated measures for measurement error.

Source	df	SS	MS	F	P (parametric)
Individual	4508	3.69589936	0.0008198535	5.69	<0.0001
Side	161	0.04523598	0.0002809688	1.95	<0.0001
Individual x side	4508	0.6495867	0.0001440964	9.79	<0.0001
Measurement error	9338	0.1373947	0.0000147135		

4.4.2 *Differences between the right and left antler sides*

The following analyses were focused on the shape variation of the left and right antler sides. The performed DFA (Table 4.3) suggested that effectively there were differences between sides (Parametric $p < 0.0001$ and T-square $p < 0.0001$).

To explore the shape differences between sides, the mean landmark configuration of each side was extracted and graphically represented,

showing very subtle changes (Fig. 4.2).

Table 4.3. Discriminant function analysis (DFA) and cross-validation test between the left (**L**) and right (**R**) antler sides.

Comparison	DFA			Cross-val.			P-values	
		R	**L**		**R**	**L**	parametric	T-square
Rigth vs. Left	**R**	171	46	**R**	139	78		
	L	39	178	**L**	72	145	<0.0001	<0.0001

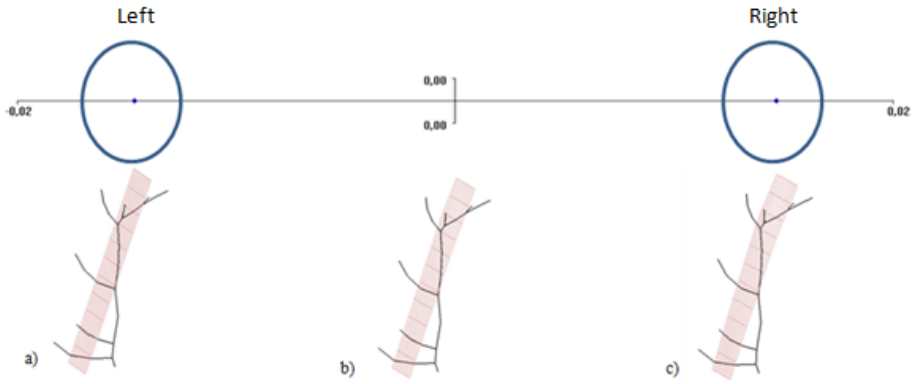

Figure 4.2. Shape variation of the average landmark configurations of left and right antler sides; a) average left antler side; b) average configuration between both antler sides; c) average right antler side.

In parallel, the possible size differences between sides were studied by calculating the corresponding values of Centroid size (CS) and log Centroid size (log CS) (Left CS = 1959.319705 and log CS = 7.324885662; Right CS = 2061.680022 and log CS = 7.325095291) (Table 4.4).

Table 4.4. Centroid size values of right and left antler sides.

Side	CS	log CS
Left side	1959.319705	7.324885662
Right side	2061.680022	7.325095291

4.4.3 *Allometric test*

The allometric effect of both antler components, symmetric and asymmetric, was tested through the corresponding regressions of shape on log CS (Fig. 4.3 and Table 4.5). In both components, taking into account the age, was observed that generally the youngest ages classes (1 and 2) had the smallest antlers (Fig. 4.3). Moreover, the allometric effect on the symmetric component was significant, explaining a 14.36% ($p < .0001$) of the total shape variation (Table 4.5), and in the asymmetric component was also significant, explaining a 2.29% ($p < .0001$) of the total shape variation (Table 4.5).

4.4.4 *PCA and MANOVA*

The shape variation associated to the symmetric and asymmetric components, was studied by performing the corresponding PCAs (Fig. 4.4 and Table 4.6). The percentage of variability explained by the first four principal components (PCs) of each PCA, was totally different for both components, representing a 63.28% of the total shape variation for the symmetric component and a 45.89% for the asymmetric component (Table 4.6).

We principally focused on the shape changes explained by each one of the first four PCs of the asymmetric component (Fig. 4.4).

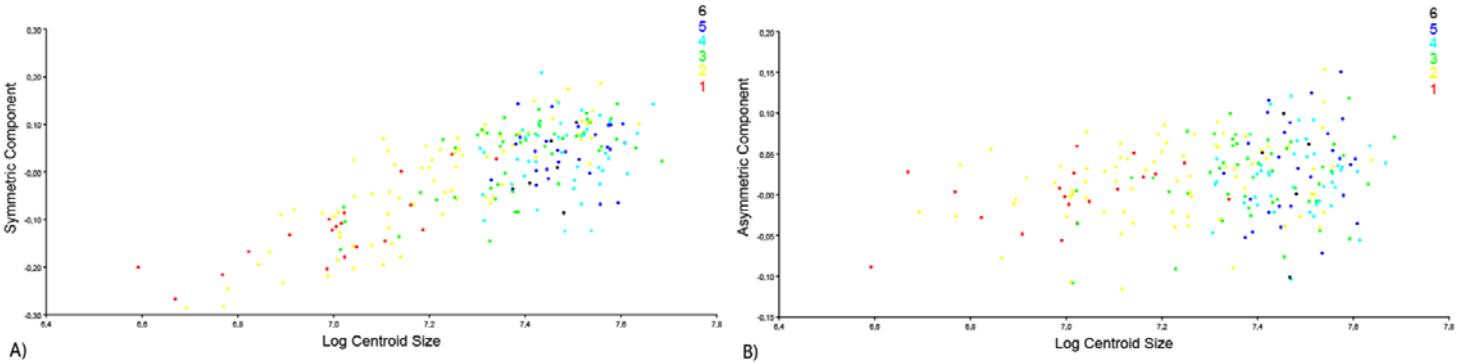

Figure 4.3. Allometric test. A) Regression between the symmetric component of antler and log CS according to age class; B) Regression between the asymmetric component of antlers and log CS according to age class. Age classes: class 1, red; class 2, yellow; class 3, green; class 4, light blue; class 5, dark blue; class 6, black.

Table 4.5. Allometric regressions between the symmetric and the asymmetric components (log CS values).

Regression	Total SS	Predicted SS	Residual SS	% predicted	p-value
Symm. comp.	8.18237322	1.17537579	7.00699743	14.36	<0.0001
Asymm. comp.	7.26394015	0.16659264	7.09734751	2.29	<0.0001

Apparently, it was not possible to establish a clear relationship between the different antler traits and the shape change explained by each PC, since general changes at beams level, general tines (eye, bez and trez tines) and crowns were observed in all of them. Thus, we statistically tested whether variables as age class, total number of tines or capture year had any influence over antler asymmetry and the corresponding shape changes, by performing MANOVAs to each fixed factor. The Wilk's lambda and Hotelling traces were calculated for each variable, being not significant in any case (Age class: Wilk's lambda= 0.008, p= 0.533, and Hotelling's T-squared= 8.270, p= 0.581; total tines: Wilk's lambda= 0, p= 0.512, and Hotelling's T-squared= 22.494, p= 0.433 and; capture year: Wilk's lambda= 0.7, p= 0.847, and Hotelling's T-squared= 4.378, p= 0.843; Table 4.7).

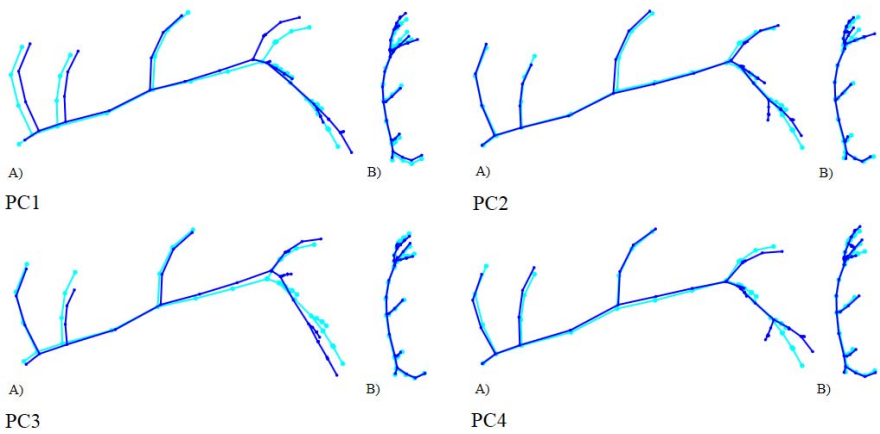

Figure 4.4. Shape change associated to the first four PC's of the asymmetric component in frontal view (A) and lateral view (B). In dark blue, the shape change associated to each PC; In light blue, the consensus figuration.

Table 4.6. PCAs of the symmetric and the asymmetric components of Iberian red deer antlers. % of total shape variability explained by the first four principal components in each case.

	PC	Eigenvalue	%Variance	Cumulative%
Symmetric Comp.	PC1	0.00970286	32.57	32.57
	PC2	0.0039774	13.35	45.93
	PC3	0.00293468	9.85	55.78
	PC4	0.00223619	7.51	63.28
Asymmetric Comp.	PC1	0.00448987	13.35	13.35
	PC2	0.00406694	12.09	25.44
	PC3	0.00358688	10.67	36.11
	PC4	0.00328836	9.78	45.89

Table 4.7. MANOVA. Test of the effect of the factors age class, total number of tines and capture year on the asymmetric component.

Factor	test	Value	F	df	p-value
Age class	Wilk's lambda	0.008	0.993	660	0.533
	Hotelling's T-squared	8.270	0.982	660	0.581
Total tines	Wilk's lambda	0	0.999	1584	0.512
	Hotelling's T-squared	22.494	1.011	1584	0.433
Capture year	Wilk's lambda	0.7	0.891	396	0.847
	Hotelling's T-squared	4.378	0.892	396	0.843

4.4.5 *Antler asymmetries on age class and capture year*

The behaviour of the fluctuating asymmetry (FA), as well as the behaviour of the total asymmetric component of antlers with respect to individuals' age and capture year was analysed. To do it, quadratic models

based on linear regressions ($Y= x^2+x+c$) and the mean values of both, the FA and the asymmetric component, were performed with the software Sigmaplot 10.0 (STATSOFT 2008). Thus, the real trend of FA in the sample was specifically observed. The corresponding regression between age and the asymmetric component showed a positive relationship ($r^2= 0.89$; Fig. 4.5A), apparently suggesting a general increasing of the right antler side development with age. The same model for the FA with the age, also showed a positive relationship ($r^2= 0.85$; Fig. 4.5B). In this case, the FA tended to increase subtly with age, reaching its maximum around age class 4 (8-9 years old), from which decreases slowly to age class 6 (12-13 years old). In addition, a one-way ANOVA performed for both comparisons, the asymmetric component with age and FA with age (Table 4.8; Annex 1), generally did not show significant differences between the different age classes (Asymmetric comp. scores, $p = 0.22553809$; FA scores, $p = 0.08415724$), except for FA values between age classes 1 and 3.

Table 4.8. ANOVA results among the asymmetric antler component and the FA scores and the different age classes groups (from 1 to 6). See also Annex 1.

ANOVA					
Asymmetric comp.	**Sum of squares**	**df**	**Mean square**	**F**	**Sig.**
between-groups	1.24003E+22	5	2.48005E+21	1.40122348	0.2255
within-groups	3.39824E+23	192	1.76992E+21		
Total	3.52225E+23	197			
FA scores	**Sum of squares**	**df**	**Mean square**	**F**	**Sig.**
between-groups	0.047283842	5	0.009456768	1.97129595	0.0842
within-groups	1.01221642	211	0.004797234		
Total	1.059500262	216			

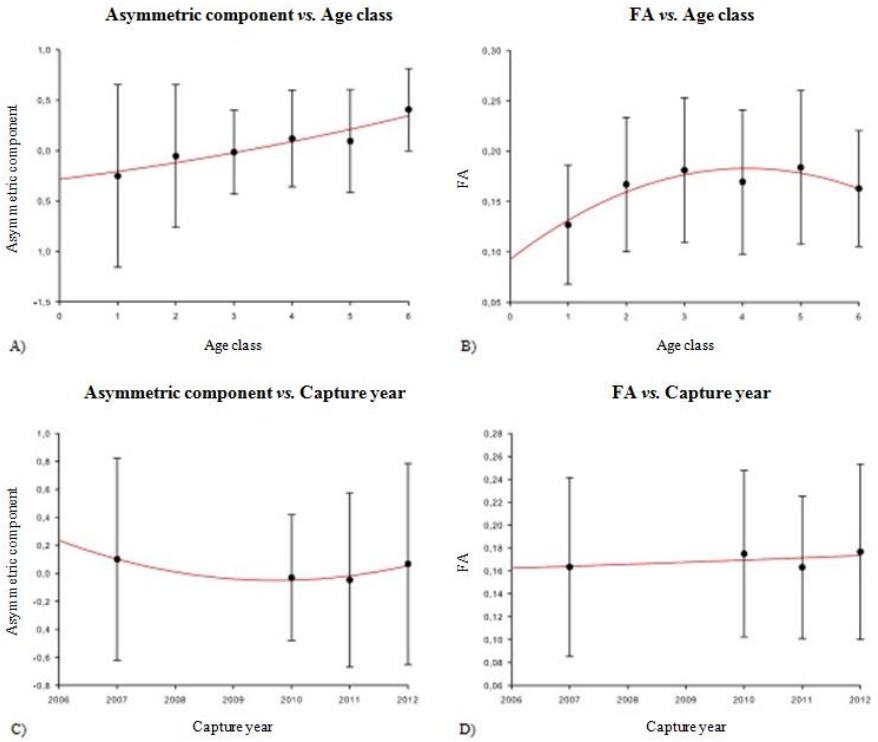

Figure 4.5. Asymmetric component and FA relationships with age and capture year respectively. In all cases the line drawn represents the best fit derived by polynomial analysis; A) Asymmetric component vs. Age class, r^2 = 0.89 and quadratic model Y= 5.79x^2 + 0.07X- 0.28); B) FA vs. Age class, r^2 = 0.85 and quadratic model Y= -5.44x^2 + 0.044X+ 0.09; C) Asymmetric component vs. Capture year, r^2 = 0.91 and quadratic model Y= 0.02x^2 - 82.83X+ 83236.67; D) FA vs. Capture year, r^2 = 0.30 and quadratic model Y= 4.025x^2 - 0.16X+ 158.94.

For the comparison of the asymmetric component of antlers and the FA with capture year, quadratic models were also used (Fig. 4.5C, D). The positive relationship of the asymmetric component and capture year (r^2= 0.91; Fig. 4.5C) did not show high variations along the different hunting seasons, although 2012 and especially 2007 apparently presented the

highest asymmetry levels. In contrast, the FA and capture year relationship was not significant (r^2= 0.30; Fig. 4.5D). The FA levels increased slowly along the different capture years, being 2012 and 2010 the highest ones.

4.5 Discussion and conclusions

The geometric morphometrics methods used in this study have allowed us to test the presence of antler asymmetries, as well as to test the presence of FA and to assess its reliability as individual quality indicator. At first, the Procrustes ANOVA results support the general hypothesis of presence of FA in the sample studied, since the individual x side effect was significant ($p < .0001$) and the measurement error was low enough to be considered negligible. However, we could not consider that the same data support the idea suggested in others works based in traditional measures and three-dimensional data (Solberg and Saether 1993; Palmer 1994; Palmer 1996; Pélabon and Van Breukelen 1998; Putman et al. 2000; Ditchkoff et al. 2001; Mateos et al. 2008; Ditckoff and Defreese 2010), that FA can be used as a reliable signal of individual quality on antlers, since in this case was the side effect (DA) the one apparently exerting a higher weight over the asymmetric component of antlers (Table 4.2).

4.5.1 *Presence of DA and FA*

As Sneddon and Swaddle (1999) said, it is not strange to find FA and DA in different magnitudes and structures of the same individual. They argued that it could be related to different functions and developmental origins of both types of asymmetry (Van Valen 1962; Moller and Pomiankowski 1993). Something similar might occur with the sample studied, despite in

this case we have both types of asymmetry in the same structure. Thus, a priori DA seems to present a more stable origin, genetically determined (Van valen 1962; Palmer 1996), which probably implies that the Iberian red deer antlers of the present sample have encoded in their genes the information about one antler side being larger than the other one, being in this case the right one (Table 4.4), as well as their potential number of tines or length (Hartl et al. 1991 and 2003). However, FA despite affecting significantly the final antler development would be based in a more unstable origin, principally determined by external stresses as the environmental ones, which could tip the balance towards a greater presence of DA or FA.

4.5.2 *Directional Asymmetry*

The presence of DA in the sample studied, provides new insights over the antler asymmetry study and its development. Although to find subtle and hardly visible but significant DA in antlers could seem strange (Fig. 4.2), it has also occurred in symmetrical features of different organisms as fly wings (see Klingenberg et al. 1998 and Klingenberg 2002 for more information). Furthermore, the DFA performed revealed the existence of statistically significant differences between the right and left antler sides (Table 4.3), reaffirming the presence of asymmetries between them. Alvarez (1995) also found a larger right antler side in a sample of fallow deer antlers. In turn, the sample presented a higher number of antlers with a longer right beam length (a 59.45% of the total sample), as occurred in the study of Bartos and Bahbouh (2006) for *Cervus elaphus*.

The relationship between the symmetric and the asymmetric components respect to the antler size (log CS) (Fig. 4.3 and Table 4.5), showed that the

symmetric one was affected by allometry, representing a 15.31% of the total shape variation in antlers, and a 2.29% in the case of the asymmetric component. Thus, size would not be the main factor causative of antler asymmetries.

The moderate difference between the left and right antler sides, may have not effect over the ability of individuals to support antlers or animal mobility, as in the case of moose (*Alces alces*) (Solberg and Saether 1993), but could be related to a more intense use of right antlers in fighting as it happens in fallow deer (*Dama dama*) (Alvarez 1995). Fights between stags imply the clash and interlock of antlers probably pointing to mechanical reasons for antler asymmetry and not with individual quality, which could affect deer fight success (Kruuk et al. 2003). However, high differences between sides could suggest that an excessive asymmetry in the studied structure could be selectively disadvantageous for deers as proposed in other organisms as house mice limb bones (Leamy 1984).

On the other hand, despite the results indicate the presence of a slightly larger right antler side, we could not consistently argue the right-handedness of Iberian red deer. To do it, it would be necessary further studies about the use of antlers in fighting and the Iberian red deer neck muscles insertion (as in Alvarez 1995). Thus, it would be possible to observe whether there is any relationship between deer locomotion, and a more frequent use of the right or left limbs when they start to walk, and the antler development, in the same way that it is known that the injury of a hind limb affect the development of the opposite antler side, usually causing malformations (Marburger et al. 1972).

In order to deepen about antler side differences, two PCAs, one for the symmetric component and other one for the asymmetric component, were

performed with the aim to define certain antler shape changes (Fig. 4.4 and Table 4.6). The first four PCs of both PCAs (Table 4.6), were obtained; however we focused on the asymmetric component results. The shape changes associated to each principal component were difficult to interpret, since widespread changes especially at beam and crown level, were observed without any specific pattern (Fig. 4.4). For that reason, the possible influence over antler asymmetries of different important variables in antler development as age, total number of tines or capture year (Azorit et al. 2002a; Carranza 2004), was statistically tested. Any of the variables studied had effect over the asymmetries observed in antlers (Table 4.7). Therefore, all these results apparently pointed again to the fact that the genetic component of individuals was acting more strongly over the antler asymmetries registered than environment. A possible explanation to it, could be the likely introduction of non-native specimens from other countries in the study area as suggested by Fierro et al. (2002).

4.5.3 *Hunter beliefs*

The results obtained in this study, especially those referred to the presence of a higher right antler side on the sampled antlers corroborate, in a way, some hunters observations. Some general hunter beliefs suggest that the antler side of highest length usually has the highest number of tines, normally corresponding to the right one. In the same way, when antlers have an odd number of tines, it is though that the right side show the higher number, which sometimes has been related to the left or right handedness of deers. Just in order to check whether these beliefs were fulfilled or not in our sample, we made a quick count of the number of tines of each branch, taking into account its length. Thus, from a total of

217 Iberian red deer antlers, 129 (a 59.45% of the sample) had a larger right beam and 88 (the 40.55% of the total sample) a larger left beam. From the 217 initial antlers, 122 had the same number of tines on both sides, of which 50 (approximately a 41% of 122) had the left side longer than the right side, and 72 (a 59%) had the right side longer than the left one. 53 of the total antlers, had a higher number of tines on the right side, from which 19 (a 36%) had the left side longer than the right one, and 34 (a 64%) had a longer right side. The remaining 42 antlers presented a higher number of tines on the left side, from which 20 (a 48%) had a longer left side and 22 (a 52%) a longer right side. These results, suggested that generally the right antler side is longer than the left one, as the mean Centroid size values showed (Table 4.4). However, it do not give enough support to the belief quoted above that the larger antler side has the higher number of tines, since only 34 antlers of 217 (representing a 15.67% of the total antlers) met the proposed requirements. On the other hand, 93 of 217 antlers (id est. a 42.86%), which represent less than a half of the sample, had an odd number of tines. From this 93 antlers, 52 (55.91%) presented a higher number of tines in the right side, while 41 (44.09%) presented the higher number in the left side. To show a higher number of tines in the left antler side is usually interpreted by hunters as presence of left-handedness in deer, regardless of the leading-limb preference of the animal, but it has not been proven in any scientific way. Therefore, we could say that only the 23.96% of the total antlers would be in agreement with the second belief quoted above, which does not seem to represent the general tendency of the sample.

4.5.4 *Influence of age and capture year over antler asymmetries*

The asymmetric component and FA behaviours were studied with respect to individual age and capture year factors, because of their importance in final antler development (Azorit et al. 2002a; Carranza 2004).

A slight positive relationship between the asymmetric component and deer age existed (Fig. 4.5A), which suggested that with increasing age the antler asymmetries tended to increase proportionally. Despite of that, we are not able to affirm it categorically, if we take into account a greater weight from the DA phenomenon, we could say that the previous relationship shows a proportional increasing of DA, and therefore and increasing of the right antler side, with age. The highest asymmetry values appeared at age class 6 (12 to 13 years old), corresponding to the oldest specimens of the study, which does not mean that is referred to the individuals with the largest antlers. It could be related to the fact that maybe mechanical constraints are the main force acting over the antlers (Solberg and Saether 1993).

According to literature, the FA could reliably reflect the genetic quality of specimens if their level decreases with age and male quality (Moller 1992;Solberg and Saether 1993). Thus, this is what we firstly expected of the relationship between FA and age (Fig. 4.5B). In this case, the FA levels tended to increase until 8-9 years old approximately (age class 4), which correspond to the 7-10 years defined by Clutton-Brock et al. (1979) for both fighting and mating success. From there the FA started to decrease. A possible explanation, for the continuous increase of FA initially observed, could be its coincidence with the rapid antler growing phase, period characterized for the high sensitivity of antlers to possible

stresses (Lincoln 1994; Pélabon and Van Breukelen 1998). The posterior FA decrease, could coincide with the end of the maximum antler development phase and the scope of sexual maturity in males (Carranza 1999; Carranza 2004), which in turn could enhance the ability to channel the use of resources in other activities such as fighting or a more symmetrical antler development (Solberg and Saether 1993). This observations contrast with the expected U-shaped relationship between the FA and age found in other studies (Putman et al. 2000; Mateos et al. 2008), or the increase of developmental instability with antler senescence (Stige et al. 2006). Moreover, it could also be related to the fact that antlers are secondary sexual traits, as beetle horns or bird spurs, and not ordinary morphological traits (Moller 1992), which are subject to a sexual selection (Bateman 2000;Mateos et al. 2008) especially as they get older, allowing us to argue that environmental stress would not be the dominant factor in the sample (Putman et al. 2000). In turn, it could be reflecting the genetic quality of individuals (Moller 1992;Solberg and Saether 1993). Furthermore, the FA decrease from 8-9 years old would be in agreement with the idea that only higher quality males are able to survive to older ages (Solberg and Saether 1993; Ditchkoff and Defreese 2010).

Studying the relationship between the asymmetric component and the capture year, only slight changes were found along the different years (Fig. 4.5C). However, the extreme capture years (2007 and 2012) presented the highest asymmetry values, especially 2007. Thinking in terms of DA, it was probably indicating that the genetic basis of the individuals hunted each capture year exercised some effect over the results. Accordingly, the individuals collected in 2007 would be those that on average had a more developed right antler side. The subsequent

decrease of asymmetry in the following capture years (2008 and 2009) could be related with the lack of information, but also with the type of individuals previously hunted. In this sense, if one year many individuals are hunted, it could be reflected in the following year in a depletion of the genetic pool of populations, which could involve some time to recover certain type of genes. The slight final increase of asymmetry in 2012, could be simply due to the natural tendency of the population genes. On the other hand, the FA and capture year relationship showed a very slight increase along time, especially in 2010 and 2012 (Fig. 4.5D).

The highest FA levels showed in these capture years (2010 and 2012) are probably due to the adverse environmental conditions observed in them. However, these results would reinforce the fact that FA could not be used as individual quality indicator, since a previous study realized with the same material study, revealed that 2010 and 2012 were the two years with the best quality antler trophies of the sample. It is in agreement with several studies, which in turn consider more reliable the use of antler size as quality indicator, in relationship with a greater role of antlers in sexual selection (Kruuk et al. 2003; Bartos and Bahbouh 2006; Bartos et al. 2007) and mating success (Mateos et al. 2008). An alternative explanation for the lack of association between the FA and capture year, could be that the environmental conditions of each hunting season were not sufficiently stressful for the sampled antlers. In addition, the apparent effect of size over FA levels could also be related with the rejection of the hypothesis of the use of FA as quality indicator (Solberg and Saether 1993). Thus, the general differences observed between the asymmetric component and the FA relationships with respect the deer age and capture year, could be

related to the influence of the other significant asymmetry in the sample, the DA.

5. Exploring integration and modularity in the antler of Iberian red deer (*Cervus elaphus hispanicus*)

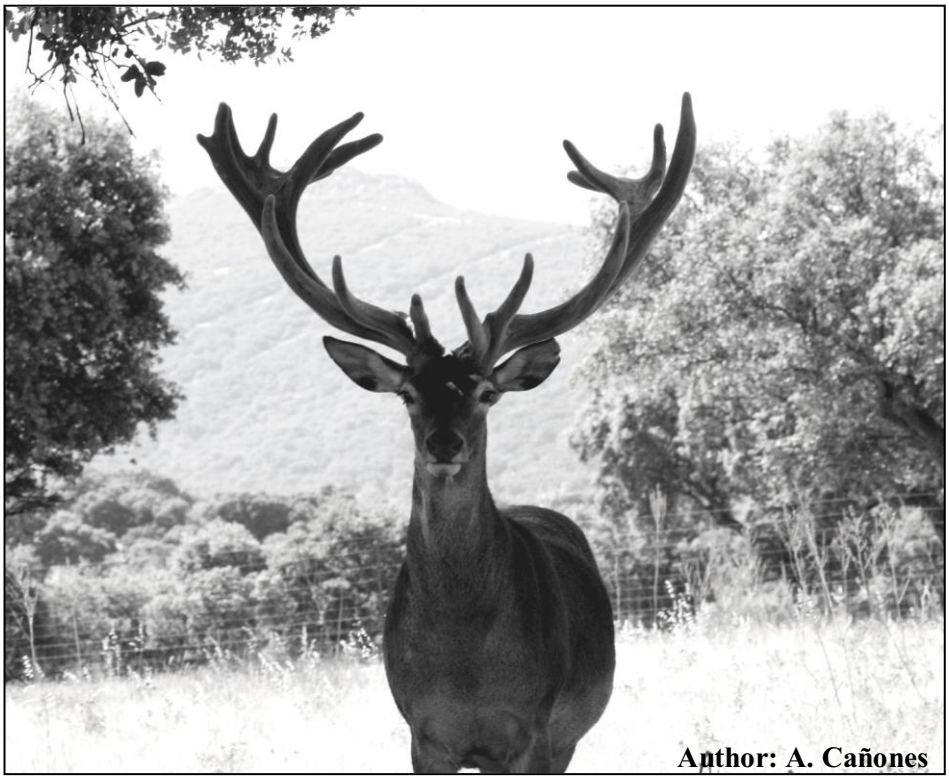

5.1 Abstract

The antler of the Iberian red deer (*Cervus elaphus hispanicus*) has long been studied as a particular model of mammal regeneration based on the interaction of multiple pathways, which could provide to antlers a modular organization. In this research, geometric morphometrics methods were used to examine the morphological data extracted from 217 Iberian red deer antlers collected from several big game states located at the Eastern part of Sierra Morena (Spain). 115 three-dimensional landmarks and semilandmarks were digitized on different antler parts. The presence of modularity and integration, focusing in both the variation among individuals and fluctuating asymmetry (FA), was assessed in the sampled antlers. Five different antler partitions were proposed based on the antler regeneration process and its genetics. The hypotheses tested showed both modularity and integration among the different antler traits, which revealed the tight relationship between both concepts. Thus, although different antler parts could be defined as separated modules, it seemed that the Iberian red deer antler generally acts as an internally homogeneous developmental structure comprised by different units, whose variation occurs in a coordinated way throughout the antler development. Furthermore, the interaction of multiple but similar pathways during the antler regeneration process would explain the high percentages of covariation observed between the hypothetic modules using partial least squares (PLS). Accordingly, the high integration found in the FA component of shape suggested that subtle perturbations suffered at direct developmental pathways may affect the entire structure.

5.2 Introduction

Generally, the organisms and its components are integrated in order to act as a functional whole (Klingenberg 2013). The integration phenomenon implies the organization of the different characters of a structure resulting from the action of several biological processes (Klingenberg 2008a). However, the different parts of a structure can be tightly integrated within them but relatively independent to other parts, which would suggest the presence of modules. Modules are defined as fully integrated units characterized by having a weak connectivity between them, which provides some independence (Klingenberg 2008a). The presence of integration apparently involves a coordinated covariation between the multiple traits of a structure (Klingenberg 2009). This covariation does not usually occur homogeneously throughout the structure (Olson and Miller 1958; Klingenberg 2013), which suggests the existence of different levels of interaction between the different parts of a structure due to the presence of modules. In addition, the apparent autonomy of modules has been considered to play an important role in evolutionary processes (Schlosser and Wagner 2004; Klingenberg 2008a; Medarde et al. 2013).

Antlers have been defined as prominent secondary sexual characters expensive to maintain, since they are lost and regrown each year (Badyaev 2004; Malo et al. 2005; Estévez et al. 2008; Dicthkoff and Defreese 2010; Emlen et al. 2012). Our previous study on the morphology of Iberian red deer antlers, revealed that shape changes occur coordinately between the different parts of the antler (see discussion section 3), which has been previously related to the presence of different units within a structure (Martínez-Vargas 2012). Thus, Iberian red deer antlers are probably a

modular structure. However, antler expression is principally considered a developmentally integrated process (Badyaev 2004), which suggests the absence of modules. Accordingly, antlers have been considered a paradox, since they should be less integrated to ease general expression, but more integrated to indicate a better physiological quality (Badyaev 2004). Consequently, antlers could have been the result of several evolutionary processes that would lead them to show a developmental integration decrease in order to produce larger antlers at low cost (Pomiankowski and Moller 1995), an increase of its functional integration and modularity levels versus external pressures, a reduction of its genetic integration with the rest of the body, or a low evolutionary integration between its different traits due to the directional selection suffered during antler development (Badyaev 2004).

The developmental interactions involved in the construction of complex morphological structures, as for example the antler and its parts, would generate covariation between those parts (Klingenberg and Zaklan 2000). In relation to this, it has been suggested that the study of fluctuating asymmetry (FA) would be the best way to distinguish the shape covariation related exclusively to variation within developmental pathways (Klingenberg and Zaklan 2000; Klingenberg et al. 2001; Klingenberg 2008a, 2009, 2013), since it would detect the presence of subtle asymmetries between the left and right antler sides originated from random perturbations (Klingenberg and Zaklan 2000; Klingenberg 2003).

The main objective of this study was thus to determine whether the Iberian red deer antler and its parts act as a single integrated structure or they rather behave as a modular entity. In order to do that, different hypothetic antler partitions were formulated based on previous studies

describing the basis of the antler regeneration process and the operation of genes involved in antler expression (for example Price and Allen 2004; Hall 2005; Price et al. 2005; Kierdorf et al. 2007; Gyurján et al. 2007; Lord et al. 2007; Molnár et al. 2007; see below). Thus, in the same way that in other structures as insect wings, rodent mandibles, or mammal skulls (Klingenberg et al. 2001; Klingenberg 2009; Klingenberg 2013), modularity and integration were assessed in antlers focusing 1) on the general variation of traits among individuals, which reflects the different mechanisms implied during antler development, and 2) on the variation related to FA, which represents exclusively interactions between developmental processes (Klingenberg et al. 2003; Klingenberg 2008a).

5.2.1 *Antler regeneration process*

The Iberian red deer antler develops from a permanent outgrowth of the frontal bone of the skull called pedicle (Price and Allen 2004; Hall 2005; Price et al. 2005; Kierdorf et al. 2007; García et al. 2010). The developmental process fits a sigmoidal curve, firstly characterized by a reduced growth rate and followed by a rapidly increase, exceeding 2 cm/day in some species including red deer, until the maximum antler size is reached (Goss 1970; Goss 1995; Price and Allen 2004). Once the antler growth ceases, the ossification process starts. Antler ossification causes a cyclical reversible osteoporosis to the animal due to the enormous mineral demand (Hillman et al. 1973; Bubenik 1983; Hall 2005; William et al. 2005; Stéger et al. 2010). Then, as the breeding season approaches, the velvet skin covering the antler is shed while the hard antler remains (Clutton-Brock et al. 1982; Muir et al 1988; Price et al. 2005). Finally,

after the breeding season, the hard antler falls and a new antler starts to grow (Fennesy and Suttie 1985).

Generally, the annual regeneration of antlers is considered a stem-cell based epimorphic process (Kierdorf et al. 2007). This process depends on testosterone secretion and photoperiod, which results in more pronounced seasonal changes as deer age (Goss 1969; Chapman 1975; Goss 1983; García et al. 2010). Thereby, during the longer days of spring, the low testosterone level allows antler casting and regrowth. Then, at late summer, when days become shorter, the testosterone level rises, stopping antler growth as well as its ossification and velvet skin shedding (Goss 1968; Lincoln et al 1972; Muir et al 1988; Gaspar-López et al. 2010). The velvet shedding is caused by changes in the blood vessels supplying the antler surface (García et al. 2010). The maximum testosterone level is reached during the breeding season (September-October; García et al. 2002). After that, the testosterone level starts to fall to a certain standard, which causes the activation of the osteoclasts at the transition area between the pedicle and the antler (Li et al. 2005). This activation leads to the resorption of the bone linking the two parts, causing the antler to fall (Suttie et al. 1984; Price et al. 2005). When the antler falls, it leaves a wound that is healed by a germination tissue originating over the pedicle (Hall 2005). This tissue is also responsible of the proliferation of fibroblasts (Goss 1969; Fowler 1993), which promote the elongation and posterior ramification of a new antler through cartilage formation and ossification (Zhou et al. 1999; Price and Allen 2004), starting a new regeneration cycle. It is also interesting to note that, at the early stages of the antler regeneration process, two growth centres appear independently from the pedicle, one for the eye tine and one for the main beam (Li et al.

2005; Kierdorf et al. 2007). Therefore, the longitudinal antler growth occurs in an appositional mode through a process of modified endochondral ossification (Banks and Newbury 1983; Price and Allen 2004; Price et al. 2005). The growth antler zones are located distally in the beam and the corresponding tines, whose appearance generates repeated splits at beam growth zone level (Kierdorf et al. 2007).

Several studies have suggested that the successive splits of the growth zone that allow antler ramification (i.e. tine formation) can already be distinguished as separate histological zones at the anterior and posterior pedicle areas prior to the start of antler growth (Price et al. 1994; Price and Allen 2004; Price et al. 2005), which could highlighting the action of previous genetic processes.

5.2.2 *Genetic basis of antler growth*

As pointed out by Price and Allen (2004), genetic studies on antler development are scarce. However, the antler development process has been considered a good system for monitoring changes in gene expression, since the mesenchymatic cells involved are able to retain their embryonic ability to give rise to both cartilage and bone (Gyurján et al. 2007). For that reason, some studies have focused on the genes involved in antler regeneration (Gyurján et al. 2007; Lord et al. 2007; Molnár et al. 2007) and the different regulatory elements affecting their expression (e.g. parathyroid hormone-related peptide (PTHrP) (Faucheaux et al. 2004); retinoic acid (RA), growing factors (e.g. IGF-I, IGF-II), cytokines and proto-oncogenes (Allen et al. 2002; Price et al. 1994; Price and Allen 2004). All these regulatory elements generally present different expression patterns at different layers defined at antler tip level (e.g. from

outermost to innermost epidermis/dermis, mesenchyme, precartilage and cartilage; Francis and Suttie 1998; Li et al. 2002). Additionally, an antler proteome map was defined by Park et al. (2004), showing antler specificity and suggesting that the different tissues involved in the regeneration process have different developmental origins.

The aforementioned studies contribute to a better knowledge of the coordinated cell differentiation and proliferation occurring during the antler regeneration process, the internal mechanisms involved, and the genes expressing at different tissues and timings during this process. No studies have been carried out on the genes governing the expression of each particular antler tine in any specific way. However, Hartl et al. (1991, 2003) showed that the presence of certain allozymes could be associated with several morphological characteristics of the antler. Furthermore, they stated that the frequencies of these allozymes could be altered with selective hunting pressure, which could lead to better trophies. Specifically, Hartl et al. (1991, 2003) indicated that *Idh-2*^{125} is especially important in young males, since it is related to a high number of tines and a fast antler development; that *Me-1*^{90} and *Acp-1*^{100} are related to the development of the small first set of antlers; and that *Acp-2*^{100} is especially important in antlers of large beams and in fully grown individuals (>7 years).

5.3 Material and methods

217 complete antlers were collected during three different hunting seasons (2007/08, 2009/10 and 2011/12), from several big game states located at the Eastern part of Sierra Morena (Jaen, South of Spain). From each

antler, a configuration including 115 landmarks (LMs; anatomically homologous points) and semilandmarks (constructed landmarks) (Van der Molen et al. 2007; Zelditch et al. 2004), corresponding to different antler parts (eye tines, bez tines, trez tines, beams and crowns), was digitized through and Immersion MicroScribe G2X (Fig. 5.1; Table 5.1).

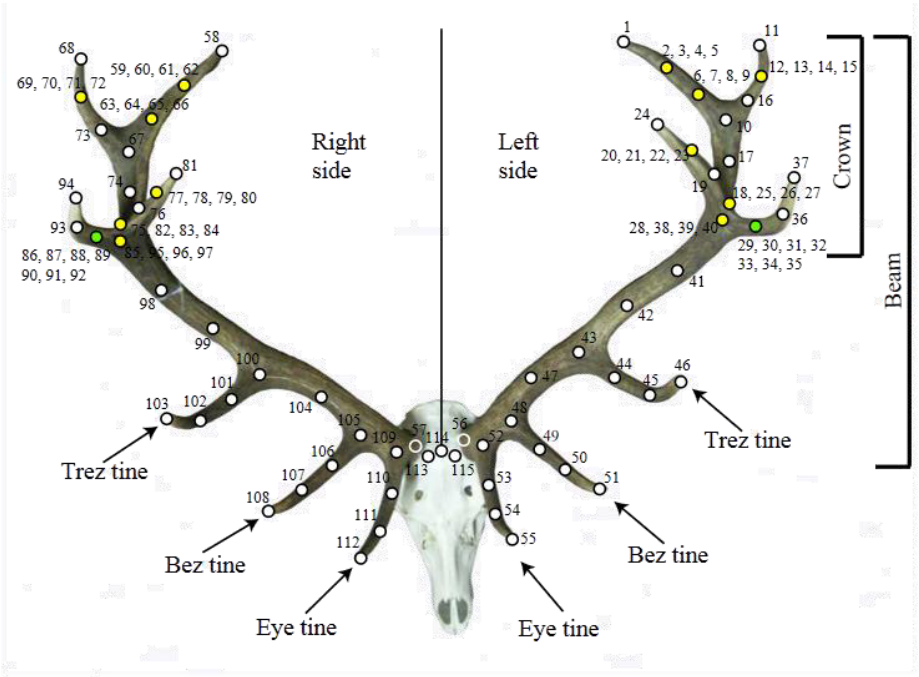

Figure 5.1. Antler anatomy and digitized landmarks. Top view. Landmarks 56 and 57, represented by empty circles, are not in the antler surface but located under the burr base. Yellow circles represent four overlapping landmarks, while green circles denote seven overlapping landmarks. This landmark overlapping is due to the potential occurrence of tines from those antler positions during development.

Table 5.1. Landmark definitions. In order to facilitate the landmark definition, the crown tines were considered from crown base until the beams' tip as first, second, third and fourth tine. The corresponding potential tines were considered as daughter tines of each one of the four principal crown tines. Abbreviation: LMs, landmarks.

Left side LMs	Definition	Right side LMs
1	Tip of the fourth crown tine	**58**
2 and 6	Semilandmarks along the fourth crown tine	**59 and 63**
3 to 5	Semilandmarks along the first potential daughter tine of the fourth crown tine	**60 to 62**
7 to 9	Semilandmarks along the second potential daughter tine of the fourth crown tine	**64 to 66**
10	Shared base of the fourth and third crown tines	**67**
11	Tip of the third crown tine	**68**
12 and 16	Semilandmarks along the third crown tine	**69 and 73**
13 to 15	Semilandmarks along the first potential daughter tine of the third crown tine	**70 to 72**
17	Crown midpoint semilandmark	**74**
18	Base of the second crown tine	**75**
19 and 23	Semilandmarks along the second crown tine	**76 and 77**
20 to 22	Semilandmarks along the first potential daughter tine of the second crown tine	**78 to 80**
24	Tip of the second crown tine	**81**
25 to 27	Semilandmarks along the second potential daughter tine of the second crown tine	**82 to 84**
28	Base of the first crown tine	**85**
29 and 36	Semilandmarks along the first crown tine	**86 and 93**
30 to 32	Semilandmarks along of the first potential daughter tine of the first crown tine	**87 to 89**
33 to 35	Semilandmarks along of the second potential daughter tine of the first crown tine	**90 to 92**
37	Tip of the first crown tine	**94**
38 to 40	Semilandmarks along of the third potential daughter tine of the first crown tine	**95 to 97**
41 and 42	Beam semilandmarks between the crown base and left trez tine base	**98 and 99**
43	Trez tine base	**100**
44 and 45	Semilandmarks along the trez tine	**101 and 102**
46	Tip of the trez tine	**103**
47	Beam semilandmark between trez tine base and bez tine base	**104**
48	Bez tine base	**105**
49 and 50	Semilandmarks along the bez tine	**106 and 107**
51	Tip of the bez tine	**108**
52	Eye tine base	**109**
53 and 54	Semilandmarks along the eye tine	**110 and 111**
55	Tip of the eye tine	**112**
56	Burr base	**57**
	Right midpoint of the coronal suture	**113**
114	Intersection between the coronal and sagittal sutures	**114**
115	Left midpoint of the coronal suture	

Two separate datasets were then constructed from those configurations, one including the complete antler (217 configurations of 115 landmarks)and another considering separately the left and right branches of each antler (434 configurations of 56 landmarks). The half antler dataset allowed us to study separately the symmetric and the asymmetric components of antler shape (Klingenberg et al. 2003; Jojic et al. 2011), through the application of Procrustes ANOVA (Klingenberg et al. 2002). The symmetric component represents shape variation among individuals, and uses the averaged shape of the left and right side to compare individuals, while the asymmetric component represents the differences between the left and right configurations of each individual (Klingenberg et al. 2002).

The sample included individuals from different age classes, which implied the presence of antlers with a variable number of tines, not always developed at the same places. For that reason, a standard configuration of landmarks and semilandmarks, including all the observed tines in the sample, was created following the criteria described by Oxnard and O'Higgins (2009). Since semilandmarks do not necessary involve true homology (Kerschbaumer and Sturmbauer 2011), they were transformed into landmarks through the software Resample (Raaum 2006). Since antlers are bilateral structures with matching symmetry, it was assumed the existence of a separate copy of the structure, with a different landmark configuration, on each body side (Klingenberg et al. 2002). Thus, when using the half antler dataset, all the landmark configurations from one side ought to be reflected, resulting in the corresponding mirror images, before the Procrustes Superimposition (GPA) (Klingenberg 2013). Then, the corresponding GPA was performed in both datasets in order to align the

landmark configurations (Zelditch et al. 2004). The possible measurement error performed during data collection could influence the asymmetries observed, especially those referred to fluctuating asymmetry (FA) (Palmer 1994). Consequently, a Procrustes ANOVA was carried out prior to any further analyses on a half antler dataset of replicated configurations to test the error, as well as the presence of FA (Klingenberg and McIntyre 1998; Klingenberg et al. 2002). If so, the measurement error was considerably smaller than the asymmetries observed, which justified the use of a single half antler configuration in the following analyses (see Table 4.2 Section 4). Furthermore, the presence of FA (Individual x side effect) was significant (see Table 4.2 Section 4).

The effect of size was evaluated through the corresponding multivariate regression of antler shape on Centroid size (CS) (Monteiro 1999) in both, the symmetric and the asymmetric components of shape. A significant allometric effect could affect the results of the integration and modularity analyses, which could be avoided by using the residual values of the multivariate regression of shape on size in subsequent analyses (Klingenberg 2009).

Five different hypothetical antler partitions were formulated to evaluate the existence of integration and modularity (Table 5.2; Fig. 5.2). They were defined following previously observed antler shape changes and also on previous studies on antler regeneration and genetics. The first hypothesis (H1) was based on a preliminary analysis of the main shape changes occurring in the complete antler (Fig. 5.3). In this hypothesis, the complete dataset was divided in two subsets of 58 and 57 LMs in order to define and analyze the covariation between the right and left antler sides (Fig. 5.2A). The presence of further modules within each half antler was

explored using four different hypotheses (Table 5.2), in which the symmetric and asymmetric components of antler shape were observed separately.

Table 5.2. Modularity hypotheses tested. Abbreviation: LMs, landmarks.

Modularity hypotheses			
Complete dataset	**Total LMs**	**Module 1 LMs**	**Module 2 LMs**
H1: Right side vs. Left side	115	58	57
Half antler dataset	**Total LMs**	**Module 1 LMs**	**Module 2 LMs**
H2: Antler crown *vs.* Antler rest	56	40	16
H3: Antler beam *vs.* Total tines	56	14	42
H4: Eye tine *vs.* Antler rest	56	4	52
H5: Trez tine *vs.* Antler rest	56	4	52

The second hypothesis proposed (H2) was based on the high shape variability observed at antler crown level and the preliminary coordinated shape changes observed between antler parts (Fig. 5.3). Thus, H2 consisted of two proposed modules: i) the crown part and its tines, represented by 40 LMs; and ii) the rest of the antler and its tines represented by 16 LMs (Fig. 5.2B). The third hypothesis (H3) envisaged the possibility to find modularity between the main antler beam, and the different antler tines. The continuity of the antler regeneration process (Pomiankowski and Moller 1995; Gyurján et al. 2007) would imply a continuous beam growth; however, it suffers several splits along its development due to the periodic appearance of tines (Kierdorf et al. 2007). These splits could suggest the presence of different modules defined by each emerging tine, leaving the main beam act as a central module. Thus, the beam was represented by 14 LMs and the tines by 42

LMs (Fig. 5.2C). The biological interest of this hypothesis was to elucidate whether the antler beam behaved independently from the antler tines and vice versa. Both the fourth and fifth hypotheses emphasized the processes determining the appearance order of antler tines. The fourth hypothesis (H4) was based on the presence of two growth centres at the start of antler development, which originated the beam and the eye tine separately (Li et al. 2005; Kierdorf et al. 2007). H4 was represented by: i) the eye tine, the first tine to appear, composed by 4 LMs; and ii) the rest of the antler, composed by the remaining 52 LMs (Fig. 5.2D). The trez tine appears later in the antler growth having its origin from a different split of the main beam (Kierdorf et al. 2007). Taking into account this, we could expect a different behaviour of the trez tines respect to the eye tine and the antler rest, which in turn would imply presence of modularity between the different antler tines and the beam. Accordingly, the fifth hypothesis (H5) defined the trez tine as a possible independent module by using 4 LMs for the trez tine and 52 for the rest of the antler (Fig. 5.2E). The hypothetic modules of both H4 and H5 could clarify whether each antler tine tends to act as a single unit, even though they were involved in the same developmental process.

The RV coefficient was used to calculate the degree of covariation between the different proposed modules for both the symmetric and asymmetric components of antler shape (Escoufier 1973). Similarly to the squared correlation coefficient, this coefficient is a scalar measure based on squared measures of the variances and covariances of the different sets of variables studied (Klingenberg 2009). A total of 10000 random partitions from each one of the hypotheses proposed were used to obtain a reliable RV value in each case (Table 5.3).

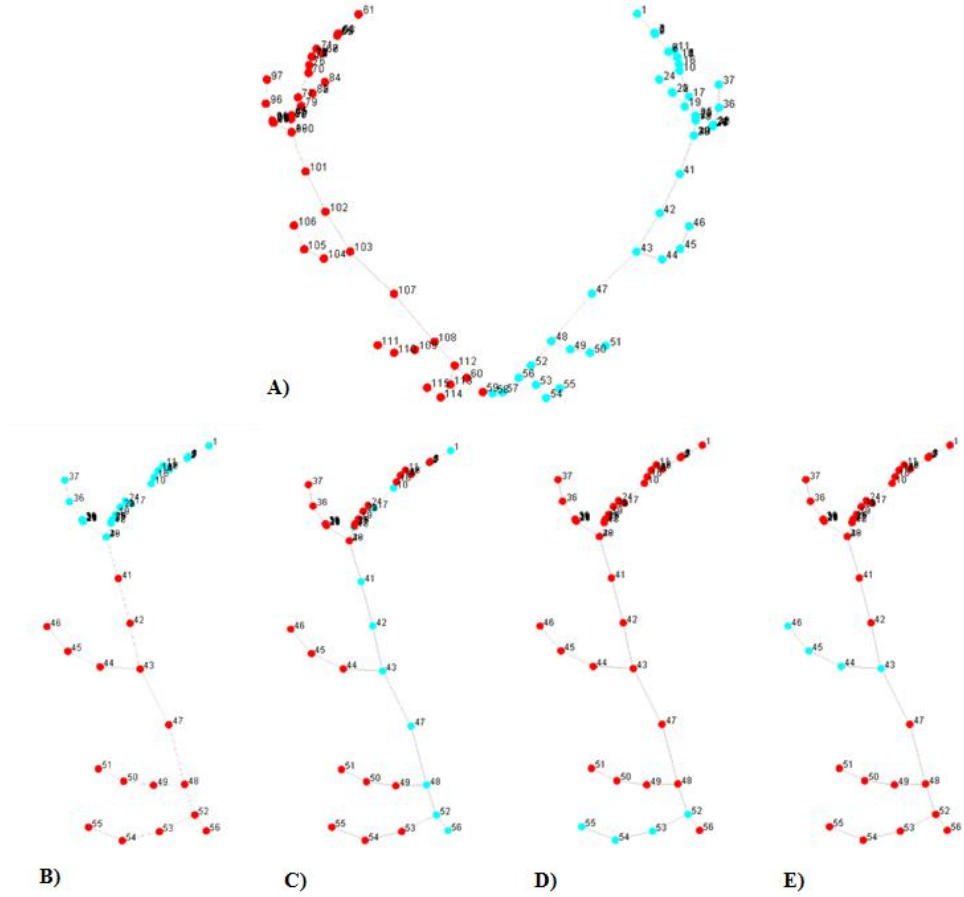

Figure 5.2. Modularity hypotheses tested. Proposed module 1 in red and proposed module 2 in blue. A) Complete dataset: right side vs. left side; B) Half antler dataset: antler crown *vs.* the rest of the antler; C) Half antler dataset: antler main beam *vs.* the rest of the tines; D) Half antler dataset: eye tine *vs.* the rest of the antler; and E) Half antler dataset: trez tine *vs.* the rest of the antler.

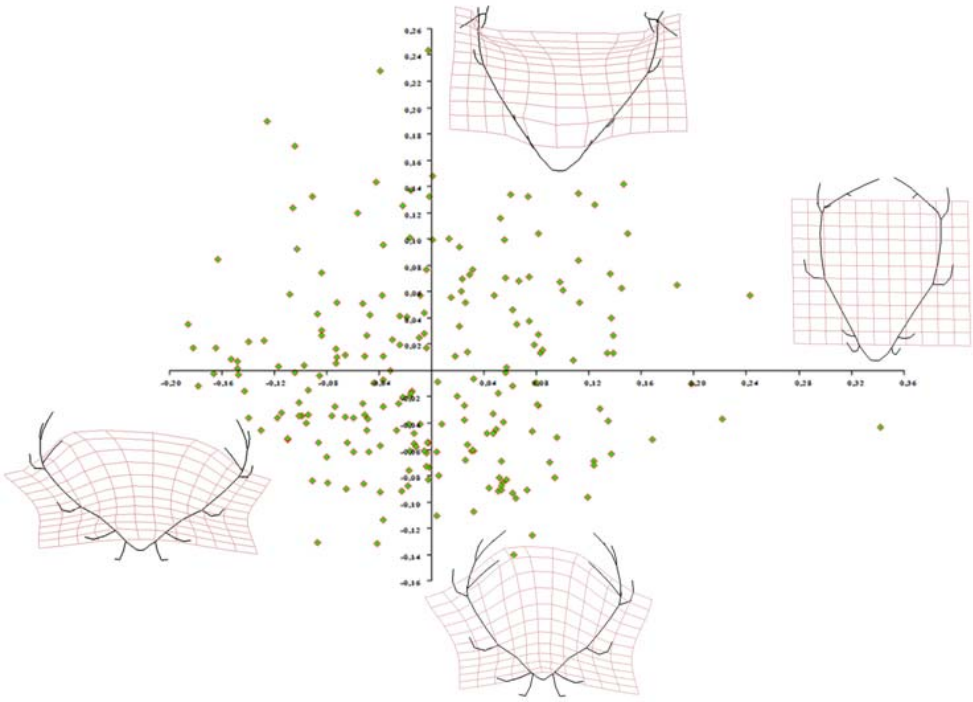

Figure 5.3. Shape changes associated to the two first principal components (PC1, X-axis; PC2, Y-axis) of a preliminary PCA performed on the complete antler dataset (115 LMs).

The significance of those tests was determined using the Bonferroni adjustment due to their permutational computation (i.e. α was set at 0.005 instead of the classical 0.05; Morgan 2007). Finally, the frequency graphs for the RV coefficient values were obtained for each hypothesis. The presence of modularity was accepted when the obtained RV value remained in the left side of the distribution, corresponding to all the possible random combinations of modules made by the permutation test. Normally, the spatially contiguous landmarks approach is preferred in modularity studies, where contiguity between LMs is satisfied when each LM of the module connects to their neighbouring LMs within the same

set, as well as with the entire peripheral margin comprised between them (Klingenberg 2009). However, in the present study all the possible random configurations between LMs had to be used instead, since our landmark configurations did not allow peripheral landmark connections in most modules.

Table 5.3. Modularity hypotheses tests performed over the symmetric and asymmetric components of antler shape. RV coefficient values corresponding to each modularity hypotheses proposed (Table 5.2, Figure 5.2) are presented before and after the allometric correction. All the p values were subjected to the Bonferroni adjustment (α= 0.005).

Complete dataset	**After correction**		**Before correction**					
	RV	**P**	**RV**	**P**				
H1: Right side *vs.* Left side	0.773	0.0000	0.805	0.0000				
Half antler datasets	**Symmetric component**				**Asymmetric component**			
	After correction		**Before correction**		**After correction**		**Before correction**	
	RV	**P**	**RV**	**P**	**RV**	**P**	**RV**	**P**
H2: Antler crown *vs.* Antler rest	0.269	0.0000	0.422	0.0000	0.189	0.0000	0.190	0.0000
H3: Antler beam *vs.* Total tines	0.627	0.0451	0.714	0.0482	0.539	0.0245	0.542	0.0225
H4: Eye tine *vs.* Antler rest	0.397	0.0360	0.521	0.0646	0.248	0.0056	0.259	0.0100
H5: Trez tine *vs.* Antler rest	0.201	0.0000	0.279	0.0011	0.124	0.0000	0.129	0.0000

After the modularity hypotheses tests, morphological integration was studied using Partial Least Squares (PLS) (Rohlf and Corti 2000; Klingenberg et al. 2001; Klingenberg 2009; Baab 2013). This method calculates pairs of functions describing the covariation between two sets

of observed variables (in this case the shape variables of each proposed module) (Sampson et al. 1989; Klingenberg and Zaklan 2000). As in other dimension reduction techniques (e.g. principal component analysis), the first function (i.e. PLS1) explains the largest percentage of covariation, and thus will be the one discussed here. Again, the PLS was performed for both the individual variation and the FA (Table 5.4). All the morphometric analyses were conducted with the software MorphoJ (Klingenberg 2008b, 2011) and Morphologika2 (O'Higgins and Jones 2006).

Table 5.4. PLS results for each modularity hypotheses proposed, after the allometric correction. For each antler partition and their corresponding shape component, the percentage of total covariation explained by the first PLS axis (%Total Cov PLS1), the correlation between subsets (Corr. PLS1) and the associated p-values (P) are shown.

Complete dataset	**%Total Cov PLS1**	**Corr. PLS1**	**P**			
H1: Right side *vs.* Left side	74.95	0.97	<0.001			
Half antler datasets	**Symmetric component**			**Asymmetric component**		
	%Total Cov PLS1	**Corr. PLS1**	**P**	**%Total Cov PLS1**	**Corr. PLS1**	**P**
H2: Antler crown *vs.* Antler rest	56.30	0.79	<0.001	40.86	0.79	<0.001
H3: Antler beam *vs.* Total tines	38.50	0.86	<0.001	39.65	0.92	<0.001
H4: Eye tine *vs.* Antler rest	60.99	0.83	<0.001	59.71	0.82	<0.001
H5: Trez tine *vs.* Antler rest	51.39	0.71	<0.001	50.98	0.59	<0.001

5.4 Results

5.4.1 *Allometric effect*

The multivariate regression of shape on CS showed a statistically significant allometric effect in the complete antler dataset ($p<0.0001$), which explained 11.43% of the total shape variation. In the half antler dataset, the allometric effect was significant on both the symmetric and the asymmetric components of antler shape ($p<0.0001$ in both cases), representing 14.36% and 2.29% of the total shape variation, respectively. Therefore, the covariance matrices of the regression residuals were used to test the presence of modularity.

5.4.2 *H1: Complete Dataset – Right antler side vs. Left antler side*

Although the frequency graph seemed to suggest different semi-independent subunits (Fig. 5.4a), the RV coefficient indicated the absence of modularity between the two subsets defined (RV= 0.773; $p < 0.0001$). In addition, the PLS1 revealed a significant percentage of covariation (74.95%; $p<0.001$) and correlation (0.97; $p<0.001$) between the proposed modules, suggesting the presence of high integration among them (Fig. 5.5a).

5.4.3 *H2: Half antler Dataset – Antler crown vs. Antler rest*

A significant RV coefficient was obtained for the symmetric component of the second hypothesis (RV= 0.269; $p< 0.001$), which indicated the presence of modularity between the subsets proposed. The presence of modularity was also evident in the frequency graph (Fig. 5.4b1), despite the distribution appearing slightly shifted to the right (which would

suggest certain degree of covariation between the two hypothetic modules). The first PLS axis showed a significant percentage of covariation (56.30%; $p<0.001$) and correlation (0.79; $p<0.001$), suggesting the presence of integration between subsets (Fig. 5.5b1). Regarding the asymmetric component, the RV value obtained was also significant, but lower than that of the symmetric component (RV= 0.189; $p< 0.0001$). The corresponding frequency graph corroborated the presence of modularity suggested by the RV value (Fig. 5.4b2). The PLS analysis also showed a significant but lower covariation respect to the symmetric component ($p<0.001$; 40.86%), and an identical correlation (0.79; $p<0.001$), again indicating integration among the subsets proposed (Fig. 5.5b2).

5.4.4 *H3: Half antler Dataset – Antler beam vs. Total tines*

The symmetric component of the third hypothesis showed a non-significant RV coefficient (RV= 0.627; p= 0.0451), although the frequency graph seemed to indicate otherwise (Fig. 5.4c1). This, confirmed the absence of modularity between the subsets proposed. The PLS1 showed a significant percentage of covariation ($p<0.001$; 38.50%) as well as a positive correlation between the modules proposed (0.86; $p<0.001$) (Fig. 5.5c1), which supports the results of absence of modularity in favour of a higher integration level. Regarding the asymmetric component, although its RV coefficient seemed significant (RV= 0.539; p= 0.0245), after the Bonferroni adjustment (α= 0.005) the presence of modularity was rejected. The corresponding frequency graph suggested certain degree of covariation between the hypothetic modules (Fig. 5.4c2). Finally, the PLS1 showed a slightly higher significant covariation

(p<0.001; 39.65%) and correlation (0.92; p<0.001) between the subsets proposed, than in the symmetric component (Figure 5.5c2). Thus, the results would indicate that the main antler beam does not act as an independent unit.

5.4.5 *H4: Half antler Dataset – Eye tine vs. Antler rest*

Both the significant RV coefficient (RV= 0.397; p = 0.0360) of the modularity test performed on the symmetric component of shape and the frequency graph (Fig. 5.4d1) suggested the presence of an independent module in the eye tine, but modularity was rejected after the Bonferroni adjustment (Table 5.3). The PLS1 showed a significant percentage of covariation (p<0.001; 60.99%; Fig. 5.5d1) and a positive correlation (0.83; p<0.001), supporting the presence of high integration levels between the subsets defined. The same analyses performed over the asymmetric component of the hypothesis, showed absence of modularity (RV= 0.248; p = 0.0056), which is not supported by the corresponding frequency graph (Fig. 5.4d2). The PLS1 resulted in a slightly lower but significant percentage of covariation (p<0.001; 59.71%) and correlation (0.82; p<0.001) between subsets than in the symmetric component (Fig. 5.5d2).

5.4.6 *H5: Half antler Dataset – Trez tine vs. Antler rest*

The modularity test of the symmetric component revealed a significant RV coefficient (RV= 0.201; p < 0.0001). This result was supported by the RV frequency graph (Fig. 5.4e1). The PLS1 suggested that, despite the presence of a considerable degree of modularity, a significant percentage of covariation (p<0.001; 51.39%) and correlation (0.71; p<0.001) between

modules also existed (Fig. 5.5e1). Regarding the asymmetric component, a higher and also significant modularity level than in the symmetric component was found (RV= 0.124; $p < 0.0001$), which is also clearly observed in the corresponding frequency graph (Fig. 5.4e2). In addition, the PLS1 of the asymmetric component resulted in a significant percentage of covariation ($p<0.001$; 50.98%) and correlation (0.59; $p<0.001$) between subsets (Fig. 5.5e2).

5.5 Discussion and conclusions

5.5.1 *Complete antler dataset*

Bilateral structures as antlers, are present in the right and left body sides of individuals and share the same genetic base, developmental programs and environment (Klingenberg and Zaklan 2000; Bartos et al. 2007). Nevertheless, it has been suggested that some bilateral structures, as for example the right and left limbs of vertebrates could act as independent modules (Schlosser and Wagner 2004). Thus, what should we expect about antlers? Our results showed observable differences between antler sides (see results section 4), which made us contemplate the possibility of both antler sides acting as independent modules. However, the first modularity hypothesis tested (H1) was rejected, and thus both antler sides could not be considered as separate units. Furthermore, it has been documented that the antler cast process may not occur synchronously between sides, since they can be lost with a day of difference (Price et al. 2005). Accordingly, the regeneration process can start with a few hours of difference between sides, which could explain why the frequency graph suggested certain degree of modularity (Fig. 5.4a).

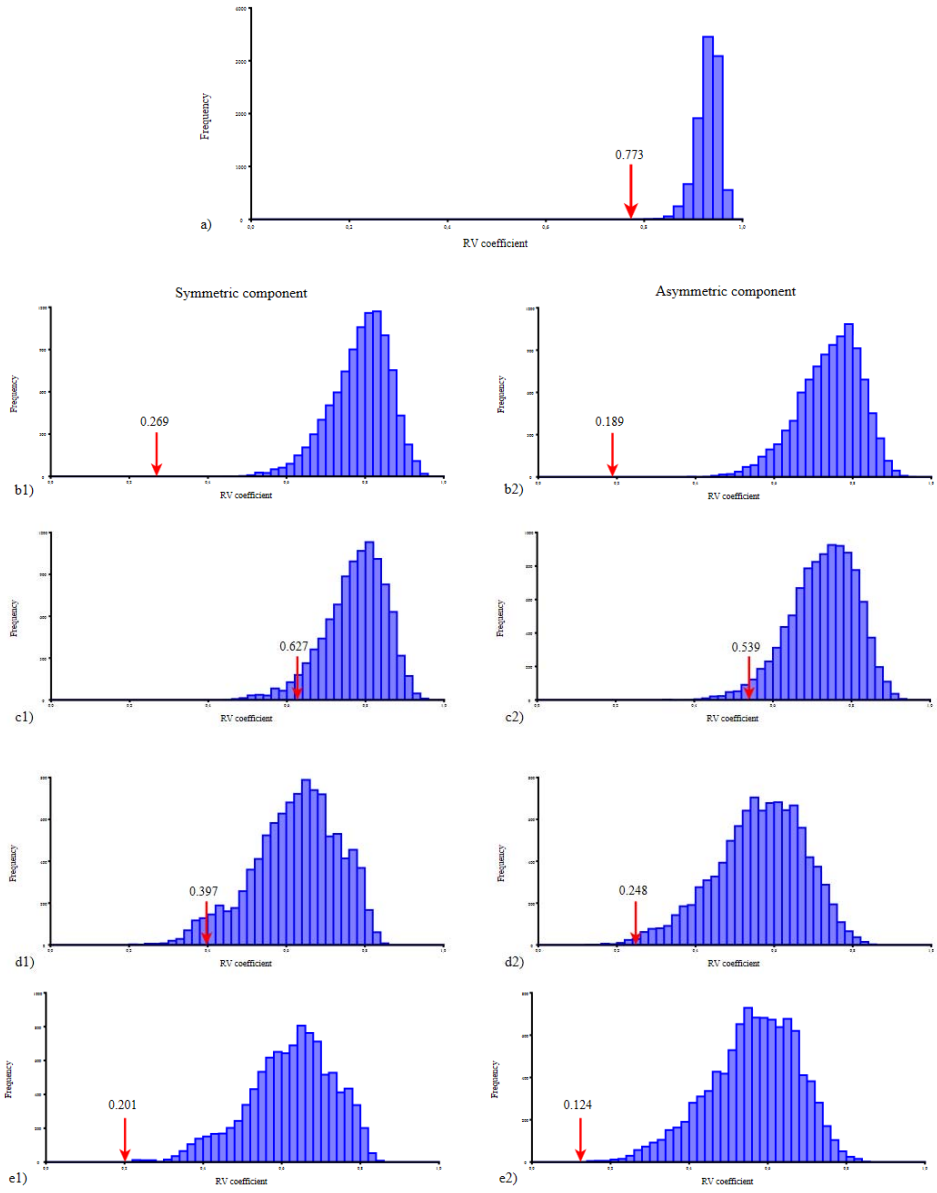

Figure 5.4. Frequency graphs of the RV coefficients for all the modularity hypotheses tested on the antler shape of Iberian red deer. In the half antler hypotheses, results for the symmetric and asymmetric components of antler shape are given separately. The red arrow represents the lowest RV coefficient value between the tested modules.

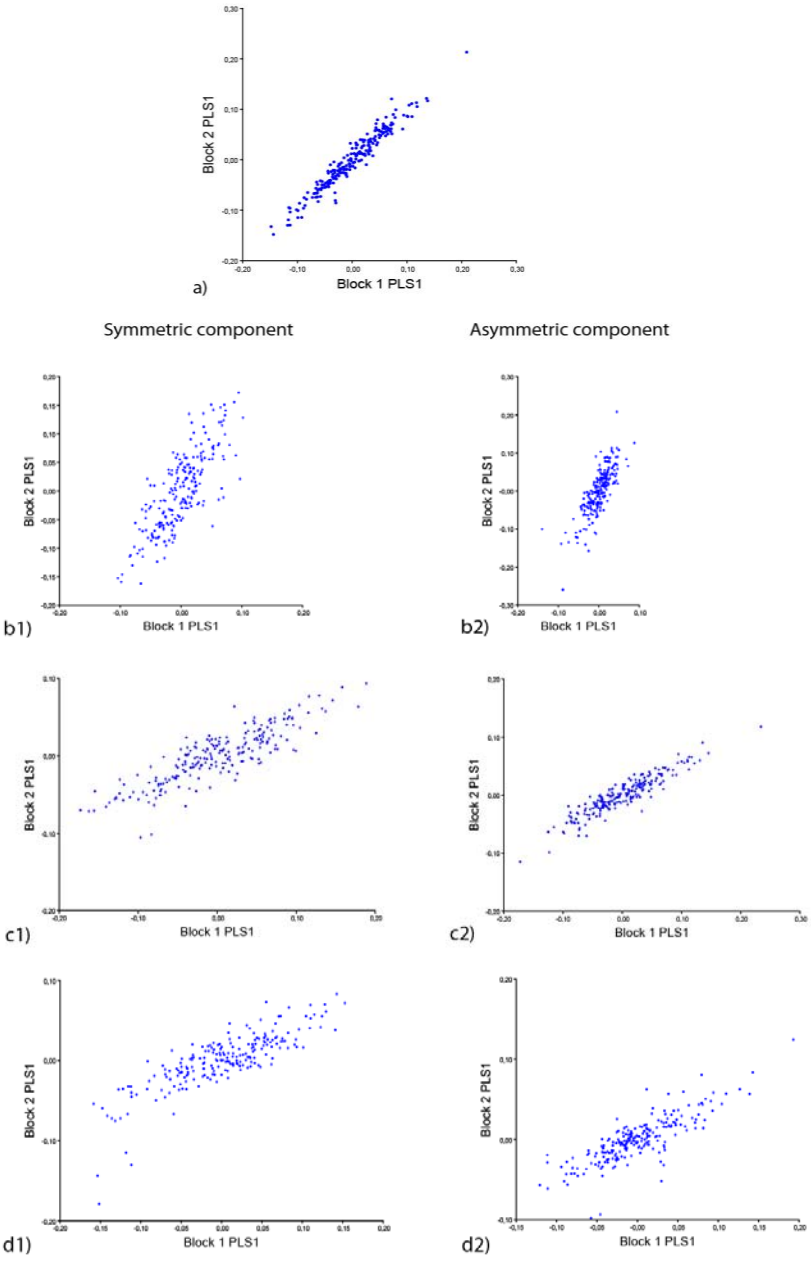
Block 2 PLS1
Block 1 PLS1
a)
Symmetric component
Asymmetric component
b1)
b2)
c1)
c2)
d1)
d2)

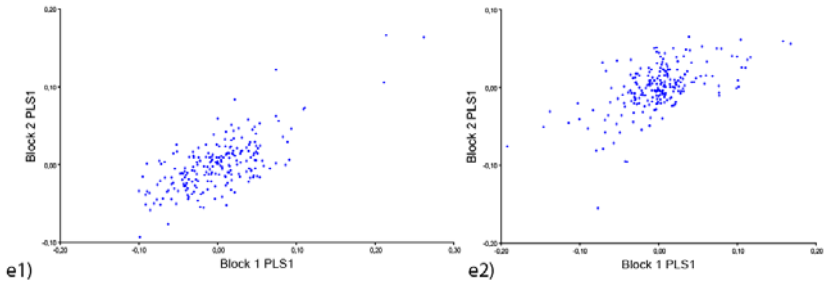

Figure 5.5. Partial Least Squares graphs for the different modularity hypotheses proposed. In the half antler hypotheses, covariation between subsets is shown separately for the symmetric and asymmetric components of antler shape (figures b1 to e2).

The high amount of significant covariation between antler sides showed by PLS1(74.95%), suggested a high integration level between antler sides, which could be related to the almost synchronous growth of both sides (Price et al. 2005), and also to their shared developmental programs (Park et al. 2004). In contrast, a previous PCA performed on the complete dataset suggested coordinated shape changes between the different parts of both antler sides (Fig. 5.3), which supported the existence of a modular structure (as in mice lower jaws; Martínez-Vargas 2012). In conclusion, the absence of modularity between antler sides suggests that the Iberian red deer antler would act as a fully integrated module comprised by different units, whose variation occurs in a coordinated way throughout the antler development.

5.5.2 *Half antler datasets*

The different antler parts would interact to perform a common function as the head and eyes protection during fights and velvet shedding (Pruitt 1966; Malo et al. 2005), or as an organ associated with deer reproductive and social success (García et al. 2010). However, the results of the

modularity analyses suggest the existence of two modules, an antler crown module and a trez tine module. Despite that, the high levels of integration found in the PLS suggest that the modules found are not completely independent of the rest of the antler, which did not constitute a separate module. Apparently, we could expect that a higher modularity level found on an organism a lower integration between its parts is observed. Conversely, to have found significant modularity and integration in the subsets compared, shows the strong relationship between both phenomena (Klingenberg 2008a and 2013). Therefore, the hypothetic modules observed along the antlers would not be as independent as expected at first, which would be consistent with the fact that modularity occurs in different degrees (Klingenberg et al. 2003; Klingenberg 2008a and 2013). In turn, the action of previous internal processes, closely linked to tissue antler differentiation, could be also signalling the existence of developmental units spatially defined (Klingenberg 2009). On the other hand, the suggested antler beam and eye tine modules were not supported by the present results.

Generally, this study shows that the variation patterns of the antler traits among individuals, as well as the variation patterns related to FA coincide, implying that the different pathways involved in both cases are responsible of the covariation observed along the sampled antlers. Thus, the continued growth observed in antlers would be influencing the integration levels found (Pomiankowski and Moller 1995; Gyurján et al. 2007), as well as the morphological variation of the different antler parts (Klingenberg 2008a). However, in the same way that the mechanisms implicated in an organism development are expected to generate

covariation between the observable traits (Klingenberg 2008a), environmental factors can affect the overall antler regeneration, promoting phenotypic changes (Alvarado 2004) that might also act as integrating factors (Klingenberg 2009), independently of the genetic control involved during the process (Li et al. 2002; Gyurján et al. 2007; Molnár et al. 2007; Lord et al. 2007).

Therefore, this study describes the general behaviour of different antler traits, suggesting that the sampled antlers would act as an internally homogeneous developmental structure.

The second hypothesis showed that the antler crown would behave as a module, which could be related to the high variation concentrated at that level, since generally as the antler crown increases in number of tines, it coordinately tends to bend with respect the antler rest causing the bow of the entire structure (see results section 3). The last fact, would be consistent with the previous coordinated shape changes observed in antlers (Fig. 5.3). However, the significant integration showed by the PLS, implied that the proposed modules are not completely independent. In addition, the positive correlation between modules, could be due to a parallel variation caused by genetic (Hartl et al. 1991 and 2003) and even environmental factors (Putman et al. 2000), similarly to what happens with the alveolar an ascending ramus of the mouse mandible (Klingenberg et al. 2003). In parallel, the variation due to direct developmental interactions was also observed in H2 through the study of the asymmetric antler component (Klingenberg and Zaklan 2000; Klingenberg et al. 2001; Klingenberg 2008a; Klingenberg 2013). These results again suggested that the variation along antler is characterized by developmental integration of modules partially independent, which is in agreement with

other studies (Leamy 1993; Klingenberg and Leamy 2001). In addition, the existence of integration at FA level, suggested that the possible effect of random perturbations suffered at direct developmental pathways could affect in a parallel way, other developmental processes being transmitted throughout the whole antler (Klingenberg and Zaklan 2000; Klingenberg et al. 2001).

Hypothesis three results suggested that both patterns of variation, among individuals and due to FA, broadly coincide as has been also found in the study of other organisms (Klingenberg and McIntyre 1998; Klingenberg and Zaklan 2000; Klingenberg et al. 2001). This coincidence probably means that the direct developmental pathways acting on antlers could be also the main mechanisms responsible for the covariation of its traits among individuals making the antler act as a single unit.

Hypothesis four, shows again a correspondence between the patterns of variation among individuals and FA, suggesting the absence of modularity in the eye tine. However, a lack of concordance between the covariation patterns among individuals and due to FA, has been observed in other studies (Debat et al. 2000; Klingenberg et al. 2002 and 2003), suggesting that the covariation among individuals would be generated in part by direct developmental interactions, but also because of the parallel action of other developmental processes, as for example allelic variations in genes (Klingenberg et al. 2003; Klingenberg 2008a, Jojic et al. 2011).

The results of the fifth hypothesis, suggest that despite the trez tine is involved in the same developmental process that the rest of the antler, its later appearance would provide it a relatively independent behaviour from the antler beam as well as from other tines, as the eye tine. It could be due

to forces acting in different moments of the antler regeneration process, such as genetic interactions suffered at antler tip level during tissue proliferation (Li et al. 2002). In this sense, developmental and genetic antler processes could be equally regulated in the same way as flowering plants, which apparently tend to show a strong functional integration within floral traits as well as within the rest of vegetative traits, but not across them (Conner and Sterling 1996; Juenger et al. 2005). Conversely, we do not known the specific genes responsible for the growth and development of each specific tine (J. Carranza personal comment). In a similar way, we cannot rule out a possible specialization of the antler tines based on the antler development process. These last two facts on tine development could again result in certain independence among the different antler parts.

On the other hand, the significant allometric effect detected in the complete dataset and both the symmetric and asymmetric components of shape in the half antler dataset, is in agreement with a previous similar study (Klingenberg 2009). Although size probably was not the primary factor of integration in the antler, its effect was nonetheless important, as shown by the decrease in the values of the RV coefficients and the increase in the modularity levels after using regression residuals to correct the allometric effect (Table 5.3).

Since the data used in this type of studies is a representation of the results of multiple developmental, genetic, functional and evolutionary interactions (Klingenberg et al. 2001, Klingenberg et al. 2003; Alvarado 2004; Klingenberg 2008a and 2009), it would be interesting for future prospects in this field to study whether separate developmental, genetic,

functional, or evolutionary modularity could be identified in antler shape, and to establish how these different types of modularity interrelate.

6. Quality assessment of the Iberian red deer antler (*Cervus elaphus hispanicus*) using a photogrammetric interactive method (PhIMM)

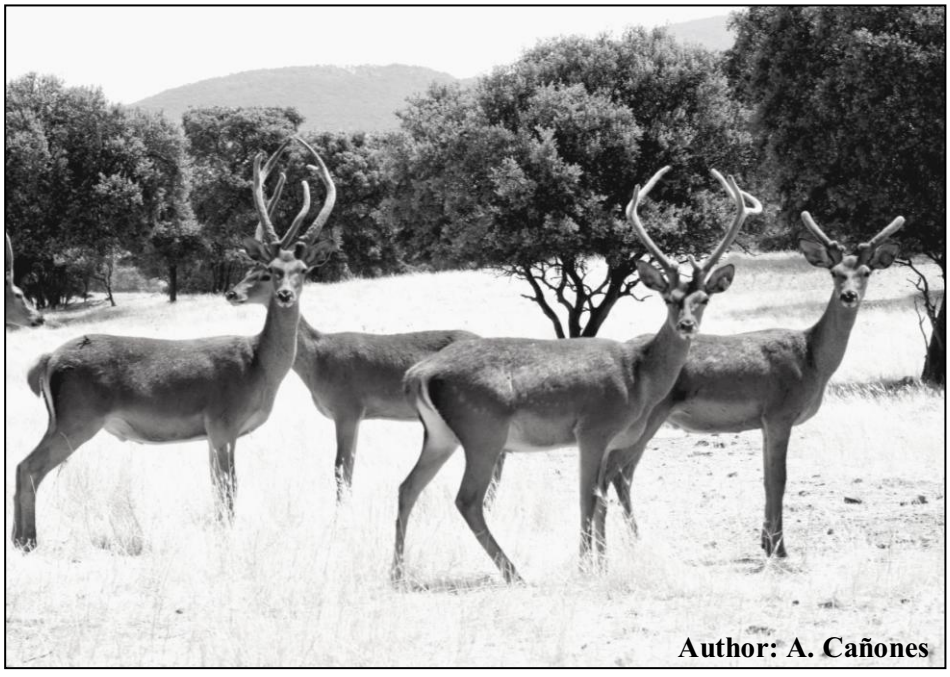

6.1 Abstract

Deer antler trophy homologation, as well as the obtention of biometric databases from antlers for subsequent analysis, have resulted in the development of different biometric tools. The present study compares three different methods of length measurement in order to develop a simple and reliable system for the quality assessment of deer hunting trophies. A set of Iberian red deer antlers (*Cervus elaphus hispanicus*) was used.

The antler lengths were determined alternatively using traditional measuring (Tape), an Articulated Arm Coordinate Measuring Machine (CMA), and a new photogrammetric technique based on a parametric computer-aided design system (CAD-3D). By means of this new photogrammetric method, a group of 3D parametric curves were generated inside the CAD system, representing the real lines to be measured on the antlers. These curves were generated according to a 3D ray tracing procedure, similarly to the projection system used in the photography. A comparison in order to assess differences between the three methods mentioned above was carried out. The three methods showed similar reliability, although the photogrammetric process, based on CAD-3D technology, was faster and more functional than the traditional measuring tape or the Articulated Arm machine. Moreover, since the photogrammetric method only requires two photographs by individual, it is possible to study a high percentage of antlers in the field. On the other hand, photogrammetric methods have the advantage of obtaining other interesting information for trophy homologation. Thus, through the photographs, it is possible to take into account different

aspects of subjective evaluation as for example the antler colour, the tines shape or the antler surface roughness, among others.

6.2 Introduction

From deer hunting point of view, there is a growing interest in antler assessment to trophy homologation, as well as in the obtention of biometric databases for later analysis. To accomplish this task, new tools and methodologies to facilitate and accelerate the collection and processing of geometric data are investigated.

Biometric tools, have been widely used for the quantification of morphological traits in individuals of different species. The latest measurement technologies applied on biological elements, provide results of high accuracy since they are supported by tools such as Coordinate Measuring Machines or 3D scanners. These tools are hardly reproducible in terms of precision either, in laboratories or controlled environments.

Articulated Arms Coordinate Measuring Machines (AACMM or CMA) are the most common measuring instruments used for the obtention of landmark coordinates. These articulated arms work acquiring the three-dimensional location of landmarks (homologous points) with regard to a reference system. Moreover, the CMA is a highly accurate method, easy to handle (Lockwood et al. 2002; Harvati 2008; Nicholson and Harvati 2006; Kimmerle et al. 2008).

However, there are several techniques that perform a highly efficient coordinate digitalization as for example 3D scanners, which are the most accurate collecting information in biometric and geometric morphometrics studies (Baltsavias 1999; Hennessy and Stringer 2002; Wang 2005; Brilakis et al. 2010; Korosec et al. 2010; Golparvar-Fard et al. 2011).

The information provided by scanners consists of clustered points, which reproduce the shape of the elements studied. From clustered points it is possible to create virtual reconstructions of biological elements for different purposes (Chin-Hung et al. 2007; Fortin et al. 2007; Shigeta et al. 2013). Due to the large amount of information obtained from scanners, data handling may be difficult. This amount of information involves performing a data selection, removing duplicate points, as well as the ones located in well-defined areas, and reducing redundant or in excess points (Golparvar-Fard et al. 2011; Ramos-Barbero and Santos-Ureta 2011). However, the digitizing process of scanners is sometimes incomplete, leaving areas without scanning, which results in a lack of information in the surfaces obtained. These faults must be corrected later through the use of other techniques. Pernot et al. (2006) used a mechanical model to simulate the curvature variation minimization. Yang et al. (2006) created and algorithm to fill n-sided holes with NURBS patches that interpolate the boundary curves. Wang and Oliveira (2007) presented and algorithm based on least squares and interpolate both, geometry and shading information. Panchetti et al. (2010) filled these holes by combining the geometric information available on the surrounding of the holes and the information contained in an image of the real object.

The three-dimensional models obtained from scanned points, do not exactly provide the information needed to be treated by biometric and geometric morphometrics techniques. Therefore, from the thousand points digitalized, only those consistent with landmarks are needed. Unfortunately, the approximation between digitalized points and landmarks is usually low. In order to solve this problem, segmentation techniques based on the identification of particular elements, such as

edges, vertexes or different sides of the 3D model, are used. The result is a 3D model of recognizable topology from which landmarks can be extracted (Zitová and Flusser 2003; Wang 2005; Wu and Yu 2005; Demarsin et al. 2007; Goyal et al. 2012). In the case of items with irregular shapes, such as some biological structures, additional difficulties could appear.

Photogrammetry consists of taking photographs from different locations called "viewpoints" and tracing rays from them to the objects. The rays obtained from different viewpoints are intersected to produce the three-dimensional coordinates of landmarks. By means of the mathematical intersection of converging rays in the space, the precise location of a point can be determined. Some advantages of photogrammetry are its flexibility, economic and small equipment, and that virtually there is no limit in the size and complexity of the objects measured. The main disadvantage of the method is the required manual processing. Nevertheless, several studies have found that photogrammetry is able to obtain similar results to contact or scanning methods, in terms of precision (Balsatvias 1999; Aguilar et al. 2005; Ramos-Barbero and Santos-Ureta 2011; Bhatla et al. 2012; Sánchez-Lasheras et al. 2012).

Therefore, many studies have used photogrammetry to obtain clustered points similarly to 3D scanners. This is achieved by a large number of photographs of the object, taken from different positions (Zitová and Flusser 2003; Baumberg et al. 2005; Shigeta et al. 2013). Generally, commercial tools based on the creation of networks of apparent contours are used to perform the photographs, but they are only useful when high accuracy is not required and the object geometry is not complex (Remondino and El-Hakim 2006; Prakoonwit and Benjamin 2007).

However, the use of photogrammetry for the obtention of clustered points do not avoid the problems mentioned above for clustered points obtained from 3D scanners. Thus, the same processes used to refine and to perform the segmentation of the information extracted from 3D scanners, are used to photogrammetric data and the obtention of the final landmarks.

The morphological data capture for the quality assessment of antlers, is usually done in situations which do not allow to take many photographs. The set of landmarks necessary for the geometric study of antlers is small compared with the number of clustered points. Accordingly, taking into account the exact definition of the landmarks selected, and leaving aside the detailed information necessary for carrying out the 3D models of antlers, the number of photographs required is considerably reduced.

Some authors addressed methods that could reduce the number of photographs (Veldhuis and Vosselman 1998; Ordóñez et al. 2008; Rodríguez et al. 2008), or proposed methods based on taking three photographs and three distances measured at three different calibrated positions (Styliadis 2008). Rodríguez et al. (2008) and Styliadis (2008), studied the use of a single image to reconstruct objects, based on known geometric restrictions of measured objects, id est. relationships among straight lines (co-planarity, parallelism, perpendicularity, symmetry and distance). These are not landmark based methods, which are applied to objects of simple shapes in other fields not related to biology.

In practice, the most versatile and accurate method to study antler morphology using a few landmarks and a reduced number of photographs by specimen, has been the recreation of the photogrammetric scene of antlers in a parametric CAD-3D environment.

The CAD modelling technique has been widely used to create human anatomical parts (bio-CAD modelling) by modelling bones and organs for the manufacture of moulds and prototypes (Sun 2005; Kurazume 2009), or in the surgical planning and assessment of bone pathologies (Minns et al. 2003). Fortin et al. (2007) developing a personalized design and adjustment of spinal braces by means of 3D visualization of the external trunk surface with the underlying 3D bone structures. Parametric CAD models have been also used in the design of body components in order to replace injured elements (Li et al. 2009). This technology has also been proved useful for the computer modelling of antlers. Specifically, virtual models of real antlers have been successfully created in order to calculate its density, as a substitute method to the less accurate based on the Archimedes principle (Paramio et al. 2012).

The method proposed in the present study develops projective techniques of photogrammetry, within a parametric software based on three-dimensional Computer Aided-design technology (CAD-3D). This software allows to reproduce virtually the real scene crossed for the light rays tracing a picture, in a three-dimensional way.

Therefore, the main objective of the study was to develop and apply a photogrammetric method, based on parametric CAD-3D technology, for which it has been necessary to refine the art of taking photographs in the field. This method only requires two photographs by individual. Thus, the reduced number of photographs allows the study of a high amount of antlers. In addition, the new technique, called Photogrammetric Interactive Measure Method (PhIMM), has been tested as a versatile tool to obtain a large amount of geometric data in a short time and even under unfavourable conditions.

6.3 Material and methods

To validate the PhIMM, an Iberian red deer (*Cervus elaphus hispanicus*) population, one of the species of greatest hunting importance in the South of Spain, has been studied in order to obtain geometric information from their antlers and to assess the quality of the animals as hunting trophies.

6.3.1 *Study area and sample*

A sample of 14 antler trophies of different sizes and tine number was used. The antler trophies came from two different public big game states located at the Northwest of Sierra Morena (Andalusia, Spain), Lugar Nuevo (LN) and Selladores-Contadero (SC). Specifically, antlers from the 2008 and 2009 hunting seasons were collected.

6.3.2 *Geometric data for antler trophy homologation*

Traditionally, trophy homologation has been based on the measure and score allocation of antlers according to the guidelines described in hunting protocols (García et al. 2010). In the case of the sampled antlers, the following elements were taken into consideration (Fig. 6.1): the main shaft length, the eye tines length, the trez tines length, the burr perimeter, the perimeters of certain antler points and the maximum internal separation of antlers. However, there are other quantitative and qualitative antler elements whose valuation is subjective, namely antler colour, tines colour and its tip shape, antler surface roughness (presence of pearls), total number of tines, crown length and its number of tines, bez tines length or total antler weight.

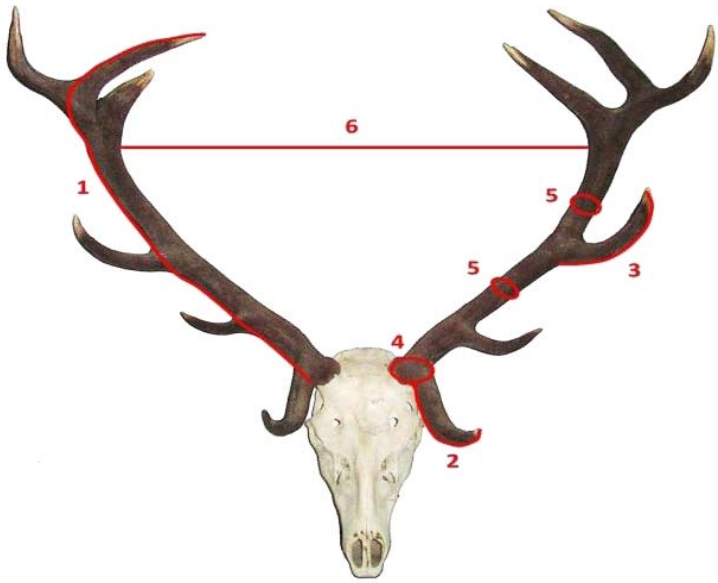

Figure 6.1. Elements to be measured in trophy homologation: 1: Main antler shaft length, 2: Eye tines length, 3: Trez tines length, 4: Burr perimeter, 5: Perimeters of certain antler points. 6: Maximum internal separation of antlers.

6.3.3 *Instrumental, hardware and software*

The corresponding photographs were taken using a handheld PowerShot SX210 IS digital camera, with a resolution of 4320x3240 pixels.

The parametric variational CAD system used was SolidWorks by Dassault Systems. A special computer was not required for the processing of the photographs using SolidWorks. However, it was necessary to have a high level graphic card to a better analysis of the photographs.

Antler measuring was performed using both, traditional methods (tapes and callipers) and an articulated arm coordinate measuring machine (AACMM or CMA) model MicroScribe G2X, with 50" of sphere and 0.009" (0.23 mm) of accuracy.

6.3.4 *Photogrammetric method and CAD-3D technology*

The photogrammetric interactive method (PhIMM) proposed consists of the representation of a structure in a three-dimensional virtual space. To carry it out, two photographs from different perspective of the structure must be taken to allow the location of common reference points.
The light rays captured by a camera are those coming from an object that fall on the plane of a photograph and pass through a lens (Fig. 6.2).

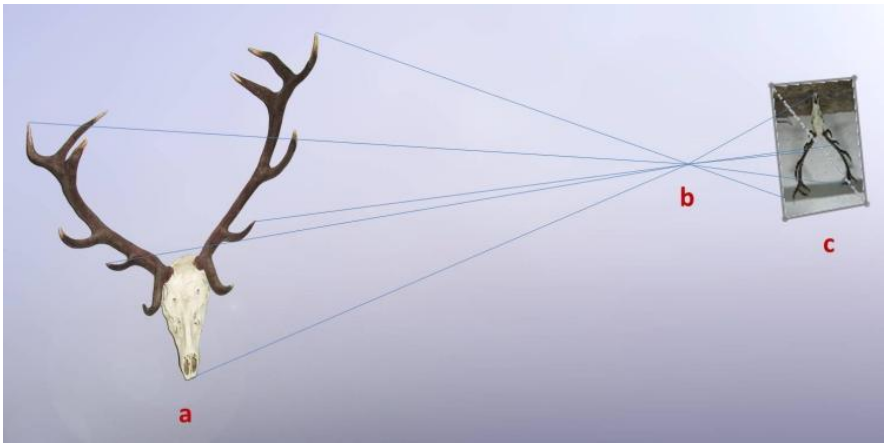

Figure 6.2. Trajectory of the rays of incidence on the plane of a photograph. a) Real object; b) position of the camera lens; and c) photograph.

Conventionally, the plane of a photograph was found in a film or negative, but at present it is found on a digital CCD reader. In the photograph plane the real image is reproduced, reduced in scale and inverted. Along the rays that run to the photograph plane, successive homological enlargements or reductions of the photograph can be located in parallel planes (Fig. 6.3). The homology centre is located at the position of the camera lens.

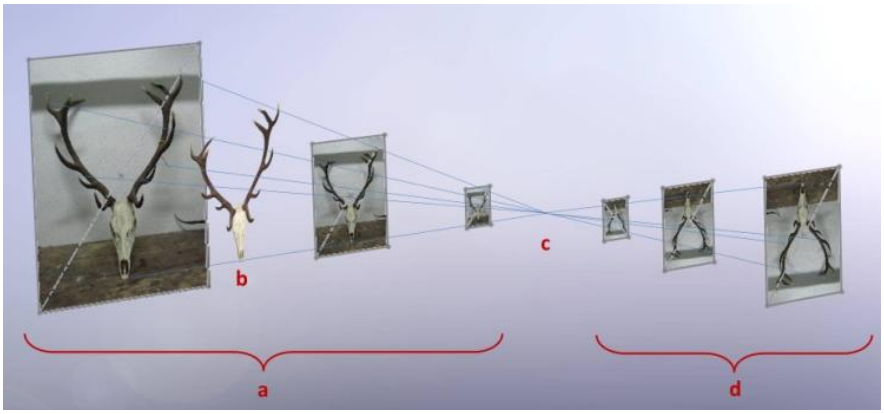

Figure 6.3. Homological images placed in parallel planes, adapted to the ray beam of a photograph. a) Non-inverted homological images; b) position of the camera lens (centre of homology); and c) Inverted homological images.

However, the obtention of non-inverted homologous images of the photograph, it is also possible. The non-inverted images would appear in planes located between the camera and the real object, or behind the real object. The proposed method, uses a non-inverted image located behind the real object with a scale factor according to the object size (Fig. 6.4).

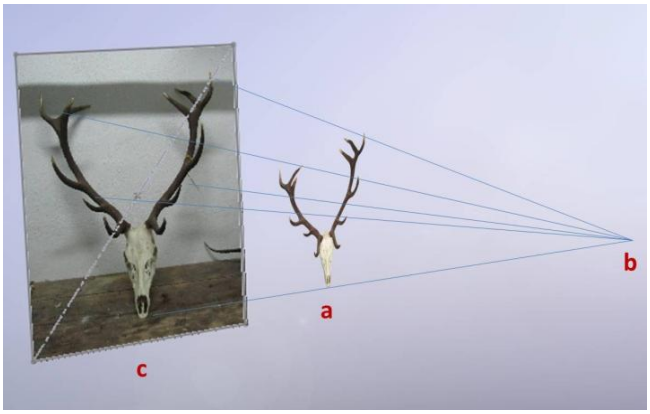

Figure 6.4. Chosen situation in the method. The object is located between the homology centre (lens) and a non-inverted photographic image. The photographic image will be always placed behind the object and will be larger than it.

In order to perform the photogrammetric measure of antlers through photographs, it is necessary to include within each photographing scene an item of known geometry and size as metric reference. In the present case, a rectangular piece of 50x50 (cm) dimensions, whose four corners must be clearly included in the photograph, was used (Fig.6.5).

Figure 6.5. Metric reference element of known dimensions (square plate of 50x50 cm).

A Computer Aided-design CAD-3D software (Solidworks) helps to represent a virtual scene from the light radiation emitted by the objects, in this case antlers, and captured on each photograph. The corresponding photograph is framed in a rectangle where a diagonal is traced. The midpoint of the diagonal corresponds to the photograph centre (Fig. 6.6a). From this central point, a line perpendicular to the plane of the photograph is traced. This line represents the axis of a pyramid whose apex will correspond later to the origin of the radiation affecting the picture (Fig. 6.6b).

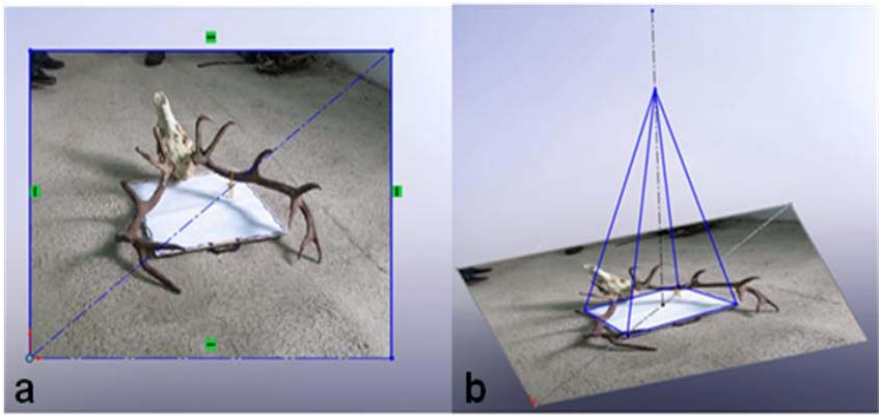

Figure 6.6. a) Creation of the rectangular frame of the photography; b) pyramidal ray beam for obtaining the homology centre.

The pyramid is built on a square, which is included in the photograph plane. Furthermore, the pyramid has four lateral edges that join in the apex of the perpendicular axis described above. The four corners of the pyramid base coincide respectively with the visualization on the picture of the four corners of the rectangular metric reference used. However, at this time, the origin of the radiation affecting the picture or the pyramid apex position, it is still not determined (Fig. 6.6b). To determine the exact position of the radiation origin, it is necessary to match the lateral edges of the pyramid with the vertexes of a square that measures the same than the metric reference (50x50 cm). Then, since the CAD system is variational parametric, the apex of the pyramid reaches a fixed position, solving the geometric problem (Fig. 6.7a). Therefore, the apex position corresponds to the exact location in which the photo was conducted, id est., the camera position. This process is repeated for a second photograph by creating a new pyramid linked to the photograph plane. Accordingly, it is possible to obtain the position of a second camera (Fig. 6.7b).

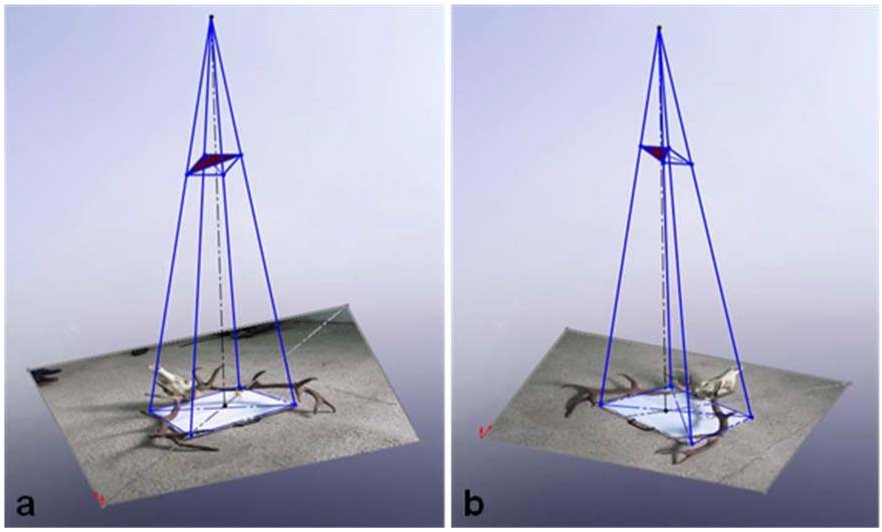

Figure 6.7. Inclusion of the metric reference in the lateral edges of the pyramid. a) Centre of homology of the first photography; b) Centre of homology of the second photography.

At this point, the same virtual scene is represented from two different points of view with two ray beams departing from each camera position, passing through the real object and affecting the plane of each photograph. Moreover, there is a common element to both ray beams in the space, the square metric reference.

Then, a new three-dimensional space where the two radiations affecting the picture match with the two reference elements contained in the lateral edges of the corresponding pyramids, is created (Fig. 6.8a). Thus, a system formed by two projective ray beams can fully represent the real scene.

The next step of the process is matching those rays of light from the two origins of radiation, which reach the plane of their corresponding

photograph. The point where the ray of light touches the photograph is matched with a specific point of the photographed item. The same is done with the ray of light of the second photograph, until matching with the corresponding element. The point where both rays of light intersect represents the real position of the studied object in the space (Fig. 6.8b).

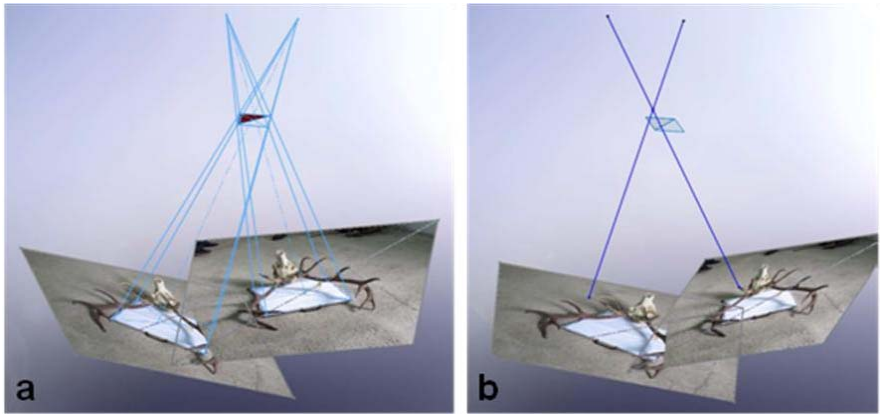

Figure 6.8. a) Superposition of the radiation of the two photographs; b) spatial location of a point from the two photographs.

The matchmaking of more rays of light allows to obtain real distances between visible points of both photographs. Example of this is that a succession of points, located along the surface of the curve of the main antler shaft, leads to the obtention of both, the real position of the curve and its length (Fig. 6.9a, b and c). The different points of the surface are joined by spline curves, which length is easily calculated by the system.
The advantage of performing this procedure by a variational parametric CAD system, is that the antler measurements relevant from the hunting point of view, can be repeated with agility and rapidity.

The statistical analysis was performed using Statgraphics Centurion XV v15.2.06 (Stat Point, Inc). Data normality and homoscedasticity assumptions were tested through a Shapiro–Wilk test and a Levene's test, respectively. Then, differences between the antlers measured using three different methods (traditional measuring (Tape), coordinate measuring machine (CMA) and the PhIMM (CAD)) were assessed. An analysis of variance (ANOVA) and a multiple comparison test were also used. Finally, a correlation coefficient was calculated to assess the relationship among the lengths obtained by the three methods.

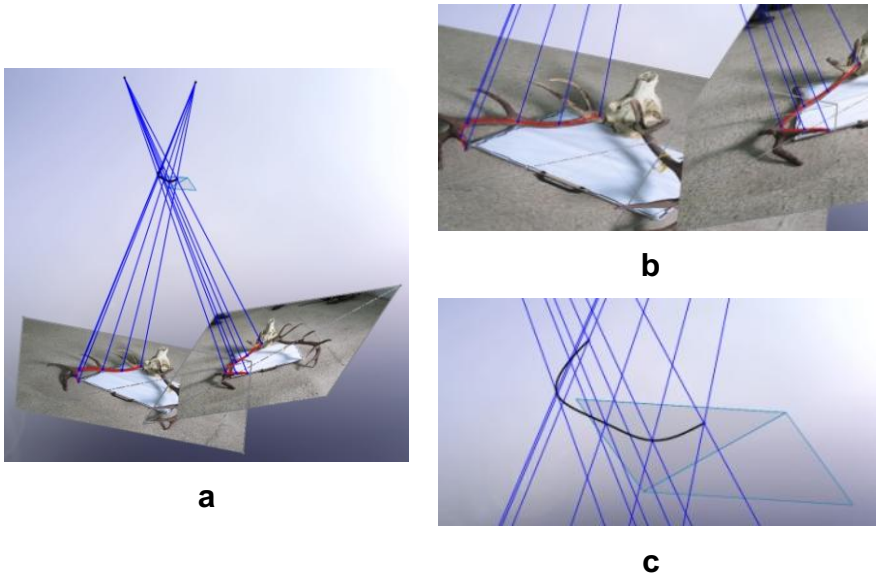

Figure 6.9. Obtention of the real position of a series of points and of the curve length joining them. a) ray beams; b) adjustment of the curves on the photographs; c) obtaining of the curve and its true magnitude.

6.4 Results and discussion

The antler shaft length, the eye tines length, the trez tines length and the maximum internal separation of the antler branches were calculated using the three different methods already quoted (Table 6.1). The comparison between the perimeters at the three positions defined in the homologation process (Fig. 1) using two methods, Tape and CAD, was performed (Table 6.2).

Table 6.1. Statistical results of eye tine lengths, trez tine lengths, main shaft length and maximum internal separation of antlers using the three methods (Tape, CAD and CMA).

			Length (cm)		ANOVA
Element	**Nº**	**Method**	**Range**	**Mean ± St. Deviation (CV)**	**(P-value)**
Eyetines	28	CAD	7.43 - 34.68	21.94 ± 6.57 (29.93%)	F= 0.2; p= 0.82
		CMA	8.17 - 31.6	22.71 ± 6.04 (26.61%)	
		Tape	6.0 - 33.0	21.68 ± 6.40 (29.52%)	
Treztines	28	CAD	8.73-34.94	18.83 ± 6.75 (35.85%)	F= 0.11; p= 0.89
		CMA	8.6- 34.9	19.47 ±6.39 (32.81%)	
		Tape	8.5- 35.0	19.61 ± 6.46 (32.94%)	
Mainshafts	14	CAD	42.76 - 85.47	66.35 ± 13.05 (19.67%)	F= 0.04; p= 0.96
		CMA	42.4 - 86.8	65.75 ± 12.90 (19.62%)	
		Tape	40.0 - 82.5	65.34 ± 12.84 (19.65%)	
Separation	14	CAD	35.14 - 77.14	56.98 ± 10.86 (19.05%)	F= 0.01; p= 0.99
		CMA	36.1 - 79.7	57.16 ± 11.00 (19.25%)	
		Tape	35.5 - 76.0	56.54 ± 10.49 (18.56%)	

There were not significant differences (with a significant level of 0.05) between lengths using any of the three methods (eye tines p = 0.8190; trez tines p = 0.8929; main shaft p = 0.9572; and maximum internal separation p = 0.9877).

The perimeters calculated either were not significantly different between positions (perimeters at the burr p = 0.6770; perimeters at position 1 p = 0.8202; and perimeters at position 2 p = 0.8455).

Table 6.2. Statistical results of Perimeters at the three positions defined by the homologation process using two methods (Tape, CAD).

			Perimeter (cm)		ANOVA
Position	**Nº**	**Method**	**Range**	**Mean ± St. Deviation (CV)**	**(P-value)**
Burr	28	CAD	10.73-21.84	16.59±2.67 (16.11%)	F= 0.18; p= 0.68
		Tape	10.5-21.0	16.32± 2.27 (13.89%)	
Position 1	28	CAD	8.49-13.6	10.97± 1.72 (15.72%)	F= 0.05; p= 0.82
		Tape	8.5-14.0	11.07±1.69 (15.29%)	
Position 2	28	CAD	7.5-13.09	10.15±1.67 (16.45%)	F= 0.04; p= 0.85
		Tape	8.0-13.0	10.23±1.65 (16.10%)	

Results were more similar in the case of higher lengths (main shaft and maximum internal separation). This fact is caused because in both CMA and CAD methods, the lengths are estimated by curves passing by a set of chosen homologous points. These curves are more adaptable for big lengths because the number of homologous points is higher. The tines usually are defined by only three or four landmarks, while the main shaft could be defined by more than 20. In the case of the internal separation of the antlers, the similarity is still higher because it fits a straight line.

Antler measurements performed by the Tape method require about 20 minutes. These measurements must be done carefully, if possible on a

table. The CMA method must be preferably applied in a laboratory, taking about 30-40 minutes by antler. Finally, the CAD method just involves some seconds in taking the two photographs by specimen. However, the photo processing takes about 30 minutes by antler, but it is carried out afterwards through a computer, and far from the field. The Tape method requires measurements taken by different people, or at least performed by trained people, to obtain good results. It is impossible to do that in the field or at a hunting day, since the number of specimens is usually high and the conditions are difficult. The CMA method is even more difficult to be carried out in the field. Taking into account the antler measurements considered by the current trophy homologation protocols, the CMA method would be the less appropriate, since it is not suitable to measure perimeters. However, this would not be inconsistent with the quality assessment of antler trophies using other criteria (e.g. TQS; Martínez-Salmerón et al. in prep.; see section 3).

6.5 Conclusions

After the validation of the PhIMM using a collection of antler trophies and the obtaining of the corresponding parameters, the results were compared with the ones observed through traditional and CMA methods. The three methods showed similar results, providing analogous values for the different antler lengths measured. Differences of size and shape among the sampled antlers were likely, since they belonged to stags from different ages and ecological conditions during the antler growth.

The Tape and CMA methods are certainly more complex and sometimes more difficult to use at the field than CAD method. Since CAD method

only requires two photographs by individual, it is possible the study of a high percentage of antlers in the field. On the other hand, photogrammetric methods have the advantage of obtaining more interesting information. By means of photographs it is possible to take into account a set of data whose valuation is rather subjective, as for example antler color, tines shape or antler surface roughness, among others.

The CAD method has become a useful tool to provide data as lengths, angles, diameters, perimeters, etc. necessary to either, trophy homologation or morphometrics analysis. In addition, the CAD or PhIMM is a low cost method, which implies low time consumption.

This work has also tried to show the usefulness of the CAD method as an optimal choice in the field of zoological studies, such as those related to geometric morphometrics of deer antlers. Additionally, performing the necessary adjustments, this method could be applied to any anatomical part of any animal species.

7. General discussion

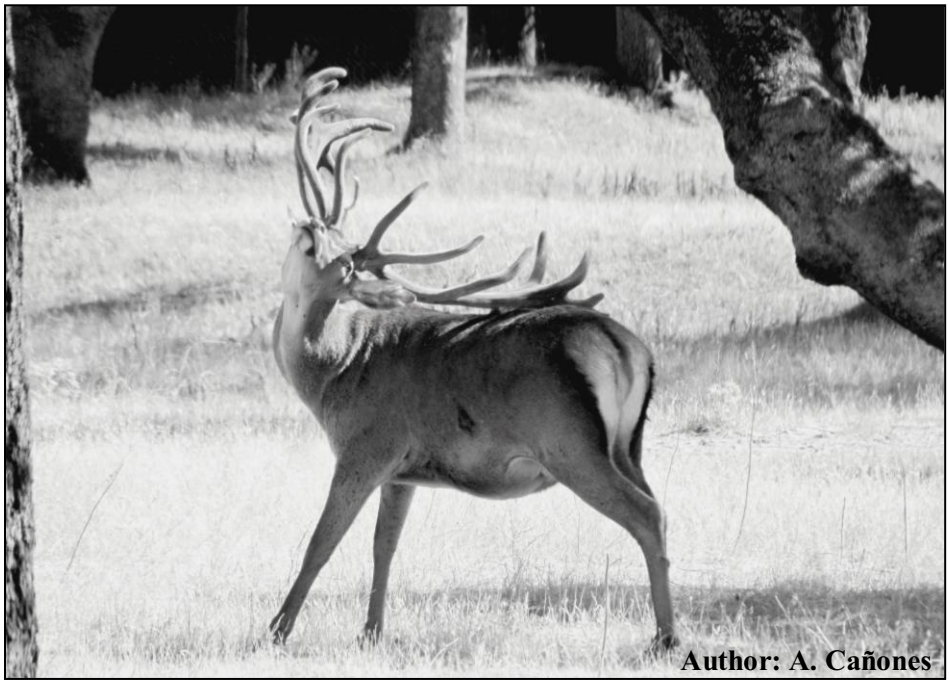

7. General discussion

Previous studies about deer antlers have provided a wealth of knowledge about them (see for example Clutton-Brock et al. 1982; Geist 1998; García et al. 2010). Antlers are scientifically interesting (Gómez et al. 2013; Landete-Castillejos et al. 2013), since they are basis of biomedicine studies, such as the synthesis of biomaterials for regenerating bone structures, or studies related to bone density (Zioupos et al. 2000; Baciut et al. 2007; Estevez et al. 2008; Landete-Castillejos et al. 2010). The emergence of new technologies, has involved a new avenue of exploration to obtain more and better information about different antler aspects. For that reason, this work especially focuses in analyzing some antler features using innovative methodologies, as geometric morphometrics and photogrammetric interactive methods.

Along this research, the economic importance of the Iberian red deer (*Cervus elaphus hispanicus*) in Sierra Morena, has been highlighted (Carranza 1999; Azorit et al. 2002a; Garde et al. 2010; García et al. 2010). Deer represent a very important source of income, not only in reference to the piece charged, but for the value given to the antlers as hunting trophies (Landete-Castillejos et al. 2013; García et al. 2010). Therefore, the morphology and structure of antlers is important.

The antler structure has been widely defined, generally referring to the order of appearance of the different tines with age (see for example Montoya 1999; Azorit et al. 2002a; Fierro et al. 2002; García et al. 2010). Nevertheless, the results obtained in this study have shown the possibility to determine in larger detail the shape changes experienced by antlers, according to age. Hence, the shape changes of common parts to all the

antlers sampled, as beams, eye tines and trez tines, have been observed and described precisely.

Such accuracy in antler shape change description, substantiate the idea that geometric morphometrics techniques, the main methodology used here, are useful for quantifying shape changes in complex structures. In addition, although this work has been based on a local sampling, this methodology could be applied to the study of the shape change patterns of other ungulate species that display antler. Thereby, antler models of similar complexity and hunting interest than Iberian red deer could be studied, as would be the case of fallow deer (*Dama dama*). In addition, geometric morphometrics could be also applied to paleontology, as for example the Irish elk (*Megaloceros giganteus*).

The increasing complexity of antlers with age, in terms of the number and position of its tines, especially occurs at antler crown level (Azorit et al. 2002a; García et al. 2010). Consequently, the crown is a highly variable part, extremely difficult to study. Apparently, it is not known the maximum number of tines that the antler crown can achieve, as well as their position. Thus, a big challenge in this field would achieve to measure and describe whether the antler crown shows a particular pattern of shape change.

According to different authors, antlers reach their maximum size development and number of tines, between 8-12 years old (Nahlik 1992; Montoya 1999). Briefly, it is assumed the existence of an optimum age for antler. In the present research it is found that individuals from age class 4 (8-9 years old) generally presented the maximum number of tines, that means producing the best trophies, which would be in agreement with

Montoya (1999). Nonetheless, an optimum trophy age was not clearly defined at the present study.

However, it is interesting to highlight the obtention of extra information, in the present research not available through the use of traditional methods; for example, the shape change visualization along the different age classes and trophy categories. Geometric morphometrics have allowed to reveal the developmental antler trend of a deer population along different years. This visualization not only provides information about what happens in populations, helping the species management, but it also allows the identification of individuals exceptionally developed, probably due to the presence of high quality genetic strains or individuals bred in excellent environmental and nutritional conditions. Therefore, the combination of both types of measures, those based on three-dimensional coordinates and on lineal measurements, would provide a more rigorous categorization of the hunting value of antlers.

Nevertheless, it would be interesting to carry out further sampling in order to obtain more homogeneous age groups in number of individuals. For example, age classes 1 and 6 are not very sampled within hunting trophies.

The main interest of deer management, is the obtaining of the best antler trophies (Landete-Castillejos et al. 2013). Consequently, deer are one of the most affected species by selective hunting. The search for the best trophies tends to focus hunting on larger specimens, with longer, symmetrical antlers and higher number of tines.

Antlers are defined as bilaterally symmetrical structures, whose right and left sides are encoded by the same genes (Solberg and Saether 1993; Lagesen and Folstad 1998; Pélabon and Jolly 2000). However, the final

antler development depends not only on genetic aspects, but it is highly influenced by external factors, such as environmental ones (Putman et al. 2000). The environmental situation, especially in terms of food availability (Carranza 1999), would be one of the principal causes of the high morphological variability observed among the antlers studied. That is why apparently it is still debated whether the quality of antlers is largely influenced by the animal condition and climate, or whether it is mostly consequence of genetics (Hartl et al. 1991).

The high variability observed, sometimes involves the presence of asymmetries between the left and right antler sides. Many studies have addressed the issue of asymmetries in deer antlers especially focusing on the fluctuating asymmetry (FA) phenomenon (Solberg and Saether 1993; Palmer 1994; Palmer 1996; Pélabon and Van Breukelen 1998; Putman et al. 2000; Ditchkoff et al. 2001; Mateos et al. 2008). Generally, FA is expected to predict developmental instability or individual fitness (Palmer and Strobeck 1986; Kruuk et al. 2003; Swaddle 2003; Mateos et al. 2008). Nonetheless, there is a lot of controversy about the use of FA as quality indicator (Kruuk et al. 2003; Ditchkoff and Defreese 2010). The last fact, together with the lack of studies dealing about the asymmetry issue in deer antlers using three-dimensional data, boosted the use of geometric morphometrics methods to study the asymmetries of the antlers sampled. Therefore, the presence of FA was studied. The results obtained were surprising, since higher values of directional asymmetry (DA) than FA, were found. This fact would support previous results that do not consider FA as a reliable indicator of individual quality.

The DA existence, which by definition implies that one side of a bilateral structure is larger than the other one (Palmer 1994). In the present

research the antler right side was the larger. Therefore, despite no function is attributed to the presence of asymmetry in antlers (Alvarez 1995), we could investigate about the reasons of the existence of such asymmetry. It is surprising that in previous studies about red deer there is no mention of the existence of DA.

The introduction of specimens from other populations in the area here studied is interesting for the species handling, since it could involve the hunting trophies improvement by increasing its economic value, but it could also mean the disappearance of the Iberian subspecies itself by excessive genetic mix (Carranza 2004). On the other hand, it has been shown that antlers are primarily used as weapons in intrasexual fights, where the right antler side of one male pushes against the left side of his opponent and vice versa (Clutton-brock 1982; Lincoln 1992). The different antler tines would prevent the rival antler from sliding along the beam reaching the head or eyes, apparently favouring the presence of more symmetric antlers (Kruuk et al. 2003; Mateos et al. 2008). However, to have found a higher right antler side in the antlers sampled, in the same way that Alvarez (1995) found in fallow deer, suggested a more intense use of that right side during fights. Accordingly, a future aspect to be addressed about Iberian red deer antlers, would be the study of their use during fights. Consequently, it could be possible to study whether there is a higher tendency to hit first the right antler side, or whether individuals tend to turn the head more often to one side than to the other one during fighting. The facts mentioned above would have consequences at neck muscles, since they are actively involved in fighting (Clutton-Brock 1982). Additionally, it could be possible to observe whether there is any relationship between the tendency of deer to start walking with the right or

left limbs and the higher development of one antler side, in the same way as leg injuries do (Marburger et al. 1972). In turn, it may allow to define whether there is left or right-handedness in deer, since there are only vague hypotheses based on different hunter observations.

Although the antler complexity can be influenced by genetics or environment, as said above, the shape changes observed along antlers usually occur in a coordinated way between its different parts. These coordinated changes suggested that antlers could be formed by units defining different anatomical parts, in the same way that organisms are composed of several components (Klingenberg 2008a).

When different identifiable parts act with some individuality respect to the rest of an organism or structural elements, we are facing the existence of modules (Wagner et al. 2007; Klingenberg 2008a). The presence of modularity is related to the concept of morphological integration (Olson and Miller 1958; Baab et al. 2012), because generally all the parts of an organism are coordinated and integrated to act as a functional whole (Klingenberg 2013). Thus, the present research served to check whether the theory previously exposed, fits antlers, similarly to other complex structures as for example flowering plants (Conner and Sterling 1996; Juenger et al. 2005). The presence of modularity and integration in both covariation patterns, that caused to all the mechanisms involved on antler development, and the other due to FA, which exclusively represents the interaction of direct developmental pathways (Klingenberg et al. 2003; Klingenberg 2008a), were studied in different antler partitions composed by a variable number of landmarks. The presence of modularity in the antler crown and trez tines, but not in the beam and eye tines, is ambiguous. At first, it was though that the covariation found at different

antler parts, was exclusively due to the action of direct developmental pathways. However, the presence of integration at FA level, suggested that alterations suffered by such developmental pathways would be affecting the overall antler (Klingenberg and Zaklan 2000; Klingenberg et al. 2001). Despite that, it has been suggested that some integration is always present in antlers, as well as in any other structure (Klingenberg 2008a), the matching between covariation patterns among modules and within modules, evidenced by their element variability, suggested that the different antler parts shared common mechanisms of covariation. Therefore, the results showed the no possibility to isolate both phenomena, integration and modularity, indicating that antlers generally act as internally coherent and coordinated modules in order to perform a common function. However, the modularity found in some antler parts, would be indicative of its relatively independent behaviour along the developmental process of the structure.

The study of the presence of different types of modules (developmental, genetic, functional and even evolutionary), would be of great interest in order to disaggregate both, the operation and contribution of each one to the final antler development.

An interesting and useful information to consider for future antler studies, would be genetic information. The emerging interest towards quantitative genetics (Baab et al. 2012), and the possibility of analyzing genetic patterns in deer populations of Sierra Morena, could help to a better understanding about the morphological variations observed in antlers. Moreover, genetics could help to detect in a more specific way, foreign introductions in a population or clarify the heredity levels of different antler traits. Likewise, this type of studies would upgrade deer

management and in turn, antler development. Other interesting topics in morphometrics, would be to carry out studies about the possible correlation between the antler shape change and the jaw and skull size of the specimens, since a pattern of change between both structures could exist (Gould, 1973; Damuth and McFadden, 1990).

Summarizing, this work has shown that geometric morphometrics methods are enough powerful biologically and statistically, to capture the complex and subtle shape changes suffered by antlers. This methodology has allowed to describe and quantify the direction and orientation of the different antler shape changes (Baab et al. 2012), not possible by using classical morphometrics methods. Furthermore, geometric morphometrics give us the tools to test differences between groups if present, as well as to determine the nature of any relationship between the shape of the structures under study and other variables (Baab et al. 2012).

In parallel, a Photogrammetric Interactive Measure Method (PhIMM) has been proposed for the study of antlers, as well as for the study of any other biological structure. This new method is interesting since it is able to provide significant advantages over data collection and the three-dimensional visualization of antlers, in a fast and economic way. Through this system and after completing the relevant digital photographs, it would not be a problem the lack of taking certain measures over the antler, since using a few landmarks it would be possible to extract all the extra interesting information later. The PhIMM validation using antler trophies, shows similar results to those obtained through traditional measurements or geometric morphometrics. Therefore, the three methods would provide analogous values for the same antler measurements.

The PhIMM, has also been proved useful for the computer modelling of antlers, showing its versatility and flexibility. Moreover, it is expected to be suitable for application to individuals in the field, and not just on hunting trophies or museum specimens. Making the necessary adjustments, the method could be also applied to any part of the animal physiognomy of any species. Thus, this work aims to establish for the first time the method mentioned as a viable option in zoological studies.

Nevertheless, it should be noted that in both cases, id est., by using geometric morphometrics methods or the PhIMM, the data collection is not invasive or cause any damage to the material used for the study. Additionally, both methods do not imply the sacrifice of more animals that those killed in the corresponding hunting seasons.

The different results and conclusions extracted from this research not only can be considered of high scientific rigor due to the type of methodologies used, but allow to assume new insights in the study of complex structures similar to the Iberian red deer antlers.

8. Resumen en español

Introducción general

Breve historia de la morfometría geométrica

El origen de la morfometría, definida como el estudio de la variación de la forma y su covariación con otras variables, se remonta a varios siglos atrás. Alberto Durero, pintor del S. XV, junto con matemáticos del S. XIX, como D'Arcy Thompson, Francis Galton, Karl Pearson, Ronald A. Fisher, Julian Huxley o Georges Teissier, entre otros, contribuyeron a formar las bases tanto de la morfometría tradicional, como de la morfometría geométrica.

Morfometría tradicional vs. Morfometría geométrica

La morfometría tradicional, aplica estadística sobre medidas lineales, las cuales proporcionan poca información sobre la forma ya que, a veces, se superponen ignorando la relación espacial entre ellas, y suelen estar altamente correlacionadas con el tamaño del objeto. Dichas medidas, al no ser exactamente independientes, pueden dar lugar a errores de medida. Estas observaciones, junto con la imposibilidad de visualizar los cambios de forma, subestiman la información sobre la forma. Por otro lado, la morfometría geométrica es un método basado en la utilización de landmarks, lo que permite deducir la forma de los objetos, entendida como la información geométrica que permanece cuando los efectos de traslación, rotación y escala son eliminados. Además, combina estadística multivariante con métodos para la visualización directa de los resultados, de manera que los cambios debidos única exclusivamente a la variación de la forma pueden ser observados.

Espacio de forma y dimensionalidad

La visualización de los cambios de forma de estructuras y organismos, se da en un espacio de forma no euclídeo representado por una superficie esférica.

Para configuraciones de más de tres landmarks, los correspondientes puntos

morfológicos pueden proyectarse sobre un espacio tangente lineal, el cual es una aproximación lineal del espacio no-euclídeo, de igual dimensión. El espacio tangente lineal permite la aplicación de estadística multivariante.

Componentes de la forma

La totalidad del cambio de forma de las estructuras se descompone en componente uniforme y no uniforme. El componente uniforme representa los cambios de forma debidos a la geometría, de manera que todos los puntos se ven afectados por igual, una vez los efectos de rotación, traslación y escala son eliminados. Por contra, el componente no uniforme hace referencia al resto de cambios potenciales, como movimientos no lineales o variaciones locales de landmarks determinados.

Método fotogramétrico interactivo (PhIMM)

El método fotogramétrico interactivo (PhIMM) se caracteriza por combinar la realización de fotografías digitales en el campo, con la aplicación de un programa basado en el uso de tecnología CAD-3D (Computer Aided-design technology). De esta manera, haciendo un par de fotografías del objeto de estudio, sería posible extraer la información geométrica del mismo y elaborar modelos tridimensionales. La validación del método se realizó mediante su aplicación en la evaluación de la calidad de astas de ciervo de Sierra Morena.

Antepasados de los ciervos con astas

A lo largo del Terciario los cérvidos, de origen tropical, evolucionaron colonizando climas fríos y originando dos subfamilias, la del Viejo Mundo y la del Nuevo Mundo.

Los primeros cérvidos eran de tamaño pequeño, con caninos superiores muy desarrollados y no tenían astas. Según el registro fósil, los cérvidos aparecen en el Oligoceno, mientras que las primeras cornamentas aparecen en el Mioceno temprano, en los géneros *Syndioceras* y *Climacoceras*. Paralelamente,

antepasados de la familia *Antilocapridae* mostraron astas caracterizadas por no ser renovables. A mediados del Mioceno aparecen los primeros cérvidos con cornamentas renovables, pertenecientes a los géneros *Dicrocerus* y *Stephanocemas,* de Asia y Europa respectivamente. Sin embargo, el considerado primer cérvido con cornamenta fue un espécimen del Viejo Mundo, *Euprox minimus*, caracterizado también por tener caninos cortos.

Durante el Plioceno tardío se produjo la radiación de las especies que dio lugar a los verdaderos ciervos, como el género *Odocoileus*. A partir de aquí, animales grandes, dotados de cornamentas más complejas y caninos reducidos aparecieron hasta dar lugar a *Cervus* sp.

Cervus elaphus hispanicus: aspectos sistemáticos y distribución

El ciervo rojo (*Cervus elaphus*) es un ungulado rumiante, perteneciente al orden Artiodáctilos y familia *Cervidae*. Dicha familia comprende 16-17 géneros dependiendo del autor, y 41 especies. *Cervus* sp. incluye 10 especies distribuidas por Asia, Europa y África. *Cervus elaphus* comprende varias subespecies, de las cuales el presente estudio se centra en *Cervus elaphus hispanicus* o ciervo Ibérico. El ciervo Ibérico se caracteriza por ser una de las subespecies más pequeñas del género, y por ser endémico de la Península Ibérica. Además, posee un pelaje más marrón que otras subespecies, con manchas blancas durante los tres primeros meses de vida. El ciervo Ibérico es crepuscular y gregario, a pesar de que ambos sexos permanecen separados durante casi todo el año. La excepción es la época de cría, momento en el que su estructura social poligínica implica la formación de harenes.

Interés económico del ciervo Ibérico de Sierra Morena

El valor socioeconómico del ciervo Ibérico en Sierra Morena es importante puesto que, es el animal

de caza más importante del Sur de España. El principal objetivo de su caza es la obtención de los mejores trofeos. Por ello, a veces, los propietarios de las fincas reponen las poblaciones de ciervo con especímenes procedentes de otros países. Dicha práctica es controvertida ya que, puede tener efectos tanto positivos como negativos en las poblaciones autóctonas, pudiendo provocar la desaparición de la subespecie ibérica. Éste y otros problemas ponen de manifiesto la necesidad de conocer ampliamente el desarrollo y estructura de las astas, para así gestionar correctamente las poblaciones, y a su vez, ayudar a conciliar la eficiencia económica con la conservación de zonas de alto valor natural.

Rasgos y estructura de las cornamentas

Las cornamentas tienen como función principal actuar como arma en luchas intraespecíficas. El desarrollo de las cornamentas es altamente sensible a densidades de población elevadas y condiciones ambientales adversas, sobre todo en cuanto a disponibilidad de alimento se refiere. Sin embargo, las mejores astas se obtienen de la conjunción de la situación genética y ambiental de los individuos. Dichas estructuras se desarrollan a partir de una excrecencia del hueso frontal denominada pedículo. A partir del pedículo surge el eje principal de la cornamenta. Los individuos más jóvenes, de aproximadamente 1 año de edad, reciben el nombre de *varetos* y no presentan astas ramificadas. De aquí en adelante, éstas tienden a ser más grandes y ramificadas (luchaderas, contraluchaderas, candiles y coronas).

Las cornamentas también son interesantes por ser estructuras óseas renovables cuya morfología varía anualmente, sobre todo debido a alteraciones ambientales sufridas durante el proceso de desarrollo. Su capacidad de regeneración es similar a la de extremidades de urodelos, lo que las convierte en uno de los tejidos de crecimiento más rápido del reino animal. El máximo

desarrollo de las cornamentas coincide con el alcance de la madurez sexual de los individuos, lo que ocurre entre los 7-12 años de edad. Seguidamente, se inicia el proceso de regresión por envejecimiento de los especímenes.

Cornamentas vs. Cuernos

Las cornamentas son óseas y los cuernos dérmicos. Además, las cornamentas son el único apéndice relleno de punta a punta, mientras que los cuernos se encuentran parcialmente huecos. Los cuernos presentan una cubierta rígida imposible de modificar una vez formada. No obstante, las cornamentas se renuevan cada año. Las astas, mesenquimáticas, crecen por la punta, mientras que los cuernos, ectodérmicos, crecen por su base. Ambos apéndices también presentan similitudes puesto que son caracteres sexuales secundarios altamente influenciados por variables ambientales como la temperatura, disponibilidad de comida o fotoperiodo.

Objetivos

El presente estudio se basa en el análisis de astas de ciervo Ibérico de la zona oriental de Sierra Morena (Jaén, España), utilizando técnicas de morfometría geométrica y otras metodologías. Con el fin de profundizar en determinados aspectos de las cornamentas, los diferentes objetivos de la investigación son:

1) Describir y cuantificar la variabilidad de forma entre cornamentas de ciervo Ibérico pertenecientes a diferentes clases de edad, utilizando morfometría geométrica, y evaluar la presencia de una edad óptima para la obtención de trofeos en la zona.

2) Cuantificar las asimetrías presentes entre las ramas izquierda y derecha de las cornamentas, tomando especial interés la evaluación de la presencia de asimetría fluctuante (FA), y su determinación como posible indicador de calidad individual.

3) Determinar si las cornamentas de ciervo Ibérico se definen como estructuras únicas integradas, o bien como entidades modulares.

4) Desarrollar y aplicar un método fotogramétrico interactivo (PhIMM) basado en tecnología CAD-3D, para la evaluación de la calidad de trofeos de caza.

Material y métodos generales

Área de estudio y material

El ciervo Ibérico habita todo tipo de áreas de la Península Ibérica, pero tiene preferencia por zonas de transición donde se dan variaciones estacionales diarias. Esto es lo que ocurre en la parte oriental de Sierra Morena (Jaén, España), el área de estudio. Dicha área presenta un clima típico mediterráneo con distribución irregular de lluvias durante el año.

217 astas fueron recolectadas de diferentes fincas de Sierra Morena, durante las temporadas de caza 2007/08, 2009/10 y 2011/12. Por lo tanto, todas las cornamentas medidas fueron trofeos de caza.

Paralelamente, variables climáticas de interés, como lluvias o temperaturas invernales, fueron extraídas de estaciones climáticas cercanas al área de estudio.

Determinación de la edad

La edad influye sobre el desarrollo de las cornamentas por lo que, su determinación fue necesaria. Para ello, la mandíbula de cada espécimen fue recogida, medida, limpiada y cortada a nivel del primer molar, con el fin de realizar el recuento de capas de cemento interadicular. Las capas de cemento forman bandas anchas y estrechas, correspondientes a marcas de rápido crecimiento y reposo del mismo. El recuento de capas implica saber que la primera de todas, aparece a los 6 meses de edad. De aquí en adelante, una nueva banda de reposo aparece cada año. Dependiendo de la edad asignada a cada espécimen, estos fueron agrupados en clases de edad de la 1 a la 6. La clase de edad 1 incluía individuos de 2-3 años, la clase 2 de 4-5 años, y así sucesivamente hasta la clase 6, donde se incluyeron individuos de 12-13 años.

Obtención y tratamiento de los datos

Landmarks y semilandmarks

Para el estudio del cambio de forma de las cornamentas mediante morfometría geométrica, la obtención de configuraciones de landmarks fue necesaria. En el presente trabajo, se utilizaron

landmarks definidos por tres coordenadas cartesianas y por lo tanto, ubicados en un espacio tridimensional. La utilización de semilandmarks también fue necesaria para la definición de curvas y superficies de la estructura. De esta manera, obtenemos configuraciones de landmarks y semilandmarks, independientes para cada individuo.

Definición de landmarks en las cornamentas

La observación de tantas cornamentas como fuera posible fue necesaria para determinar la posición más adecuada de los landmarks y semilandmarks en la estructura. Al comparar cornamentas de diferentes edades, la muestra comprendía estructuras con diferente número de ramificaciones. Para solventar ese problema, la digitalización de coordenadas se hizo siguiendo el criterio establecido por Oxnard y O'Higgins (2009). Teniendo en cuenta lo anterior, un total de 115 landmarks fueron digitalizados por cornamenta.

Tamaño del centroide y alometría

Eliminar el efecto escala antes de cualquier análisis de la forma, implica separar forma y tamaño. Forma y tamaño no son estadísticamente independientes, sino que se encuentran asociados por la alometría, la cual se define como la influencia del tamaño sobre la forma. Por ello, el efecto alométrico fue testado, para alcanzar cada uno de los objetivos de esta tesis, mediante la correspondiente regresión de forma sobre tamaño. El estimador del tamaño en morfometría geométrica es el centroide. El centroide se calcula como la raíz cuadrada de la suma de distancias al cuadrado de cada landmark respecto al centro de la forma, y es el único matemáticamente independiente a la forma.

Superimposición Procrustes (GPA)

Antes de empezar a trabajar con las coordenadas de todas las cornamentas de la muestra, es

necesario eliminar los efectos de rotación, escala y translación de cada configuración de landmarks independiente. Para ello, se efectúa la Superimposición Procrustes (GPA).

El GPA da lugar a una configuración consenso de todas las configuraciones de landmarks de la muestra. A partir de aquí, es posible obtener toda una serie de variables, denominadas deformaciones parciales (*partial warps*; PW), las cuales facilitan la interpretación de los resultados en análisis posteriores.

Estadística multivariante

Tras el GPA y la obtención de las PW, se extrae la matriz de covarianza de las variables a estudiar. Sobre dicha matriz es posible aplicar estadística multivariante, como por ejemplo Análisis de Componentes Principales (PCA). El PCA produce nuevas variables llamadas componentes principales (PCs), los cuales permiten estudiar los patrones de variación de forma de toda la muestra, proporcionando la máxima cantidad de información sin que ésta se repita y reduciendo su dimensionalidad. Por otro lado, también es posible observar diferencias entre grupos, mediante Análisis de Variables Canónicas (CVA), o entre pares de grupos, mediante Análisis de Función Discriminante (DFA). La aplicación de Análisis de la varianza (ANOVA) o Análisis Multivariante de la varianza (MANOVA) entre otros, también es posible en función de los objetivos establecidos.

Simetría y asimetría

Las astas de ciervo muestran *Matching symmetry*. Por lo tanto, una copia separada de la estructura existe en cada mitad del plano de simetría del cuerpo. Así, las dos ramas de la cornamenta son imagen especular la una de la otra. Las desviaciones de la simetría ocurren debido a factores tanto genéticos como ambientales, generando diferencias entre los lados izquierdo y derecho de las estructuras. Los principales tipos de asimetría son, fluctuante (FA) y

direccional (DA). Para cuantificar los niveles de FA y DA en la muestra, se evaluaron las diferencias entre las configuraciones originales de landmarks y sus correspondientes imágenes especulares. La evaluación se realizó a través de un análisis de Procrustes ANOVA, el cual se caracteriza por proporcionar información sobre la acción de efectos como la FA, DA y el efecto individuo, en la muestra. Del mismo modo, permite calcular el posible error de medida.

Integración y modularidad

Generalmente, los organismos están compuestos por diferentes partes, las cuales pueden ser relativamente independientes entre sí sugiriendo la presencia de módulos. Integración y modularidad, son dos fenómenos

altamente relacionados por lo que, a pesar de la presencia de módulos, siempre hay cierto grado de integración entre ellos. Con el fin de identificar la presencia de hipotéticos módulos entre las diferentes partes de las cornamentas de ciervo Ibérico, diversos métodos analíticos fueron aplicados. Previamente, el efecto alométrico de los datos fue corregido. Para las diferentes hipótesis de modularidad propuestas se obtuvo el coeficiente RV, indicador del grado de asociación entre los módulos. Seguidamente, el estudio de la covariación entre los conjuntos de datos, se llevó a cabo mediante análisis de mínimos cuadrados parciales (PLS).

Métodos de digitalización

Cintas métricas o pies de rey son los métodos de medida más utilizados en estudios de morfometría tradicional. Sin embargo, la recolección de datos para estudios de morfometría geométrica requiere herramientas más específicas como escáneres tomográficos, brazos digitalizadores o fotografías digitales. El uso de fotografías digitales resulta rápido y económico, pero no permite trabajar directamente en tres dimensiones. Paralelamente,

existen dispositivos adaptados para trabajar en 3D, como es el caso del brazo digitalizador, modelo MicroScribe G2X utilizado en este trabajo, o el uso de escáneres para la obtención de tomografías computerizadas, los cuales son efectivos pero poco económicos.

Herramientas para la aplicación de un método fotogramétrico interactivo (PhIMM)

El PhIMM comprende dos tipos de herramientas. Por un lado, implica realizar dos fotografías desde diferentes perspectivas de cada cornamenta. Cada fotografía debe incluir una referencia métrica de 50x50 cm con el fin de localizar puntos comunes entre cornamentas. En este caso, las fotografías se realizaron con una cámara digital PowerShot SX210 IS de 4320x3240 píxeles. Por otro lado, el procesado de las fotografías requiere la utilización del software SolidWorks basado en tecnología CAD-3D, la cual permite recrear virtualmente el espacio en el que se encuentran los objetos haciendo modelizaciones 3D.

Morfometría geométrica de la cornamenta de ciervo Ibérico (*Cervus elaphus hispanicus*)

Resumen

El presente estudio describe y cuantifica la variación de forma de cornamentas de ciervo Ibérico, con el fin de caracterizar cambios relacionados con la edad e identificar una edad óptima para los trofeos de caza. La variación de forma de partes comunes a todas las cornamentas, así como la covariación de diversos factores ambientales y del desarrollo, con respecto a la forma y tamaño de las mismas fue estudiada mediante morfometría geométrica. Los individuos más jóvenes (2-3 años) presentan cornamentas alargadas cerca del cráneo con ramas principales acortadas distalmente, mientras que las de individuos maduros (6-9 años) son más cortas cerca del cráneo y arqueadas distalmente. Variaciones de forma ligadas a puntas específicas también fueron identificadas, siendo candiles y luchaderas más rectas y orientadas verticalmente en individuos jóvenes, y más largas y curvadas en individuos maduros.

Un PCA mostró el progresivo cambio de las cornamentas para acomodar un mayor número de puntas a lo largo de la vida, alargando y separando las ramas principales, pero también reorientando candiles, luchaderas y coronas. Los principales factores asociados con el tamaño y diferencias de forma de las cornamentas fueron: presencia o no de contraluchaderas, edad, puntas totales y puntas de la corona. Sin embargo, los efectos ambientales (año de captura) también fueron significativos. A cada cornamenta se le asignó una categoría y calificación de calidad como trofeo (TQS), la cual aumentaba entre las clases de edad 2 y 4 (4 a 9 años), y disminuía a partir de las clases 5 y 6 (10 a 13 años). Estos resultados tienen implicaciones para el manejo y conservación de la subespecie ibérica.

Introducción y objetivos

La principal subespecie cinegética del Sur de España, es el ciervo Ibérico. De ahí la creciente tendencia a optimizar la calidad de las astas, tomando especial importancia su tamaño y simetría. El asta de ciervo, incrementa el número de puntas, especialmente en la corona, con la edad. Ello se prolonga hasta los 8-12 años de edad. Seguidamente, el número de puntas regresiona.

El área de estudio, Sierra Morena Oriental, presenta un clima típico mediterráneo marcado por la irregularidad de precipitaciones. La humedad del suelo determina la calidad y disponibilidad de alimento durante la primavera, época de desarrollo de las cuernas, lo que a su vez estaría condicionado por el régimen de lluvias invernales. Por ello, además de la edad, la variable año de captura representa un factor de aproximación ambiental que puede afectar a la calidad final de las astas. Los objetivos del estudio son, describir y cuantificar las variaciones morfológicas de partes comunes a todas las cornamentas de la muestra, y determinar la presencia de una edad óptima para las mismas.

Material y métodos

Técnicas de morfometría geométrica fueron utilizadas para cuantificar la variación morfológica de las astas. El grado de covariación del tamaño y forma de las cornamentas respecto a factores de desarrollo (edad, presencia o no de contraluchaderas, puntas de la corona y puntas totales) y ambientales (año de captura) fue testado. 209 cornamentas procedentes de fincas cinegéticas de la parte oriental de Sierra Morena (Jaén, España) fueron medidas durante las temporadas de caza 2007/08, 2009/10 y 2011/12. Coordenadas tridimensionales de 35 landmarks y semilandmarks fueron digitalizadas para cada cornamenta. A continuación, se efectuó un análisis generalizado de Procrustes (GPA) y seguidamente, un análisis de componentes principales (PCA). El efecto del

tamaño de las cornamentas sobre su forma, se testó a través de la correspondiente regresión. El mismo tipo de regresión se utilizó para cuantificar la relación entre la forma de las cornamentas y los factores ambientales y de desarrollo mencionados anteriormente. Para determinar la edad de cada individuo se procedió a la recolección y corte a nivel del primer molar (M1) de su mandíbula inferior. Posteriormente, se hizo el recuento de capas de cemento interadicular y se clasificó a los especímenes en seis clases de edad. La determinación de una edad óptima para los trofeos se realizó mediante la:elaboración de un índice propio (TQS) basado en medidas de protocolos de caza, que permitió categorizar la calidad de los trofeos de la muestra.

Finalmente, para la interpretación de TQS se estipuló que los trofeos de ente 71 y 80 puntos eran muy buenos (VG), los de 61 a 70 buenos (G), los de 51 a 60 de calidad media (M), los de 41 a 50 de calidad pobre (P), los de 31 a 40 de mala calidad (B), y los de 30 o menor puntuación de muy mala calidad (VB).

Resultados

Los 6 primeros PCs del PCA, representaron un 68,53% de la variación total de forma. Valores positivos de PC1 (28,10%) mostraron astas alargadas cerca del cráneo con ramas próximas entre sí, y luchaderas y candiles rectos y orientados apicalmente. Valores negativos de PC1, representaron cuernas acortadas cerca del cráneo, con ramas más distantes, candiles ligeramente curvados y luchaderas orientadas más hacia abajo que en el consenso. Valores positivos de PC2 (15,79%), representaron astas acortadas por la parte próxima al cráneo y curvadas, con una parte distal más larga y arqueada, candiles largos y curvados, y luchaderas largas y orientadas frontalmente.

Valores negativos de PC2 mostraron forma de V, con candiles más cortos y orientados hacia arriba que la forma consenso,

y luchaderas acortadas y lateralizadas.

Los valores positivos de PC3 (8,10%), representaron cuernas más estrechas, con luchaderas y candiles más largos mientras, sus valores negativos mostraron cuernas más amplias, con candiles y luchaderas más cortas y rectas.

PC4 (7,02%) mostró cornamentas de ramas curvadas en la base de la corona, con candiles más cortos y de curvatura similar a los del consenso. En cambio, valores negativos de PC4 mostraron cuernas en forma de V, con ramas rectas y candiles largos y curvados por la base.

De valores negativos a positivos, PC5 (5,25%) mostró una orientación frontal progresiva de los candiles, y una posición más horizontal de las luchaderas.

Los valores positivos de PC6 (4,27%) mostraron astas proyectadas cranealmente por su parte superior y puntas largas, sobre todo las luchaderas. Mientras valores negativos de PC6 mostraron cuernas proyectadas caudalmente por su parte superior y de puntas más cortas.

La mayor separación entre ramas de las cornamentas se dio en la base de la corona, lo que coincide con el punto de máxima curvatura de la estructura.

El efecto alométrico fue significativo. Los individuos más jóvenes (clases 1 y 2) presentaron astas de morfologías similares a valores positivos de PC1, con ramas esbeltas junto al cráneo y próximas entre sí, y candiles y luchaderas rectas y orientadas verticalmente. En cambio, individuos maduros (clases 2 y 4) mostraron morfologías similares a valores positivos de PC2, con cuernas cortas junto al cráneo y arqueadas distalmente, y luchaderas y candiles largos y curvados.

El efecto de factores referentes al desarrollo de las cornamentas sobre la variación de forma observada, fue significativo. Por contra, la aproximación ambiental utilizada (año de captura) mostró el efecto más pequeño.

La relación entre la morfología de las cornamentas y el TQS, resultó similar a la relación entre forma y tamaño. Por otro lado, la observación de la forma media asociada a cada valor de TQS, sugirió que las puntuaciones más altas se asociaban a cuernas más arqueadas, con puntas más largas y curvadas. A mayor TQS la variación de forma incrementaba. Sin embargo, la variabilidad de forma encontrada en cada clase de edad, no permitió definir una edad óptima para las astas, puesto que los mejores trofeos aparecieron entre las clases 2 y 5 (4-9 años).

Discusión y conclusiones

¿Cómo afectan los factores estudiados a la morfología de las cornamentas?

El cambio de forma de las cornamentas se relaciona con la edad, pero también con el número de puntas totales y puntas de la corona. La separación entre ramas, se relaciona tanto con el incremento del número de puntas como con el tamaño de la estructura. Los ciervos más jóvenes (clases 1 y 2), con la mínima separación entre ramas y el menor número de puntas, presentan los valores más positivos de PC1. En PC2, el aumento de curvatura sufrida en la parte superior de las cornamentas se asociaría con un incremento de la corona y del número de puntas en la misma. Asimismo, los valores positivos de PC2 generalmente se atribuyen a individuos maduros (clases 3 y 4) cuya cornamenta ya ha alcanzado el máximo desarrollo. PC3, presenta una relación inversa a lo observado en PC1 ya que, el desplazamiento caudal de la punta central de la corona a mayor número de puntas, ocurre a medida que los valores de PC1 disminuyen y los de PC3 aumentan. De esta manera, los tres primeros PCs describirían la progresiva transformación de las cornamentas para acomodar el creciente número de puntas que aparece a lo largo de la vida, tanto alargando y separando sus ramas como reorientando los candiles, luchaderas y coronas. PC4 describe el paso de cuernas jóvenes a

adultas, donde las ramas y coronas dejan de estar alineadas. PC5, afectado por el efecto tamaño, podría representar cambios alométricos a lo largo del desarrollo de las cornamentas. PC6 se relacionaría con ciertas asimetrías observadas entre ramas. Así, la morfometría geométrica permitiría el estudio del cambio de forma asociado a cada uno de los factores que afectan a la morfología de las cornamentas.

Reflexiones sobre la optimización de la calidad de las cornamentas

La influencia de la edad y disponibilidad de alimento sobre el tamaño de las astas, así como la aparente relación con las condiciones invernales, sugirió una relación de TQS con la edad y el ambiente. La edad afectó a TQS (41,31%; p= <0.0001), puesto que los individuos más jóvenes (clase 1) presentaron las puntuaciones más bajas (VB). Las puntuaciones más elevadas (VG) pertenecieron a las clases 3 y 4. Los trofeos de buena calidad (G) aparecieron entre las clases 2 y 5, lo que podría ser indicativo de la presencia de individuos de gran calidad genética, capaces de generar buenos trofeos a edades tempranas. La escasez de buenos trofeos en las clases 5 y 6 podría explicarse por el proceso de regresión de las cuernas. A pesar de ello, no se encontró una edad óptima para los trofeos de la muestra basándonos únicamente en su morfología. El año de captura también afectó a TQS (2.42 %, p = 0.0209). Sin embargo, los resultados obtenidos en los diferentes años estudiados no parecen reflejar que las lluvias y temperaturas invernales sean buenos predictores de la calidad de las cornamentas de la muestra.

¿Modularidad en el desarrollo de las cornamentas?

Aparentemente, los cambios de forma explicados por cada PC ocurren de manera coordinada entre las partes superior e inferior de las astas, siendo el candil la parte media de la estructura. Una parte superior muy desarrollada se asocia con puntas largas y curvadas, lo que a su vez se asocia

con cambios de orientación. Ello, sugiere presencia de modularidad durante el desarrollo de las astas.

Interacciones entre factores

La gran variabilidad observada en la muestra, no permitió hallar morfologías características para cada clase de edad. La ausencia de contraluchaderas en la mayoría de individuos de clase 1 y algunos de la 2, sugirió que dicho factor afectaría mayoritariamente a individuos más maduros. La asignación de un número de puntas determinado para cada clase de edad tampoco fue posible, puesto que los individuos más jóvenes (clase 1) presentaron entre 6 y 11 puntas, mientras que los individuos de clase 2, presentaron de 9 hasta 14. La mayoría de los especímenes presentaron 12-14 puntas, lo que contrasta con las 10 observadas en estudios previos, y sugiere un incremento en la calidad de las cornamentas del área de estudio. Dicho incremento, podría deberse a la introducción de individuos procedentes de otros países en la zona. En la clase 6 el número de puntas desciende, lo que se relaciona con el receso de las astas a partir de los 12 años de edad. En general, los individuos de clase 4 presentaron el máximo número de puntas, y por lo tanto los mejores trofeos. Los individuos más jóvenes (clase 1) presentaron de 2 a 8 puntas en la corona, mientras que la mayoría de individuos de la clase 2 presentó entre 5 y 7. Ello reafirma el hecho de que individuos de 4 años en adelante, deben presentar de 10 a 12 puntas para ser considerados buenos trofeos en España. De la clase 3 en adelante, el número de puntas en la corona fue similar al de la clase 2 produciéndose un progresivo aumento en la categoría de los trofeos, hasta llegar a la clase 6.

Estudio de la asimetría de la cornamenta de ciervo Ibérico (*Cervus elaphus hispanicus*) mediante el uso de morfometría geométrica

Resumen

Debido a la complejidad de las cornamentas, se propuso el uso de morfometría geométrica en 3D para observar la presencia de asimetrías. Se evaluó la presencia de asimetría fluctuante (FA) y su fiabilidad como indicador de calidad individual. Para ello, 56 landmarks y semilandmarks de 434 medias cornamentas fueron digitalizados. Un Procrustes ANOVA realizado sobre un primer subconjunto con réplicas, determinó que el error de medida era suficientemente pequeño como para no ser tenido en cuenta. Por lo tanto, las asimetrías observadas eran reales. La FA de las cornamentas fue significativa. Sin embargo, el nivel de asimetría direccional (DA) también lo fue, siendo predominante. La DA encontrada en este caso, se correspondió con una rama derecha ligeramente más desarrollada. Un análisis de función discriminante (DFA) mostró diferencias significativas entre los lados izquierdo y derecho de las astas. Estos resultados sugirieron que la FA encontrada no era útil como indicador de calidad individual. Paralelamente, el efecto sobre el componente asimétrico de diferentes variables importantes en el desarrollo final de las cornamentas (edad, puntas totales y año de captura), fue testado mediante MANOVA. Ninguna de las variables estudiadas tuvo efecto significativo sobre las cornamentas, lo que apuntó a que la genética de los individuos era la principal causa de la presencia de asimetrías en la muestra.

La presencia de DA en la muestra, proporcionó una nueva visión acerca de la asimetría de las astas y su desarrollo. Ello planteó nuevas cuestiones como por ejemplo, si la presencia de DA implica limitaciones mecánicas sobre las cornamentas, tan útiles durante las luchas intraespecíficas.

Introducción y objetivos

La cornamenta se define como un carácter sexual secundario difícil de mantener. Dicha estructura es bilateral, y posee dos ramas genéticamente programadas para desarrollarse simétricamente. Sin embargo, su desarrollo final depende tanto de factores genéticos como ambientales. La cornamenta es una buena estructura para estudios de asimetría ya que, su renovación anual refleja las dificultades a las que los especímenes se ven sometidos durante el año. Así, solo aquellos machos de mayor calidad serían capaces de producir astas grandes y simétricas. Por esta razón, el estudio FA y DA es de interés. La FA definida como medida epigenética de estrés, se da cuando pequeñas diferencias ocurridas al azar aparecen en caracteres bilaterales, por lo que suele utilizarse como indicador de estabilidad del desarrollo y *fitness*. En cambio, la DA, de base genética, refleja diferencias sistemáticas entre lados del cuerpo, mostrando la propensión a desarrollarse siempre más un lado que el otro. Lo estudios de asimetría en cornamentas generalmente consideran la presencia de FA y no de DA. No obstante, otros estudios sugieren la posibilidad de pasar de FA a DA. El principal objetivo de este estudio fue testar la presencia de FA en cornamentas de ciervo Ibérico utilizando morfometría geométrica en 3D, y evaluar su fiabilidad como indicador de calidad individual. De esta manera, se espera un descenso de FA tanto con la edad como con tamaño, así como un incremento de FA en los años con peor clima.

Material y métodos

Las cornamentas del estudio fueron recolectadas en diferentes fincas cinegéticas de Sierra Morena (Jaén, España), durante las temporadas de caza 2007/08, 2009/10 y 2011/12.

De 434 medias cornamentas, se digitalizaron 56 landmarks y semilandmarks.

Especímenes de diferentes edades y por lo tanto, con diferente

número y localización de puntas en las cornamentas, fueron incluidos en la muestra. Para su medida, se siguió el criterio establecido por Oxnard y O'Higgins (2009).

A continuación, se llevó a cabo la superimposición Procrustes (GPA) de todas las configuraciones de landmarks caracterizadas por ser imágenes especulares las unas de las otras. Un subconjunto conformado por 132 medias cornamentas y sus réplicas, permitió calcular el error de medida mediante la aplicación de Procrustes ANOVA. Dicho análisis proporcionó información acerca de efectos como: el propio de cada individuo, el efecto lado (DA) y el efecto Individuo x lado (FA). Seguidamente, se realizó un nuevo Procrustes ANOVA aplicado a la totalidad de la muestra (434 medias cornamentas), sin réplicas. Posibles diferencias entre lados de las cornamentas se analizaron mediante un análisis de tipo discriminante (DFA). El efecto alométrico del tamaño sobre la forma de las cornamentas también fue testado. La cuantificación de los cambios de forma asociados al componente simétrico y asimétrico de la forma de las cornamentas se realizó mediante dos análisis de componentes principales (PCA). El efecto de la edad, puntas totales y año de captura sobre las asimetrías observadas, se analizó mediante análisis multivariante de la varianza (MANOVA). Los individuos de la muestra, fueron clasificados en clases de edad de la 1 a la 6 (de 2 a 13 años de edad).

Resultados

El error de medida fue suficientemente pequeño como para no afectar a los resultados, lo que justifica la utilización de una sola copia para cada cornamenta en siguientes análisis.

Se observó significancia del efecto lado (DA) y del efecto Individuo x lado (FA), siendo el efecto DA casi el doble de FA. El DFA sugirió diferencias significativas entre lados.

Paralelamente, las diferencias de tamaño entre lados fueron obtenidas por el cálculo del valor

del centroide (Izquierdo: CS = 1959,319705 y log CS = 7,324885662; Derecho: CS = 2061,680022 y log CS = 7,325095291).

El efecto alométrico del tamaño sobre la forma de las cornamentas, fue testado tanto para el componente simétrico como para el asimétrico de las mismas. En ambos casos, el efecto alométrico fue significativo, explicando un 14,36% ($p < 0,0001$) de la variabilidad total de forma en el componente simétrico, y un 2,29% ($p < 0,0001$) en el asimétrico.

El porcentaje de variabilidad explicada por los cuatro primeros componentes (PCs) del PCA del componente simétrico de las cornamentas fue de 63,28%, mientras que para el componente asimétrico fue de 45,89%. No fue posible establecer relaciones claras entre los diferentes caracteres de las cornamentas y el cambio de forma asociado a cada PC de dicho componente asimétrico. A su vez, el efecto sobre el componente asimétrico de variables como la edad, número total de puntas y año de captura, no fue significativo en ningún caso. Modelos cuadráticos, mostraron una relación positiva entre el componente asimétrico y la edad ($r^2= 0,89$). La relación de FA con la edad, también fue positiva ($r^2= 0,85$) alcanzando su máximo alrededor de la clase 4 (8-9 años) y decreciendo hasta la clase 6 (12-13 años). La aplicación de ANOVA de un factor, tanto para el componente asimétrico como para la FA con respecto a la edad, apenas mostró diferencias entre los valores generales de asimetría y los de FA para cada clase de edad (Comp. asimétrico, $p= 0.2255$; FA, $p= 0.0842$). La relación positiva del componente asimétrico con el año de captura ($r^2= 0,91$), no mostró grandes diferencias entre años. Por contra, la relación de FA con el año de captura no fue significativa ($r^2= 0,30$).

Discusión y conclusiones

Los resultados corroboran la presencia de FA en la muestra. Sin embargo, los datos no apoyan la utilización de FA como indicador

de calidad individual, ya que en este caso es la DA la que ejerce un mayor peso sobre el componente asimétrico de las cornamentas.

Presencia de DA y FA

El origen de la DA sería estable debido a su predeterminación genética. En cambio, el origen de FA, principalmente determinado por estreses externos, podría inclinar la balanza hacia una mayor presencia de DA o FA en la muestra.

Asimetría direccional (DA)

La presencia de DA en la muestra, relacionada con un mayor lado derecho, proporciona una nueva visión acerca de la asimetría de las cornamentas y su desarrollo. El DFA reafirmó la presencia de asimetrías entre lados de las cornamentas.

El efecto alométrico encontrado sobre el componente asimétrico de las mismas, no representó la principal causa de asimetría. Las diferencias observadas entre ramas, podrían relacionarse con un uso más intenso del lado derecho de las cornamentas durante las luchas, lo que apuntaría a razones mecánicas para la presencia de asimetría y no a la calidad individual. El mayor desarrollo de la rama derecha no permite determinar si los ciervos muestreados son diestros o no. Debido a la difícil interpretación de los cambios de forma observados en el PCA del componente asimétrico, se observó la influencia de variables como la edad, puntas totales o el año de captura. Ninguna de ellas tenía efecto sobre las asimetrías observadas. Por lo tanto, sería el componente genético de los individuos el que actuaría con mayor intensidad sobre las asimetría de las cornamentas y no el ambiente.

Influencia de la edad y el año de captura sobre las asimetrías de las cornamentas

La relación de la asimetría de las astas con la edad, sugirió un aumento conjunto de ambos. El efecto de DA, supondría el aumento progresivo del lado derecho de las cuernas con la edad. FA, aumentaba hasta los 8-9 años, edad de éxito reproductivo y lucha

de los ciervos, para luego disminuir. El aumento inicial de FA, coincidiría con la fase de rápido crecimiento de las cuernas. La posterior disminución de FA coincidiría con el alcance de la madurez sexual, y una mayor capacidad para usar recursos en actividades como la lucha o el desarrollo de cuernas más simétricas. La relación del componente asimétrico con el año de captura, mostró que los años 2007 y 2012 tenían los valores más elevados de asimetría. Con respecto a DA, ello podría ser indicativo del peso genético de los individuos cazados cada año. Así, si un año se cazan muchos individuos, ello podría reflejarse al año siguiente en un agotamiento de la reserva genética de las poblaciones. Los mayores valores de FA se registraron en 2010 y 2012, probablemente debido a las condiciones ambientales adversas registradas esos años. Estos resultados refuerzan la imposibilidad de usar FA como indicador de calidad individual, puesto que estudios previos sobre el mismo material de estudio, revelaron que esos años (2010 y 2012) fueron los que trofeos de mayor calidad presentaron. Las diferencias observadas entre el componente asimétrico de las cuernas y la FA, podrían ser debidas a la influencia de DA en la muestra.

Explorando la presencia de integración y modularidad en la cornamenta de ciervo Ibérico (C*ervus elaphus hispanicus*)

Resumen

El asta de ciervo Ibérico (*Cervus elaphus hispanicus*), representa un modelo particular de regeneración en mamíferos que podría proporcionar una organización modular a la misma. El presente estudio, examina los datos morfológicos de 217 cornamentas. De cada cornamenta, 115 landmarks y semilandmarks fueron digitalizados. La presencia de modularidad e integración tanto a nivel de variación entre individuos como a nivel de asimetría fluctuante (FA), fue evaluada. Para ello, cinco particiones distintas basadas en información acerca del proceso de regeneración y genética de las cornamentas, fueron propuestas. Las hipótesis testadas mostraron modularidad e integración entre los diferentes caracteres de las astas, lo que reveló una estrecha relación entre ambos conceptos. El comportamiento general de diferentes caracteres del asta, sugiere que dicha estructura, actúa como una unidad de desarrollo homogénea y coherente, compuesta por diferentes módulos, cuya variación ocurre de manera coordinada durante el desarrollo.

La interacción de múltiples vías durante el proceso de regeneración de las astas, explicaría los elevados porcentajes de covariación entre módulos observados tras un análisis de mínimos cuadrados parciales (PLS). Asimismo, la elevada integración encontrada a nivel de FA, sugirió que las perturbaciones sufridas en vías directas del desarrollo afectarían a la totalidad de la estructura.

Introducción y objetivos

Generalmente, los organismos y sus componentes se integran para actuar como un todo. Sin embargo, las diferentes partes de una estructura pueden encontrarse integradas y ser relativamente

independientes entre sí, sugiriendo presencia de módulos. La integración en una estructura, implica la covariación coordinada de múltiples caracteres de manera no homogénea. Estudios previos acerca de la morfología de la cornamenta de ciervo Ibérico, revelaron cambios de forma coordinados entre sus partes, lo que se relaciona con la presencia de módulos.

Sin embargo, la expresión de las cornamentas se considera un proceso de desarrollo integrado.

Las interacciones implicadas en la construcción de estructuras complejas, tales como las astas y sus partes, generan covariación entre dichas partes. Por ello, el análisis de FA, es la mejor manera de estudiar la covariación debida exclusivamente a la variación producida en vías del desarrollo.

El principal objetivo de este estudio es determinar si las cornamentas de ciervo Ibérico actúan como unidades integradas o bien, como estructuras modulares. Para ello, cinco hipótesis de modularidad basadas en el proceso de regeneración de las cornamentas y su genética, fueron propuestas. En cada hipótesis, la presencia de modularidad e integración fue evaluada con respecto a la variación general de los caracteres entre individuos, donde todos los mecanismos implicados en el desarrollo de las cornamentas se ven reflejados, y con respecto a la variación relacionada con la FA, donde se únicamente se representan las interacciones entre vías de desarrollo.

Proceso de regeneración de la cornamenta

Las astas se desarrollan a partir de una excrecencia permanente del hueso frontal denominada pedículo.

La regeneración de las cornamentas sigue un crecimiento sigmoidal, caracterizado por un reducido crecimiento inicial seguido de un rápido incremento, hasta alcanzarse el máximo desarrollo. Tras el cese del crecimiento se da la osificación de la cornamenta. La regeneración de

las cornamentas depende de los niveles de testosterona y el fotoperiodo. Así, bajos niveles de testosterona en primavera, implican la muda y recrecimiento de las astas, mientras que altos niveles de testosterona a finales del verano, frenan el proceso de crecimiento y osificación, e implican la muda del terciopelo. En las primeras etapas del proceso de regeneración, se distinguen dos centros de crecimiento en el pedículo, uno para la luchadera y otro para el eje principal. El crecimiento de las cornamentas es aposicional, y se da por la parte distal tanto del eje principal, como de las puntas. Éstas últimas se generan a partir de diversas divisiones ocurridas en la zona de crecimiento del eje principal.

Base genética del crecimiento de la cornamenta

Existen estudios que analizan los genes implicados en la regeneración de las cornamentas, y los diferentes elementos reguladores que afectan a su expresión. Dichos elementos, presentan diferentes patrones de expresión en las diferentes capas definidas en el extremo más distal de cada punta. El mapa proteómico de las cornamentas también se conoce. A pesar de que no se conocen genes específicos que determinen la expresión particular de cada una de las puntas de la cornamenta, sí se conoce la existencia de ciertas aloenzimas asociadas con la expresión de diferentes caracteres morfológicos.

Material y métodos

217 cornamentas fueron recolectadas durante las temporadas de caza 2007/08, 2009/10 y 2011/12, procedentes de diferentes fincas cinegéticas de la parte oriental de Sierra Morena (Jaén, España). A partir de la información recogida dos conjuntos de datos distintos fueron construidos, uno para la cornamenta completa (217 cornamentas + 115 landmarks), y otro para medias cornamentas (434 medias cornamentas + 56 landmarks) para estudiar los componentes simétrico y

asimétrico de la forma por separado. Una configuración de landmarks fue registrada para cada cornamenta. Previamente a trabajar con el conjunto de datos referente a media cornamenta, se obtuvo la imagen especular de cada mitad. A continuación, un análisis de superimposición Procrustes (GPA) fue aplicado en ambos conjuntos de datos. Un Procrustes ANOVA aplicado sobre un subconjunto de medias cornamentas con réplicas, sirvió para testar la presencia de FA y el posible error de medida. Las correspondientes regresiones de la forma simétrica y asimétrica de las cornamentas sobre tamaño, permitió observar el efecto alométrico. La posible influencia de dicho efecto sobre los niveles de modularidad e integración, implicó utilizar los valores residuales de las regresiones anteriores para siguientes análisis.

Cinco hipótesis distintas sirvieron para evaluar la existencia de modularidad e integración en las astas.

La primera hipótesis (H1), referente a la cornamenta completa, definió cada lado de la estructura como dos módulos distintos de 58 y 57 LMs. El resto de hipótesis, se definieron utilizando sólo media cornamenta.

La segunda hipótesis (H2), propuso como módulos la corona y sus puntas (40 LMs), y el resto de la cornamenta con sus puntas (16 LMs).

La tercera hipótesis (H3), sirvió para buscar modularidad entre el eje principal de las cornamentas (14 LMs) y sus puntas (42 LMs).

La cuarta hipótesis (H4), propuso como módulos la luchadera (4 LMs) y el resto de la cornamenta (52 LMs). Finalmente la quinta hipótesis (H5), define el candil (4 LMs) y el resto de la cornamenta (52 LMs) como hipotéticos módulos.

El coeficiente RV y gráficos de frecuencias, fueron calculados con el fin de observar el grado de modularidad en cada hipótesis. La significación del coeficiente RV fue determinada usando el ajuste de Bonferroni. La presencia de integración morfológica para cada hipótesis fue estudiada mediante

análisis de mínimos cuadrados parciales (PLS).

Resultados

Efecto alométrico

La regresión de forma sobre tamaño correspondiente a la cornamenta completa, mostró un efecto alométrico significativo ($p<0,0001$) que explicó el 11,43% de la variabilidad total de forma. El mismo efecto sobre media cornamenta, también fue significativo tanto para el componente simétrico de la forma como para el componente asimétrico ($p<0,0001$ en ambos casos), representando un 14,36% y un 2,29% de la variabilidad total de forma respectivamente.

H1: Cornamenta completa - Lado derecho vs. Lado izquierdo

El coeficiente RV indicó ausencia de modularidad en H1 (RV= 0,773; $p < 0,0001$). El PLS reveló una covariación significativa (74,95%; $p<0,001$), así como una correlación positiva entre módulos (0,97; $p<0,001$), sugiriendo presencia de integración.

H2: Media cornamenta - Corona vs. Resto de la cornamenta

El componente simétrico de H2 mostró presencia de modularidad (RV= 0,269; $p< 0,001$). Sin embargo, el PLS mostró una covariación significativa (56,30%; $p<0,001$) y una correlación positiva entre módulos (0,79; $p<0,001$), sugiriendo presencia de integración. El componente asimétrico de H2, también fue significativo en modularidad (RV= 0,189; $p< 0,0001$). El análisis de PLS, mostró covariación significativa entre módulos ($p<0,001$; 40,86%), y una correlación idéntica a la del componente simétrico (0,79; $p<0,001$), sugiriendo nuevamente presencia de integración.

H3: Media cornamenta - Eje principal vs. Puntas totales

El componente simétrico de H3 mostró ausencia de modularidad (RV= 0,627; p= 0,0451). El PLS reveló un porcentaje de covariación significativo ($p<0,001$; 38,50%), así como una correlación positiva ente módulos (0,86; $p<0,001$),

reforzando ausencia de modularidad y presencia de integración. La presencia de modularidad en el componente asimétrico de H3, fue rechazada (RV= 0,539; p= 0,0245). El análisis de PLS en este caso, mostró covariación significativa (p<0,001; 39,65%) y correlación positiva entre módulos (0,92; p<0,001), indicando presencia de integración.

H4: Media cornamenta - Luchadera vs. Resto de la cornamenta

La significación del coeficiente RV obtenido en el componente simétrico de H4 (RV= 0,397; p = 0,0360), fue rechazada descartando presencia de modularidad. El correspondiente PLS, mostró un porcentaje de covariación significativo (p<0,001; 60,99%), y correlación positiva entre módulos (0,83; p<0,001), dando soporte a la presencia de integración. Los mismos análisis realizados sobre el componente asimétrico, mostraron ausencia de modularidad (RV= 0,248; p = 0,0056). El PLS también mostró un porcentaje de covariación significativo (p<0,001; 59,71%) y correlación positiva (0,82; p<0,001) entre los módulos propuestos.

H5: Media cornamenta - Candil vs. Resto de la cornamenta

El componte simétrico de H5 reveló modularidad significativa (RV= 0,201; p < 0,0001). Sin embargo, el PLS mostró covariación significativa (p<0,001; 51,39%) y correlación (0,71; p<0,001) entre los módulos de dicho componente, sugiriendo cierta integración. El componente asimétrico de H5, presentó una modularidad aún mayor (RV= 0,124; p < 0,0001). Finalmente, el PLS del componente asimétrico resultó en una covariación significativa (p<0,001; 50,98%) y una correlación positiva (0,59; p<0,001) entre los módulos propuestos.

Discusión y conclusiones

Cornamenta completa

Estructuras bilaterales como las cornamentas, comparten la misma

base genética, programas de desarrollo y ambiente. Con todo, se sabe que algunas estructuras bilaterales como por ejemplo, las patas de vertebrados, pueden actuar como módulos independientes. Por lo tanto ¿qué podríamos esperar de las cornamentas? Para averiguarlo H1 fue planteada. Dicha hipótesis fue rechazada, impidiendo considerar las dos ramas de las cornamentas como módulos distintos. Por otro lado, se sabe que el proceso de caída de las ramas no tiene por qué ocurrir de manera sincronizada. En consecuencia, el proceso de regeneración empezaría con pocas horas de diferencia entre lados. Ello podría implicar cierta modularidad entre ramas. Sin embargo, la significativa covariación encontrada implicó presencia de integración, probablemente debida al crecimiento prácticamente sincronizado de ambas ramas. Por lo tanto, la ausencia de modularidad entre ramas, sugirió que las cornamentas actuarían como un módulo integrado, compuesto por diferentes partes cuya variación ocurre de manera coordinada.

Media cornamenta

Las diferentes partes de la cornamenta interactúan para llevar a cabo funciones comunes. Los resultados sugieren la existencia de dos módulos, corona y candil. Sin embargo, los niveles de integración observados, sugieren que dichos módulos no son del todo independientes al resto de la cornamenta. La modularidad e integración encontrada en los módulos propuestos, pone en evidencia la fuerte relación existente entre ambos conceptos. Asimismo, los hipotéticos módulos observados no serían tan independientes como se pensaba en un principio. La acción de procesos internos previos, relacionados con la diferenciación tisular de las cornamentas, podría señalizar la existencia de unidades definidas en la estructura. Los resultados obtenidos no dieron soporte a la idea de considerar el eje principal de las cornamentas o

las luchaderas, como módulos independientes.

El presente estudio muestra que los patrones de variación de los caracteres de las cornamentas entre individuos, así como los patrones de variación relacionados con la FA coinciden, de manera que las diferentes vías implicadas en ambos casos, serían las responsables de toda la covariación observada a lo largo de las cornamentas. Así, el comportamiento general de los diferentes caracteres de la cornamenta, sugiere que dicha estructura actúa como una unidad de desarrollo homogénea internamente coherente.

La segunda hipótesis, mostró que la corona de las cornamentas se comportaría como un módulo, pudiendo estar relacionado con la gran variabilidad concentrada a ese nivel. Ello coincidiría con cambios de forma coordinados observados previamente. Sin embargo, la integración observada, sugirió que los módulos propuestos no son completamente independientes. Además, la correlación positiva entre módulos, podría ser debida a una variación paralela causada por factores tanto genéticos como ambientales. La integración observada en el componente asimétrico de H2, sugiere que la variación observada a lo largo de las cornamentas se caracteriza por la integración del desarrollo de módulos parcialmente independientes. Los resultados de H3, muestran de nuevo dicha coincidencia de los patrones de variación entre individuos y debido a FA, lo que sugiere que las vías implicadas directamente en el desarrollo de las cornamentas, podrían ser a la vez los principales mecanismos responsables de la covariación entre individuos, haciendo que la estructura actúe como una unidad.

La correspondencia entre patrones de variación nuevamente se repite en H4, sugiriendo ausencia de modularidad en la luchadera. En el caso de H5, se sugiere que a pesar de que el candil se encuentre implicado en el mismo proceso de desarrollo que el resto de la cornamenta, su aparición tardía le

proporcionaría un comportamiento relativamente independiente al resto de partes de la estructura. Ello, podría ser debido a la acción de fuerzas en diferentes momentos durante el proceso de regeneración de las cornamentas. Por otra parte, no se conocen genes específicos responsables del crecimiento y desarrollo específico de cada punta de la cornamenta, y no se puede descartar la posible especialización de las puntas de las cornamentas a lo largo del proceso de desarrollo.

Otro aspecto a destacar, es el efecto alométrico detectado tanto en el conjunto de datos referente a la cornamenta completa, como en los componentes simétrico y asimétrico del conjunto de datos referente a media cornamenta. A pesar de que el tamaño no es el principal factor causante de la integración en las cornamentas, su efecto es igualmente importante ya que su eliminación implicó un descenso de los valores de coeficiente RV y por lo tanto, un incremento de los niveles de modularidad.

Valoración de la calidad de las cornamentas de ciervo Ibérico (*Cervus elaphus hispanicus*) mediante la aplicación de un método fotogramétrico interactivo (PhIMM)

Resumen

El interés por la homologación de cornamentas de ciervo como trofeos de caza, así como por la obtención de datos biométricos de las mismas, ha dado lugar al desarrollo de distintas herramientas biométricas. El presente estudio, testa la simplicidad y fiabilidad de tres métodos distintos de medida, sobre un conjunto de cornamentas de ciervo Ibérico. Concretamente, las medidas realizadas sobre las cornamentas, se llevaron a cabo mediante cinta métrica, brazo digitalizador y un nuevo sistema fotogramétrico basado en tecnología CAD-3D (PhIMM). A través del PhIMM, se generan curvas paramétricas 3D, las cuales representan las líneas reales a medir sobre las cornamentas. Las diferentes medidas de las cornamentas fueron estimadas y comparadas utilizando los tres métodos, los cuales mostraron resultados similares. Sin embargo, el PhIMM fue el sistema más rápido y funcional. Debido a que el PhIMM únicamente requiere de la realización de dos fotografías por individuo, permite el estudio de un elevado porcentaje de cornamentas en el campo. Por otro lado, los métodos fotogramétricos tienen la ventaja de permitir registrar otra información igualmente interesante para la homologación de trofeos directamente sobre las fotografías, como es por ejemplo el color de las cornamentas, la forma de sus puntas o la rugosidad de la superficie de la estructura.

Introducción y objetivos

El interés por la valoración de las astas de ciervo como trofeos de caza, así como la obtención de datos biométricos para su posterior análisis, implica el desarrollo de nuevas metodologías.

Herramientas biométricas como brazos articulados (CMA), son los

más utilizados para la obtención de landmarks y por lo tanto, para la cuantificación morfológica de individuos de diferentes especies. No obstante, los escáneres 3D son los más precisos en la obtención de datos geométricos. La gran cantidad de información proporcionada por los escáneres resulta difícil de manejar, por lo que una selección de los datos es necesaria. El resultado son modelos 3D de topología reconocible, de los que pueden extraerse landmarks. La fotogrametría consiste en la toma de fotografías a partir de diferentes localizaciones desde donde se trazan rayos hasta los objetos. Los rayos se cruzan en el espacio para la obtención de las coordenadas 3D de landmarks de interés. La fotogrametría es flexible, no tiene límite de tamaño y complejidad de los objetos a medir, y resulta económica. Su principal desventaja es el procesado manual que requiere. No obstante, sus resultados son similares a los obtenidos con escáneres y CMA. La recolección de datos morfológicos para la evaluación de la calidad de las cornamentas, suele darse en situaciones poco adecuadas para la toma de fotografías, e implica el uso de landmarks. El método fotogramétrico interactivo (PhIMM) propuesto en este estudio desarrolla técnicas proyectivas basadas en la utilización de tecnología CAD-3D. Así, a partir de pocos landmarks y un par de fotografías por espécimen, es capaz de recrear el escenario tridimensional de gran cantidad de cornamentas en un espacio corto de tiempo y bajo condiciones desfavorables.

Material y métodos

Área de estudio y muestra

Una muestra de 14 trofeos de caza de diferentes tamaños y número de puntas fue utilizada. Los trofeos, procedentes de diferentes fincas del noreste de Sierra Morena, fueron obtenidos durante las temporadas de caza 2008 y 2009.

Datos geométricos para la homologación de trofeos

La homologación de trofeos se basa en la medida y asignación de puntuaciones a las cornamentas según lo descrito en protocolos de caza. Para las cornamentas de la muestra se tuvo en cuenta: la longitud del eje principal, la longitud de las luchaderas, la longitud de los candiles, el perímetro de la roseta, el perímetro de ciertos puntos de la cornamenta y la máxima separación entre ramas.

Herramientas, hardware y software

Las correspondientes fotografías fueron realizadas mediante una cámara digital modelo SX210 IS. El sistema CAD paramétrico variacional utilizado, fue SolidWorks. Las medidas de las cornamentas se realizaron mediante cinta métrica (Tape) y un brazo articulado (CMA).

Método fotogramétrico y tecnología CAD-3D

El PhIMM, permite la representación tridimensional de estructuras, a partir de dos fotografías tomadas desde diferente perspectiva, con el fin de localizar puntos de referencia comunes.

Los rayos de luz capturados por una cámara son aquellos procedentes de un objeto, que caen en el plano de la fotografía y pasan a través de la lente. En el plano de una fotografía se reproduce la imagen real de las estructuras, reducida en escala e invertida. El PhIMM utiliza una imagen no invertida localizada tras el objeto de estudio. Para la medida fotogramétrica de las cornamentas se debe incluir una referencia métrica de tamaño conocido en cada fotografía. Las correspondientes fotografías se enmarcan en un rectángulo donde se traza una diagonal. El centro de dicha diagonal se corresponde con el centro de la fotografía. Desde dicho centro se proyecta una línea perpendicular al plano de la fotografía que representa el eje de una pirámide cuyo vértice será el origen de la luz incidente sobre la imagen. La base de la pirámide se

incluye en el plano de la fotografía, coincidiendo con las esquinas de la referencia métrica utilizada. Mediante el uso de tecnología CAD, el vértice de la pirámide alcanza una posición fija que coincide con la localización exacta de la cámara fotográfica. El proceso se repite para una segunda cámara. De esta manera, tras la proyección de dos haces de luz distintos se representa el mismo escenario virtual desde dos puntos de vista diferentes. Los rayos de luz que tocan la correspondiente fotografía coinciden con algún elemento fotografiados. Donde los rayos de ambas fotografías se cruzan, representa la posición real del objeto en el espacio.

La normalidad de los datos, así como su homocedasticidad fueron testados Las medidas obtenidas de cada cornamenta, a partir de la utilización. de tres métodos distintos (tradicional (*Tape*), medidora de coordenadas (CMA) y PhIMM (CAD)), fueron evaluadas. Un análisis de la varianza (ANOVA), así como un test de comparación múltiple también fueron utilizados. Finalmente, se calculó el coeficiente de correlación entre las diferentes longitudes obtenidas con los tres métodos.

Resultados y discusión

Las longitudes del eje principal, luchaderas y candiles, así como la máxima separación entre ramas de las cornamentas fueron calculadas usando tres métodos (Tape, CMA y CAD). Se realizó la comparación de determinados perímetros de la estructura utilizando los métodos Tape y CAD.

No se encontraron diferencias significativas entre las longitudes de las luchaderas usando los tres métodos (luchaderas p= 0.82; candiles p= 0.89; eje principal p= 0.96; y máxima separación interna p= 0.99). Los perímetros calculados tampoco fueron significativamente diferentes (roseta, p = 0,68; posición 1, p = 0,82; y posición 2, p= 0.85).

Los resultados mostraron una mayor similitud en aquellas longitudes más grandes (eje principal y máxima separación

interna). Ello es consecuencia de que tanto en CMA como en CAD, las longitudes son estimadas por curvas que pasan a través de una serie de puntos homólogos escogidos. Dichas curvas son más adaptables, cuanto mayor es el número de puntos homólogos utilizados. De esta manera, mientras las luchaderas se definen por un máximo de 3-4 puntos, el eje principal de las cornamentas puede definirse por más de 20. En cuanto a la máxima separación entre ramas, la similitud entre métodos es todavía mayor puesto que, se representa por una línea recta.

Conclusiones

Tras la validación del PhIMM mediante una colección de trofeos de caza, los resultados fueron comparados con los obtenidos mediante los sistemas Tape y CMA. Las medidas realizadas con el sistema tradicional (Tape) requieren de unos 20 minutos por cornamenta. Los resultados fueron similares en los tres casos, proporcionando valores análogos para las diferentes longitudes medidas.

Los métodos Tape y CMA, son más difícilmente aplicables en el campo que el método CAD, ya que éste sólo requiere dos fotos por espécimen. Ello a su vez permite el estudio de un elevado porcentaje de cornamentas en el campo. Además, los métodos fotogramétricos permiten la obtención de otra información de interés, lejos del campo.

El PhIMM o método CAD, es útil en la obtención de datos necesarios tanto para la homologación de trofeos como para la obtención de datos para análisis de tipo morfométrico. Es un método de bajo coste y rápida aplicación. Asimismo, dicho método sería aplicable en el campo de la zoología.

Discusión general

La aparición de nuevas tecnologías ha supuesto una nueva vía de exploración para la obtención de más información y de mejor calidad sobre diferentes aspectos de las cornamentas. Así, el presente estudio analiza características de las astas de ciervo Ibérico, mediante la utilización de morfometría geométrica y un método fotogramétrico interactivo.

El peso económico del ciervo Ibérico, especialmente en referencia al valor de sus astas como trofeos de caza, destaca la importancia de la morfología de la estructura.

Los resultados obtenidos han permitido determinar con mayor detalle, cambios experimentados por las cornamentas según la edad de los especímenes. La precisión en la descripción de los cambios, fundamenta la idea de usar morfometría geométrica para la cuantificación de los mismos en estructuras complejas. Además, dicha metodología podría ser aplicada al estudio de los cambios de forma de astas de otras especies de ungulados como el gamo, o bien, en estudios paleontológicos.

La creciente complejidad de las cornamentas con la edad, ocurre sobre todo a nivel de corona. Aparentemente, no se conoce ni la posición ni el máximo número de puntas que la corona puede alcanzar, lo que supondría un reto a considerar en este campo.

Las cornamentas, alcanzan su máximo desarrollo a los 8-12 años. El presente trabajo mostró que los individuos de la clase de edad 4 (8-9 años), generalmente presentaban el máximo número de puntas siendo los mejores trofeos de la muestra. Sin embargo, una edad óptima para los trofeos no pudo ser definida.

La morfometría geométrica también permitió visualizar los cambios de forma de las astas en las diferentes clases de edad y categorías de trofeos. Dicha visualización, reveló la tendencia del desarrollo de las cornamentas con los años, y permitió la identificación de individuos excepcionalmente desarrollados, lo

que permite una categorización más rigurosa del valor de las astas. Las astas son estructuras simétricamente bilaterales. Sin embargo, su desarrollo final depende tanto de aspectos genéticos como ambientales, sobre todo en cuanto a disponibilidad de alimento se refiere. Ello, implica gran variabilidad morfológica entre las estructuras estudiadas, dando lugar, en ocasiones, a la presencia de asimetrías entre ramas. Muchos estudios evalúan la presencia de asimetría fluctuante (FA) en cornamentas ya que, dicha asimetría aparentemente predice la inestabilidad de desarrollo o la *fitness* de los individuos. Con todo, existe gran controversia sobre el uso de FA como indicador de calidad individual.

En este caso, se evaluó la presencia de FA. Sin embargo, se encontraron valores más elevados de asimetría direccional (DA), lo que rechazó la posibilidad de considerar FA como indicador de calidad individual.

La existencia de DA dio lugar a una rama derecha más grande. Una razón para la existencia de DA, pudo ser la introducción de especímenes procedentes de otras poblaciones en el área de estudio. Por otro lado, el tener la rama derecha más desarrollada, y el hecho de que las cornamentas son principalmente utilizadas como armas en combates intraespecíficos, sugirió un uso más intenso de dicha rama durante las luchas. Asimismo, sería posible observar si hay relación entre la tendencia de los ciervos a iniciar la marcha con las extremidades derechas o izquierdas y un mayor desarrollo de un lado de la cornamenta, del mismo modo que ocurre cuando se dan lesiones en las patas.

Los cambios de forma observados a lo largo de las astas suelen ocurrir de manera coordinada entre sus partes, sugiriendo la existencia de diferentes unidades anatómicas en la estructura. Cuando dichas unidades actúan con cierta independencia con respecto al resto de la estructura, se habla de la existencia de módulos. La presencia de modularidad, está

relacionada con el concepto de integración morfológica, puesto que todas las partes de un organismo suelen coordinarse para actuar como un todo. En el caso de las cornamentas, se encontró presencia de modularidad en la corona y candiles, pero no en el eje principal y las luchaderas. En un principio, se pensó que la covariación encontrada entre las diferentes partes de la estructura era debida a la acción de vías implicadas directamente en el desarrollo (FA). Sin embargo, la presencia de integración en FA sugirió alteraciones en dichas vías que afectarían a la totalidad de la estructura. La coincidencia entre los patrones de covariación entre módulos y dentro de los módulos, sugirió que las diferentes partes del asta compartían mecanismos de covariación. Así, no fue posible aislar los fenómenos de modularidad e integración, indicando que las cornamentas generalmente actúan como módulos coordinados internamente coherentes, con el fin de realizar una función común. A pesar de ello, la modularidad encontrada en determinadas partes de la estructura, es indicativo de su comportamiento relativamente independiente a lo largo del proceso de desarrollo.

Paralelamente, un método fotogramétrico interactivo de medida (PhIMM) fue propuesto para completar el estudio de las astas. Dicho método es interesante puesto que proporciona ventajas significativas para la recolección de datos, y la visualización tridimensional de las astas, de manera rápida y económica. Tras las realización de las fotografías digitales pertinentes, la falta de la toma de ciertas medidas en el campo no es problema, ya que a partir de pocos landmarks es posible extraer toda la información de interés con posterioridad. La validación del PhIMM usando trofeos de caza, mostró resultados similares a los obtenidos tanto con morfometría geométrica como con métodos tradicionales. Además, el PhIMM ha demostrado ser útil tanto para la modelización tridimensional de astas, mostrando

gran versatilidad y flexibilidad, como para ser aplicado en el campo, y no únicamente sobre trofeos de caza o especímenes de museo. De esta manera, se establece por primera vez el PhIMM como una opción viable en estudios de zoología.

Conclusiones generales

1. El estudio del cambio de forma de estructuras complejas, como las astas de ciervo Ibérico, mediante el uso de morfometría geométrica es adecuado ya que, permite obtener resultados similares a los obtenidos con métodos tradicionales, pero con mayor detalle, consiguiendo un estudio más preciso del cambio de forma asociado a los diferentes factores que afectan a la morfología de la estructura.

2. A pesar del efecto considerable de la edad sobre la variación de forma de las cornamentas, factores como el número total de puntas, el numero de puntas presente a nivel de la corona, o la presencia o ausencia de contraluchaderas, son aquellos que sufren una tasa de cambio más elevada.

3. La separación interna entre las ramas izquierda y derecha de las cornamentas aumenta con el número de puntas desarrollado, del mismo modo que ocurre con el tamaño de las mismas. Los individuos de las clases de edad 3 y 4, muestran astas relativamente cortas en su parte próxima al cráneo y arqueadas distalmente. Por otro lado, los ciervos más jóvenes, pertenecientes a las clases de edad 1 y 2, muestran astas de ejes próximos distalmente y relativamente alargados en su parte más próxima al cráneo, y tienen un escaso número de puntas. De manera que, existe una transformación progresiva de las cornamentas, con el fin de acomodar el creciente número de puntas.

4. La variación de forma de puntas específicas, como los candiles y las luchaderas, está influenciado por su nivel de desarrollo según la edad. En consecuencia, los candiles y luchaderas son más rectos y más verticalmente orientados en los individuos más jóvenes, haciéndose más largas y curvadas en individuos maduros.

5. De acuerdo con el índice de calidad de las cornamentas TQS, no fue posible encontrar una edad óptima para los trofeos de la muestra, basándose únicamente en su forma. Sin embargo, el estudio de factores que afectan a la forma de las

astas, sugiere que los individuos pertenecientes a la clase de edad 4 (8-9 años de edad), producen los mejores trofeos. No obstante, es interesante destacar que los trofeos de buena calidad comienzan a aparecer a partir de la clase de edad 2 y su aparición se prolonga hasta la 5. Ello indica la presencia de individuos de calidad genética excepcional, y/o criados en mejores condiciones ambientales y nutricionales, capaces de producir trofeos de buena calidad a edades tempranas.

6. A pesar de que efectos ambientales, como el régimen de lluvias invernales o las temperaturas invernales, afectan al desarrollo final de las cornamentas, no fue posible considerarlos como buenos predictores de la calidad de las mismas, considerando TQS.

7. No fue posible encontrar una forma característica para cada clase de edad, ya que las interacciones entre factores estudiados dieron lugar a una gran cantidad de variabilidad. De acuerdo con ello, no hubo posibilidad de asignar un número particular de puntas a cada clase de edad, puesto que los individuos de la clase de edad 1 tenían entre 6 y 11 puntas, los de la clase de edad 2 entre 9 y 14 y, de aquí en adelante, la mayoría de especímenes presentaron entre 12 y 14 puntas.

8. La presencia de asimetría fluctuante (FA) en las cornamentas ha sido tradicionalmente utilizada como indicador de calidad individual. Sin embargo, la aplicación de morfometría geométrica revela que, en la presente muestra, la asimetría direccional (DA) sería el efecto que ejercería mayor peso sobre el componente asimétrico de las astas. El error de medida cometido durante la recolección de datos fue suficientemente bajo para no afectar a los resultados, lo que apoya lo observado.

9. A pesar de que previas investigaciones registraron la tendencia natural de las cornamentas a presentar niveles elevados de FA, ello no se cumple en la muestra estudiada ya que, los niveles más elevados fueron los de DA. La coexistencia de DA y FA no es extraña, puesto que se relaciona con los diferentes orígenes evolutivos de ambos tipos de asimetría, y con el hecho de que es la combinación de genética más ambiente la responsable del desarrollo final de la estructura. Así,

a pesar de que FA afecta al desarrollo final de las astas, su origen evolutivo más inestable, principalmente determinado por estreses externos, podría inclinar la balanza hacia una mayor presencia de DA o FA.

10. El haber encontrado DA en las cornamentas de ciervo Ibérico, proporciona nuevos conocimientos acerca del estudio de su asimetría y desarrollo, ya que presentar un lado derecho más desarrollado podría relacionarse con un uso más intenso de esa parte del cuerpo durante las luchas, lo cual a su vez podría influir sobre el éxito en la lucha y apareamiento. Por otro lado, ello podría estar relacionado con ciertos hábitos de la locomoción de ciervos.

11. Las diferencias generales observadas entre el componente asimétrico de las cornamentas y FA, con respecto a la edad y el año de captura, están influenciadas por la DA encontrada, así como por la condición de caracteres sexuales secundarios de las mismas.

12. La alometría significativa detectada en los componentes simétrico y asimétrico de las cornamentas, tanto del conjunto de datos de las astas completas como de medias astas, no fue el principal factor de integración en la estructura.

13. La modularidad e integración encontradas en las cornamentas mostraron la imposibilidad de separar ambos fenómenos, lo cual refuerza el hecho de que la modularidad es una cuestión de grados, y que el crecimiento continuo observado en la estructura podría influir a los niveles de integración encontrados, y a la variación morfológica de sus partes.

14. A pesar de que en el desarrollo de toda la cornamenta se encuentran generalmente involucrados los mismos procesos de desarrollo, la aparición tardía de algunas partes durante el crecimiento les proporcionaría un comportamiento relativamente independiente, como es el caso de los candiles. Este hecho podría estar relacionado con la progresiva especialización de las diferentes puntas de las astas, del mismo modo que ocurre con la luchaderas de los caribús.

15. La cornamenta de ciervo Ibérico actuaría como un módulo completamente integrado por diferentes unidades, cuya variación se caracterizaría por ocurrir de manera coordinada a lo largo del desarrollo, y cuyo propósito sería actuar como arma durante las luchas influyendo sobre el éxito social y reproductor de los ciervos.

16. El método fotogramétrico interactivo (PhIMM) proporciona resultados para la evaluación de la calidad de las cornamentas idénticos a aquellos obtenidos mediante métodos tradicionales (cinta métrica), o mediante morfometría geométrica (Landmarks), de manera rápida y económica. Además, dicho método permite obtener volúmenes y perímetros de las estructuras.

17. El PhIMM representa ventajas significativas en la recolección de datos geométricos de todo tipo de estructuras, por lo que se considera adecuado para la aplicación directa en individuos en el campo y no sólo sobre trofeos de caza o especímenes de museo. Al mismo tiempo, el PhIMM ha sido considerado útil para la modelización de cornamentas mediante ordenador, dando lugar a la representación tridimensional de las mismas. A su vez, dichos modelos resuelven la falta de toma de ciertas medidas en el campo, ya que permiten recolectar posteriormente información extra de interés.

18. Llevando a cabo los ajustes necesarios sobre el PhIMM, es posible su aplicación a la morfología de cualquier especie. De esta manera, este trabajo establece por primera vez el PhIMM como una opción viable para estudios zoológicos.

9. Conclusions

9. General conclusions

1. The shape change study of complex structures as Iberian red deer antlers through the use of geometric morphometrics methods is suitable, since it allows to obtain similar results than traditional methods but in larger detail, getting a more precise study of the shape change associated to the different factors affecting the antler morphology.

2. Although the great effect of age on antler shape variation, are factors like the total number of tines, the number of tines present at antler crown level or the presence or absence of bez tines, those exerting a higher change rate.

3. The degree of separation between antler branches increases at the upper part of the antler with the number of tines developed, in the same way as occurs with antler size. Individuals from age classes 3 and 4, show antlers relatively shorter near the skull and arched distally. Instead, youngest deer (from age classes 1 and 2) show antler beams closer distally and relatively elongated near the skull, since they have a few number of tines. Accordingly, there is a progressive antler transformation, in order to accommodate the increasing number of tines.

4. The shape variation of specific tines, as the trez and eye tines, is influenced by its developmental level according to age. Consequently, the trez and eye tines are straighter and more vertically oriented in youngest individuals, becoming longer and more curved in older individuals.

5. According to the TQS antler quality index, it was not possible to find an optimum trophy age based on antler shape alone. However, the study of factors affecting the antler shape suggests that age class 4 (8 to 9 years

old) produces the best quality trophies, but it is also interesting to note that good quality trophies start to appear from age classes 2 to 5, indicating the presence of individuals of exceptional genetic quality, or bred in best environmental and nutritional conditions, able to produce good antler trophies at early ages.

6. Although environmental effects as the winter rainfall and winter temperature levels affect the final antler development, we cannot consider them as good predictors of antler quality considering the TQS.

7. A characteristic shape was not found to any specific age class, since the interactions among the factors studied create a huge pool of variability. In agreement, there is no possibility to establish a particular number of tines to the different age classes, since individuals from age class 1 used to have between 6 and 11 tines, those of age class 2 ranged from 9 to 14 tines, and hereafter most of the specimens had between 12 and 14 tines.

8. The presence of Fluctuating asymmetry (FA) in antlers has been traditionally used as a reliable individual quality indicator. However, geometric morphometrics methods revealed that in this case, the Directional asymmetry (DA) would be the effect exerting a higher weight over the asymmetric component of antlers. The measurement error committed during data collection was low enough to be considered negligible, which gives support to that observed.

9. Although previous research registered that natural trend of antlers is to present higher levels of FA, it is not fitted by the antlers of the sample, since they showed higher values of DA. The coexistence and significance of DA and FA in antlers is not surprising, because it is related to the different developmental origins of both types of asymmetry and the fact

that it is the combination of genetics and environment the responsible of the final antler development. Thus, despite FA affects the final antler development, its more unstable origin principally determined by external stresses, could tip the balance towards a greater presence of DA or FA.

10. To have found DA on Iberian red deer antlers, provides new insights over the study of its asymmetry and development, since the fact of presenting a more developed right antler side, could be related to a more intense use of the right body side during fights, which could influence its fight and mating success. On the other hand, it could be related to certain locomotion habits of deer.

11. The general differences observed between the asymmetric component of antlers and the FA relationships with respect deer age and capture year are influenced by the significant Directional asymmetry (DA) found in the sample, as well as by the secondary sexual character condition of antlers.

12. The significant allometry detected in the symmetric and asymmetric antler components of the complete and half antler datasets, was not the primary factor of integration in antlers.

13. The significant modularity and integration found in antlers, showed the no possibility to separate both phenomena, which reinforces the fact that modularity is a matter of degrees and that the continued growth observed in antlers could be influencing the integration levels found, and the morphological variation of the different antler parts.

14. Although the overall antler development is generally involved by the same developmental processes, the later appearance of some parts during antler growth would provide a relatively independent behaviour, as

occurred with the trez tines. This fact could be related to the progressive specialization of the different antler tines, in the same way as occur with the eye tines in caribous.

15. The Iberian red deer antler would act as a fully integrated module comprised by different units, whose variation is characterized by occur in a coordinated way throughout its development, and whose purpose would be to act as a weapon during fights influencing the social and mating success of deer.

16. The Photogrammetric Interactive Method (PhIMM) is able to provide the same results to those obtained for the quality assessment of antlers with traditional methods (tapes) or geometric morphometrics methods (landmark coordinates), in a fast and economic way. Furthermore, the method is able to obtain volumes and perimeters of structures.

17. The PhIMM represents significant advantages over geometric data collection of all type of structures, since it is expected to be suitable for application to individuals in the field, and not just about hunting trophies or museum specimens. Moreover, the PhIMM has also been proved useful for the computer modelling of antlers allowing the three-dimensional representation of them. In turn, these models solve the lack of taking certain measurements in the field, since they allow to collect extra interesting information later.

18. Performing the necessary adjustments over the PhIMM, it could be also applied to the morphology of any species. Thus, this work establishes for the first time the PhIMM as a viable option in zoological studies.

10. Literature cited

10. Literature cited

Adams, DC, Rohlf, FJ and Slice, DE (2004). Geometric morphometrics: ten years of progress following the "revolution". *Ital. J. Zool.* **71:** 5-16.

Aguilar, MA, Aguilar, FJ, Agüera, F and Carvajal, F (2005). The Evaluation of close-range photogrammetry for the modelling of mouldboard plough surfaces. *Biosyst. Eng.* **90:** 397-407.

Allen, SP, Maden, M and Price, JS (2002). A role of retinoic acid in regulating the regeneration of deer antlers. *Dev. Biol.* **251:** 409-423.

Alvarado, A (2004). Regeneration and the need for simpler model organisms. *Phil. Trans. R Soc. Lond. B* **359:** 759-763.

Alvarez, F (1995). Functional directional asymmetry in fallow deer (*Dama dama*) antlers. *J. Zool. Lond.* **236:** 563-569.

Aristóteles, 1990. Libro IX. Castración de los cuadrúpedos. In: *Historia de los animales*. Vara-Donado, J (ed), pp. 600. Madrid: Akal SA.

Azorit, C (2011). Guía para la determinación de la edad del ciervo Ibérico (*Cervus elaphus hispanicus*) a través de su dentición: revisión metodológica y técnicas de elección. *Anales* **24:** 237-264.

Azorit, C, Analla, M, Carrasco, R, Calvo, JA and Muñóz-Cobo, J (2002c). Teeth eruption pattern in red deer (*Cervus elaphus hispanicus*) in southern Spain. *An. Biol.* **24:** 107-114.

Azorit, C, Analla, M, Carrasco, C, Carrasco, R and Muñóz-Cobo, J (2002b). Astas, esqueleto y edad del ciervo (*Cervus elaphus hispanicus*) de Sierra Morena oriental: Estudio de correlación. *An. Biol.* **24**: 195-200.

Azorit, C, Analla, M, Carrasco, R and Muñóz-Cobo, J (2002a). Influence of age and environment on antler traits in Spanish red deer (*Cervus elaphus hispanicus*). *Z. Jagdwiss*. **48**: 137-144.

Azorit, C, Analla, M, Hervas, J, Carrasco, R, Muñoz-Cobo, J (2002e). Growth marks observation: preferential techniques and teeth for ageing of Spanish red deer (*Cervus elaphus hispanicus*). *Anat. Histol. Embryol.* **31:** 303-307.

Azorit, C, Analla, M and Muñóz-Cobo, J (2003). Variation of mandible size in red deer *Cervus elaphus hispanicus* from southern Spain. *Acta Theriol.* **48:** 221-228.

Azorit, C, Hervas, J, Analla, M, Carrasco, R, Muñoz-Cobo, J (2002f). Histological thin sections: a method for the microscopic study of teeth in Spanish red deer (*Cervus elaphus hispanicus*). *Anat. Histol. Embryol.* **31:** 224-227.

Azorit, C, Muñoz-Cobo, J, Analla, M (2002d). Seasonal deposition of cementum in first lower molars from *Cervus elaphus hispanicus*. *Mamm. Biol.* **67:** 243-245.

Azorit, C, Muñoz-Cobo, J, Hervas, J and Analla, M (2004). Aging through growth marks in teeth of Spanish red deer (*Cervus elaphus hispanicus*). *Wildlife Soc. B* **32:** 702-710.

Baab, KL (2013). The impact of superimposition choice in geometric morphometric approaches to morphological integration. *J Hum. Evol.* **65:** 689-692.

Baab, KL, McNulty, KP and Rohlf, FJ (2012). The shape of human evolution: A geometric morphometrics perspective. *Evol. anthropol.* **21**: 151-165.

Baciut, M, Baciut, G, Simon, V, Albon, C, Coman, V, Prodan, P, Florian, SI and Bran, S (2007). Investigation of deer antler as a potential bone regenerating biomaterial. *J. Optoelectro. Adv. M* **9:** 2547-2550.

Badyaev, A (2004). Developmental perspective on the evolution of sexual ornaments. *Evol. Ecol. Res.* **6:** 1-17.

Baltsavias, EP (1999). A comparison between photogrammetry and laser scanning. *ISPRS J. Photogramm. Remote Sens.* **54:** 83-94.

Banks, JW and Newbury, WJ (1983). Antler development as a unique modification of mammalian endochondral ossification. *Antler Dev. Cervidae* **1:** 279-306.

Bartos, L and Bahbouh, R (2006). Antler size and fluctuating asymmetry in red deer (*Cervus elaphus*) stags and probability of becoming and harem holder in rut. *Biol. J. Linn. Soc.* **87:** 59-68.

Bartos, L, Bahbouh, R and Vach, M (2007). Repeatability of size and fluctuating asymmetry of antler characteristics in red deer (*Cervus elaphus*) during ontogeny. *Biol. J. Linn. Soc.* **91:** 215-226.

Bateman, PW (2000). The influence of weapon asymmetry on male-male competition sucess in a sexually dimorphic insect, the African King Cricket *Libanasidus vittatus* (Orthoptera: Anostostomatidae). *J. Insect Behav.* **13:** 157-163.

Baumberg, A, Lyons, A and Taylor, R (2005). 3D S.O.M.—A commercial software solution to 3D scanning. *Graph. models* **67:** 476-495.

Bennett, ET (2005). *Cervus elaphus barbarus*, 1833. In: Mammal Species of the World (MSW). A Taxonomic and Geographic Reference (3rd ed), Wilson, DE and Reeder, DM (eds), pp. 2142. Baltimore: Johns Hopkins University Press.

Berglund, A, Bisazza, A and Pilastro, A (1996). Armaments and ornaments: an evolutionary explanation of traits of dual utility. *Biol. J. Linn. Soc.* **58:** 385-399.

Bhatla, A, Choe, SY, Fierro, O and Leite, F (2012). Evaluation of accuracy of as-built 3D modeling from photos taken by handheld digital cameras. *Automat. Constr.* **28:** 116-127.

Blackith, R and Reyment, RA (1971). Multivariate morphometrics. pp. 412. New York: Academic Press.

Bookstein, FL (1982). Foundation of morphometrics. *Annu. Rev. Ecol. Evol. S* **13:** 451-470.

Bookstein, FL (1984). A statistical method for biological shape comparisons. *J. theor. Biol.* **107:** 475-520.

Bookstein, FL (1991). Morphometric tools for landmark data: Geometry and biology. pp. 435. New York: Cambridge University Press.

Bookstein, FL (1996). Combining the tools of geometric morphometrics. *Nato. Adv. Sci. Inst. Se.* **284:** 131-151.

Bookstein, FL (1998). A hundred years of morphometrics. *Acta Zool. Acad. Sci. Hung.* **44:** 7-59.

Bookstein, FL, Chernoff, B, Elder, RL, Humphries, JM, Smith, GR and Strauss, RE (1985). Morphometrics in evolutionary biology: the geometry of size and shape change. pp. 277. Philadelphia: Academy of Natural Sciences Press.

Bookstein, FL, Gunz, P, Mitteroecker, P, Prossinger, H, Schaefer, K and Seidler, H (2003). Cranial integration in *Homo*: singular warps analysis of the midsagittal plane in ontogeny and evolution. *J. Hum. Evol.* **44:** 167-187.

Brilakis, I, Lourakis, M, Sacks, R, Savarese, S, Christodoulou, S, Teizer, J and Makhmalbaf, A (2010). Toward automated generation of parametric BIMs based on hybrid video and laser scanning data. *Adv. Eng. Inform.* **24:** 456-465.

Bubenik, GA (1983). The endocrine regulation of the antler cycle. In: *Antler development in Cervidae*. Brown, RD (ed), pp. 480. Kingsville: Caesar Kleberg Wildlife research Institute.

Carranza, J (1999). Aplicaciones de la Etología al manejo de las poblaciones de ciervo del suroeste de la Península Ibérica: producción y conservación. *Etología* **7:** 5-18.

Carranza, J (2004). Ciervo-*Cervus elaphus* Linnaeus, 1758. In: *Enciclopedia Virtual de los Vertebrados Españoles*. Carrascal, LM and Salvador, A (eds). Madrid: Museo Nacional de Ciencias Naturales.
http://www.vertebradosibericos.org.

Chapman, DI (1975). Antler-bones of contention. *Mammal Re*v. **5:** 121-172.

Chin-Hung, T, Yun-Sheng, C and Wen-Hsing, H (2007). Constructing a 3D trunk model from two images. *Graph. Models* **69:** 33-56.

Chritz, KL, Dyke, GJ, Zazzo, A, Lister, AM, Monaghan, NT and Sigwart, JD (2009). Palaeobiology of an extinct Ice Age mammal: Stable isotope and cementum analysis of giant red deer teeth. *Palaeogeogr. Palaeocl.* **282:** 133-144.

Clements, MN, Clutton-Brock, TH, Albon, SD, Pemberton, JM and Kruuk, LEB (2010). Getting the timing right: antler growth phenology and sexual selection in a wild red deer population. *Oecología* **164:** 357-368.

Clutton-Brock, TH (1982). The Functions of Antlers. *Behaviour* **79:** 108-125.

Clutton-Brock, TH, Albon SD, Gibson, RM and Guinness, FE (1979). The logical stag: adaptative aspects of fighting in red deer (*Cervus elaphus L.*). *Anim. Behav.* **27:** 211-225.

Clutton-Brock, TH, Guinnes, FE and Albon, SD (1982). Red deer: Behavior and ecology of two sexes. pp. 250. Chicago: University of Chicago Press.

Conner, JK and Sterling, A (1996). Selection for independence of floral and vegetative traits: evidence from correlation patterns in five species. *Can. J. Bot.* **74:** 642-644.

Corbet, GB (1978). The mammals of the Paleartic Region: A taxonomic review. pp. 314. London: British Museum.

Corti, M and Crosetti, D (1996). Geographic variation in the grey mullet: a geometric morphometric analysis using partial warp scores. *J. Fish. Biol.* **48:** 255-269.

Damuth, JD and McFadden, BJ (1990). Body Size in Mammalian Paleobiology: Estimation and Biological Implications. pp. 397. Cambridge: Cambridge University Press.

Debat, V, Alibert, P, David, P, Paradis, E and Auffray, JC (2000). Independence between developmental stability and canalization in the skull of the house mouse. *Proc. R. Soc. Lond. B Biol. Sci.* **267:** 423-430.

De los Reyes, AD (1990). Los venados de nuestras sierras. pp. 228. Madrid: Aldaba Ediciones S.A.

Demarsin, K, Vanderstraeten, D, Volodine, T and Roose, D (2007). Detection of closed sharp edges in point clouds using normal estimation and graph theory. *Comput. Aided Des.* **39:** 276-283.

Ditchkoff, SS and Defreese, RL (2010). Assessing fluctuating asymmetry of white-tailed deer antlers in a three-dimensional context. *J. Mammal.* **91:** 27-37.

Ditchkoff, SS, Lochmiller, RL, Masters, RE, Hoofer, SR and Van Den Bussche, RA (2001). Major-histocompatibility-complex-associated variation in secondary sexual traits of white-tailed deer (*Odocoileus virginianus*): Evidence for good-genes advertisement. *Evolution* **55:** 616-625.

Douglas, MJW (1970). Dental cement layers as criteria of age for deer in New Zealand with emphasis on Red deer, *Cervus elaphus*. *New Zeal. J. Sci.* **13:** 352-358.

Drake, AG and Klingenberg, CP (2008). The pace of morphological change: historical transformation of skull shape in St. Bernard dogs. *Proc. R. Soc. Lond. B Biol. Sci.* **275:** 71-76.

Dryden, IL and Mardia, KV (1998). Statistical shape analysis. pp. 384. Chichester: John Wiley and Sons.

Dürer, A (1528). Vier Bücher von menschlicher Proportion. pp. 264. Nuremberg: Hieronymus Formschneyder.

Elewa, AMT (2010). Morphometrics for non morphometricians. pp. 367. London: Springer.

Ellerman, JR and Morrison-Scott, TCS (1951). Check list of Paleartic and Indian Mammals 1758-1946. pp. 810. London: Natural History Museum.

Emlen, DJ, Warren, IA, Johns, A, Dworkin, I and Lavine, LC (2012). A Mechanism of Extreme Growth and Reliable Signaling in Sexually Selected Ornaments and Weapons. *Science* **337:** 860-864.

Escoufier, Y (1973). Le traitement des variables vectorielles. *Biometrics* **29:** 751-760.

Estévez, JA, Landete-Castillejos, T, García, AJ, Ceacero, F and Gallego, L (2008). Population management and bone structural effects in composition and radio-opacity of Iberian red deer (*Cervus elaphus hispanicus*) antlers. *Eur. J. Wild. Res.* **54:** 215-223.

Faucheaux, C Allen, S, Nicholls, BM, Danks, JA, Horton, MA and Price, JS (2004). Recapitulation of the parathyroid hormone-related peptide-Indian hedgehog pathway in the regenerating deer antler. *Devl. Dynam.* **231:** 88-97.

Fennessy, PF and Suttie, JM (1985). Antler growth: Nutritional and endocrine factors. In: *Biology of deer production*. *R Soc. N Z Wellington Bull.* **22:** 239-250.

Fierro, Y, Gortazar, C, Landete-Castillejos, T, Vicente, J, García, A and Gallego, L (2002). Baseline values for cast antlers of Iberian red deer (*Cervus elaphus hispanicus*). *Z. Jagdwiss*. **48**: 244-251.

Fisher, RA (1935). The logic of inductive inference. *J. R. Stat. Soc.* **98:** 39-82.

Fortin, D, Cheriet, F, Beauséjour, M, Debanné, P, Joncasm J and Labelle, H (2007). A 3D visualization tool for the design and customization of spinal braces. *Comput. Med. Imag. Grap.* **31:** 614-624.

Fowler, ME (1993). Horns and antlers. In: *Zoo and wildlife medicine: Current therapy 4*. Fowler, ME, Miller, RE (eds), pp. 512. St. Louis: Saunders Elsevier.

Francis, SM and Suttie, JM (1998). Detection of growth factors and proto-oncogene mRNA in the growing tip of red deer (*Cervus elaphus*) antler using reverse-transcriptase polymerase chain reaction (RT-PCR). *J. Exp. Zool.* **281:** 36-42.

Frieß, M (2003). An application of the relative warps analysis to problems in human paleontology–with notes on raw data quality. *Image Anal. Stereol.* **22:** 63-72.

García, AJ, Gaspar-López, E, Estévez, JA, Gómez, JA, Ceacero, F, Olguín, A, Carrión, D, Landete-Castillejos, T and Gallego, L (2010). El trofeo en los cérvidos: caracterización funcional del crecimiento de la cuerna usando como modelo el ciervo. In: *Ungulados silvestres de España: biología y tecnologías reproductivas para su conservación y aprovechamiento cinegético*. Instituto Nacional de Investigación y Tecnología Agraria y Alimentaria (INIA) (ed), pp. 300. Madrid: Ministerio de Ciencia e Innovación.

García, AJ, Landete-Castillejos, T, Garde, J and Gallego, L (2002). Reproductive seasonality in female Iberian red deer. *Theriogenology* **58:** 1553-1562.

Garde, JJ, Fernández-Santos, MR, Soler, AJ, Esteso, MC, Maroto-Morales, A, García-Álvarez, O, García-Díaz, AJ, Ortiz, JA and Ramón, M (2010). Ciervo Ibérico (C*ervus elaphus hispanicus*, Hilzheimer 1909). In: *Ungulados silvestres de España: biología y tecnologías reproductivas para su conservación y aprovechamiento cinegético*. Instituto Nacional de Investigación y Tecnología Agraria y Alimentaria (INIA) (ed), pp. 300. Madrid: Ministerio de Ciencia e Innovación.

Gaspar-López, E, García, AJ, Landete-Castillejos, T, Carrión, D, Gómez, JA, Estévez, JA and Gallego, L (2007). Descripción del crecimiento de la primera cuerna en ciervo ibérico (*Cervus elaphus hispanicus*). *Galemys* **19:** 115-127.

Gaspar-López, E., Landete-Castillejos, T., Estévez, J.A., Ceacero, F., Gallego, L. and García, A.J. (2010). Biometrics, Testosterone, Cortisol and AntlerGrowth Cycle in Iberian Red Deer Stags (*Cervus elaphus hispanicus*). *Reprod. Domest. Anim.* **45:** 243-249.

Geist, V (1998). Deer of the world: their evolution, behaviour and ecology. pp. 432. Mechanisburg: Stackpole Books.

Gingerich, PD (1984). Pleistocene extinctions in the context of origination-extinction equilibrium in Cenozoic mammals. In: *Quaternary extinctions: A prehistoric revolution*. Martin, PS and Klein, RG (eds), pp. 892. Tucson: University of Arizona Press.

Golparvar-Fard, M, Bohn, J, Teizer, J, Savarese, S and Peña-Mora, F (2011). Evaluation of image-based modeling and laser scanning accuracy for emerging automated performance monitoring techniques. *Automat. Constr.* **20:** 1143-1155.

Gómez, S, García, AJ, Luna, S, Kierdorf, U, Kierdorf, H, Gallego, L and Landete-Castillejos, T (2013). Labeling studies on cortical bone formation in the antlers of red deer (*Cervus elaphus*). *Bone* **52:** 506-515.

Gómez-Robles, A, Martinón-Torres, M, Bermúdez de Castro, JM, Margvelashvili, A, Bastir, M, Arsuaga, JL, Pérez-Pérez, A, Estebaranz, F and Martínez, LM (2007). A geometric morphometric analysis of hominin upper first molar shape. *J. Hum. Evol.* **53:** 272-285.

Goss, RJ (1968). Inhibition of growth and shedding of antlers by sex hormones. *Nature* **220:** 83-85.

Goss, RJ (1969). Photoperiod control of antler cycles in deer II. Alterations in amplitude. *J. Exp. Zool.* **171:** 311-324.

Goss, RJ (1970). Problems of antlerogenesis. *Clin. Orthop.* **69:** 227-238.

Goss, RJ (1983). Deer antlers: Regeneration, Function and Evolution. pp. 336. New York: Academic Press.

Goss, RJ (1995). Future directions in antler research. *Anat. Rec.* **241:** 291-302.

Gould, SJ (1973). The origin and function of "bizarre" structures: antler size and skull size in the "Irish elk", *Megaloceros giganteus*. *Evolution* **28:** 191-220.

Goyal, M, Murugappan, S, Piya, C, Benjamin, W, Fang, Y, Liu, M and Ramani, K (2012). Towards locally and globally shape-aware reverse 3D modeling. *Comput. Aided Des.* **44:** 537-553.

Graham, JH, Freeman, DC and Emlen, JM (1994). Antisymmetry, directional asymmetry and dynamic morphogenesis. In: *Developmental instability: Its origins and evolutionary implications*. Markow, TA (ed), pp. 448. Netherlands: Springer.

Graham, JH, Roe, KE and West, TB (1993). Effects of lead and benzene on the developmental stability of *Drosophila melanogaster*. *Ecotoxicology* **2:** 185-195.

Gyurján, IJr, Molnár, A, Borsy, A, Stéger, V, Hackler, LJr, Zomborszky, Z, Papp, P, Duda, E, Deák, F, Lakatos, P, Puskás, LG and Orosz, L (2007). Gene expression dynamics in deer antler: mesenchymal differentiation toward chondrogenesis. *Mol. Genet. Genomics* **277:** 221-235.

Hall, BK (2005). Antlers. In: *Bones and cartilage: developmental and evolutionary skeletal biology*. pp. 792. London: Elsevier Academic Press.

Hartl, GB, Lang, G, Klein, F and Willing, R (1991). Relationships between allozymes, heterozygosity and morphological characters

in red deer (C*ervus elaphus*) and the influence of selective hunting on allele frequency distributions. *Heredity* **66:** 343-350.

Hartl, GB, Zachos, F and Nadlinger, K (2003). Genetic diversity in European red deer (C*ervus elaphus L.*): anthropogenic influences on natural populations. *C. R. Biologies* **326:** S37-S42.

Harvati, K (2003). Quantitative analysis of Neanderthal temporal bone morphology using three-dimensional Geometric Morphometrics. *Am. J. Phys. Anthropol.* **120:** 323-338.

Hennessy, RJ and Stringer, CB (2002). Geometric morphometric study of the regional variation of modern human craniofacial form. *Am. J. Phys. Anthropol.* **117:** 37-48.

Hillman, JR, Davis, RW and Abdelbaki, YZ (1973). Cyclic bone remodeling in deer. *Calc. Tiss. Res.* **12:** 323-330.

Hilzheimer, J (1909). Neigen inselbewohnende Säugetiere zu einer Abnahme der Körpergröße? *Arch. f. Rass.- u. Gesellschbiol.* **6:** 305-313.

Huxley, JS (1931). The relative size of antlers in deer. *Proc. Zool. Soc. London* **72:** 819-864.

Huxley, JS (1932). Problems of relative growth. pp. 276. Baltimore: Johns Hopkins University Press.

Jojic, V, Blagojevic, J and Vujosevic, M (2011). B chromosomes and cranial variability in yellow-necked field mice (*Apodemus flavicollis*). *J. Mammal.* **92:** 396-406.

Juenger, T, Pérez-Perez, JM, Bernal, S and Micol, JL (2005). Quantitative trait loci mapping floral and leaf morphology traits in *Arabidopsis thaliana*: evidence for modular genetic architecture. *Evol. Dev.* **7:** 259-271.

Junta de Andalucía (March, 2012). www.juntadeandalucia.es

Junta Nacional de Homologacion de Trofeos de Caza (October, 2010). http://www.fedecaza.com/esp/menuprincipal/menuprincipal/otros_organismos/fedyorg/homologa.asp

Kendall, D (1977). The diffusion of shape. *Adv. Appl. Probab.* **9:** 428-430.

Kendall, D (1981). The statistics of shape. In: *Interpreting multivariate data*. Barnett, V (ed), pp. 374. New York: Wiley & Sons.

Kendall, D (1984). Shape-manifolds, Procrustean metrics and complex projective spaces. *B. Lond. Math. Soc.* **16:** 81-121.

Kerschbaumer, M and Sturmbauer, C (2011). The Utility of Geometric Morphometrics to Elucidate Pathways of Cichlid Fish Evolution. *Int. J. Evol. Biol.* **2011:** 1-8.

Kierdorf, U, Kierdorf, H and Szuwart, T (2007). Deer antler regeneration: cells, concepts and controversies. *J. Morphol.* **268:** 726-738.

Kimmerle, EH, Ross, A and Slice, D (2008). Sexual dimorphism in America: Geometric Morphometric Analysis of the craniofacial region. *J. Forensic. Sci.* **53:** 54-57.

Klein, RG, Wolf, C, Freeman, LG and Allwarden, K (1981). The use of dental crown heights for constructing age profiles of red deer and similar species in archaeological samples. *J. Archaeol. Sci.* **8:** 1-31.

Klingenberg, CP (2002). Morphometrics and the role of the phenotype in studies of the evolution of developmental mechanisms. *Gene* **287:** 3-10.

Klingenberg, CP (2003). A developmental perspective in developmental instability: theory, models and mechanisms. In: *Developmental instability*: *Causes and Consequences*. Polak, M (ed), pp. 459. New York: Oxford University Press.

Klingenberg, CP (2008a). Morphological integration and developmental modularity. *Annu. Rev. Ecol. Evol. Syst.* **39:** 115-132.

Klingenberg, CP (2008b). MorphoJ. Faculty of life sciences. Manchester: University of Manchester. http://www.flywings.org.uk/MorphoJ_page.htm

Klingenberg, CP (2009). Morphometric integration and modularity in configurations of landmarks: tools for evaluating a prior hypotheses. *Evol. Dev.* **11:** 405-421.

Klingenberg, CP (2011). MorphoJ: an integrated software package for geometric morphometrics. *Mol. Ecol. Resour.* **11:** 353-357.

Klingenberg, CP (2013). Cranial integration and modularity: insights into evolution and development from morphometric data. *Hystrix, It. J. Mamm.* **24:** 1-16.

Klingenberg, CP, Badyaev, AV, Sowry, SM and Beckwith, NJ (2001). Inferring developmental modularity from morphological integration: Analysis of individual variation and asymmetry in bumblebee wings. *Am. Nat.* **157:** 11-23.

Klingenberg, CP, Barluenga, M and Meyer, A (2002). Shape analysis of symmetric structures: quantifying variation among individuals and asymmetry. *Evolution* **56**: 1909-1920.

Klingenberg, CP and McIntyre, GS (1998). Geometric morphometrics of developmental instability: analyzing patterns of fluctuating asymmetry with Procrustes methods. *Evolution* **52:** 1363-1375.

Klingenberg, CP, McIntyre, GS and Zaklan, SD (1998). Left-right asymmetry of fly wings and the evolution of body axes. *Proc. R. Soc. Lond. B Biol. Sci.* **265:** 1255-1259.

Klingenberg, CP, Mebus, K and Auffray, JC (2003). Developmental integration in a complex morphological structure: how distinct are the modules in the mouse mandible? *Evol. Dev.* **5:**522-531.

Klingenberg, CP and Leamy, LJ (2001). Quantitative genetics of geometric shape in the mouse mandible. *Evolution* **55:** 2342-2352.

Klingenberg, CP, Wetherill, L, Rogers, J, Moore, E, Ward, R, Autti-Rämö, I, Fagerlund, A, Jacobson, SW, Robinson, LK, Hoyme, HE, Mattson, SN,Li, TK, Riley, EP, Foroud, T and CIFASD Consortium (2010). Prenatal alcohol exposure the patterns of facial asymmetry. *Alcohol* **44:** 649-657.

Klingenberg, CP and Zaklan, SD (2000). Morphological integration between developmental compartments in the *Drosophila* wing. *Evolution* **54:** 1273-1285.

Korosec, M, Duhovnik, J and Vukasinovic, N (2010). Identification and optimization of key process parameters in noncontact laser scanning for reverse engineering. *Comput. Aided Des.* **42:** 744-748.

Kruuk, LEB, Slate, J, Pemberton, JM and Clutton-Brock, TH (2003). Fluctuating asymmetry in a secondary sexual trait: no associations with individual fitness, environmental stress or inbreeding, and no heritability. *J. Evolution. Biol.* **44:** 135-142.

Kurazume, R, Nakamura, K, Okada, T, Sato, Y, Sugano, N, Koyama, T, Iwashita, Y and Hasegawa, T (2009). 3D reconstruction of a femoral shape using a parametric model and two 2D fluoroscopic images. *Comput. Vis. Image Underst.* **113:** 202-211.

Kurtén, B and Anderson, E (1980). Pleistocene mammals of North America. pp. 442. New York: Columbia University Press.

Lagesen, K and Folstad, I (1998). Antler asymmetry and immunity in reindeer. *Behav. Ecol. Sociobiol.* **44:** 135-142.

Landete-Castillejos, T, Garcia, A, Ceacero, F and Gallego, L (2013). La composición y propiedades mecánicas de cuernas y huesos de ciervo como fuente de información para gestionar ecosistemas. *Ecosistemas* **22:** 68-75.

Landete-Castillejos, T, Currey, JD, Estévez, JA, Fierro, Y, Calatayud, A, Ceacero, F, García, A and Gallego, L (2010). Do drastic weather effects on diet influence changes in chemical composition, mechanical properties and structure in deer antlers? *Bone* **47:** 815-825.

Leamy, L (1984). Morphometric studies in inbreed and hybrid house mice. V. Directional and fluctuating asymmetry. *Am. Nat.* **123:** 579-593.

Leamy, L (1993). Morphological integration of fluctuating asymmetry in the mouse mandible. *Genetica* **89:** 139.153.

Li, C, Clark, DE, Lord, EA, Stanton, JL and Suttie, JM (2002). Sampling technique to discriminate the different tissue layers of growing antler tips for gene discovery. *Anat. Rec.* **268:** 125-130.

Li, C, Suttie, JM and Clark, DE (2005). Histological examination of antler regeneration in red deer (*Cervus elaphus*). *Anat. Rec.* **282A:** 163-174.

Li, N, Zhang, H and Ouyang, H (2009). Shape optimization of coronary artery stent based on a parametric model. *Finite Elem. Anal. Des.* **45:** 468-475.

Lincoln, GA (1992). Biology of antlers. *J. Zool.* **226**: 517-528.

Lincoln, GA (1994). Teeth, horns and antlers: the weapons of sex. In: *The differences between sexes*. Short RV, Balaban E (eds), pp. 479. Cambridge: Cambridge University Press.

Lincoln, GA, Guinness, F and Short, RV (1972). The way in which testosterone controls the social and sexual behavior of the red deer stag, *Cervus elaphus*. *Horm. Behav.* **3:** 375-396.

Linnaeus, C (1758). Systema Naturae 10th edition. Ratio editions, pp 824. Stockholm: Laurentius salvius.

Lockwood, CA, Lynch, JM and Kimbel, WH (2002). Quantifying temporal bone morphology of great apes and humans: an approach using geometric morphometrics. *J. Anat.* **201:** 447-464.

López-Parra, JE, Estévez, JA, Landete-Castillejos, T, Gaspar-López, E, Olguín, CA, Ceacero, F, García, AJ and Gallego, L (2009). Comparación de parámetros estructurales, mecánicos y químicos de cuernas de ciervo ibérico (*Cervus elaphus hispanicus*) de fincas cinegéticas con diferente gestión. Sociedad Española de Ovinotecnia y Caprinotecnia (SEOC) (ed), pp. 613. Huesca: Comunicaciones cinegéticas.

Lord, E, Martin, SK, Gray, JP, Li, C and Clark, DE (2007). Cell cycle genes PEDF and CDKN1C in growing deer antlers. *Anat. Rec.* **290:** 994-1004.

Low, WA and Cowan, IM (1963). Age determination of deer by annular structure of dental cementum. *J. Wildlife Manage.* **27:** 466-471.

Ludt, CJ, Schroeder, W, Rottman, O and Kuehn, R (2004). Mitochondrial DNA phylogeography of red deer (*Cervus elaphus*). *Mol. Phylogenet. Evol.* **31**: 1064-1083.

Ludwig, W (1932). *Das Rechts-Links Problem im Tierreich und beim Menschen*, pp. 516. Berlin: Springer.

Malo, AF, Roldán, ERS. Garde, J, Soler, A and Gomendio, J (2005). Antlers honestly advertise sperm production and quality. *P. Roy. Soc. Lond. B Bio.* **272:** 149-157.

Marburger, RG, Robinson, RM, Thomas, JW, Andregg, MJ and Clark, KA (1972). Antler malformation produced by leg injury in white-tailed deer. *J. Wildlife Dis.* **8:** 311-314.

Marcos, J (1989). Biología, manejo poblacional, cinegético del ciervo. pp. 32. Zaragoza: Diputación General de Aragón.

Marcus, LF (1990). Traditional morphometrics. In: *Proceedings of the Michigan morphometrics workshop, Spec. Publ. Nº2*. Rohlf, FJ and Bookstein, FL (eds), pp. 396. Michigan: University of Michigan Museum of Zoology.

Martínez, M, Rodríguez-Vigal, C, Jones, OR, Coulson, T and San Miguel, A (2005). Different hunting strategies select for different weights in red deer. *Biol. Lett.* **1:** 353-356.

Martínez-Vargas, J (2012). Effect of the Robertsonian translocations of the modular organization of *Mus musculus domesticus* mandible in the Robertsonian system of Barcelona. Master degree in Biodiversity, University of Barcelona.

Mateos, C, Alarcos, S, Carranza, J, Sánchez-Prieto, C and Valencia, J (2008). Fluctuating asymmetry of red deer antlers negatively

relates to individual condition and proximity to prime age. *Anim. Behav.* **75:** 1629-1640.

Medarde, N, Muñoz-Muñoz, F, López-Fuster, MJ and Ventura, J (2013). Variational modularity at the cell level: insights from the sperm head of the mouse. *BMC Evol. Biol.* **13:** 179-191.

Minns, RJ, Bibb, R, Banks, R and Sutton, RA (2003). The use of a reconstructed three-dimensional solid model from CT to aid the surgical management of a total knee arthroplasty: a case study. *Med. Eng. Phys.* **25:** 523-526.

Mitchell, B (1967). Growth layers in dental cement for determining the age of Red deer (*Cervus elaphus L.*). J. *Anim. Ecol.* **36:** 279-293.

Moller, AP (1992). Patterns of fluctuating asymmetry in weapons: evidence for reliable signalling of quality in beetle horns and bird spurs. *P. Roy. Soc. Lond. B Bio.* **248:** 199-206.

Moller, AP (1994). Directional selection on directional asymmetry: testes size and secondary sexual characters in birds. *Proc. R. Soc. Lond. B* **258:** 147-151.

Moller, AP and Pomiankowski, A (1993). Fluctuating asymmetry and sexual selection. *Genetica* **89:** 267-279.

Molnár, A, Gyurján, I, Korpos, E, Borsy, A, Stéger, V, Buzás, Z, Kiss, I, Zomborszky, Z, Papp, P, Déak, F and Orosz, L (2007). Identification of differentially expressed genes in the developing antler of red deer *Cervus elaphus*. *Mol. Genet. Genomics* **277:** 237-248.

Monteiro, LR (1999). Multivariate regression models and geometric morphometrics: the search for causal factors in the analysis of shape. *Syst. Biol.* **48:** 192-199.

Montoya, JM (1999). El ciervo y el monte. Manejo y conservación (*Cervus elaphus L.*). pp. 308. Madrid: Editorial Mundi-prensa.

Morgan, JF (2007). P value fetishism and use of the Bonferroni adjustment. *EBMH Notebook* **10:** 34-35.

Mosimann, JE (1970). Size allometry: size and shape variables with characterizations of the lognormal and generalized gamma distributions. *J Am. Stat. Assoc.* **65:** 930-945.

Moyes, K, Morgan, BJT, Morris, A, Morris, SJ, Clutton-Brock, TH and Coulson, T (2009). Exploring individual quality in a wild population of red deer. *J Anim. Ecol.* **78:** 406-413.

Muir, PD, Sukes, AR and Barrel, GK (1988). Changes in blood content and histology during growth of antlers in red deer (*Cervus elaphus*) and their relationship to plasma testosterone levels. *J. Anat.* **158:** 31-42.

Nahlik, AJ (1992). Management of Deer and their Habitat. pp. 271. Dorset: Wilson Hunt.

Nicholson, E and Harvati, K (2006). Quantitative analysis of human mandibular shape using three-dimensional Geometric Morphometrics. *Am. J. Phys. Anthropol.* **131:** 368-383.

O'Higgins, P and Jones, N (2006). Tools for statistical shape analysis. Hull York Medical School. http://sites.google.com/site/hymsfme/resources

Olson, EC and Miller, RL (1958). *Morphological integration*. pp. 376. Chicago: University Chicago Press.

Ordóñez, C, Arias, P, Herráez, J, Rodríguez, J and Martín, MT (2008). Two photogrammetric methods for measuring flat elements in buildings under construction. *Automat. Constr.* **17:** 517-525.

Oxnard, C and O'Higgins, P (2009). Biology Clearly Needs Morphometrics. Does Morphometrics Need Biology? *Biol. Theor.* **4:** 84-97.

Palmer, AR (1994). Fluctuating asymmetry analyses: A primer. In: *Developmental Instability: Its Origins and Evolutionary Implications*. Markow, TA (ed), pp. 448. Netherlands: Springer.

Palmer, AR (1996). Waltzing with asymmetry. *BioScience* **46:** 518-532.

Palmer, AR (March, 2013). http://www.biology.ualberta.ca/palmer.hp/asym/asymmetry.htm

Palmer, AR (2004). Symmetry breaking and the evolution of development. *Science* **306:** 828-833.

Palmer, AR and Strobeck, C (1986). Fluctuating asymmetry: Measurement, analysis, patterns. *A. Rev. Ecol. Syst.* **17:** 391-421.

Panchetti, M, Pernot, JP and Véron, P (2010). Towards recovery of complex shapes in meshes using digital images for reverse engineering applications. *Comput. Aided Des.* **42:** 693-707.

Paramio, MAR, Muñoz-Cobo, J, Moro, J, Gutierrez, R, Oya, A, Tellado, S and Azorit, C (2012). Assessing red deer antlers density with water displacement method versus a new parametric volume modelling technique using CAD-3D. *Anim. Prod. Sci.* **52:** 750-755.

Park, HJ, Lee, DH, Park, SG, Lee, SC, Cho, S, Kim, HK, Kim, JJ, Bae, H and Park, BC (2004). Proteome analysis of red deer antlers. *Proteomics* **4:** 3642-3653.

Parsons, PA (1990). Fluctuating asymmetry: an epigenetic measure of stress. *Biol. Rev.* **65:** 131-145.

Parsons, PA (1992). Fluctuating asymmetry: a biological monitor of environmental and genomic stress. *Heredity* **68:** 361-364.

Pearson, K (1985). Note on regression and inheritance in the case of two parents. *Proc. R. Soc. Lond.* **58:** 240-242.

Pélabon, C and Joly, P (2000). What, if anything, does visual asymmetry in fallow deer antlers reveal? *Anim. Behav.* **59:** 193-199.

Pélabon, C and van Breukelen, L (1998). Asymmetry in antler size in roe deer (*Capreolus capreolus*): an index of individual and population conditions. *Oecologia* **116:** 1-8.

Pérez-González, J, Carranza, J, Torres-Porras, J and Fernández-García, JL (2010). Low heterozygosity at microsatellite markers in Iberian red deer with small antlers. *J. heredity* **101:** 553-561.

Pernot, JP, Moraru, G and Véron, P (2006). Filling holes in meshes using a mechanical model to simulate the curvature variation minimization. *Comput. Graph.* **30:** 892-902.

Pomiankowski, A and Moller, AP (1995). A resolution of the lek paradox. *Proc. R. Soc. Lond. B* **260:** 21-29.

Prakoonwit, S and Benjamin, R (2007). 3D surface point and wireframe reconstruction from multiview photographic images. *Image Vision Comput.* **25:** 1509-1518.

Price, J and Allen, S (2004). Exploring the mechanisms regulating regeneration of deer antlers. *Phil. Trans. R. Soc. Lond. B* **359:** 809-822.

Price, JS, Allen, S, Faucheux, C, Althnaian, T and Mount, JG (2005). Deer antlers: a zoological curiosity or the key to understanding organ regeneration in mammals? *J. Anat.* **207**: 603-618.

Price, JS, Oyajobi, BO, Oreffo, RO and Russell, RG (1994). Cells cultured from the growing tip of red deer antler express alkaline phosphatase and proliferate in response to insulin-like growth factor-I. *J. Endocrinol.* **143:** R9-R16.

Pruitt, WOJr (1966). The function of the brow-tine in caribou antlers. *Arctic* **19:** 111-113.

Putman, RJ and Staines, BW (2004). Supplementary winter feeding of wild red deer *Cervus elaphus* in Europe and North America: justifications, feeding practice and effectiveness. *Mammal Rev.* **34:** 285-306.

Putman, RJ, Sullivan, MS and Langbein, J (2000). Fluctuating asymmetry in antlers of fallow deer (*Dama dama*): the relative roles of environmental stress and sexual selection. *Biol. J. Linn. Soc.* **70:** 27-36.

Raaum, R (2006). Resample. Version 1, NYCEP Morphometrics Group.

Ramos-Barbero, B and Santos-Ureta, E (2011). Comparative study of different digitization techniques and their accuracy. *Comput. Aided Des.* **43:** 188-206.

Remondino, F and El-Hakim, S (2006). Image-based 3D modelling: a review. *Photogramm. Rec.* **21:** 269-291.

Reyment, RA (1991). Multidimensional paleobiology. pp. 539. New york: Pergamon Press.

Rodríguez, J, Martín, MT, Arias, P, Ordóñez, C and Herráez, J (2008). Flat elements on buildings using close-range photogrammetry and laser distance measurement. *Opt. Lasers Eng.* **46:** 541-545.

Rohlf, FJ and Corti, M (2000). Use of Two-Block Partial Least-Squares to study covariation in shape. *Syst. Biol.* **49:** 740-753.

Rohlf, FJ and Slice, D (1990) Extensions of the Procrustes method for the optimal superimposition of landmarks. *Syst Zool* **39**, 40–59.

Sadeghi, S, Adriaens, D and Dumont, HJ (2009). Geometric morphometric analyses of wing shape variation in ten european populations of *Calopterix splendens* (Harris, 1782) (Zygoptera: Odonata). *Odonatologica* **38:** 343-360.

Saénz de Buruaga, M, Lucio, A and Purroy, FJ (1991). Reconocimiento de sexo y edad en especies cinegéticas. pp. 127. Vitoria: Gobierno Vasco.

Sampson, PD, Streissguth, AP, Barr, HM, and Bookstein, FL (1989). Neurobehavioral effects of prenatal alcohol: part II. Partial Least square analysis. *Neurotoxicol. Teratol.* **11:** 477-491.

Sánchez-Lasheras, F, Fernández, RI, Cuesta, E, Álvarez, BJ and Martínez, S (2012). Study of the technical feasibility of photogrammetry and Coordinated Measuring Arms for the inspection of welded structures. *AIP Conf. Proc.* **1431:** 311-318.

Santiago-Moreno, J, Toledano-Díaz, A, Gómez-Brunet, A, Picazo, RA, Salas-Vega, R and López-Sebastián, A (2010). El trofeo en los bóvidos silvestres: caracterización funcional del crecimiento del cuerno. In: *Ungulados silvestres de España: biología y tecnologías reproductivas para su conservación y aprovechamiento cinegético.* Instituto Nacional de Investigación y Tecnología Agraria y Alimentaria (INIA) (ed), pp. 242. Madrid: Ministerio de Ciencia e Innovación.

Schlosser, G and Wagner, GP (2004). Introduction: the modularity concept in developmental and evolutionary biology. In:

Modularity in development and evolution, pp. 600. Chicago: The University of Chicago Press.

Schmidt, KT, Stien, A, Albon, SD and Guinness, FE (2001). Antler length of yearling red deer is determined by population density, weather and early life-history. *Oecologia* **127:** 191-197.

Shigeta, Y, Hirabayashi, R, Ikawa, T, Kihara, T, Ando, E, Hirai, S, Fukushima, S and Ogawa, T (2013). Application of photogrammetry for analysis of occlusal contacts. *J. Prosthodont. Res.* **57:** 122-128.

Skog, A, Zachos, FE, Rueness, EK, Feulner, PGD, Mysterud, A, Langvatn, R, Lorenzini, R, Hmwe, SS, Lehoczky, I, Harti, GB, Stenseth, NC and Jakobsen, KS (2009). Phylogeography of red deer (*Cervus elaphus*) in Europe. *J. Biogeogr*. **36:** 66-77.

Sneddon, LU and Swaddle, JP (1999). Asymmetry and fighting performance in the shore crab *Carcinus maenas*. *Anim. Behav.* **58:** 431-435.

Sokal, RR and Rohlf, FJ (1997). Biometry: the principles and practice of statistics in biological research. pp. 880. New York: WH Freeman & Company.

Solberg, EJ and Saether, BE (1993). Fluctuating asymmetry in the antlers of moose (*Alces alces*): does it signal male quality? *P. Roy. Soc. Lond. B* **254:** 251-255.

Sommer, RS, Zachos, FE, Street, M, Skog, A and Beneche, N (2008). Late quaternary distribution dynamics and phylogeography of red deer (*Cervus elaphus*) in Europe. *Quaternary Sci. Rev.* **27:** 714-733.

Spoor, F, Jeffrey, N and Zonneveld, F (2000). Using diagnostic radiology in human evolutionary studies. *J. Anat.* **197:** 61-76.

SPSS for Windows Vers. 15.0 (1997). Chicago: SPSS Inc.

STATSOFT (2008). Statistics for windows 8.0. Tulsa: StatSoft Inc.

Stéger, V, Molnár, A, Borsy, A, Gyurján, I, Szabolcsi, Z, Gábor, D, Molnár, J, Papp, P, Nagy, J, Puskás, L, Barta, E, Zomborszky, Z, Hom, P, Podani, J, Semsey, S, Lakatos, P and Orosz, L (2010). Antler development and coupled osteoporosis in the skeleton of red deer *Cervus elaphus*: expression dynamics for regulatory and effector genes. *Mol. Genet. Genomics* **284:** 273-287.

Stige, LC, Hessen, GO and Vollestad, LA (2006). Fitness, developmental instability, and the ontogeny of fluctuating asymmetry in *Daphnia magna*. *Biol. J. Linn. Soc.* **88:** 179-192.

Styliadis, AD (2008). Historical photography-based computer-aided architectural design: Demolished buildings information modeling with reverse engineering functionality. *Automat. Constr.* **18:** 51-69.

Sun, W, Starly, B, Nam, J and Darling, A (2005). Bio-CAD modeling and its applications in computer-aided tissue engineering. *Comput. Aided Des.* **37:** 1097-1114.

Suttie, JM, Fennessy, PF, Crosbie, SF, Corson, ID, Laas, FJ, Elgar, HJ and Lapwood, KR (1991). Temporal Changes in LH and testosterone and their relationship with the first antler in red deer (*Cervus elaphus*) stags from 3 to 15 months of age. *J. Endocrinol.* **131:** 467-474.

Suttie, JM, Lincoln, GA and Kay, RNB (1984). Endocrine control of antler growth in red deer stags. *J. Reprod. Fertil.* **71:** 7-15.

Swaddle, JP (2003). Fluctuating asymmetry, animal behaviour, and evolution. *Adv. Stud. Behav.* **32:** 169-207.

Terrádez-Gurrea, M (2002). Análisis de Componentes Principales. Cataluña: Universitat Oberta de Catalunya, 11.

Thompson, DAW (1917). On growth and form. pp. 204. Cambridge: Cambridge University Press.

Toga, AW and Thompson, PM (2003). Mapping brain asymmetry. *Nat. Rev. Neurosci.* **4:** 37-48.

Torres-Porras, J, Carranza, J and Pérez-González, J (2009a). Combined effects of drought and density on body and antler size of male Iberian red deer (*Cervus elaphus hispanicus*): implications for climate change prospects. *Wildlife Biol.* **15:** 1-9.

Torres-Porras, J, Carranza, J and Pérez-González, J (2009b). Selective culling of Iberian red deer stags (*Cervus elaphus hispanicus*) by selective montería in Spain. *Eur. J. Wildl. Res.* **55**: 117-123.

Ullrey, DE (1982). Nutrition and antler development in white-tailed deer. In: *Antler development in Cervidae*. Brown, RD (ed), pp. 49-58. Kingsville: Caesar Kleberg Wildlife Research Institute.

Van der Molen, S, Martínez, NA and González-José, R (2007). Introducción a la Morfometría Geométrica. Curso teórico práctico, pp. 89. Centro Nacional Patagónico and University of Barcelona.

Van valen, L (1962). A study of fluctuating asymmetry. *Evolution* **16:** 125-142.

Veldhuis, H and Vosselman, G (1998). The 3D reconstruction of straight and curved pipes using digital line photogrammetry. *ISPRS J. Photogramm. Remote Sens.* **53:** 6-16.

Wagner, GP, Pavlicev, M and Cheverud, JM (2007). The road to modularity. *Nature Rev. Genet.* **8:** 921-931.

Walvius, MR (1961). A discussion of the size of recent red deer (*Cervus elaphus L.*) compared with prehistoric specimens. *Beaufortia* **9:** 75-82.

Wang, CCL (2005). Parameterization and parametric design of mannequins. *Comput. Aided Des.* **37:** 83-98.

Wang, J and Oliveira, MM (2007). Filling holes on locally smooth surfaces reconstructed from point clouds. *Image Vis. Comput.* **25:** 103-113.

Whitehead, GK (1993). The whitehead encyclopedia of deer. pp. 597. Shrewsbury: Swan Hill Press.

William, JBJr, Glenwood, PE, Robert, AK and Robert, WD (2005). Antler growth and osteoporosis I. Morphological and morphometric changes in the costal compacta during the antler growth cycle. *Anat. Record* **162:** 387-397.

Wu, H and Yu, Y (2005). Photogrammetric reconstruction of free-form objects with curvilinear structures. *Visual Comput.* **21:** 203-216.

Yan, YJ, Yong, JH, Zhang, H, Paul, JC and Sun, JG (2006). A rational extension of Piegl's method for filling n-sided holes. *Comput. Aided Des.* **38:** 1166-1178.

Zelditch, ML, Swiderski, DL, Sheets, HD and Fink, WL (2004). Geometric morphometrics for biologists: A Primer. pp. 428. San Diego: Elsevier Academic Press.

Zhou, S and Wu, S (1979). A preliminary study of quantitative and character inheritance of antlers. *Acta. Gen. Clin.* **6:** 434-440.

Zioupos, P, Currey, JD and Casinos, A (2000). Exploring the effects of hypermineralisation in bone tissue by using an extreme biological example. *Connect Tissue Res.* **41:** 229-248.

Zitová, B and Flusser, J (2003). Image registration methods: a survey. *Image Vis. Comput.* **21:** 977-1000.

11. Supplementary material

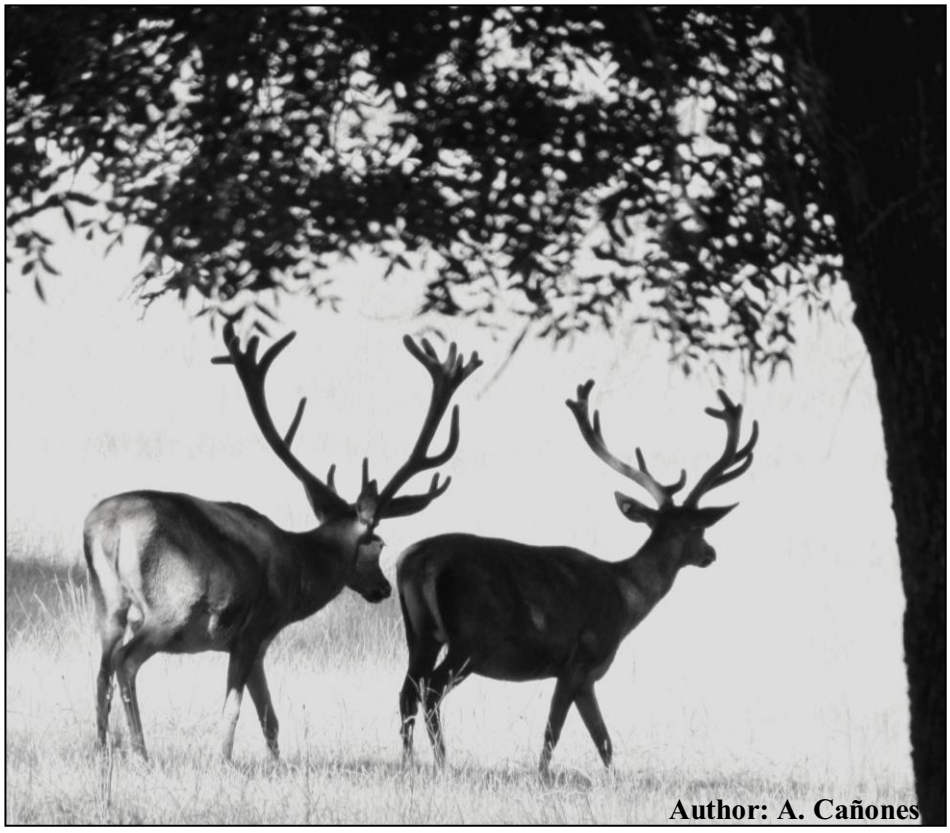

Annex I (section 4)

Table I. ANOVA. Test of homogeneity of variances (Levene test) for asymmetric component scores among the different age classes.

Levene statistic	df1	df2	Sig.
0.997613941	5	192	0.4205

Table II. (a) ANOVA. Post-hoc tests for determining possible mean differences between the asymmetric component scores of the different age classes (Age c). The mean difference is significant at 0.05 level.

	Age c	Age c	Mean difference	St. Error	Sig.	Confidence intervals 95%	
	(I)	(J)	(I-J)			Upper limit	Lower limit
HSD de Tukey	1	2	-5725387377	11706261738	0.9965	-39424455410	27973680657
		3	-2434748853	12176933410	1.0000	-37488749578	32619251872
		4	-9639240472	12537809502	0.9724	-45732102983	26453622038
		5	-16410529498	13469097893	0.8275	-55184311976	22363252980
		6	-47319616285	21554662670	0.2447	-1.09369E+11	14730255829
	2	1	5725387377	11706261738	0.9965	-27973680657	39424455410
		3	3290638523	8004655985	0.9985	-19752537228	26333814275
		4	-3913853096	8543622023	0.9974	-28508562000	20680855809
		5	-10685142121	9859686009	0.8874	-39068432796	17698148554
		6	-41594228909	19503853285	0.2751	-97740391834	14551934016
	3	1	2434748853	12176933410	1.0000	-32619251872	37488749578
		2	-3290638523	8004655985	0.9985	-26333814275	19752537228
		4	-7204491619	9177942072	0.9698	-33625231325	19216248086
		5	-13975780645	10414151507	0.7612	-43955223101	16003661812
		6	-44884867432	19789932703	0.2124	-1.01855E+11	12084838480
	4	1	9639240472	12537809502	0.9724	-26453622038	45732102983
		2	3913853096	8543622023	0.9974	-20680855809	28508562000
		3	7204491619	9177942072	0.9698	-19216248086	33625231325
		5	-6771289025	10833905641	0.9891	-37959086758	24416508707
		6	-37680375813	20014005002	0.4160	-95295123483	19934371857
	5	1	16410529498	13469097893	0.8275	-22363252980	55184311976
		2	10685142121	9859686009	0.8874	-17698148554	39068432796
		3	13975780645	10414151507	0.7612	-16003661812	43955223101
		4	6771289025	10833905641	0.9891	-24416508707	37959086758
		6	-30909086788	20610199590	0.6649	-90240112672	28421939097
	6	1	47319616285	21554662670	0.2447	-14730255829	1.09369E+11
		2	41594228909	19503853285	0.2751	-14551934016	97740391834
		3	44884867432	19789932703	0.2124	-12084838480	1.01855E+11
		4	37680375813	20014005002	0.4160	-19934371857	95295123483
		5	30909086788	20610199590	0.6649	-28421939097	90240112672

Table II. (b) ANOVA. Post-hoc tests for determining possible mean differences between the asymmetric component scores of the different age classes (Age c). The mean difference is significant at 0.05 level.

	Age c	Age c	Mean difference	St. Error	Sig.	Confidence intervals 95%	
	(I)	(J)	(I-J)			Upper limit	Lower limit
Bonferroni	1	2	-5725387377	11706261738	1	-40520806934	29070032181
		3	-2434748853	12176933410	1	-38629181921	33759684215
		4	-9639240472	12537809502	1	-46906333225	27627852281
		5	-16410529498	13469097893	1	-56445762158	23624703163
		6	-47319616285	21554662670	0.4401	-1.11388E+11	16748960672
	2	1	5725387377	11706261738	1	-29070032181	40520806934
		3	3290638523	8004655985	1	-20502214365	27083491412
		4	-3913853096	8543622023	1	-29308716075	21481009883
		5	-10685142121	9859686009	1	-39991843021	18621558779
		6	-41594228909	19503853285	0.5134	-99567027848	16378570030
	3	1	2434748853	12176933410	1	-33759684215	38629181921
		2	-3290638523	8004655985	1	-27083491412	20502214365
		4	-7204491619	9177942072	1	-34484792729	20075809490
		5	-13975780645	10414151507	1	-44930561867	16979000578
		6	-44884867432	19789932703	0.3666	-1.03708E+11	13938267300
	4	1	9639240472	12537809502	1	-27627852281	46906333225
		2	3913853096	8543622023	1	-21481009883	29308716075
		3	7204491619	9177942072	1	-20075809490	34484792729
		5	-6771289025	10833905641	1	-38973737654	25431159603
		6	-37680375813	20014005002	0.9188	-97169537825	21808786199
	5	1	16410529498	13469097893	1	-23624703163	56445762158
		2	10685142121	9859686009	1	-18621558779	39991843021
		3	13975780645	10414151507	1	-16979000578	44930561867
		4	6771289025	10833905641	1	-25431159603	38973737654
		6	-30909086788	20610199590	1	-92170363699	30352190124
	6	1	47319616285	21554662670	0.4401	-16748960672	1.11388E+11
		2	41594228909	19503853285	0.5134	-16378570030	99567027848
		3	44884867432	19789932703	0.3666	-13938267300	1.03708E+11
		4	37680375813	20014005002	0.9188	-21808786199	97169537825
		5	30909086788	20610199590	1	-30352190124	92170363699

Table III. ANOVA. Test of homogeneity of variances (Levene test) for FA scores among the different age classes.

Levene statistic	df1	df2	Sig.
0.303430866	5	211	0.9105

Table III. (a) ANOVA. Post-hoc tests for determining possible mean differences between the FA scores of the different age classes (Age c). The mean difference is significant at 0.05 level.

	Age c	Age c	Mean difference	St. Error	Sig.	Confidence intervals 95%	
	(I)	(J)	(I-J)			Upper limit	Lower limit
HSD de Tukey	1	2	-0.040056151	0.017765346	0.2176	-0.091150963	0.011038661
		3	-0.054326844	0.018773076	0.0476	-0.108319984	-0.000333705
		4	-0.042610552	0.019149566	0.2307	-0.097686512	0.012465407
		5	-0.056907429	0.020740332	0.0711	-0.116558581	0.002743723
		6	-0.035998765	0.034812826	0.9060	-0.136123739	0.064126209
	2	1	0.040056151	0.017765346	0.2176	-0.011038661	0.091150963
		3	-0.014270693	0.012769647	0.8737	-0.050997403	0.022456017
		4	-0.002554401	0.013316958	1	-0.040855229	0.035746427
		5	-0.016851278	0.01551763	0.8866	-0.061481447	0.027778891
		6	0.004057386	0.031977623	1	-0.087913275	0.096028048
	3	1	0.054326844	0.018773076	0.0476	0.000333705	0.108319984
		2	0.014270693	0.012769647	0.8737	-0.022456017	0.050997403
		4	0.011716292	0.014634283	0.9672	-0.030373288	0.053805872
		5	-0.002580585	0.016661864	1	-0.05050168	0.04534051
		6	0.018328079	0.03254826	0.9932	-0.075283789	0.111939948
	4	1	0.042610552	0.019149566	0.2307	-0.012465407	0.097686512
		2	0.002554401	0.013316958	1	-0.035746427	0.040855229
		3	-0.011716292	0.014634283	0.9672	-0.053805872	0.030373288
		5	-0.014296877	0.017084941	0.9603	-0.06343478	0.034841026
		6	0.006611787	0.032766854	1	-0.087628778	0.100852352
	5	1	0.056907429	0.020740332	0.0711	-0.002743723	0.116558581
		2	0.016851278	0.01551763	0.8866	-0.027778891	0.061481447
		3	0.002580585	0.016661864	1	-0.04534051	0.05050168
		4	0.014296877	0.017084941	0.9603	-0.034841026	0.06343478
		6	0.020908664	0.033721242	0.9895	-0.076076812	0.117894141
	6	1	0.035998765	0.034812826	0.9060	-0.064126209	0.136123739
		2	-0.004057386	0.031977623	1	-0.096028048	0.087913275
		3	-0.018328079	0.03254826	0.9932	-0.111939948	0.075283789
		4	-0.006611787	0.032766854	1	-0.100852352	0.087628778
		5	-0.020908664	0.033721242	0.9895	-0.117894141	0.076076812

Table III. (b) ANOVA. Post-hoc tests for determining possible mean differences between the FA scores of the different age classes (Age c). The mean difference is significant at 0.05 level.

	Age c	Age c	Mean difference	St. Error	Sig.	Confidence intervals 95%	
	(I)	(J)	(I-J)			Upper limit	Lower limit
Bonferroni	1	2	-0.040056151	0.017765346	0.3777	-0.092801349	0.012689047
		3	-0.054326844	0.018773076	0.0631	-0.110063987	0.001410299
		4	-0.042610552	0.019149566	0.4070	-0.099465491	0.014244386
		5	-0.056907429	0.020740332	0.0989	-0.118485341	0.004670482
		6	-0.035998765	0.034812826	1	-0.139357822	0.067360293
	2	1	0.040056151	0.017765346	0.3777	-0.012689047	0.092801349
		3	-0.014270693	0.012769647	1	-0.052183693	0.023642307
		4	-0.002554401	0.013316958	1	-0.042092363	0.036983562
		5	-0.016851278	0.01551763	1	-0.062923022	0.029220467
		6	0.004057386	0.031977623	1	-0.09088397	0.098998743
	3	1	0.054326844	0.018773076	0.0631	-0.001410299	0.110063987
		2	0.014270693	0.012769647	1	-0.023642307	0.052183693
		4	0.011716292	0.014634283	1	-0.031732801	0.055165385
		5	-0.002580585	0.016661864	1	-0.052049553	0.046888383
		6	0.018328079	0.03254826	1	-0.078307496	0.114963655
	4	1	0.042610552	0.019149566	0.4070	-0.014244386	0.099465491
		2	0.002554401	0.013316958	1	-0.036983562	0.042092363
		3	-0.011716292	0.014634283	1	-0.055165385	0.031732801
		5	-0.014296877	0.017084941	1	-0.065021957	0.036428203
		6	0.006611787	0.032766854	1	-0.090672792	0.103896366
	5	1	0.056907429	0.020740332	0.0989	-0.004670482	0.118485341
		2	0.016851278	0.01551763	1	-0.029220467	0.062923022
		3	0.002580585	0.016661864	1	-0.046888383	0.052049553
		4	0.014296877	0.017084941	1	-0.036428203	0.065021957
		6	0.020908664	0.033721242	1	-0.079209488	0.121026817
	6	1	0.035998765	0.034812826	1	-0.067360293	0.139357822
		2	-0.004057386	0.031977623	1	-0.098998743	0.09088397
		3	-0.018328079	0.03254826	1	-0.114963655	0.078307496
		4	-0.006611787	0.032766854	1	-0.103896366	0.090672792
		5	-0.020908664	0.033721242	1	-0.121026817	0.079209488

12. Acknowledgements

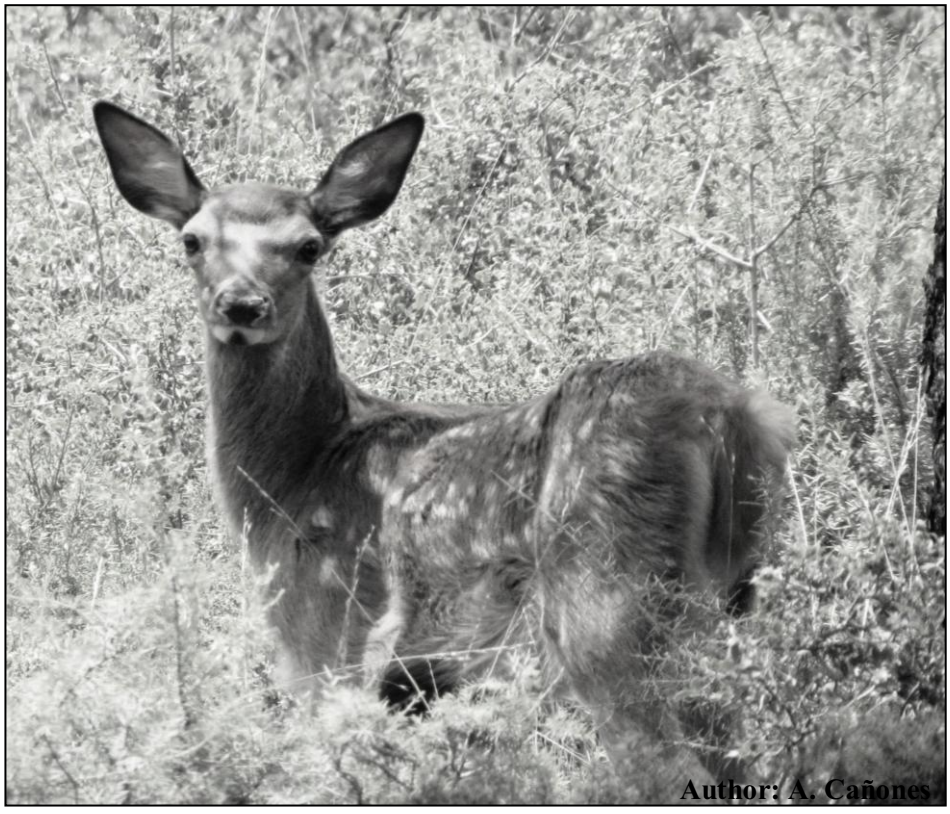

12. Acknowledgements

En primer lugar, quiero agradecer a mi director de tesis Adrià Casinos el haber depositado su confianza en mí a lo largo de todo este tiempo, y haberme brindado la oportunidad de llevar a cabo este trabajo. De la misma manera, quiero agradecer a Concepción Azorit su codirección y enseñanzas durante mis estancias en Jaén, así como durante la elaboración de esta tesis. Le agradezco al Dr. Jacint Ventura el haberme introducido en el mundo de la morfometría geométrica. Quiero agradecerle a Miguel Ángel Rubio su gran colaboración y aportación, sin la cual no se podría haber realizado el sexto capítulo de esta tesis. Agradezco al taxidermista Ismael Blanco y a toda su familia y trabajadores, la amabilidad con la que me han tratado siempre durante todo el proceso de recogida de material para este estudio. Sé que aún hoy en día, siempre estarán dispuestos a ayudar en lo que sea. Tampoco olvido a todas aquellas personas como Antonio Cañones, que han puesto su granito de arena abriéndome las puertas de sus fincas o cediéndome fantásticas fotografías utilizadas para ilustrar este trabajo. Gracias a todos aquellos como Francesc Muñoz, Albert Cama o Hugo A. Benítez, entre otros, que habéis ayudado a solventar numerosas dudas contestando a mis correos electrónicos, o simplemente me habéis dedicado palabras amables durante una etapa de mi vida, que reconozco a veces me ha parecido una tortura.

Le quiero agradecer enormemente a Paul O'Higgins su gran ayuda en la recta final de esta tesis, ya que gracias a él recuperé parte de la confianza que en algún momento perdí y realmente empecé a ver que podía alcanzar la luz al final del túnel. También le doy las gracias a todas aquellas personas del HYMS que hicieron que mi estancia en York fuera mucho más placentera y provechosa de lo esperado, así que, Vivi, Thomas,

Ricardo, Miguel, Karen, Andrew, Esther, Sam, Phil, Roxanna, Paul, *I would like to extent to you warm thanks*.

Muchas otras personas me han ayudado a lo largo de esta tesis, en momentos muy distintos y de maneras muy diferentes. Por ello, no puedo olvidar a mi *troupe* de Jaén. Esa Mari Sierra y ese Ismael que tan amablemente me adoptaron cuando anduve por tierra de olivos, y me enseñaron lo que eran las tapas de verdad EA! Sin olvidar toda la buena gente que allí conocí, como Óscar, Bea, Carmen, Jose, Terri, ... y todos los compis de la facultad con los que lo he pasado en grande celebrando fiestas del amigo invisible.

Luego está mi querido "depart", ahí donde nos concentramos todos los que compartimos penas y glorias. Cómo nos hemos reído juntos en esas cenas de navidad, charlas de despacho, charlas de bar, picnics cumpleañeros o fiestas de barrio, cosa que espero sigamos haciendo a lo largo de los años. Y cuánto nos hemos agobiado también. Caras nuevas llegan y las viejas se van, pero siempre nos quedará el haber sido del departamento de Biología animal, por eso vivan los "pajarólogos", "peixateros", y "bichólogos varios", sin vosotros el día a día no hubiera sido lo mismo. No me olvidaré de Isa, Albert, Alberto, Blanca, Josep Lluís, Toni, Javi, Laura, Teresa, Vero, Jose, Zuzanna, Nicole, Karla, Carolina, Irene, Francesc, David, Oriol, Mario, Manolo, ni de Miguel o José Luis. Tampoco me olvidaré de otros compañeros de departamento con los que no he tenido tanto trato como Fabi, Morgana, Marcel, Oriol, Carme o Jaime. Por supuesto, no me olvido de la genética del grupo, Gemma, ni de su pastel de zanahoria, o de mis compis de despacho Nuria, Urtzi, Eudald, Alex y Marc. Recordaré esas tardes de risas haciendo

abdominales y estiramientos en el centro cívico contigo Olatz, así como nuestras charlas y múltiples proyectos fallidos para ir a patinar.

A esa persona que aún no he mencionado, quiero que sepa que no me he olvidado, pero es que se merecía un apartado especial. Ese eres tú Eloy, puesto que para mi has sido un gran mentor y un mejor compañero de batalla, me he reído contigo muchísimo y me has guiado y aconsejado como el que más. Lo he pasado genial compartiendo estos años contigo, y si tuviera que repetir no se me ocurriría una manera mejor de volverlos a pasar, así que para ti van unas gracias bien grandes rodeadas de luces de neón.

Antes de embarcarme en un doctorado siempre hubo gente a mi alrededor animándome y compartiendo todas mis andanzas. Personas especiales que espero sigan muchos muchos muchos más años a mi lado, así que para mi Nurieta, Aurora, Víctor, Noe, Nati, Aran, Eli e Ivy, también van millones de gracias. No puedo olvidarme de mi Helen, toda una vida juntas, y ahora que la pequeña Laia está entre nosotros es aún mejor, así que agradezco enormemente tu apoyo por duplicado.

Leo lo que escribo y pienso qué bonito todo, si en realidad me lo he pasado bien. Pues sí, han habido muchas experiencias buenas, pero desde luego también las ha habido estresantes. Esos momentos en los que la bipolaridad mental acecha y piensas, "quién me mandaría a mi hacer un doctorado", "yo no sirvo para esto" o "en menudo embolado me he metido", no los echaré de menos para nada. Sin embargo, he de admitir que todo ello ha supuesto un gran desafío en mi vida, del que al parecer he salido airosa. El doctorado ha sacado la superviviente que llevaba dentro, esa persona capaz de aprender y superar retos y sobre todo, la que ha comprendido que eso son grandes virtudes. Y qué orgulloso te sientes

cuando eres capaz de verlo por ti mismo. Por ello, para mí el agradecimiento más importante es el que le doy a mi familia. Sin ellos, yo no estaría aquí ni sería quien soy. Para mí el mayor aprendizaje en mi vida no es lo que me haya podido aportar la ciencia, sino el consejo y apoyo de mis padres. Ojalá llegue a ser la mitad de sabia que ellos, así que gracias papá y gracias mamá, sois los mejores padres que una puede desear. Otros pilares igualmente importantes de los que no me olvido, son mi tete, Anna, y especialmente mi Angelito, gracias por haber estado siempre a mi lado.

Para finalizar he aquí mi pincelada filosófica:

El verdadero saber
es saber que se sabe lo que se sabe
y que no se sabe lo que no se sabe.
(*Confucio*)